



Provided by the author(s) and University of Galway in accordance with publisher policies. Please cite the published version when available.

Title	MicroRNAs as biomarkers and therapeutics in breast cancer
Author(s)	O'Brien, Killian
Publication Date	2017-05-25
Item record	http://hdl.handle.net/10379/6921

Downloaded 2024-05-18T21:25:20Z

Some rights reserved. For more information, please see the item record link above.



MicroRNAs as Biomarkers and Therapeutics in Breast Cancer

A thesis submitted to the National University of Ireland as partial fulfilment of the requirements for the degree of Doctor of Philosophy (PhD)

By

Killian O'Brien

BSc, MSc



Under the supervision of

Dr. Róisín M Dwyer

Discipline of Surgery, School of Medicine, National University of Ireland, Galway

May 2017

Table of Contents

Acknowledgements.....	vi
List of Tables	vii
List of Figure.....	xi
Abbreviations.....	xv
Communications Arising from This Work	xviii
Abstract.....	xx
Chapter 1 Introduction.....	1
1.1 Breast Cancer:	3
1.1.1 Breast tumour classification:	3
1.1.2 Breast cancer detection:	5
1.1.3 Breast cancer treatment:	6
1.2 MicroRNAs	8
1.2.1 MicroRNA Background:.....	8
1.2.2 miRNA Biogenesis:	9
1.2.3 miRNAs in normal biological processes:	11
1.2.4 miRNAs in Cancer:.....	11
1.2.5 Circulating miRNAs in Breast Cancer:	12
1.2.6 Sample Source:.....	13
1.2.7 Impact of Haemolysis:.....	16
1.2.8 Impact of Variations in extraction methods:	16
1.2.9 Impact of Endogenous Controls:.....	17
1.2.10 Therapeutic potential of miRNAs:.....	19
1.2.11 miR-379:.....	20
1.3 Mesenchymal Stem Cells:	20
1.4 Exosomes:	22
1.4.1 Biogenesis:	23
1.4.2 Exosome Isolation and Characterisation:	24
1.4.3 Exosome Contents:	26
1.4.4 Biomarker Potential:	26
1.4.5 Uptake by Recipient Cells:	27
1.4.6 Therapeutic Potential:	27
1.4.7 Engineering Exosomes:	28

1.5: Thesis Aims.....	32
Chapter 2 Materials and Methods.....	33
2.1 Ethics and Consent.....	35
2.2 Sample Preparation:	35
2.1 Gene and MiRNA Expression Analysis:	35
2.1.1 RNase Contamination:	35
2.1.2 RNA Extraction:	36
2.1.5 Determining RNA Quality and Quantity:.....	41
2.1.6 Reverse Transcription for Gene Expression Analysis:.....	42
2.1.7 Reverse Transcription for miRNA Analysis:.....	43
2.1.8 Real-time Quantitative Polymerase Chain Reaction (RQ-PCR):	43
2.2 Cell Culture.....	46
2.2.1 Overview of Cell Culture:	46
2.2.2 Immortalised Breast Cancer Cell lines:	47
2.2.3 Mesenchymal Stem Cells:	47
2.2.4 Feeding Cells:	48
2.2.5 Subculturing:	48
2.2.6 Cell Counting:	49
2.2.7 Cryopreservation of Cells:.....	51
2.2.8 Recovering Cells:	52
2.2.9 Transduction of MSCs:	52
2.2.10 Examining Cells by Fluorescence Microscopy:.....	54
2.2.11 Cell Proliferation Assay:	54
2.2.12 Cell Migration Assay:.....	55
2.3 Exosomes	56
2.3.1 Exosome Isolation:	56
2.3.2 Indirect Exosome Quantification:	57
2.3.3 Direct Exosome Quantification:	58
2.3.4 Transmission Electron Microscopy:	59
2.3.5 Confocal Microscopy of Exosome Transfer:.....	60
2.4 Investigating the impact of miR-379 <i>In vivo</i>	61
2.4.1 Ethics and Licensing:	61
2.4.2 Animal Facility:.....	62
2.4.3 Animal Model:.....	62

2.4.5 <i>In vivo</i> Investigation of therapeutic potential of miR-379:	65
2.5 Histological Analysis.....	66
2.5.1 Tissue processing and embedding:	66
2.5.2 Sectioning of tissue:	67
2.5.3 Haematoxylin and Eosin Staining:.....	67
2.5.4 Fluorescent staining of tissue samples:	68
2.5.5 Immunohistochemistry:.....	69
Chapter 3 Circulating miRNAs as Biomarkers of Breast Cancer.....	71
3.1 Introduction:	73
3.2 Aims:	74
3.3 Materials and Methods.....	75
3.3.1 Ethical Approval:	75
3.3.2 Patient Clinicopathological Details:	75
3.3.3 Sample Collection and Analysis:	75
3.4 Results:.....	76
3.4.1 Analysis of Circulating miR-138 in EDTA Collected Whole Blood:	76
3.4.2 Analysis of Circulating miR-504 in EDTA Collected Whole Blood:	76
3.4.3 Impact of Collection, Storage and Extraction Method on miRNA Profile:	77
3.4.4 Impact of Starting Material on Endogenous Control Profile:	78
3.4.5 Detecting Haemolysis in Cell-Free Sources:.....	79
3.4.6 Qualitative Analysis of the Impact of Starting Material on Circulating miRNAs:.....	79
3.4.7 miR-138 as Potential Biomarker of Breast Cancer:.....	81
3.4.8 miR-504 as Potential Biomarker of Breast Cancer:.....	83
3.4.9 miR-379 as Potential Biomarker of Breast Cancer:.....	85
3.5 Discussion:	86
Chapter 4 Evaluation of miR-379 as Tumour Suppressor miR In Vivo	93
4.1 Introduction:	95
4.2 Aims:	96
4.3 Materials and Methods:.....	97
4.4 Results.....	98
4.4.1 Confirmation of HCC1954 Transduction:	98
4.4.2 Impact of Transduction on HCC1954 Cell Viability:	98

4.4.3 Subcutaneous vs Mammary Fat Pad Tumour Administration:.....	99
4.4.4 <i>In vivo</i> Imaging of Tumour Vascularity:.....	100
4.4.5 Histological Analysis of Tumours:	101
4.4.6 Evaluation of Lymph Node Infiltration:.....	102
4.4.7 Confirmation of miR-379 Enrichment <i>In vivo</i> :	103
4.4.8 Impact of Elevated miR-379 Expression on COX-2 Expression:	104
4.4.9 Analysis of Tumour Vascularity:.....	106
4.4.10 Impact of Elevated miR-379 Expression on Tumour Cell Proliferation:	107
4.5 Discussion:	108
Chapter 5 Evaluating Therapeutic Impact of Systemic Delivery of miR-379	115
5.1 Introduction:	117
5.2 Aim:	118
5.3 Materials and Methods:.....	118
5.4 Results:.....	120
5.4.1 Optimisation of MSC Transduction:.....	120
5.4.2 Transduction of MSCs:	121
5.4.3 Impact of miR-379 Enrichment on MSCs:	123
5.4.4 Characterisation and Quantification of Exosomes:	124
5.4.5 Quantification of Exosome-Encapsulated miR-379:	127
5.4.6 Confocal Microscopy of Exosomal Co-Localisation:.....	127
5.4.7 Impact of Exosomal Transfer on Breast Cancer Cell Proliferation:.....	128
5.4.8 Evaluating Therapeutic Efficacy of Systemically Administered Engineered MSCs:	129
5.4.9 Therapeutic Impact of Systemic Administration of Cell-Free Engineered Exosomes:	131
5.5 Discussion:.....	133
Chapter 6 Discussion	141
6.1 Discussion:	143
6.2 Future Work:	148
6.3 Conclusion:.....	149
Chapter 7 References	151
Chapter 8 Appendices	169
8.2 LAST Training Certificate:.....	Error! Bookmark not defined.
8.3 Patient Consent Form:	Error! Bookmark not defined.

Acknowledgements

Firstly I want to thank my supervisor Dr Roisin Dwyer. There is nothing that I can write here that will do justice to the endless hours of help that she has provided me with over the course of my PhD. Her work ethic and integrity have set a benchmark that I will aspire to over the course of my career. I am eternally grateful for her unwavering support throughout this thesis.

I would also like to thank Professor Michael Kerin who has supported me throughout the course of my research. I truly appreciate the time he gave me and the role he played over the last few years. His enthusiasm for research both inspires and motivates me.

I would like to thank all the staff within the Discipline of Surgery, namely Emer Hennessy, Eimear Ramphul, Catherine Curran and Grace Clarke who have displayed endless hours of patience with me and have always provided assistance whenever needed. I also want to thank all the other researchers who have been in the lab with me for making the research experience far more fruitful.

I would also like to thank the Irish Cancer Society and BREAST-PREDICT. They have given me opportunities to present my research both nationally and internationally. Thank you to the entire BREAST-PREDICT team that consistently helped me over the last few years.

I must say a special word of thanks to my parents, Chris and Ellen. I can't thank them enough for what they have done to get me to this point. They have laid the foundation that I stand on today and provided me with the support that allowed me to overcome any adversity. I would also like to thank my brother, Rory and sister, Emily who have always been there for me throughout. Lastly, I must say thank you to Pat, her endless support helped me in ways beyond her comprehension.

List of Tables

Table 1.1: 5-year survival of patients based on stage of disease at diagnosis [2]	3
Table 1.2: Hormone receptor status of breast cancer subtypes.	4
Figure 1. 1: miRNA biogenesis and mechanism of action[48]	10
Table 1.3: Overview of starting material used in studies analysing circulating miRNAs in breast cancer.	14
Table 1.4: Different extraction methods used in analysis of circulating miRNAs in breast cancer. (X indicating at least 1 published use of technique)	17
Table 1.5: Variation in endogenous controls used in literature of circulating miRNAs in breast cancer.	17
Figure 1. 2: Overview of MSC differentiation capabilities[149].....	21
Figure 1. 3: Exosome biogenesis[174].	24
Figure 2. 1: Automated protocol for extraction of RNA on MagNA pure compact [220].	40
Figure 2. 2: Example of Nanodrop result with peak at 260 nm and optimum absorbance ratio highlighted	42
Table 2 1 Components of mastermix used for reverse transcription of miRNA.....	43
Figure 2. 3: Example of plate outline used for RQ-PCR.....	44
Table 2 2: Components of mastermix used for reverse transcription of miRNA....	45
Table 2 3: Components of mastermix used for RQ-PCR of miRNA.....	45
Table 2 4: Media Requirements.....	47
Figure 2. 4: Outline of protocol to determine the number of viable cells in a given solution [225].	50
Figure 2. 5: Outline of nucleocassette (Chemometec) used for cell count [226]. ...	51
Figure 2. 6: Lentiviral construct used for transduction of cells (Adapted from the SMARTchoice shMIMIC Lentiviral miRNA Technical Manual)	53
Figure 2. 7: Example of transwell insert and experimental set-up for evaluating migratory potential of cells.....	55
Figure 2. 8: Graphical representation of migration experiment setup.....	55
Figure 2. 9: Fields of view used to count number of migrated cells on excised insert	56
Figure 2. 10: Protocol used to isolate exosomes from cell conditioned media.....	57
Figure 2. 11: Evaluating size and concentration of exosomes in sample by nanoparticle tracking analysis [227].	59
Figure 2. 12: Anatomy of mouse mammary glands exploited for tumour induction (Image adapted from aegiscreative.com).....	63
Figure 2. 13: (a) Image of Photoacoustic Imaging System (b) Picture taken of mouse prepared to undergo photoacoustic imaging	64
Figure 2. 14: Outline of In vivo study timeline	65
Table 2 5: Primary and Secondary antibody information Abcam: Supplier used ...	70
Table 3. 1: Patient clinicopathological details on EDTA collected whole blood	75
Figure 3. 1: miR-138 levels in whole blood of breast cancer patients and healthy controls. Central horizontal line represents the median, represents the mean and the vertical lines represent the minimum and the maximum of the data	76

Figure 3. 2: miR-138 levels in whole blood of breast cancer patients and healthy controls. Central horizontal line represents the median, represents the mean and the vertical lines represent the minimum and the maximum of the data	77
Figure 3. 3: miR-16 expression in EDTA collected whole blood and RNA extracted by modified TRIzol™ BD method (Red line -). PAXgene™ collected whole blood and RNA extracted by PreAnalytix method (Blue line -).....	78
Figure 3. 4: Analysis of miR-16 expression in whole blood, serum and plasma	78
Table 3. 2: Measuring miR-16, miR-144 and miR-451 for presence of haemolysis in serum and plasma samples.....	79
Figure 3. 5: Qualitative analysis of miR-138 in whole blood, serum and plasma ...	80
Figure 3. 6: Qualitative analysis of miR-504 in whole blood, serum and plasma ...	80
Figure 3. 7: Qualitative analysis of miR-379 in whole blood, serum and plasma ...	81
Table 3. 3: Patient clinicopathological details on PAXgene™ collected whole blood	81
Figure 3. 8: Analysis of circulating miR-138 in controls and patients with breast cancer. Central horizontal line represents the median, represents the mean and the vertical lines represent the minimum and the maximum of the data	82
Figure 3. 9: Analysis of miR-138 between healthy controls and across each subtype of breast cancer. Central horizontal line represents the median, represents the mean and the vertical lines represent the minimum and the maximum of the data	83
Figure 3. 10: Analysis of miR-504 expression in healthy controls and patients with breast cancer. Central horizontal line represents the median, represents the mean and the vertical lines represent the minimum and the maximum of the data	84
Figure 3. 11: Analysis of miR-504 between healthy controls and breast cancer subtypes. Central horizontal line represents the median, represents the mean and the vertical lines represent the minimum and the maximum of the data	84
Figure 3. 12: Analysis of miR-379 in healthy control and breast cancer patient samples. Central horizontal line represents the median, represents the mean and the vertical lines represent the minimum and the maximum of the data	85
Figure 3. 13: Analysis of miR-379 expression in healthy controls and each subtype of breast cancer. Central horizontal line represents the median, represents the mean and the vertical lines represent the minimum and the maximum of the data	86
Figure 4. 1: Confirmation of transduction of breast cancer cell line HCC1954 with lentivirus by (a)RQ-PCR analysis of miR-379 expression in HCC-NTC compared to HCC-379 cells and (b)Visualisation of Red Fluorescing Protein (RFP) in HCC-NTC cells following lentiviral transduction (10X, scale bar 400 µm).	98
Figure 4. 2: MTS assay establishing any impact of miR-379 enrichment on HCC-379 cells compared to HCC-NTC cell lines over a 72hr period.....	99
Figure 4. 3: H & E staining of both MFP and SC tumours imaged at 10X and 20X100	
Figure 4. 4: Ultrasound and Photoacoustic images from a HCC-NTC tumour, A (i,ii) and compared to a HCC-379 tumour, B (i,ii). Images taken in the range of 680 – 970 nm allowing for detection of oxy and deoxyhaemoglobin	101

Figure 4. 5: Images from sectioned MFP tumours derived from HCC-NTC, (A) and HCC-379, (B) cells stained for H & E and imaged at 10X (i), 20X (ii) and 40X (iii) .	102
Figure 4. 6: Fluorescence microscopy imaging of DAPI stained (i)HCC-NTC and (ii) HCC-379 sentinel lymph nodes	103
Figure 4. 7: RQ-PCR confirmation of enriched expression of miR-379 in (a) subcutaneous HCC-379 tumours and (b) mammary fat pad HCC-379 tumours ..	104
Figure 4. 8: RQ-PCR data of miR-379 expression plotted against COX-2 gene expression in the same Ex-Vivo tumour samples	104
Figure 4. 9: Image of COX-2 primary antibody free negative control of In vivo tumour sample, with Haematoxylin stained nuclei (blue) (magnification 20X) ...	105
Figure 4. 10: Images from sectioned MFP tumours derived from (A) HCC-NTC, and (B) HCC-379, cells stained for the COX-2 protein and imaged at 10X (i), 20X (ii) and 40X (iii)	105
Figure 4. 11: (a) Image of tonsil tissue which served as a primary antibody free negative control and a (b) positive control, both images at 4X magnification.....	106
Figure 4. 12: Images from sectioned MFP tumours derived from (A) HCC-NTC, and (B) HCC-379, cells stained for the CD31 protein and imaged at 10X (i), 20X (ii) and 40X (iii)	107
Figure 4. 13: Images from sectioned MFP tumours derived from (A) HCC-NTC, and (B) HCC-379, cells stained for the PCNA protein and imaged at 10X (i), 20X (ii) and 40X (iii)	107
Figure 5. 1: MTS assay analysing impact of varying concentrations of Polybrene on MSC viability following 72hrs.....	120
Figure 5. 2: MTS assay analysing impact of Puromycin concentrations on MSC viability over the course of 7 days	121
Figure 5. 3: Light (i,ii) and fluorescent (iii,iv) images taken at 10X of MSCs before and after puromycin selection. Fluorescent images of (v) DAPI and Phalloidin (vi) MSCs readily expressing RFP following transduction, imaged at a magnification of 40X	122
Figure 5. 4: (a) RQ-PCR confirmation of enriched miR-379 expression in MSC-379 cells following transduction	123
Figure 5. 5: MTS assay to determine impact of miR-379 enrichment on cell viability in MSC-NTC and MSC-379 cell lines	123
Figure 5. 6: Migration assay quantifying the number of migrated cells at a magnification of 20X	124
Figure 5. 7: TEM image at 40,000X of isolated exosomes	125
Figure 5. 8: Images from NTA of isolated exosomes. (a,c) Graph showing size distribution of and average of 5 analyses of isolates showing SEM in red. (b,d) Snapshot from video analysis showing individual exosomes or aggregates	126
Table 5. 1: Correlation between quantification by protein estimation and NTA .	126
Figure 5. 9: RQ-PCR analysis of miR-379 expression in exosomes isolated from MSC-NTC and MSC-379 cell lines	127
Figure 5. 10: (a) 20X, (b) 60X image of HCC1954 cells incubated with PBS. (c) 20X, (d) 60X image of HCC1954 cells incubated with engineered exosomes derived from MSCs.....	128

Figure 5. 11: MTS assay evaluating impact of MSC derived exosomes on cell viability.....	129
Figure 5. 12: (a) IVIS imaging and quantification of bioluminescence of tumours over 6 weeks. (b) Sample images of mice before and following administration of MSC-NTC and MSC-379 cell	130
Figure 5. 13: (a) IVIS imaging and quantification of bioluminescence of tumours over 6 weeks. (b) Sample images of mice before and following repeat doses of miR-379 enriched exosomes and NTC exosomes	132

List of Figure

Table 1.1: 5-year survival of patients based on stage of disease at diagnosis [2]	3
Table 1.2: Hormone receptor status of breast cancer subtypes.	4
Figure 1. 1: miRNA biogenesis and mechanism of action[48]	10
Table 1.3: Overview of starting material used in studies analysing circulating miRNAs in breast cancer.	14
Table 1.4: Different extraction methods used in analysis of circulating miRNAs in breast cancer. (X indicating at least 1 published use of technique)	17
Table 1.5: Variation in endogenous controls used in literature of circulating miRNAs in breast cancer.	17
Figure 1. 2: Overview of MSC differentiation capabilities[149].....	21
Figure 1. 3: Exosome biogenesis[174].	24
Figure 2. 1: Automated protocol for extraction of RNA on MagNA pure compact [220].	40
Figure 2. 2: Example of Nanodrop result with peak at 260 nm and optimum absorbance ratio highlighted	42
Table 2 1Components of mastermix used for reverse transcription of miRNA.....	43
Figure 2. 3: Example of plate outline used for RQ-PCR.....	44
Table 2 2: Components of mastermix used for reverse transcription of miRNA....	45
Table 2 3: Components of mastermix used for RQ-PCR of miRNA	45
Table 2 4: Media Requirements.....	47
Figure 2. 4: Outline of protocol to determine the number of viable cells in a given solution [225].	50
Figure 2. 5: Outline of nucleocassette (Chemometec) used for cell count [226]. ...	51
Figure 2. 6: Lentiviral construct used for transduction of cells (Adapted from the SMARTchoice shMIMIC Lentiviral miRNA Technical Manual)	53
Figure 2. 7: Example of transwell insert and experimental set-up for evaluating migratory potential of cells.....	55
Figure 2. 8: Graphical representation of migration experiment setup.....	55
Figure 2. 9: Fields of view used to count number of migrated cells on excised insert	56
Figure 2. 10: Protocol used to isolate exosomes from cell conditioned media.....	57
Figure 2. 11: Evaluating size and concentration of exosomes in sample by nanoparticle tracking analysis [227].	59
Figure 2. 12: Anatomy of mouse mammary glands exploited for tumour induction (Image adapted from aegiscreative.com).....	63
Figure 2. 13: (a) Image of Photoacoustic Imaging System (b) Picture taken of mouse prepared to undergo photoacoustic imaging	64
Figure 2. 14: Outline of In vivo study timeline	65
Table 2 5: Primary and Secondary antibody information Abcam: Supplier used ...	70
Table 3. 1: Patient clinicopathological details on EDTA collected whole blood	75
Figure 3. 1: miR-138 levels in whole blood of breast cancer patients and healthy controls. Central horizontal line represents the median, represents the mean and the vertical lines represent the minimum and the maximum of the data	76

Figure 3. 2: miR-138 levels in whole blood of breast cancer patients and healthy controls. Central horizontal line represents the median, represents the mean and the vertical lines represent the minimum and the maximum of the data	77
Figure 3. 3: miR-16 expression in EDTA collected whole blood and RNA extracted by modified TRIzol™ BD method (Red line -). PAXgene™ collected whole blood and RNA extracted by PreAnalytix method (Blue line -).....	78
Figure 3. 4: Analysis of miR-16 expression in whole blood, serum and plasma	78
Table 3. 2: Measuring miR-16, miR-144 and miR-451 for presence of haemolysis in serum and plasma samples.....	79
Figure 3. 5: Qualitative analysis of miR-138 in whole blood, serum and plasma ...	80
Figure 3. 6: Qualitative analysis of miR-504 in whole blood, serum and plasma ...	80
Figure 3. 7: Qualitative analysis of miR-379 in whole blood, serum and plasma ...	81
Table 3. 3: Patient clinicopathological details on PAXgene™ collected whole blood	81
Figure 3. 8: Analysis of circulating miR-138 in controls and patients with breast cancer. Central horizontal line represents the median, represents the mean and the vertical lines represent the minimum and the maximum of the data	82
Figure 3. 9: Analysis of miR-138 between healthy controls and across each subtype of breast cancer. Central horizontal line represents the median, represents the mean and the vertical lines represent the minimum and the maximum of the data	83
Figure 3. 10: Analysis of miR-504 expression in healthy controls and patients with breast cancer. Central horizontal line represents the median, represents the mean and the vertical lines represent the minimum and the maximum of the data	84
Figure 3. 11: Analysis of miR-504 between healthy controls and breast cancer subtypes. Central horizontal line represents the median, represents the mean and the vertical lines represent the minimum and the maximum of the data	84
Figure 3. 12: Analysis of miR-379 in healthy control and breast cancer patient samples. Central horizontal line represents the median, represents the mean and the vertical lines represent the minimum and the maximum of the data	85
Figure 3. 13: Analysis of miR-379 expression in healthy controls and each subtype of breast cancer. Central horizontal line represents the median, represents the mean and the vertical lines represent the minimum and the maximum of the data	86
Figure 4. 1: Confirmation of transduction of breast cancer cell line HCC1954 with lentivirus by (a)RQ-PCR analysis of miR-379 expression in HCC-NTC compared to HCC-379 cells and (b)Visualisation of Red Fluorescing Protein (RFP) in HCC-NTC cells following lentiviral transduction (10X, scale bar 400 µm).	98
Figure 4. 2: MTS assay establishing any impact of miR-379 enrichment on HCC-379 cells compared to HCC-NTC cell lines over a 72hr period.....	99
Figure 4. 3: H & E staining of both MFP and SC tumours imaged at 10X and 20X100	
Figure 4. 4: Ultrasound and Photoacoustic images from a HCC-NTC tumour, A (i,ii) and compared to a HCC-379 tumour, B (i,ii). Images taken in the range of 680 – 970 nm allowing for detection of oxy and deoxyhaemoglobin	101

Figure 4. 5: Images from sectioned MFP tumours derived from HCC-NTC, (A) and HCC-379, (B) cells stained for H & E and imaged at 10X (i), 20X (ii) and 40X (iii) .	102
Figure 4. 6: Fluorescence microscopy imaging of DAPI stained (i)HCC-NTC and (ii) HCC-379 sentinel lymph nodes	103
Figure 4. 7: RQ-PCR confirmation of enriched expression of miR-379 in (a) subcutaneous HCC-379 tumours and (b) mammary fat pad HCC-379 tumours ..	104
Figure 4. 8: RQ-PCR data of miR-379 expression plotted against COX-2 gene expression in the same Ex-Vivo tumour samples	104
Figure 4. 9: Image of COX-2 primary antibody free negative control of In vivo tumour sample, with Haematoxylin stained nuclei (blue) (magnification 20X) ...	105
Figure 4. 10: Images from sectioned MFP tumours derived from (A) HCC-NTC, and (B) HCC-379, cells stained for the COX-2 protein and imaged at 10X (i), 20X (ii) and 40X (iii)	105
Figure 4. 11: (a) Image of tonsil tissue which served as a primary antibody free negative control and a (b) positive control, both images at 4X magnification.....	106
Figure 4. 12: Images from sectioned MFP tumours derived from (A) HCC-NTC, and (B) HCC-379, cells stained for the CD31 protein and imaged at 10X (i), 20X (ii) and 40X (iii)	107
Figure 4. 13: Images from sectioned MFP tumours derived from (A) HCC-NTC, and (B) HCC-379, cells stained for the PCNA protein and imaged at 10X (i), 20X (ii) and 40X (iii)	107
Figure 5. 1: MTS assay analysing impact of varying concentrations of Polybrene on MSC viability following 72hrs.....	120
Figure 5. 2: MTS assay analysing impact of Puromycin concentrations on MSC viability over the course of 7 days	121
Figure 5. 3: Light (i,ii) and fluorescent (iii,iv) images taken at 10X of MSCs before and after puromycin selection. Fluorescent images of (v) DAPI and Phalloidin (vi) MSCs readily expressing RFP following transduction, imaged at a magnification of 40X	122
Figure 5. 4: (a) RQ-PCR confirmation of enriched miR-379 expression in MSC-379 cells following transduction.....	123
Figure 5. 5: MTS assay to determine impact of miR-379 enrichment on cell viability in MSC-NTC and MSC-379 cell lines	123
Figure 5. 6: Migration assay quantifying the number of migrated cells at a magnification of 20X.....	124
Figure 5. 7: TEM image at 40,000X of isolated exosomes	125
Figure 5. 8: Images from NTA of isolated exosomes. (a,c) Graph showing size distribution of and average of 5 analyses of isolates showing SEM in red. (b,d) Snapshot from video analysis showing individual exosomes or aggregates	126
Table 5. 1: Correlation between quantification by protein estimation and NTA .	126
Figure 5. 9: RQ-PCR analysis of miR-379 expression in exosomes isolated from MSC-NTC and MSC-379 cell lines.....	127
Figure 5. 10: (a) 20X, (b) 60X image of HCC1954 cells incubated with PBS. (c) 20X, (d) 60X image of HCC1954 cells incubated with engineered exosomes derived from MSCs.....	128

Figure 5. 11: MTS assay evaluating impact of MSC derived exosomes on cell viability.....	129
Figure 5. 12: (a) IVIS imaging and quantification of bioluminescence of tumours over 6 weeks. (b) Sample images of mice before and following administration of MSC-NTC and MSC-379 cell	130
Figure 5. 13: (a) IVIS imaging and quantification of bioluminescence of tumours over 6 weeks. (b) Sample images of mice before and following repeat doses of miR-379 enriched exosomes and NTC exosomes	132

Abbreviations

°C	Degrees Centigrade
(-NTC)	Lentivirus encoding scramble sequence
(-379)	Lentivirus enriching miR-379 expression
µg	Microgram
µl	Microlitre
µm	Micrometre
AAV	Adeno-Associated Virus
ANOVA	Analysis of variance
ATCC	American Type Culture Collection
BCA	Bicinchoninic Acid
BSA	Bovine Serum Albumin
cDNA	complimentary DNA
cm	centimetre
COX-2	Cyclooxygenase-2
Ct	Cycle threshold
DAPI	4',6-diamidino-2-phenylindole
DCIS	Ductal Carcinoma In Situ
DPX	Distrene, Plasticiser, Xylene
EDTA	Ethylenediaminetetracetic acid

EGFR	Epidermal Growth Factor Receptor
ER	Estrogen Receptor
FGF	Fibroblast Growth Factor
FBS	Fetal Bovine Serum
HER2	Human Epidermal Growth Factor Receptor
hr	hour
IU	International Unit
i.v.	Intravenous
IVIS	<i>In vivo</i> Imaging System
MFP	Mammary Fat Pad
min	Minute
miRNA	MicroRNA
ml	millilitre
MRI	Magnetic Resonance Imaging
MSC	Mesenchymal Stem Cell
NFW	Nuclease Free Water
nm	Nanometre
NTA	Nanoparticle Tracking Analysis
PAI	Photoacoustic Imaging System
PBS	Phosphate Buffer Saline

PR	Progesterone Receptor
RFP	Red Fluorescent Protein
RPM	Revolutions Per Minute
RQ-PCR	Relative Quantity-PCR
sec	Second
siRNA	small/short interfering RNA
TEM	Transmission Electron Microscopy
UTR	Untranslated Region

Communications Arising from This Work

Published Book Chapter:

- **O'Brien KP**, Ramphul E, Howard L, Gallagher WM, Malone C, Kerin MJ and Dwyer RM. (2017) 'Circulating microRNAs in Cancer' for Book entitled 'MicroRNA Profiling: Methods and Protocols' Springer Science + Business Media, LLC, New York. Methods Mol Biol. 2017;1509:123-139. PMID 27826923

Oral Presentation:

- American Association of Cancer Researchers (AACR, Washington DC), 'Engineering Mesenchymal Stem Cells to support tumour-targeted delivery of exosome-encapsulated microRNA-379'. **KP O'Brien**, K Gilligan, S Khan, B Moloney, K Thompson, P Lalor, P Dockery, H Ingoldsby, MJ Kerin, RM Dwyer, April 2017.
- Irish Association for Cancer Researcher (IACR, Kilkenny), 'Employing Mesenchymal Stem Cells as Tumour-Targeted Delivery Vehicles of Exosomal microRNA-379'. **KP O'Brien**, K Gilligan, S Khan, B Moloney, K Thompson, P Lalor, P Dockery, H Ingoldsby, MJ Kerin, RM Dwyer. Feb 2017
- Sir Peter Freyer Surgical Symposium (Galway),
 - 'Understanding the Tumour Suppressive Role of microRNA-379 and Developing a Tumour-Targeted Method of Therapeutic Delivery'. **KP O'Brien**, S Khan, K Thompson, DP Joyce, P Lalor, P Dockery, H Ingoldsby, MJ Kerin, RM Dwyer. Sept 2016, (Plenary Session).
 - 'Clinical application of circulating microRNAs as biomarkers is hindered by lack of standardised protocols'. **KP O'Brien**, E Ramphul, L Howard, C Malone, MJ Kerin, RM Dwyer. Sept 2015
- 6th Small Animal SPECT Imaging Workshop (Arizona), 'Mesenchymal Stem Cell-mediated imaging and therapy of Breast Cancer'. **KP O'Brien** and RM Dwyer. Jan 2016
- Matrix Biology Ireland Conference (Dubin), 'Modification of Mesenchymal Stem Cell-Derived Exosome: Potential for Breast Cancer Therapy'. **KP O'Brien**, S Khan, DP Joyce, MJ Kerin, RM Dwyer. Dec 2015
- College of Medicine, Nursing and Health Science (CMNHS) postgraduate research day (Galway), 'Clinical application of circulating microRNAs as biomarkers is hindered by lack of standardised protocols'. **KP O'Brien**, E Ramphul, L Howard, C Malone, MJ Kerin, RM Dwyer. May 2015

Poster Presentation:

- San Antonio Breast Cancer Symposium (Texas), 'Engineering Mesenchymal Stem Cells(MSCs) to secrete tumour-suppressing exosomes for breast cancer therapy'. **KP O'Brien**, S Khan, K Thompson, D Joyce, P Lalor, P Dockery, H Ingoldsby, MJ Kerin, RM Dwyer. Dec 2016

- Breast Cancer Now Symposium (London), ‘Engineering Mesenchymal Stem Cells (MSCs) for exosome mediated delivery of microRNAs’. **KP O’Brien**, S Khan, DP Joyce, P Lalor, K Thompson, P Dockery, MJ Kerin, RM Dwyer. July 2016
- European Association of Cancer Researchers (EACR, Manchester), ‘Examining the tumour suppressive capabilities of microRNA-379 and elucidating a clinically relevant means of delivery’. **KP O’Brien**, S Khan, M Mannion, DP Joyce, P Lalor, P Dochery, H Ingoldsby, MJ Kerin, RM Dwyer. July 2016
- Matrix Biology Europe (Athens), ‘Modification of Mesenchymal Stem Cell-Derived Exosomes: Potential for Breast Cancer Therapy’. **KP O’Brien**, S Khan, R Smyth, DP Joyce, P Lalor, K Thompson, P Dockery, MJ Kerin, RM Dwyer. June 2016
- Irish Association for Cancer Researcher (IACR),
 - ‘Investigating the tumour suppressor capabilities of microRNA-379 and the potential for therapeutic application’. **KP O’Brien**, S Khan, M Mannion, DP Joyce, M.J. Kerin and R.M. Dwyer. Feb 2016
 - ‘The impact that the variation in approaches has to the analysis of circulating microRNAs and their potential as biomarkers of disease’. **KP O’Brien**, D Joyce, E Ramphul, M.J. Kerin and R.M. Dwyer. Feb 2015
 - ‘Dysregulation of MicroRNA-504 Expression is Associated with Breast Cancer’. **KP O’Brien**, S. Khan, H. Quachthithu, C. Brougham, C. Curran, M.J. Kerin, R.M. Dwyer. Feb 2014

Awards and Honours:

- Received a plaque and €300 for the Prof. John Fitzpatrick Award for best oral poster presentation, Feb 2017.
- Travel Bursary worth €400 to attend 6th Small Animal SPECT Imaging Workshop, Jan 2016
- Bursary worth €120 to attend Matrix Biology Ireland conference, Dec 2015
- 3rd place in THREESIS, Oct 2014
- Awarded first prize in Higher Education Authority (HEA) funded ‘Making an Impact’ competition, Mar 2014

Abstract

Micro(mi)RNAs have potential as both therapeutics and circulating biomarkers of disease. This study investigates potential breast cancer biomarkers miR-138, miR-504 and miR-379. Furthermore, it investigates the impact that differences in starting material, collection, storage and extraction have on the miRNA profile. These variables alone, impacted the expression of stably expressed endogenous control, miR-16. Different starting material also impacted on the presence or absence of miR-138 and miR-504. While miR-504 was significantly elevated in the whole blood of patients with breast cancer when compared to healthy controls irrespective of methods of collection, storage or extraction.

While miR-379 did not function as a biomarker for detecting breast cancer, previous work has shown it to be significantly reduced in primary breast tumour tissue and having therapeutic potential. This study used an invasive breast cancer cell line, HCC-1954, to further evaluate miR-379 as a therapeutic miRNA. Cells were transduced for enriched miR-379 expression (HCC-379) or a scramble sequence (HCC-NTC) and administered into an animal model. *Ex vivo* analysis revealed an increase in tumour necrosis and a decrease in lymph node invasion in tumours with elevated miR-379 expression. Investigation of a potential role for miR-379 in regulating COX-2, revealed an inverse relationship at an mRNA level, further confirmed at a protein level.

For delivery of miR-379, the tumour homing capacity of Mesenchymal Stem Cells(MSCs) were employed. MSC-secreted exosomes natively package and deliver miRNAs and may reflect the tumour targeted potential of parent MSCs. To exploit this, MSCs were transduced for enriched expression of miR-379 in both the parent cell and secreted exosomes. An *in vivo* study was established to investigate any therapeutic efficacy of either MSC-379 or MSC-NTC cells, or exosomes secreted by the cells. Quantitative bioluminescence revealed a significant reduction in tumour activity in animals that received exosomes enriched with miR-379 systemically.

Data presented highlights factors impacting the potential for clinical utility of miRNAs as circulating biomarkers of disease. Furthermore, this data also supports miR-379 as a potential therapeutic in breast cancer. Engineering MSC secreted exosomes enriched with miR-379 holds exciting potential as a novel therapy for breast cancer.

Chapter 1

Introduction

Chapter 1: Introduction

1.1 Breast Cancer:

Breast cancer is the most common cancer among women worldwide[1]. In Ireland, there are roughly 2,700 cases diagnosed each year in women and 18 – 20 cases in men, making it the second most common malignancy in women [2, 3]. There has been a reduction in mortality rates associated with breast cancer due to improvements in treatments and earlier detection. BreastCheck was introduced into the east of Ireland in 2001 and subsequently into the South and West of the country in 2007 [2]. This service offers free biannual screening to women between 50-64 years of age. Similar to most types of cancer, patients diagnosed with advanced Stage disease suffer from significantly lower rates of survival (Table 1.1). Disease stage is determined following consideration of tumour size (T), lymph node infiltration (N) and whether or not the tumour has metastasised (M). This is subsequently scored from (I-IV) based on severity and is referred to as the TNM classification system which was initially defined by the American Joint Committee on Cancer (AJCC) [4]. Lower rates of survival at late stage diagnosis is the result of metastatic advancement and few patients that suffer from metastatic disease are cured, with treatments often resulting in substantial side effects [5].

	5-year Survival
Stage I	96.1%
Stage II	89.5%
Stage III	66.4%
Stage IV	28.1%

Table 1.1: 5-year survival of patients based on stage of disease at diagnosis [2]

This table underlines the importance of early detection of the disease and the necessity for a screening program such as Breast Check. Despite improvements, roughly 690 women die from breast cancer annually in Ireland so there is still a need for better methods of detecting the disease as well as treating patients with treatment refractory disease [2].

1.1.1 Breast tumour classification:

Upon presentation, breast tumours are classified based on Stage, Grade and Epithelial Subtype. Such classification ensures the most appropriate treatment strategy will be devised for a particular patient.

1.1.1.1 Tumour grade:

The grade of a tumour is assessed microscopically where cell morphology is evaluated. A scoring system based on the amount of gland formation, the nuclear features and the mitotic activity allow Pathologists grade a tumour [6]. Less than 10% of the tumour area forming glands would be regarded as the most aggressive morphology and receive the highest score. Nuclei with variations in size and shape would be associated with high grade tumours. A high number of mitotic figures would also be associated with high grade tumours. Overall, based on these scoring criteria, well differentiated tumours would be classed as Grade 1 while the most aggressive undifferentiated tumours would be classed as Grade 3 [7].

1.1.1.2 Epithelial subtypes of breast cancer:

Breast cancer is a heterogenous disease that can now be broken down into individual subtypes based on the distinct gene expression profiles identified by Perou et al. [8, 9]. There are five major subtypes recognised in clinical practice, which are outlined in (Table 1.2). These subtypes are defined based on the expression of three receptors, estrogen receptor (ER), progesterone receptor (PR) and human epidermal growth factor receptor-2 (HER-2).

Subtype	Receptor Status
Luminal A	ER+ PR+ HER2-
Luminal B	ER+ PR+ HER2-/+
HER2+	ER- PR- HER+
Basal-like	ER- PR- HER2-
Normal-like	ER+/- PR+/- HER2-

Table 1.2: Hormone receptor status of breast cancer subtypes.

Table 1.2: Hormone receptor status of breast cancer subtypes.

Therapies are targeted based on receptor expression of each subtype, which further highlights the importance of the molecular classification of breast cancer [10].

The estrogen receptor α (ER α) is present on roughly 70-80% of breast cancers and can be targeted quite effectively [11]. The ER α is targeted by a Selective Estrogen Receptor Modulator (SERM) e.g. Tamoxifen which binds to the receptor and subsequently prevents any estrogen from binding to and activating the receptor [12]. Another method of treating ER+ patients is with the use of Aromatase Inhibitors (AI's), such as anastrozole, preventing the conversion of androgen into estrogen by inhibiting the enzyme aromatase. This reduces the amount of

estrogen available to activate the receptors [13]. While both approaches are successful for patients that express the estrogen receptor, those that lack expression of ER must avail of alternative treatment options. Trastuzumab is a monoclonal antibody that targets the extracellular domain of the HER2 receptor and inhibits activation of the internal tyrosine kinase domain [14]. Combining Trastuzumab and AI's has shown potency for patients with Luminal B cancer [15]. Patients with HER2 amplified cancer have responded well to combinations of trastuzumab and chemotherapy [5]. Triple negative subtype of breast cancer lack expression of all three receptors, thus removing the therapeutic target exploited by the previously described drugs. Basal tumours are not exclusively triple-negative but are defined by mitotic index and cytokeratin expression [16]. This subgroup form an aggressive type of tumour with current treatment options relying on chemotherapy [17].

1.1.2 Breast cancer detection:

Currently, the gold standard for detecting breast cancer is mammography. Simply, a mammogram is an x-ray that primarily detects the presence of calcifications within the breast and any other changes that may be associated with breast cancer development [18, 19]. The current standard of care follows that once a mass is detected by mammography, the subsequent steps involve an ultrasound to further investigate the mass and to evaluate whether it is solid or cyst like. Once imaging is completed and the integrity of the mass is determined, a fine needle biopsy is then carried out to evaluate the mass for the presence of cancer. Mammography does have certain drawbacks. False positives can result in further unnecessary imaging and biopsies for the patient, while false negatives result in no detection and therefore a lost opportunity to receive treatment at as early a stage as possible. Interval cancers are one limitation of screening that is also worthy of consideration [20]. An interval cancer is a tumour that becomes palpable between 2 rounds of screening. Concerns also exist relating to overdiagnosis, for example, patients with ductal carcinoma in situ (DCIS), a disease that is not necessarily a precursor of invasive disease and one with poorly understood prognosis and treatment can result in unnecessary treatments for an individual patient [21].

In addition to the standard of care, different modalities can be implemented to aid in detection of breast cancer. Magnetic resonance imaging (MRI) can be used

on select patients, those with a genetic susceptibility or previously treated using radiation therapy. MRI has a higher sensitivity than mammography but it can result in a greater amount of false positives while also being more expensive than mammography [22]. When both modalities are used together the detection rate is higher than if either was used on its own [23].

1.1.3 Breast cancer treatment:

A landmark in breast cancer treatment came in 1880 when the radical mastectomy was introduced as a treatment option for breast cancer [24]. Since then, different treatments have evolved including more refined surgery along with chemotherapy, radiation therapy as well as the biological approaches outlined previously, consisting of monoclonal antibodies and hormone therapy.

There are various methods of treating breast cancer surgically. A lumpectomy is performed to remove the tumour and surrounding tissue from a patient's breast. In circumstances where this is not possible due to large multicentric tumours, a mastectomy is carried out [25]. This completely removes the breast and is sometimes performed as a preventative measure in the case of patients with a genetic predisposition to developing breast cancer. Biopsies from the sentinel lymph nodes are also taken in order to allow staging of the disease and in certain cases, axillary clearance is required for those with positive nodes [26].

Chemotherapy refers to the use of cytotoxic drugs, usually administered in cycles, which inhibit cell division in fast replicating cells. As tumour cells divide at a higher frequency than most healthy cells, this approach has garnered some success in the field of cancer therapy. Chemotherapy is not tumour targeted and is quite a crude treatment option with certain drawbacks. As certain healthy cells have high cell turnover they can subsequently become targets of the chemotherapy. This results in harsh side effects in the form of reduced haematopoiesis, sterility and gastric side effects [27]. Neoadjuvant chemotherapy is given to the patient prior to surgical intervention with the aim of reducing the tumour size before resection eg. Cisplatin [28]. Adjuvant therapy refers to the combination of chemotherapy along with primary treatment. Often, adjuvant therapy is administered once all visible signs of the tumour have been removed and this therapy targets any tumour cells that may have spread from the primary site or may be left behind [29].

Chapter 1: Introduction

Radiotherapy is generally performed along with other means of therapy, such as surgery or chemotherapy. Radiotherapy functions through ionizing radiation targeted to the DNA of tumour cells, preventing continuation of the cell cycle and halting further cell growth [30]. Radiotherapy is regarded as an essential treatment that results in either the cure or palliation of patients with carcinoma. The frequency at which radiotherapy is used varies in the literature, but one study suggests its use for up to 83% of patients with breast carcinoma [31].

Biological therapies were developed with the aim of improving on available chemotherapeutics and reducing the harsh side effects associated with them. The first biological therapy to receive approval from the US Food and Drug Administration (FDA) was the previously mentioned anti-HER2 monoclonal antibody trastuzumab in 1998. This has shown to be efficacious when used in conjunction with chemotherapy [14]. This breakthrough allowed for the development of further biotherapeutics. These may include more monoclonal antibody based drugs, biological agents that target differentiation, metastasis and angiogenesis as well as vaccine or gene based therapies [32]. Anastrozole and Tamoxifen are two examples of biological therapies that show efficacy in clinical practice [33, 34]. Despite such therapies reaching clinical implementation there is still a desire for a treatment that can effectively treat patients with advanced disease.

As tumours are derived from multiple cell types, issues can arise when therapies targeting only the epithelial tumour cells are administered to these heterogenous populations. Therapeutic resistance is attributed to changes in the tumour microenvironment as well as the tumour cells. Tumour vasculature can be affected by the dense nature of the tumour stroma compressing the vessels, leading to inefficient blood flow and increased interstitial pressure resulting in ineffective drug delivery to tumour cells [35]. Cells of the immune system also contribute to both inherent and acquired resistance, where macrophage abundance is thought to inhibit therapeutic response [35]. Targeting the epithelial cancer cells is not sufficient for treatment response. Developing knowledge has resulted in therapies designed to target features of the tumour environment with drugs targeting stromal fibroblasts, tumour vasculature and the immune cells showing promise [35]. Cancer stem cells (CSCs) are another population of cells

present within a tumour that can be responsible for initiation and metastasis of cancers while also playing a role in recurrence and drug resistance [36]. Improved understanding of the many cell populations present in a tumour and development of targeted strategies could result in improved patient survival.

While treatment strategies evolve, early detection of breast cancer remains the best strategy for improving patient survival. Biomarkers of disease present in the circulation would allow for a non-invasive method of detecting the cancer. One circulating biomarker employed in breast cancer is CA15-3. Although not employed for disease diagnosis, this is a glycoprotein that can detect recurrence in patients with breast cancer [37]. However, this marker was shown to be ineffective in the detection of locoregional relapse or contralateral breast cancer. This same study further states that Ca 15-3 alone is not effective as a marker for detecting relapse [38].

Whether it be imaging based, blood based or tissue based, current methods of diagnosing breast cancer are limited. There is a desire to improve current approaches in detecting breast cancer at as early stage as possible and to also provide information on recurrence and predict response of individual patients to therapy. Such personalised diagnostics will allow for more efficient evaluation and treatment options for patients. Circulating biomarkers offer a lot of promise, but despite the large degree of research invested into elucidating a biomarker, clinical implementation of novel, sensitive and specific circulating biomarkers for breast cancer have yet to be established.

While breast cancer diagnostics and therapy are both rapidly developing, there is still an unmet need for a sensitive and specific biomarker for breast cancer.

MicroRNAs have been heralded as potential circulating biomarkers of disease. An ideal biomarker should be sensitive, specific and proportional in abundance to the tumour load and miRNAs have been proven to match this criteria [39].

1.2 MicroRNAs

1.2.1 MicroRNA Background:

MicroRNAs (miRNAs) and their mechanism of action was first described in 1993 in the nematode *C.Elegans*[40]. Since then, these molecules of roughly 19-25 nucleotides have garnered a lot of interest from researchers for their use as both biomarkers of disease as well as potential therapeutic agents. miRNAs are capable

of regulating genes through translational repression of corresponding mRNAs and subsequently impacting important cellular pathways [41]. It is predicted that miRNAs could potentially regulate roughly 30% of the human protein-coding genome. Theoretically, one miRNA could target multiple mRNAs while one mRNA could be targeted by many different miRNAs [42, 43]. A surge of interest has developed in miRNAs with the online database miRbase containing 28,645 reported miRNAs from a total of 206 species [44].

1.2.2 miRNA Biogenesis:

miRNAs begin as primary (Pri-)miRNAs in the nucleus following transcription mediated by either RNA polymerase II or III, and are several hundred or thousand nucleotides in length while containing at least one miRNA stem loop [45] (Figure 1.1). The RNase III enzyme Drosha along with the double stranded binding partner the DiGeorge Syndrome Critical Region 8 (DGCR8) cleaves this pri-miRNA transcript, where up to 6 precursor (pre-)miRNAs could be derived from the original pri-miRNA. These pre-miRNAs are roughly 70-90 nucleotides in length and contain a hairpin structure. This structure is required for the transport of the molecules from the nucleus into the cytoplasm which is mediated by Exportin-5 [46]. Finally, in the cytoplasm, the hairpin structures are cropped by the endonuclease Dicer and its binding partner Tans-Activator RNA Binding Protein (TRBP), forming a small double stranded RNA duplex. Within this duplex lies the mature miRNA along with its complimentary strand. The mature miRNA incorporates into a miRNA associated RNA-induced silencing complex (miRISC). Subsequently, miRISC interacts with complimentary mRNAs where it carries out its functional impact [47].

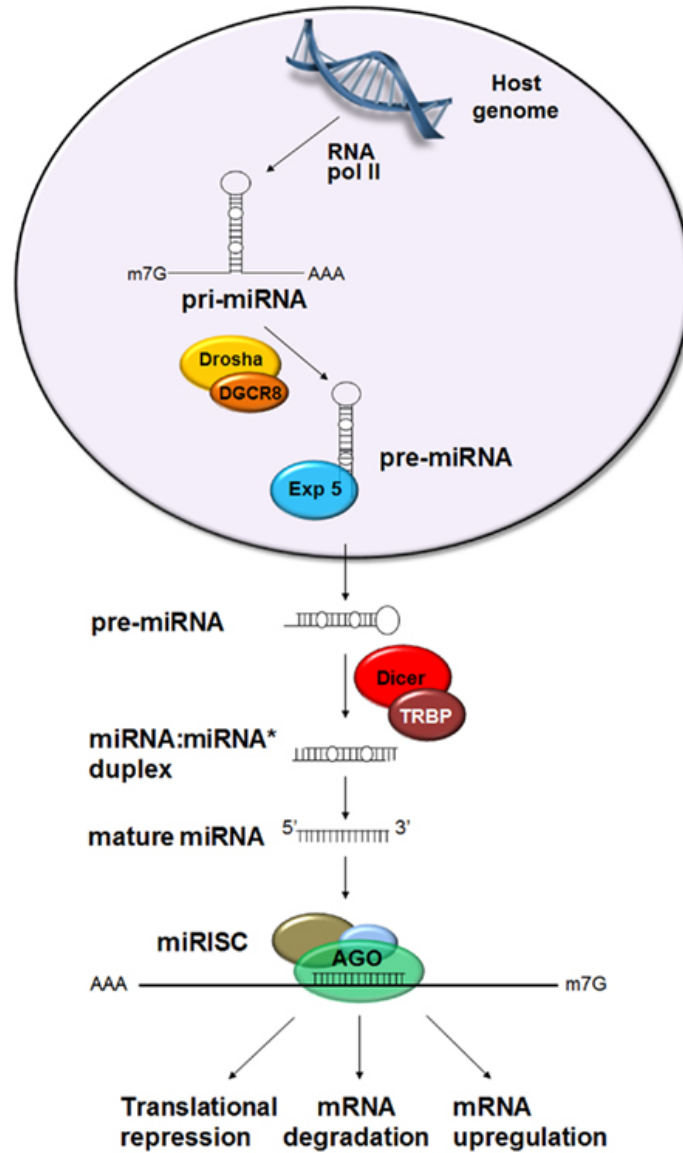


Figure 1. 1: miRNA biogenesis and mechanism of action[48]

There are two main methods by which miRNAs exert their function, either through degradation of a complimentary mRNA or translational repression. In instances where the miRISC has perfectly complimentary binding to a certain mRNA, the mRNA, through activation of an RNA mediated interference pathway, is cleaved and degraded. The second method is through the imperfect binding of the miRNA to the 3' untranslated region (UTR) or 5' UTR of partially complimentary mRNAs [49, 50]. Some reports have suggested that miRNA binding can have positive effects on the mRNA level through promotion of transcription, stabilization of the transcript resulting in an increase in translation [51-53].

1.2.3 miRNAs in normal biological processes:

miRNAs are potent regulators of gene expression and have been known to serve important roles in normal development. Many studies have shown miRNAs featuring in normal muscle development, embryonic development and lymphocyte differentiation [54]. However, in relation to normal breast physiology, little research has been carried out. One study showed that 7 groups of miRNAs are associated with distinct phases of the breast development when examined in juvenile and adult mouse mammary glands [55]. Research such as this is critical, as an understanding of normal miRNA function will allow scientists to understand how aberrant miRNA function influences carcinogenesis.

1.2.4 miRNAs in Cancer:

The first mention of miRNA involvement in cancer came in 2002 when it was discovered that miR-15a and miR-16-1 were located in a region of chromosome 13q14 that is commonly deleted in B-cell chronic lymphocytic leukaemia. Both miRNAs were shown to be down-regulated and this study was the first to suggest a tumour suppressor role for miRNAs [56]. Following from this study many have suggested roles for multiple miRNAs in a variety of human cancers. miRNAs that are found to be dysregulated in the tissue of patients with cancer when compared to control samples have been suggested as potential biomarkers or even therapeutic targets. Many miRNAs dysregulated in tumours tend to be down-regulated due to transcriptional repression, epigenetic silencing, genetic loss or defects in their biogenesis pathway [57]. miRNAs that are down-regulated in cancer could have potential as tumour suppressor miRs while those that are up-regulated could function as oncomiRs [58]. In breast cancer, miRNAs have been linked to many aspects of metastasis relating to migration, invasion, motility and angiogenesis [59]. Adding to this, some miRNAs have distinct expression profiles between the molecular subtypes of breast cancer [60, 61].

Initial work on miRNAs in the cancer setting was based on tumour tissue expression profiles, and one study illustrated the effectiveness of miRNA expression in distinguishing between normal (n=10) and breast cancer tissue (n=76) [62]. This study highlighted 15 miRNAs that could distinguish between both tissue types with 100% accuracy, however, the number of normal samples analysed would have to be increased in the baseline study in multiple populations. This could then be validated and potentially result in clinical implementation. As

well as identifying tumour cells, miRNAs were also shown to be prognostic predictors in Chronic Lymphocytic Leukaemia (CLL) [63]. In patients with CLL, high levels of a 70-kD zeta-associated protein, ZAP-70 are associated with aggressive disease. Here, 13 miRNAs were found to identify cases of CLL that exhibited low levels of ZAP-70 showing that miRNAs can have an association with disease progression. miRNAs have also been shown to elucidate poorly differentiated tumours that have uncertain histological origin which will allow for improved treatment planning [58]. Showing promise as tissue biomarkers of disease, there was a further surge of interest in elucidating a miRNA that would serve as a biomarker from a liquid biopsy.

1.2.5 Circulating miRNAs in Breast Cancer:

Once miRNAs were shown to be detectable in the circulation of patients with cancer, a surge of interest regarding implementation of these molecules as biomarkers quickly ensued. Further research discovered that miRNAs could be protein bound or encapsulated in vesicles in the circulation [64].

In the breast cancer field alone, this breakthrough has resulted in the emergence of a significant number of studies analysing breast cancer patient blood samples for the possibility of identifying clinically relevant miRNAs [65]. Despite tremendous potential, over the past decade miRNAs have not yet been implemented in the clinical setting as a biomarker of disease. There is not a standardised approach to investigating these molecules, resulting in many different methods being employed. All three starting materials (whole blood, plasma or serum) have been analysed followed by differing methods of extraction (TRIzol™ or column-based) with data generated being normalised to a large variety of endogenous controls. This variance in approaches to circulating miRNAs has resulted in opposing published results. Such contradictions based solely on different methodologies employed stagnate potentially promising miRNAs from achieving the criteria necessary for clinical implementation. Contradictory results can be seen in this field even when the same target miRNA is being investigated. For example, in one study circulating levels of miR-10b were found at significantly higher levels in the serum of breast cancer patients when compared to healthy controls, while another study reported no significant difference in the whole blood of patients versus healthy individuals [66, 67]. This pattern was mirrored in other studies where miR-106a and miR-155 were found to be elevated in the

serum of patients with breast cancer when compared to healthy individuals [68, 69]. However, when these miRNAs were analysed in plasma samples by other research groups, no significant change was observed in breast cancer patients compared to healthy controls [68, 69]. miR-145 was also analysed in the plasma and serum of breast cancer patients and compared to healthy controls by two separate groups [66, 70]. Analysing miR-145 in the serum suggested a significant increase in the patient cohort, while it was found to be decreased in the plasma of patients when compared to healthy controls [66, 70].

However, separate studies using different source materials can achieve similar results. For example, two separate groups carried out analysis of miR-21 in serum and plasma respectively, and both concluded that it was up-regulated in patients when compared to healthy controls [68, 70]. A robust method of analysing circulating miRNAs is required to overcome inter laboratory variations.

Variation is not limited to starting material, but is also witnessed in methods of extracting miRNA with some implementing TRIzol™ based methods, while others opt for column-based approaches on the same source material [71, 72]. Storage and handling of samples vary across the studies also, with some utilising storage of whole blood at -80 °C in PAXgene™ tubes while others report storage in EDTA tubes at 4 °C [67, 73]. These contrasting approaches to analysis could impact results seen, thus inhibiting publication of consistent findings and preventing the progression of the field into the clinical setting.

1.2.6 Sample Source:

Circulating miRNAs have been analysed in serum, plasma and whole blood of breast cancer patients and healthy controls. miRNAs are found to be relatively stable in these starting materials as well as other fluids such as saliva and urine. This is due to being either protein bound or encapsulated in exosomes, making each source material a viable option for analysis [64]. It is imperative for these samples to be stored appropriately. Whichever starting material is routinely collected in the host lab is likely to be the greatest influencing factor for researchers when choosing a starting material. A review of the literature revealed publications using each of these sources, with serum employed in the majority of studies (Table 1.3).

Source of extracted miRNAs	Number of Studies Published	References
Whole Blood	8	[67, 73-79]
Serum	31	[57, 66, 68, 71, 72, 80-105]
Plasma	16	[69, 70, 103, 106-119]

Table 1.3: Overview of starting material used in studies analysing circulating miRNAs in breast cancer.

1.2.6.1 Whole Blood:

8 papers have published results analysing circulating miRNAs in the whole blood of patients with breast cancer. This would be an ideal source of identifying and analysing circulating miRNAs as it could be tested after taking a simple pin prick sample from an individual. While some studies reported use of whole blood collected in standard EDTA tubes, more recently, PAXgene™ tubes have been employed for analysis of whole blood. PAXgene™ tubes contain a blend of proprietary reagents that lyse all cells, allowing immediate stabilisation of RNA. This stability is maintained for 3 days when stored at room temperature, and up to 8 years when stored at -80 °C [120]. RNA extracted from whole blood will result in greater amounts of RNA available for downstream analysis when compared to the lower, but adequate, quantity of RNA extracted from serum and plasma.

However, whole blood contains many cellular constituents, which may impact upon levels of miRNAs being detected. The presence of red blood cells can impact particular miRNAs. For example, miR-16 and miR-451 have been found to be at much higher levels on erythrocytes [121]. As a result of the many cellular elements existing in whole blood, a published study took white cell counts, haemoglobin and haematocrit levels into account in order to reduce the likelihood of sample-to-sample variability [67].

An issue when using whole blood as a source of miRNAs is storage of the sample. Samples can be collected in EDTA and PAXgene™ tubes and can then be frozen for long term storage at -80 °C. However, some studies also reported the long term storage of whole blood in EDTA tubes at 4 °C [67]. EDTA prevents coagulation of the sample but does not prevent against RNA degradation. Stabilising the RNA in the collected sample is crucial, as it is now understood that certain miRNAs have very short half-lives, some as short as an hour [122]. This highlights the necessity to standardise methods of collecting samples in order to reduce potential variability associated with particular miRNA instability.

1.2.6.2 Plasma:

As whole blood contains many factors such as erythrocytes that are capable of effecting levels of particular miRNAs, cell free sources have been employed to analyse circulating miRNAs. There have been 16 published papers that analysed this source in the breast cancer setting. As with the two other sources of circulating miRNAs, many publications did not provide a rationale as to why plasma was chosen. Plasma is obtained through a centrifugation process and contains certain clotting factors such as fibrinogen, requiring the addition of anti-coagulants such as Heparin. This addition has been shown to inhibit the downstream process of PCR analysis while citrate and EDTA have been deemed acceptable [123]. Plasma is advantageous when used for retrospective studies as it is routinely stored at -80 °C where it has been reported to remain stable and suitable for subsequent analysis. One study has shown that freeze thawing of plasma samples stored at -80 °C does not affect miRNAs present at high levels [124]. There is a risk of contaminating plasma samples with cells when aspirating the sample as this can subsequently result in detection of cellular based miRNAs as well as increasing levels of certain circulating miRNAs in the extracted RNA [123].

There are certain pre-analytic variabilities associated with plasma. The time between sample collection and processing can significantly impact sample quality so it is important to standardise this time for each sample [123]. Differences can also be seen in how samples are centrifuged. Some studies report that samples were spun at 1,300 $\times g$ for 20 min at 10 °C, and others at 600 $\times g$ for 15 min at room temperature [70, 108].

1.2.6.3 Serum:

The most studied source of circulating miRNAs is serum and this is represented by 31 published studies in breast cancer alone. Serum is also a cell free source, but unlike plasma, the sample must first undergo the coagulation process prior to centrifugation [123]. Similar to plasma, serum can be stored at -80 °C for long periods of time. A study was carried out where plasma and serum samples from the same group of individuals were compared for certain miRNAs [125]. This study found miR-15b, -16 and -24 to be detected at higher levels in plasma when compared to serum of matched individuals. This study stated that results from serum and plasma samples are not interchangeable when looking at miRNA levels.

It states the need for a rigorous protocol for centrifugation to be set in place in order to standardise this method. It was also discovered that haemolysis can lead to the detection of artificially high levels of miR-15b and miR-16 [125].

1.2.7 Impact of Haemolysis:

A very important issue to consider when using serum and plasma as a source for miRNA analysis is haemolysis. Haemolysis is the rupturing of erythrocytes and can be measured by quantifying levels of free haemoglobin in the sample. This is achieved using a spectrophotometer to analyse levels of haemoglobin, which is detected when peaks at wavelength $\lambda = 414$ are observed indicating that a sample is haemolysed [121]. Another method of detecting haemolysis is to analyse particular miRNAs that are known to be enriched in erythrocytes, such as miR-451 [121]. These steps are necessary when determining the quality of the source material as haemolysis does have an effect on the portrait of miRNAs seen in these samples.

Haemolysis is an issue that was ignored at first but as the field has developed it became far too great a problem not to be addressed. It has been shown to effect levels of certain miRNAs, such as miR-16, miR-15b and miR-24 [121]. As miR-16 has been employed as endogenous control for studies looking at circulating miRNAs in both serum and plasma, it makes the issue of haemolysis a major factor in data analysis and something that cannot be ignored [83, 109].

1.2.8 Impact of Variations in extraction methods:

There is a large variation in extraction methods across publications regarding circulating miRNAs in breast cancer, with nine different methods employed, eight of which are column-based (Table 1.4).

Method	Whole Blood	Serum	Plasma
mirVana miRNA isolation kit		X	X
mirVana PARIS kit		X	
miRNeasy mini kit	X	X	X
TRIzol™ LS method		X	X
TRIzol™ BD method	X	X	X
BioChain miRNA isolation kit		X	
MagMax viral RNA isolation kit		X	
Norgens RNA purification kit		X	X
Allprep DNA/RNA micro kit	X		

Table 1.4: Different extraction methods used in analysis of circulating miRNAs in breast cancer. (X indicating at least 1 published use of technique)

1.2.9 Impact of Endogenous Controls:

Following a similar pattern, there is also inconsistency in relation to which endogenous controls are employed for the analysis of circulating miRNAs in breast cancer, with twelve different endogenous controls used for analysis of serum miRNAs alone (Table 1.5). An endogenous control would ideally be stably expressed across all samples included for analysis whether healthy or control. Sample-to-sample variability can then be accounted for, as well as variations in template loading and varying efficiencies of reaction.

Endogenous Control	Whole Blood	Serum	Plasma
5s rRNA		X	
18S rRNA		X	
cel-miR-39		X	X
miR-16	X	X	X
GAPDH		X	
miR-1825		X	
U6 snRNA		X	
RNU6B		X	X
miR-191		X	
miR-484		X	
SNORD44		X	
miR-192		X	
U6 RNA	X		X
U6			X
miR-92			X

Table 1.5: Variation in endogenous controls used in literature of circulating miRNAs in breast cancer.

These endogenous controls range from miRNAs to ribosomal RNAs, to spiked in controls. Entire studies are carried out to establish appropriate endogenous controls for analysis of blood [126]. Many published studies determine suitability

of endogenous control across a range of samples to ensure that it is stably expressed prior to employment [100].

miR-16 is seen as an appropriate endogenous control for each source material and one that has featured in several publications [71, 73, 77, 83, 84, 109, 111, 112]. There has also been work stating that miR-16 along with other miRNAs are impacted by blood cells and haemolysis [127]. One study chose to normalise the data to the mean and median of all miRNAs measured in a sample [74]. As endogenous controls heavily influence data analysis it is crucial that there is not a large degree of variability seen in this sector of the field. Standardisation of starting material, methods of harvesting, storage and extraction will impact endogenous controls.

There are a number of issues that have a significant impact on the outcome of circulating miRNA studies. This in turn is preventing the realisation of the full potential of miRNAs as biomarkers of disease. Standardisation of approaches to analysing miRNAs in the circulation could help establishment of these molecules as clinically relevant biomarkers.

Whole blood, plasma and serum have all been shown to be appropriate for analysing circulating miRNAs, and each with varying methods of sample collection and storage. This shows that there are many ways of analysing miRNAs and that overall, no one method is necessarily superior to another. The issue is reproducibility, and that the different starting materials are not suitable for comparison. Consistency is required to support reliable comparison of data generated by different groups. Until the factors influencing miRNA presence, stability and detection in the circulation are clearly defined it is imperative that there is an attempt at standardisation.

Understanding and addressing the mitigating factors that can negatively impact upon a study, such as haemolysis, is critical in achieving standardisation across this field and resulting in more consistent and reproducible findings. If achieved, this may allow miRNAs to fulfil their potential as circulating biomarkers of many diseases.

Work in this thesis analyses certain miRNAs as biomarkers of breast cancer and the impact that starting material, collection and storage has on circulating

miRNAs. miR-138, miR-504 and miR-379 were selected based on previous work performed within this group. miR-138 was found to have elevated expression in patients with breast cancer and this was further evaluated in this thesis [128]. miR-379 was analysed previously, however, the method of collection, storage and extraction differed [129]. miR-504 was found to have dysregulated expression in breast tumour tissue (unpublished) and its potential as a circulating biomarker was determined.

1.2.10 Therapeutic potential of miRNAs:

Due to the dysregulated expression of miRNAs in a variety of pathologies, much research has been invested into evaluating the therapeutic potential of these molecules. In diseases that express abnormally high levels of a particular miRNA, investigators employ antisense oligonucleotides. These molecules can be designed to specifically target given miRNAs [130]. This was shown in a study where an antisense oligonucleotide designed to target miR-122 in an *In vivo* model resulted in an increase in the expression of the miRNAs target genes. It also resulted in degradation of miR-122 and ultimately reduced plasma cholesterol [131].

In diseases where miRNA expression is reduced, therapies can be based on restoration of native miRNA expression or enriching expression of a miRNA which has tumour suppressive capabilities. In order to deliver miRNAs, viral vectors are used as vehicles of delivery. Using an adeno-associated virus to deliver miR-26a to liver tumours, Kota et al found therapeutic benefit to the reintroduction of the miRNA [132]. This study systemically administered an adeno-associated virus (AAV) with a serotype that allowed targeting to the liver and efficient transduction of the targeted hepatocellular carcinoma cells *in vivo*. Clinically, systemic administration of AAV can evoke an immune response, potentially hindering future implementation [133]. Both strategies of either replacing or knocking out native miRNA function have shown promise in the *in vivo* setting. While direct administration of miRNAs to the sites of the tumour can be effective, such methods are not relevant in circumstances of metastatic disease. Despite promising preclinical data, targeted and safe delivery of therapeutic miRNA directly to tumour cells *in vivo* remains a challenge. In subsequent sections, the utilisation of Mesenchymal Stem Cells (MSCs) and secreted exosomes will be highlighted as a potential method of delivering exosome encapsulated miRNA as a breast cancer therapy.

1.2.11 miR-379:

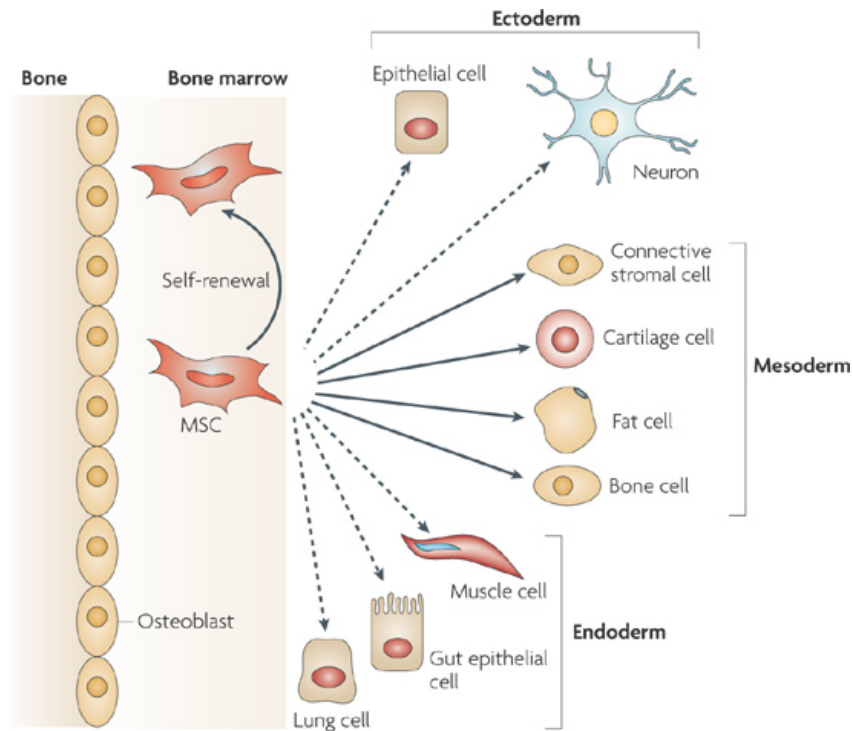
miR-379 is a miRNA which has previously been shown, by this group, to be significantly reduced in the primary tumour tissue of patients with breast cancer [129]. The miRNA was shown to inversely correlate with cell-cycle regulatory protein, Cyclin B1. Subsequent functional assays revealed direct miR-379 regulation of Cyclin B1 expression. Similarly, another study has found reduced expression of miR-379 expression in Hepatocellular carcinoma tissues [134]. This same study also revealed a relationship between miR-379 and TNM stage and metastasis. In cell lines, forcing increased expression of miR-379 reduced proliferation and migration in colorectal and hepatocellular cancer cell lines [134-136]. In mesothelioma, Interleukin (IL)-18 was shown to be targeted by miR-379 and over-expression of the miRNA resulted in an inhibition of invasion [137]. One study published contrasting results based on clinical samples available on an online database showing that elevated miR-379 expression in prostate cancer correlated with patient free survival [138]. miR-379 is located on chromosomal region 14q32.31, which is inactivated in many cancers through epigenetic mechanisms including hyper-methylation [139, 140]. This region was shown to contain tumour suppressor genes that are commonly down-regulated in multiple cancers, including glioblastoma [141].

Cyclooxygenase (COX)-2 is one of two isoenzymes of the COX enzyme system. The enzyme expression has been linked with the pathogenesis of breast cancer [142]. High expression of COX-2 in breast tumour tissue has been associated with angiogenesis, lymph node metastasis and apoptosis [143]. Increased COX-2 expression has also been shown to relate to larger tumour size, negative hormone receptor status and the presence of the Her2/neu amplification [144, 145]. One study has shown downregulation of COX-2 gene expression after enriching the expression of miR-379 in a breast cancer cell line, MDA-MB-231 [146]. Following from this finding, predictive algorithms revealed putative binding site for miR-379 on the 3'UTR of the COX-2 mRNA.

1.3 Mesenchymal Stem Cells:

MSCs are non-haematopoietic adult derived multipotent stem cells. MSCs have garnered a lot of interest in tissue regeneration as these cells have the capacity to differentiate into cells of the mesoderm, including osteoblasts, chondrocytes and adipocytes (Figure 1.2) [147]. While Figure 1.2 shows an ability of the cells to

transdifferentiate into cells of both the endoderm and ectoderm, this remains controversial. MSCs are defined by three criteria [148]. Firstly, the cells must have the ability to adhere to plastic surfaces in standard culture conditions. Secondly cells must have specific surface antigen expression which consists of expression of CD105, CD73 and CD90 in over 95% of the cell population while lacking expression of CD45, CD34, CD14, CD19 and HLA-DR. Finally, cells must have the ability to differentiate into osteoblasts, adipocytes and chondroblasts [148].



Nature Reviews | Immunology

Figure 1. 2: Overview of MSC differentiation capabilities[149]

MSCs have shown an ability to migrate to areas of tissue damage or injury when injected systemically in animal models [150]. As the tumour can be thought of as a wound that never heals, MSCs have also been shown to migrate to the sites of multiple tumours [151, 152]. Due to expression of particular surface adhesion molecules MSCs are capable of permeating and escaping from blood vessels [149]. Furthermore, through a P-selectin and vascular cell-adhesion molecule 1 (VCAM-1) dependent manner, MSCs exhibit rolling and adhesion on endothelial cells [149]. Although it is not fully understood how exactly MSCs target tumour cells, it is believed to be in part chemokine mediated. Studies have confirmed that when injected systemically, MSCs are capable of migrating and engrafting into the site

of the tumour [153]. In a xenograft animal model of breast cancer, MSC homing to the sites of lymph node metastasis was shown to be in part mediated by monocyte chemoattractant protein-1 (MCP-1) [154]. This makes MSCs promising tumour targeted delivery vehicles as they possess the ability to locate and engraft into tumours. Further adding to the promise of these cells as a therapeutic delivery vehicle is the ability of these cells to evade host immune response. This is thought to be mediated through multiple interactions with aspects of both the innate and adaptive immune response. This includes regulation of neutrophils, T-cells, B-cells, Dendritic cells and natural killer cells [149]. MSCs produce growth factors that promote tumour angiogenesis such as vascular endothelial growth factor (VEGF), fibroblast growth factor (FGF) and platelet-derived growth factor (PDGF). There are concerns that MSCs may promote tumour growth rather than hinder it when administered therapeutically [150]. Co-administration of MSCs and tumour cells have yielded conflicting results with one study reporting inhibition of primary tumour growth and formation of metastases [155]. This study administered the MSCs with Lewis lung carcinoma cells at a ratio of 2:1. Contrastingly, studies mixing MSCs with ovarian and breast cancer cells at ratios of 1:1 and 3:1 have resulted in larger and more aggressive tumours [156, 157]. Other studies have co-mixed MSCs with colon cancer and breast cancer cells at a ratio as high as 10:1 resulting in faster growing and more aggressive tumours [158, 159]. However, in studies that administered MSCs in animal models with established tumours, no promotion of tumour growth was witnessed [160-166]. Evidence in the literature suggests that MSCs may be potent tumour targeted delivery vehicles [167]. As it is possible to genetically engineer MSCs there also lies further potential to exploit the cells native characteristics for therapeutic delivery in the breast cancer setting. Among the abundance of secretory factors released by MSCs, are exosomes [168]. Following migration of the MSCs to the site of the tumour, exosomes may be engineered to ensure delivery of therapeutic agents to the cancer cells.

1.4 Exosomes:

In 1981, extracellular vesicles were first observed in neoplastic cell lines where particles that were shed contained membrane-bound enzymes [169]. This same study coined the term exosome in relation to 'exfoliated membrane vesicles with 5'-nucleotidase activity'. It was observed that these vesicles could be taken up by

recipient cells and the authors predicted that this method could be a means of transferring information between cells [169]. The definition of an exosome has varied and been disputed throughout the years and now certain criteria have been established to define an exosome. This definition currently stands as vesicles ranging from 40-120nm in size, with the presence of tetraspanin proteins (CD63, CD9 and CD81), originating from the endosome and they are released through multivesicular endosome fusion with the plasma membrane [170]. Exosomes have been shown to be secreted by all cell types in cell culture as well as being naturally present in bodily fluids such as blood, saliva, urine and breast milk [171]. Exosomes have also been shown to reflect the characteristics of the cell of origin [172]. For this reason, exosomes could be perceived as a fingerprint for that cell. Such realisations resulted in interest in these vesicles as both diagnostics and therapeutics [173].

1.4.1 Biogenesis:

As research into the vesicles progressed, much has been understood regarding exosome biogenesis (Figure 1.3) [174]. The early endosome is the first endocytic compartment that takes cargo that has been internalised from the plasma membrane [175]. This matures into the late endosomal compartment where cytoplasmic cargo is gathered through inward budding of intraluminal vesicles (ILVs). In this process, certain ILVs will direct particular cargo for lysosomal degradation while different cytoplasmic components will be directed for exosome encapsulated cellular release [176]. The formation of exosomes is ceramide dependent while relatively independent of the Endosomal Sorting Complex Required for Transport (ESCRT). As exosomes undergo two membrane inversions during formation the vesicles retain similar topology as the plasma membrane. The surface of exosomes express tetraspanins (CD63, CD81, CD9), heat shock proteins (Hsc70), lysosomal proteins (Lamp2b) and fusion proteins (CD9, flotillin, Annexin) [177]. While not fully understood, packaging of content into exosomes depends on interactions with certain lipids, proteins and the tetraspanin web [176].

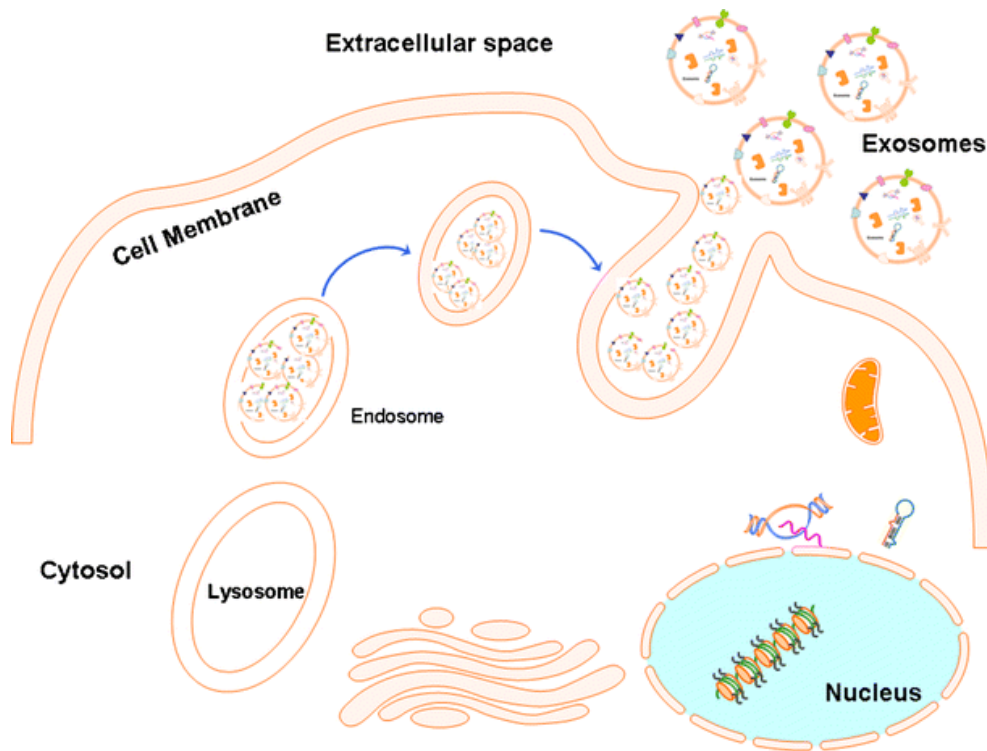


Figure 1. 3: Exosome biogenesis[174].

1.4.2 Exosome Isolation and Characterisation:

Different methods of isolating exosomes exist in the literature to date. As mentioned, exosomes can be sourced from a variety of bodily fluids, resulting in many different isolation methods. Ideally isolation methods would result in exosomes and not apoptotic bodies or microvesicles. However, current isolation methods yield heterogenous populations of vesicles. These can be partly differentiated based on size, however there is an overlap as microvesicles are 50-1000nm and apoptotic bodies are 50-5000nm. Microvesicles are also derived directly from the plasma membrane while apoptotic bodies are formed through fragmentation of the cell. While microvesicles lack any characteristic markers, apoptotic bodies are positive for Annexin-V [170]. The current gold standard method for isolating exosomes from culture medium is through differential centrifugation and subsequent ultracentrifugation [178]. Firstly, intact cells and large cellular debris are removed by differential centrifugation. This is followed by microfiltration through either a 0.1 μm or 0.22 μm filters to remove microvesicles in the size range of 500-2000 nm in diameter [179, 180]. Variations of this method include the use of a sucrose gradient for centrifugation which allows for the

removal of protein aggregates from isolated exosomes [178]. Using commercially available kits it is also possible to isolate exosomes without the need for ultracentrifugation. These methods are costly and are generally reserved for small sample sizes. This method is based on immuno-magnetic isolation where a specific exosomal surface protein is targeted allowing specific isolation of exosomes [181]. Other possible methods of isolating exosomes include high-pressure liquid chromatography-gel exclusion chromatography (HPLC-GEC), solvent precipitation, ultrafiltration, immunoaffinity capture and field flow fractionation [182]. There are challenges associated with isolating the vesicles. Current methods of exosome isolation can result in contamination with non-exosomal proteins and other types of vesicles resulting in inaccurate conclusions relating to exosomal activity [183]. Targeting to surface proteins while improving yields can bias results as a population of exosomes may not ubiquitously express the given protein [184]. While the commercially available kits ExoQuick™ and Total Exosome Isolation™ are easier to use, the isolates have been shown to contain a greater degree of contaminating proteins and reduced enrichment of exosomal marker proteins [185]. As the contents of these kits are not disclosed the chemicals within them may have an impact on the biology of the isolated exosomes [184].

Upon isolation of exosomes it is necessary to characterise the vesicles to ensure successful isolation of exosomes. For now, exosomes are characterised based on size, morphology and the expression of particular surface proteins. Size and morphology are assessed by transmission electron microscopy (TEM). Nanoparticle tracking analysis coupled with high resolution flow cytometry allows visualisation of exosomes and provides a size distribution based on Brownian motion of the isolated vesicles [186]. Protein analysis, such as Western Blot is performed to confirm the presence of surface proteins, CD9, CD63 and CD81, which ensures successful isolation of exosomes [180]. Due to such variations in approaches in the literature, recently a crowdsourcing knowledgebase (<http://evtrack.org>) has been established to increase transparency and to facilitate replicability of experiments [187]. Such an initiative should serve to improve and accelerate advancements in exosomal research.

1.4.3 Exosome Contents:

As exosomal research developed it was realised that these vesicles are capable of exerting a functional impact on recipient cells. On further analysis of the exosomal contents, specific mRNAs and miRNAs were detected [188]. This discovery realised the possibility of transferring specific genetic contents directly to recipient cells and the field grew exponentially [189]. It is now understood that exosomes are formed in the endosome where they package protein, DNA and RNA. A subset of cellular proteins have been shown to preferentially package into exosomes suggesting a non-random loading of the vesicles [180]. Furthermore, the protein content of exosomes originating from patients with cancer have been shown to differ from the content isolated from healthy individuals [190]. Analysis of 384 miRNAs showed that the exosomal miRNA content strongly reflected that of the parent cell [191]. This illustrates the selectivity of exosomal packaging and how they appear to reflect the cell of origin. Although directing exosomal packaging is not fully understood, the content of glioblastoma derived exosomes found an enrichment for tumour promoting mRNA, miRNA and proteins [192]. The lipid composition of exosomes differs from that of the whole cell membrane. Exosomes are enriched in cholesterol, sphingomyelin, ceramide and phosphatidylserine while interestingly not in lysobisphosphatidic acid, which is a lipid known to be present in multivesicular body intraluminal vesicles [193] This suggests that exosomes may also be selective in lipid composition. For now, a database, ExoCarta, has been established to bank information collected on exosomal content and it currently stands at 41,860 proteins entries, 4,946 mRNA entries, 2,838 miRNA and 1,116 lipid entries which have been collected from 286 studies [194]. While only recently established, EV-TRACK will serve as an online database for individuals to upload specific details relating to the exosomal experiments performed[187]. This will provide a bank of information for researchers to better understand current issues, such as quantification, characterisation and analysis of exosomes.

1.4.4 Biomarker Potential:

As exosomes are believed to contain genetic material that reflects the cell of origin, they show promise in diagnostics. Furthermore, these vesicles provide comparable sensitivity and specificity when compared to conventional biomarkers obtained from serum, due to the stability of the exosomes in the circulation [195].

In the cancer setting, studies have shown that tumour cells release exosomes containing tumour-specific RNA that could be exploited to aid in the diagnosis of lung adenocarcinoma [196]. As exosomes are readily sourced from many body fluids, including saliva, they may serve as an ideal non-invasive biomarker of disease [197]. While not yet implemented clinically, exosomes possess great potential as circulating biomarkers of disease.

1.4.5 Uptake by Recipient Cells:

Exosomes can transfer to recipient cells in a juxtacrine, paracrine or endocrine manner. Exosome uptake can take place via phago-lysosome intermediates, receptors specific to exosomal surface proteins or via the T-cell immunoglobulin mucin protein 4 (Tim-4) receptor [198]. Following uptake, the exosomal protein, mRNA, miRNA, DNA and lipids are either localised within the late endosome or released by the phagolysosome [198]. These genetic components can subsequently exert a phenotypic effect on the recipient cells. Furthermore, the targeting of exosomes to recipient cells while not fully elucidated is thought to be directed, potentially through specific cell surface receptors, like integrins [199, 200]. Another study showed that injection of pancreatic cancer derived exosomes retro-orbitally in a mouse model prior to tumour cell injection increased liver metastases [201]. This data suggests that pancreatic ductal adenocarcinoma derived exosomes target F4/80+ Kupffer cells, in the liver. The exosomes subsequently function in establishing an environment suitable for the migration and engraftment of pancreatic tumour cells [201]. The results of this study show that exosomes can target specific cells, exert phenotypic effects on targeted cells and reflect their parent cell.

1.4.6 Therapeutic Potential:

Depending on the cell of origin, exosomes are capable of exerting a therapeutic effect onto recipient cells. Exosomes derived from mast cells that were exposed to oxidative stress transfer a protective message to recipient cells undergoing oxidative stress and ultimately reduces cell death [202]. Another study harvested exosomes secreted from cardiosphere-derived cells (CDCs) and showed that these exosomes can inhibit apoptosis and promote proliferation of cardiomyocytes as well as increasing angiogenesis. In an animal model of acute myocardial infarction (MI), exosomes derived from CDCs that were injected into the MI zone resulted in reduced scar mass, greater viable mass and increased infarcted wall thickness

when compared to controls [203]. While this effect was thought to be mediated by natively packaged exosome encapsulated miR-146a, it was proven, as expected, not to be the sole exosome encapsulated contributor to the therapeutic effect. As exosomes exhibit native therapeutic effects in particular disease settings, there remains promise for engineering the content of exosomes. This study highlights the possibility of engineering exosomes to elicit therapeutic impacts on targeted recipient cells.

1.4.7 Engineering Exosomes:

Exosomal content can be engineered to achieve effective delivery of therapeutic protein, RNA or even drugs. Different methods of engineering exosomes are present in the literature. Some studies have availed of direct engineering of the exosomes and other have engineered the exosomal content indirectly via engineering of the parent cell.

1.4.7.1 Direct Engineering:

RNA can be incorporated into exosomes by electroporation of the vesicles. Pioneering work demonstrated enrichment of short interfering (si)RNA into exosomes derived from dendritic cells [204]. This resulted in knockdown of the target GAPDH mRNA in regions of the brain in a murine model when modified exosomes were systemically administered [204]. While effective, electroporation may not be suitable for all forms of RNA as it has been unsuccessful for the enrichment of miRNA into exosomes [205]. While the majority of research engineering exosomal content is RNA based, it is also possible to employ exosomes as drug delivery vehicles. Chemotherapeutic agents, such as Doxorubicin have been enriched in immature mouse dendritic cell derived exosomes by electroporation [206]. Not only did this method deliver a therapeutic impact it also reduced adverse effects to non-targeted organs. Another study, using a zebrafish brain cancer model, delivered exosome-encapsulated Doxorubicin [207]. This showed exosomes crossing the blood brain barrier following systemic administration while also resulting in reduced tumour size. siRNA has also been packaged into exosomes by using transfection reagents such as lipofectamine [208]. Another group enriched expression of miR-150 in exosomes through a 1 hour incubation period at 37 °C [209].

1.4.7.2 Indirect Engineering:

For delivery of therapeutic proteins, the gene encoding the desired protein can be fused to another gene that is known to be packaged within the exosome. This was achieved by one group through the fusion of the N-terminus of the chicken egg ovalbumin (OVA) peptide to the C1C2 domain of lactadherin, a known exosomal protein [210]. Transfection of the origin fibrosarcoma cells resulted in enriched expression of the OVA protein in secreted exosomes. Exosomal RNA, similarly, can be enriched through forced elevated expression of the targeted RNA in the parent cell of the secreted exosomes. This has proven successful for miRNAs and mRNA [205, 211]. Both mentioned methods of exosomal enrichment result in functional impacts. Transfection of miR-134 in parent Hs578Ts(i)₈ cells resulted in increased expression of the miRNA in secreted exosomes [191]. Transfer of the enriched exosomes onto Hs578Ts(i)₈ cells *In vitro* resulted in reduced migration and invasion of the cells while targets of miR-134, STAT5B and Hsp90, were also down-regulated. Another group focused on glioblastoma multiforme. miR-9 is up-regulated in glioma and has been shown to suppress mesenchymal differentiation of glioblastoma multiforme cells [212]. As miR-9 indirectly affects the increase of P-glycoprotein expression, which is involved in chemoresistance, this study aimed to target the miRNA. MSC-derived exosomes were engineered with anti-miR-9 by transfection of the parent cell. When taken up by recipient glioblastoma multiforme cells *In vitro*, there was a reversal in expression of the multidrug transporter resulting in sensitization of the cells to temozolomide [212]. *In vivo*, another group engineered MSC-derived exosomes through transfection of the parent cell to have enriched expression of miR-146 and subsequently injected the exosomes intra-tumourally into an orthotopic rat model. Following one injection of the engineered MSC-derived exosomes, there was a significant reduction in growth of the glioma [213].

1.4.7.3 Engineering Surface Expression of Exosomes:

Targeting exosomes to specific recipient cells can be achieved through engineering of the surface of the vesicles. This was exploited in the delivery of doxorubicin to breast cancer cells *In vivo* through fusion of the iRGD peptide to the exosome protein Lamp2b which targeted the αv integrin expressing cancer cells [206]. Another study engineered exosomes derived from human embryonic kidney (HEK293) cells to specifically target epidermal growth factor receptor (EGFR) expressing breast cancer cells *In vivo* [205]. These exosomes were enriched

for expression of let-7a as well as having the membrane engineered for expression of the GE-11 peptide, a peptide specific to the EGFR. Engineering of the surface was achieved through cloning of the GE-11 peptide sequence onto the transmembrane domain of platelet-derived growth factor receptor. This allowed targeted delivery of a therapeutic miRNA which resulted in a significant reduction in tumour growth [205]. Another published study utilised HEK293T cells and engineered the cells to express exosomal protein, Lamp2b fused to a fragment of Interleukin 3 (IL3) ligand. [214]. The IL3 receptor is overexpressed in the cells of the target disease, Chronic Myeloid Leukaemia blasts. The exosomes were loaded with the drug Imatinib and administered twice a week for 3 weeks intraperitoneally at a dose of 100 µg. There was a significant reduction in tumour volume when analysed 24 days after treatment.

1.4.7.4 MSCs and Exosomes:

As exosomes tend to reflect the native characteristics of the parent cell, it is essential that an appropriate cell is utilised for the propagation of exosomes [215]. Conditioned media from MSCs was found to significantly reduce the infarct size in both mouse and pig animal models of myocardial infarction when administered before reperfusion [216]. The active component of this therapeutic effect was subsequently shown to be MSC secreted exosomes [217]. MSCs have been heralded as the only cell to potentially match the burden of mass production of exosomes suitable for possible future clinical implementation [218]. Native characteristics of MSC-derived exosomes show therapeutic promise leading to the engineering and exploitation of these cell derived exosomes in the cancer setting [217].

1.4.7.5 Current Landscape of Exosomal Research:

Currently, enrichment of exosomal miRNA content is predominantly achieved through forced elevated expression in the parent cell. Targeting exosomes to recipient cells has been shown in studies engineering the surface of exosomes [206, 219]. Studies administering exosomes into an *In Vivo* model have quantified exosomes based on protein estimation but it is now thought that it does not correlate with the actual number of exosomes [201, 204, 206, 219]. NTA would appear a more suitable method of quantifying exosomes as it allows identification of each individual vesicle. All *In vivo* studies to date have been performed over a short time period not allowing time to determine any resurgence of the disease

[204-206]. Further studies analysing exosomes in tumour bearing immune competent mice will aid in the understanding of exosomes as therapeutic delivery vehicles. One study analysed systemic exosome delivery in immune competent mice and did not see any negative immune related impact from exosome administration [204]. This research is evolving with new methods of exploiting exosomes consistently being developed. The promise these vesicles have shown for therapeutic impact is remarkable and further research will aim to progress current developments into a clinical setting. Exosomes offer promise for systemic delivery of therapeutic miRNAs. As the vesicles reflect the characteristics of their parent cell, MSC-secreted exosomes packaging a therapeutic miRNA could serve as a novel treatment strategy for advanced breast cancer.

1.5: Thesis Aims

The overarching aims of this study were to first investigate the factors impacting the potential of circulating miRNAs as biomarkers for breast cancer and secondly to determine potential for miR-379 as a novel therapy for breast cancer.

The work presented addresses two core hypotheses with associated aims.

The potential for circulating miRNAs as biomarkers for breast cancer is impacted by the method of collection, storage, extraction and endogenous control used.

- To evaluate miR-138 and miR-504 as circulating biomarkers of breast cancer in EDTA collected whole blood samples.
- To determine the impact that collection, storage, extraction method and starting material have on the miRNA profile.
- To analyse miR-138, miR-504 and miR-379 in PAXgene™ stabilised whole blood samples.

miR-379 is a tumour suppressor. The tumour homing capacity of MSCs can be exploited for exosome mediated and tumour targeted delivery of the miRNA while MSC secreted exosomes may mimic the tumour homing potential of the donor cells.

- To evaluate miR-379 as a tumour suppressor in an *In vivo* model of breast cancer.
- To elucidate a mechanism of action for miR-379 in breast cancer.
- To engineer MSC secreted exosomes for enriched expression of miR-379.
- To assess the therapeutic impact of systemically administered MSCs, or MSC-derived exosomes enriched with miR-379 on tumour progression *In vivo*

Chapter 2

Materials and Methods

2.1 Ethics and Consent

When acquiring samples from patients or healthy individuals written, informed consent was obtained (Appendix 8.3). This study was approved by the ethics review board of Galway University Hospital (GUH).

2.2 Sample Preparation:

Depending on the source material, preparation varied. To analyse the RNA content of cells grown *In vitro*, the cells were centrifuged at 2,000 x g for 5 min following trypsinisation. The media was removed and the pelleted cells were stored at -80 °C until required for extraction. For RNA extraction from exosomes and conditioned media samples were stored at -80°C following isolation.

For analysis of tissue RNA, samples from the animals were placed directly into RNeasy® solution (Ambion, USA), immediately upon harvest. This prevents degradation of the RNA by RNases. The tissue remained in the RNeasy® solution for a maximum of one week at RT before removing the solution and the tissue was then stored at -80 °C until required for further use.

Whole blood samples were either collected in EDTA tubes and stored at 4 °C until required, or were stored in PAXgene™ tubes and allowed to incubate at RT for 2 hours before long term storage in the PAXgene™ tubes at -80 °C. To obtain serum, whole blood was collected in serum separating tubes, allowed to stand for 30 min for the sample to coagulate and subsequently centrifuged at 3,000 x g for 5 min. Top layer serum was removed placed in a tube and put in long term storage at -80 °C. For collection of plasma, whole blood was placed directly into an EDTA tube to prevent coagulation of the sample, prior to centrifugation at 3,000 x g for 5 min. Top layer plasma was removed and placed in long term storage at -80 °C.

2.1 Gene and MiRNA Expression Analysis:

2.1.1 RNase Contamination:

For all analysis relating to RNA it was essential to maintain the integrity and purity of the sample so as to ensure high quality results. To achieve this, many steps were taken to prevent degradation of the RNA by RNases, including:

- Each phase of the RNA extraction was carried out within a Class II Safety Cabinet (ECSCO®) and appropriate personal protective equipment (PPE) was worn at all times, which consisted of a lab coat and gloves.

- Prior to carrying out the procedure, the hood and each item entering it were cleaned with 70% IMS.
- Gilson pipettes and barrier pipette tips which were reserved for RNA extraction use only, were used for all reagents.
- All sample material remained on ice unless otherwise stated in the protocol.

2.1.2 RNA Extraction:

2.1.2.1 RNA Extraction from Cell Pellets:

The method of extraction varied depending on the sample material used. For extraction of RNA from cell pellets derived from *In vitro* culture the RNeasy[®] Minikit (Qiagen) was employed and the method was performed according to manufacturer's instruction. Cell pellets were removed from storage at -80 °C and thawed on ice. Once thawed, 1 ml of TRIzol™ was added to the 15 ml Falcon tube that the pellet was stored in. Using a pipette the sample was mixed through repeated pipetting of the solution to lyse the cells within the cell pellet. 200 µl of chloroform was subsequently added to the solution before being vortexed for 15 sec. Following this, the mixture was let stand at RT for 5-10 min. The mixture was then centrifuged at 12,000 x g for 15 min at 4 °C. This resulted in a phase separation of the sample with the RNA migrating to the upper aqueous phase while larger cell debris remained in the lower fraction. Carefully, the clear aqueous phase was removed ensuring not to disturb the remaining layers of the sample. Once the entire clear fraction was removed it was transferred to a 15 ml falcon tube where 3.5 times the volume of 100% ethanol was added to the sample and mixed by pipetting gently. 700 µl of the mixture was carefully pipetted onto the RNeasy[®] column ensuring not to touch the filter paper. The column was centrifuged at 14,000 x g for 21 sec at 4 °C which allowed the RNA bind to the column and isolated it from the sample. After centrifugation, the flow through was discarded and the step was repeated with the remaining sample. The column was then washed by centrifugation with RW1 buffer at the same speed and time as the previous step. To remove any DNA from the sample, ensuring the highest quality yield of pure RNA, a DNase digestion step was carried out which consisted of the addition of 80 µl of a DNase mixture which was prepared by the addition of reagents from the RNase free DNase set (Qiagen). This was let stand for 15 min at

RT. Further wash steps using the RW1 buffer were performed prior to two further wash steps using 500 μ l of the RPE buffer, with the second addition of the RPE buffer being centrifuged for 2 min allowing the membrane to dry. Finally, the RNA was eluted by adding 55 μ l of cold nuclease-free water (NFW) directly to the membrane. This was then centrifuged at 14,000 x g for 1 min at 4 °C. The RNA was then transferred to designated, autoclaved tapered tubes. 1.1 μ l of the sample was taken for quantification using the NanoDrop 1000 spectrophotometer (NanoDrop Technologies) (Section 2.1.5). The remaining sample was stored at -80 °C until required for further use.

2.1.2.2 RNA Extraction from Whole Blood:

In this study, RNA was extracted from whole blood by two methods. Firstly, whole blood collected in EDTA tubes and stored at 4 °C was extracted using a modified version of the TRI Reagent BD co-purification technique (Molecular Research Centre, Inc.) [67]. Secondly, another cohort of whole blood samples collected in PAXgene™ tubes were extracted using the recommended PreAnalytix (GmbH) column based method of extraction. For whole blood collected in EDTA tubes, RNA was extracted as follows: 3 ml of Trizol™ and 200 μ l of 1-bromo-4-methoxybenzene (BAN) were added to 1 ml of whole blood and thoroughly mixed until the sample was homogenous. Samples were let stand for 5 min at RT before centrifugation at 18,000 x g for 15 min at 4 °C resulting in a phase separation. 1 ml of the upper aqueous layer of the sample containing the RNA was removed and added to 1 ml of isopropanol and let stand for 5 min at RT. The mixture was centrifuged at 18,000 x g for 5 min at 18 °C which resulted in the formation of a pellet of RNA. The supernatant was carefully removed, disposed of, and 1 ml of 75% ethanol was added to the pellet and vortexed. The pellet was again centrifuged at 18,000 x g for 5 min at 18 °C before the ethanol was removed, replaced with 75% ethanol once more and the centrifugation step was repeated. Following this, the ethanol was removed and the pellet was let stand for 5 min at RT to air dry. Once dry, 30 μ l of NFW was added and the sample was vortexed to resuspend the RNA. This was let stand for 5 min, placed in tapered tube and analysed on the Nanodrop Spectrophotometer as described in Section 2.1.5.

For PAXgene™ collected whole blood the RNA was extracted as follows: the frozen blood sample was thawed at RT for 1 hour. Once thawed, the whole blood was centrifuged at 4,500 x g for 10 min forming a pellet from which the supernatant

was subsequently removed. 4 ml of RNase-free water was added and the sample was vortexed, resuspending the pellet before centrifugation at 4,500 x g for 10 min. The supernatant was removed from the pellet and resuspended in 350 µl of buffer BM1 by vortexing. The mixture was then transferred to a 1.5 ml microcentrifuge tube and 300 µl of buffer BM2 along with 40 µl proteinase K were added to the mixture and vortexed for 5 sec. Mixed samples were then incubated for 10 min at 55 °C and 900 RPM on a shaker-incubator (Grant-Bio PHMT). Following incubation, the sample was added to a PAXgene™ Shredder spin column and centrifuged at 20,000 x g for 3 min. The supernatant was subsequently removed from the pellet and mixed with 700 µl of isopropanol, vortexed, added to a PAXgene™ RNA spin column and centrifuged at 20,000 x g for 1 min. This was repeated until the entire sample passed through the PAXgene™ RNA spin column. 350 µl of buffer BM3 was added to the column to purify the RNA and centrifuged at 20,000 x g for 15 sec. 10 µl of DNase 1 stock solution was added to 70 µl buffer RDD and the 80 µl mixture was added to the column and allowed incubate for 15 min at RT. Buffer BM3 was added once more and centrifuged prior to the addition of 500 µl of buffer BM4 and centrifugation at 20,000 x g for 2 min. This was repeated before centrifugation at 20,000 x g for 1 min to dry the column. 40 µl of BM5 was added to the column and centrifuged at 20,000 x g for 1 min and this step was repeated. 80 µl of the buffer BM5 containing the RNA was added to a tapered tube prior to quantification on the Nanodrop spectrophotometer.

2.1.2.3 RNA Extraction from Serum and Plasma:

RNA was extracted from serum and plasma using the miRCURY™ kit (Exiqon). As both serum and plasma were stored at -80°C the samples were initially thawed on ice. Once thawed, the samples were centrifuged at 3,000 x g for 5 min before 200 µl of the total volume of the sample was placed in a microcentrifuge tube for extraction. 60 µl of Lysis solution Biofluid (BF) was added and the mixture was vortexed for 5 sec and left to incubate for 5 min at RT. Following incubation, 20 µl of protein precipitation solution BF was added to the solution and vortexed for 5 sec before incubation for 1 min and centrifugation at 11,000 x g for 3 min. The resulting supernatant was removed from the formed pellet and mixed with 270 µl isopropanol and again vortexed for 5 sec. The mixture was added to a miRNA Mini Spin Column BF, incubated for 2 min and centrifuged at 11,000 x g for 30 sec. This was repeated until all the sample passed through the column. 100 µl wash

solution 1 BF was added to the column and centrifuged at 11,000 x g for 30 sec. 700 µl of wash solution 2 BF was added and then centrifuged for 30 sec before another 250 µl of wash solution 2 BF was added and centrifuged for 2 min. Finally, 50 µl of RNase free water was placed onto the column and incubated for 1 min at RT before centrifugation at 11,000 x g for 1 min. Isolated RNA was subsequently placed in a tapered tube and stored at -80 °C following quantification on the Nanodrop Spectrophotometer.

2.1.2.4 RNA Extraction from Tissue:

For extraction of RNA from tissue samples a semi-automated system was used, MagNA pure compact (Roche). This system uses a magnetic-bead based technology for the isolation of RNA as outlined in Figure 2.1. the tissue was removed from storage at -80°C, thawed and roughly minced using a scalpel on a petri dish within a fume hood. This was subsequently placed directly into MagNA Lyser Green Beads tube with 450 µl of lysis buffer. The tubes were then placed into the MagNA Lyser (Roche) and set to 6,500 RPM for 50 sec, removed and allowed to cool on ice before returning for another cycle of 50 sec. This caused homogenisation of the tissue sample by rapid shaking of the beads within the tubes. Samples were then placed on ice for 30 min before centrifugation at 13,000 x g for 2 min. 350 µl was pipetted from the mixture ensuring not to disrupt the pellets. This sample was placed into the MagNA pure compact (Roche). RNA was extracted following the RNA extraction protocol on the MagNA pure compact (Figure 2.1).

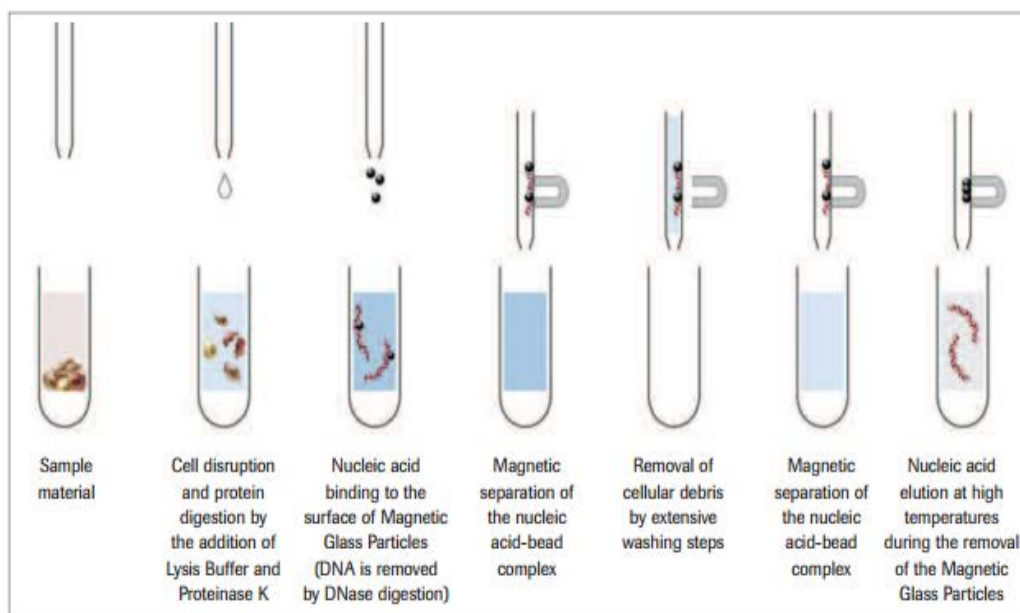


Figure 2. 1: Automated protocol for extraction of RNA on MagNA pure compact [220].

Eluted samples were removed, quantified, and stored at -80 °C until required.

2.1.2.5 RNA Extraction from Exosomes and Conditioned Media:

For extraction of RNA from exosomes, samples were removed from -80°C storage and allowed thaw on ice. The *mirVana*[™] miRNA Isolation Kit was employed for extraction of miRNA. 400 µl TRIzol[™] added to the solution and was vortexed before standing at RT for 5 min. 140 µl chloroform was added, vortexed and left stand for 10 min at RT. The sample was then centrifuged at 12,000 x g for 15 min at 4°C. Following centrifugation, the upper aqueous phase was removed and a third the volume of 100% ethanol was added. 700 µl of the mixture was added to a filter placed in a fresh tube and centrifuged at 12,000 x g for 15 sec at 4°C. Flow through was collected and steps were repeated until all the solution passed through the column. Two-thirds of the total volume 100% ethanol was then added and the previous step was repeated with a fresh filter. This time the flow through was discarded. Once the entire sample passed through the filter, 700 µl wash solution 1 was added to the filter and centrifuged at 12,000 x g for 10 sec at 4°C. Flow through was removed and 500 µl of wash solution 2/3 was added to the filter and centrifuged for 10 sec. This was repeated with the flow through disposed of each time. Centrifugation was performed at 12,000 x g for 1 min with the filter alone to allow it to dry. 50 µl of pre-heated elution solution was added to the filter after it was placed in a fresh tapered tube. This was centrifuged at 12,000 x g for 1 min. This step was repeated with a further 10 µl of elution

solution. The flow through was collected and stored at -80 °C until further required.

For RNA extraction from conditioned media, the *mirVana*[™] miRNA Isolation Kit was also used. 700 µl of TRIzol[™] was added to 1 ml of thawed conditioned media. The mixture was vortexed and incubated at room temperature for 5 min. 140 µl of chloroform was added and the sample was vortexed and left stand at room temperature for 5 min again. The mixed sample was centrifuged at 12,000 x g for 15 min at 4°C. All steps from this step on are the same as those performed for miRNA extraction from the exosomes.

2.1.5 Determining RNA Quality and Quantity:

Following each extraction method, the quality and quantity of large RNA as well as miRNA in each sample was assessed using the Nanodrop ND-1000[®]

Spectrophotometer (NanoDrop Technologies). To analyse total RNA the extinction coefficient was set as 40, while for miRNA the extinction coefficient was set to 33.

Before assessing each sample, 1.1 µl of the eluent was initially placed on the pedestal of the spectrophotometer to wash the instrument. After this, the extinction coefficient was adjusted for the analyte and another 1.1 µl was added to serve as a blank for the extracted samples. The sample was held on the pedestal with the sample arm and measurements were done with a path length of 0.1 cm. The concentration of RNA was determined automatically using the equation:

$$\text{RNA concentration (ng/}\mu\text{l)} = (A_{260} \times e) / b$$

A_{260} = Absorbance at 260 nm, e = extinction coefficient (ng-cm/mL), b = path length (cm).

To determine the purity of RNA in the sample an absorbance ratio was calculated based on 260 and 280 nm (A_{260}/A_{280}) measurements. A ratio between 1.8 and 2.2 would be indicative of a high quality sample (Figure 2.2). The ratio can be offset due to the presence of contaminants that absorb at 280nm such as proteins or phenols. The A_{260}/A_{230} ratio should also lie within the range of 1.8 and 2.2 and this can be disrupted by the presence of substances such as EDTA and TRIzol[™] which are often used in extraction methods.

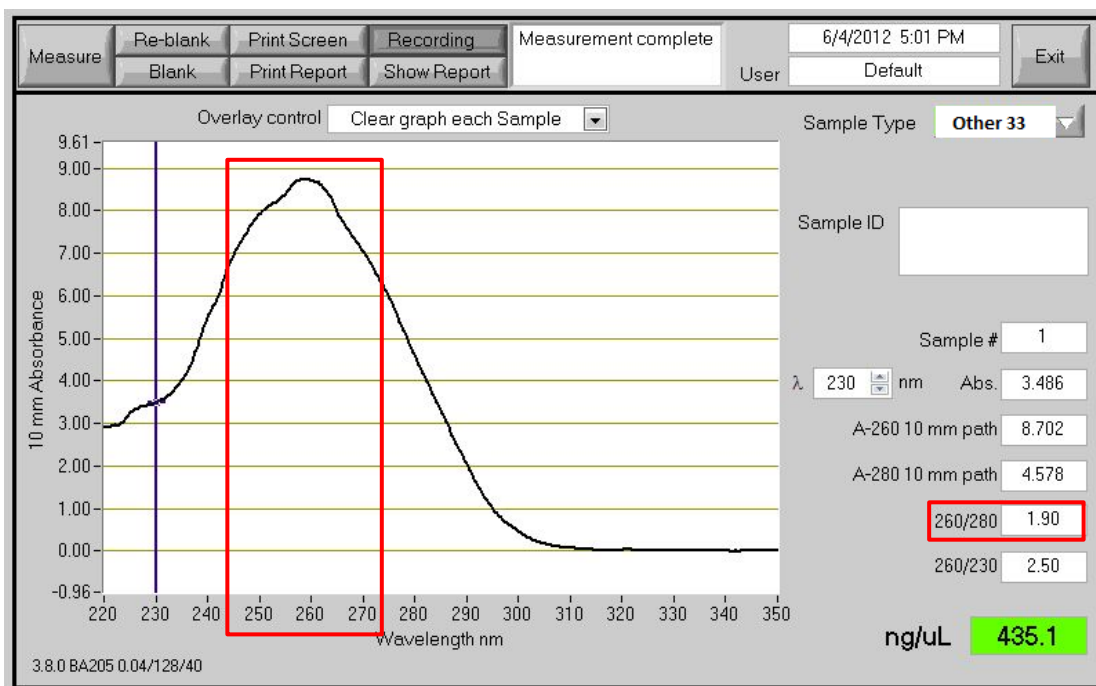


Figure 2. 2: Example of Nanodrop result with peak at 260 nm and optimum absorbance ratio highlighted

2.1.6 Reverse Transcription for Gene Expression Analysis:

All work was carried out while wearing appropriate PPE such as gloves and lab coat and handling of all materials was done within a BioSafety cabinet that was sprayed with 70 % IMS and treated with a U.V. light for 15 min prior to use. For quantification of mRNA it was first necessary to reverse transcribe the mRNA transcripts to complimentary DNA (cDNA). To achieve this, M-MLV reverse transcriptase enzyme was coupled with random primers to form the double stranded cDNA. A standard amount of 1 μg RNA was loaded for each reaction and reverse transcribed using the SuperScript™ III Reverse Transcriptase enzyme (200U/ μl , Invitrogen, Carlsbad, USA). Initially a mixture of RNA (1 μg), dNTP mix (10mM), and a master mix (3 $\mu\text{g}/\mu\text{l}$) were added together. For every batch of samples reverse transcribed a control sample (RT-blank) lacking any RNA was added as a negative control. All the samples were then placed in a GeneAmp® thermal cycler (9700, Applied Biosystems, USA) in order to denature the RNA with an initial incubation step at 65 °C for 5 min. Following the denaturation step a second mastermix was added which consisted of SuperScript III reverse transcriptase (200U/ μl), 5X reverse transcriptase buffer, dithiothreitol (DTT) (0.1M) and RNaseOut (40U/ μl). Samples were returned to the GeneAmp® thermal cycler for a further incubation at 25 °C for 5 min, 50 °C for 60 min and 70 °C for 15

min which denatured double-stranded duplexes that were present in the samples. Once completed, 30 μ l of NFW was added to each sample and was stored at -20 °C until required.

2.1.7 Reverse Transcription for miRNA Analysis:

Similarly, miRNA (5-100 ng), depending on amount of starting material, were reverse transcribed to cDNA using the TaqMan® MiRNA Reverse Transcription Kit (Applied Biosystems). Depending on the miRNA being analysed, a specific primer was obtained from Applied Biosystems. A mastermix was made up of the following constituents (Table 2.1).

Constituent	Volume (μ l)
dNTP Mix (100mM)	0.17
10X RT Buffer	1.65
Nuclease Free Water	4.57
RNase Inhibitor (20U/ μ l)	0.21
Multiscribe (50U/ μ l)	1.1
Stem Loop Primer	3.1
miRNA	5

Table 2.1 Components of mastermix used for reverse transcription of miRNA.

The mixture was placed in a GeneAmp® thermal cycler for incubation at 16 °C for 30 min, 42 °C for 30 min and 85 °C for 5 min to denature the sample. Similar to gene expression analysis, an RT blank was included which served as a negative control.

2.1.8 Real-time Quantitative Polymerase Chain Reaction (RQ-PCR):

Quantification of either mRNA or miRNA was achieved from amplification of the targeted cDNA by PCR. The reaction for amplification consists of denaturation, primer annealing and template extensions followed by a plateau or non-exponential phase where the reaction was limited by reducing agents. This reaction results in an approximate doubling of the target and the presence of a fluorescent probe targeting the sequence allowed real time detection of the product. Once this fluorescent signal reaches the threshold for detection, referred to as the cycle threshold (Ct), the target can be quantified. The amount of the target present was inversely proportional to the Ct value, the greater amount of sample present at the beginning of the reaction, the sooner the Ct will be achieved resulting in a low Ct value for high amounts of the target. A negative control which lacked any cDNA (NTC) was included in each RQ-PCR run.

Each RQ-PCR run was carried out using a 96-well plate as outlined in (Figure 2.3). A total volume of 10 µl was added to each well. Each sample was added in triplicate and two controls mentioned previously, RT-blank and NTC were also included in triplicate. On each plate either miR-A, B or C served as an endogenous control. Endogenous controls are targets that maintain a stable level of expression in a biological sample irrespective of whether they originate from a cancer patient or a healthy individual. An inter-assay control (IAC) was also added to every plate. This is a sample that has consistent expression that will ensure consistency of experimental parameters for each sample inserted into the AB7900HT (Applied Biosystems). The IAC allows for multiple different plates to be compared and included in one large study. The reaction consisted of a 10 min incubation period of 40 cycles at 95 °C for 15 seconds respectively which resulted in the formation of single stranded DNA and was followed by an annealing step at 60 °C for 60 seconds.

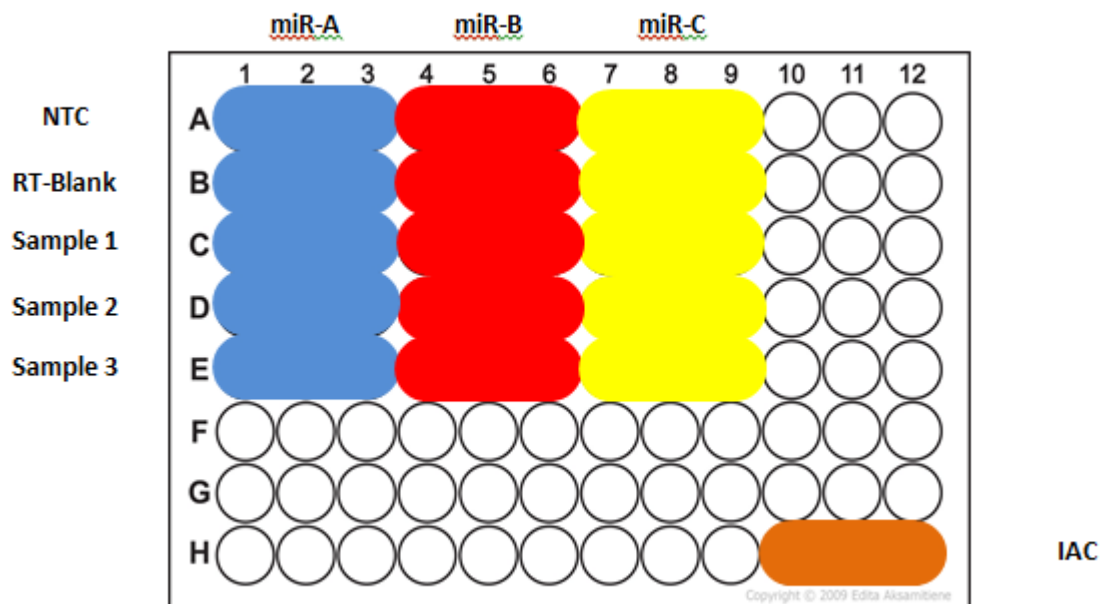


Figure 2. 3: Example of plate outline used for RQ-PCR

2.1.8.1 Analysis of Gene Expression:

For analysis of mRNA expression a mixture consisting of pre-developed assay reagents (PDARs) and Mastermix obtained from Applied Biosystems were made up as outlined in (Table 2.2).

Reagent	Volume (μ l)
TaqMan FAST Mastermix	5
Nuclease Free Water	3.5
mRNA PDAR	0.5
cDNA	1

Table 2 2: Components of mastermix used for reverse transcription of miRNA

The total volume of 10 μ l was added in triplicate to each plate and made specifically for each target mRNA. All work was carried out in aseptic conditions within a fume hood and appropriate PPE worn throughout. Reference genes known as endogenous controls were used for mRNA analysis and for this study Peptidylprolyl Isomerase A (PPIA) and Mitochondrial Receptor Protein L-19 (MRPL19) were chosen [221]. Data was expressed relative to both endogenous controls.

2.1.8.2 Analysis of miRNA Expression:

Similarly, a mixture composed of PDARs and Mastermixes obtained from Applied Biosystems were made up to 10 μ l and carried out in triplicate. For miRNA analysis the components were made up as outlined in (Table2.3).

Reagents	Volume (μ l)
TaqMan Fast Mastermix	5
Nuclease Free Water	3.8
miRNA PDAR	0.5
cDNA	0.7

Table 2 3: Components of mastermix used for RQ-PCR of miRNA

This 10 μ l mixture was made for each miRNA of interest.

2.1.8.3 Analysis of RQ-PCR Data:

In order to attain relative quantification, all data was normalised to endogenous controls. A standard deviation of less than 0.3 is required from at least two of the triplicates analysed to confirm the accuracy of the assay before data analysis can be carried out. The Ct value of the endogenous control was subtracted from that of the gene of interest. This results in what is known as the delta Ct (Δ Ct) [222].

$$\Delta\text{Ct} = \text{average Ct miRNA/gene of interest} - \text{average Ct endogenous control}$$

One sample with the highest Δ Ct value was selected and was then subtracted from every sample in the cohort which resulted in the delta delta Ct ($\Delta\Delta$ Ct).

$$\Delta\Delta\text{Ct} = \Delta\text{Ct sample} - \Delta\text{Ct lowest expressor}$$

In order to determine the fold change or relative quantification (RQ) the $\Delta\Delta C_t$ was converted to $2^{-\Delta\Delta C_t}$ [222]. If the range within the sample group was too broad then each was log transformed to create normal distribution of the cohort. Minitab 16.0 (Minitab Ltd) was used to carry out independent two-sample t-tests or one-way-ANOVA analysis between different sample groups greater than two. A p-value lower than 0.05 was considered to be statistically significant.

2.2 Cell Culture

2.2.1 Overview of Cell Culture:

Cell culture in the Discipline of Surgery, is carried out in one of three rooms. These rooms have restricted access and are segregated based on the type of cell work carried out in each. One room is used for the growth of immortalised cancer cell lines which would have originally been derived from the American Type Culture Collection (ATCC). The second room is restricted for Primary Culture which is the growth of fresh patient tissue samples acquired directly from the operating theatre. Mesenchymal Stem Cells (MSCs) which would have originated from the iliac crest of healthy individuals are also cultured in this room. The third room is designated for work related to the transduction of cells with viruses as well as any cell type that has been previously transduced with a virus. This room has a limited user base as specialised training and an environmental protection agencies (EPA) licence is required to work with a virus for any cellular transduction procedures. Each room has restricted access and is isolated from the main laboratory and requires the use of a designated lab coat for work carried out within the room. Each room is equipped with two laminar air flow Hoods (LAF), a bench top centrifuge, microscope, heated water baths, fridge and two High Efficiency Particulate Air Filter (HEPA) incubators.

Cell culture refers to the growing, or culturing, of cells in controlled laboratory conditions. All cells are grown using strict aseptic techniques which aims to reduce the possibility of bacterial contamination of the cells or any cross contamination between different cell lines. To achieve this, all work manipulating cells is carried out within a LAF hood. The hood is exposed to an ultraviolet (UV) light for 15 min prior to being opened and switched on. It is subsequently cleaned with 70% industrial methylated spirits (IMS) and appropriate PPE is worn, such as gloves and lab coats at all times when working within the LAF hoods or when handling any equipment associated with cellular manipulations. 70% IMS is used

to clean every item that enters the LAF hoods which all serve to reduce the possibility of contamination. Furthermore, the LAF hoods remain turned on for 15 min between different cell lines to prevent any cross contamination of cell lines. All cell lines are grown in a controlled Stericycler CO₂ incubator-HEPA class 100 at 37°C and 5% CO₂. All incubators, water baths and LAF hoods are rigorously cleaned weekly to reduce any possibility of contamination or infection of the cell lines.

2.2.2 Immortal Breast Cancer Cell lines:

During the course of this study breast cancer cell lines representative of different subtypes of the disease were employed (Table 2.4). Media for each breast cancer cell line was supplemented with 10% Fetal Bovine Serum (FBS) (Gibco) and 100 IU/ml Penicillin / 100 µg/ml Streptomycin (Pen/Strep, Lonza).

Cell Line	Epithelial Subtype	Receptor Profile	Media Components
T47D	Luminal A	ER+, PR+, HER2 low	RPMI 1640 w/L-glutamine +10% FBS + Pen/Strep
HCC1954	HER2 Overexpressing	ER-, PR-, HER2+	RPMI 1640 w/L-glutamine +10% FBS + Pen/Strep
MDA-MB-231	Basal	ER-, PR-, HER2 low	Leibovitz-15 w/L-glutamine +10% FBS + Pen/Strep
Mesenchymal Stem Cells (MSCs)	N/A	N/A	MEM- Alpha +10% HyClone FBS + Pen/Strep Human FGF Basic (50µg)

Table 2 4: Media Requirements

2.2.3 Mesenchymal Stem Cells:

Mesenchymal stem cells (MSCs) derived from the bone marrow of the iliac crest of healthy individuals were obtained following ethical approval and informed patient consent. Cells were supplied by the Regenerative Medicine Institute (REMEDI) following isolation and characterisation [223]. MSCs are characterised based on three different criteria, firstly, they must be adherent to plastic under normal tissue culture conditions. Secondly, they must be positive for the presence of markers CD105, CD90 and CD73 while negative for markers CD45, CD34, CD14, CD11b, CD79alpha, CD19 and HLA-DR. Thirdly, the cells must have the capacity to

differentiate into osteoblasts, adipocytes and chondrocytes under appropriate *In vitro* conditions [147]. Once characterised, MSCs were cultured in Alpha Minimum Essential Medium (α -MEM Biosciences) which contained L-glutamine and 1,000 mg/L glucose and was supplemented with pre-selected FBS (10%) (Hyclone Ltd) and Pen/Strep(Biosciences). Fibroblast Growth Factor (FGF, Peprotech) was also added to the media at a working concentration of 1 ng/ml. Fibroblast growth factors are associated with angiogenesis and wound healing and have also been shown to promote MSC proliferation [224]. The FGF (50 μ g) was reconstituted in 0.1% BSA PBS, following sterile filtration, and was aliquoted using low adhesion siliconized tips. Each 40 μ l aliquot was at a stock concentration of 100 ng/ μ l stored at -20°C in siliconized tubes (Sigma). From one stock, 40 aliquots at a concentration of 4 ng/ μ l in a volume of 25 μ l were made and stored at -20°C. When required, these working stocks were removed from -20°C storage and kept at 4°C, for a maximum length of 7 days. FGF in the culture media was used at a concentration of 1 ng/ml.

2.2.4 Feeding Cells:

Growth media used to culture cells was changed 3 times every week to maintain sufficient levels of nutrients in the media for optimal cellular growth and to remove cellular waste produced by cultured cells. All media was warmed to 37°C in a water bath prior to addition to the cells to prevent any temperature shock to the cells. The cell media was initially visualised to ensure that the pH-sensitive colour indicator in the media did not change and that there was no overt contamination. Cells were viewed using a light microscope to ensure appropriate morphology, adequate confluency and to detect any traces of contamination prior to feeding. Cell media was discarded into a waste container and fresh, warmed media was added to the flask on the side that does not contain the cells to prevent any cellular disruption. The flask of cells was then returned to the incubator at 37°C and 5% CO₂. The amount of media added to the cells depended on the size of flask used, 8ml of media for a T-25 cm², 12ml of media for a T-75 cm² and 25ml for a T-175 cm². Each flask used for culturing cells was purchased from Sarstedt that contained a vented cap to ensure efficient gas exchange.

2.2.5 Subculturing:

When cells were needed for experimentation or when they reached an appropriate degree of confluency, cells were subcultured. This is to ensure that

the cells remain in the log phase of growth because if they were to reach 100% confluency they could begin to senesce. Media, phosphate buffer saline (PBS) (Biosciences) and 0.25% Trypsin/EDTA (T/E) (Biosciences) were placed into a water bath and warmed to 37°C. The media was decanted from the cells and PBS was added to the cell monolayer. This was to remove any traces of FBS that was contained in the media which would inhibit the T/E from working. The PBS which was Ca²⁺/Mg²⁺ free was poured off the cells once washed and the T/E was subsequently added. The T/E was maintained at 37°C as it is a protease that functions best at this temperature. This remained on the cells for 45 sec at RT in the LAF hood in order to penetrate the layer of cells. Following this, the excess T/E was poured off and the flask was placed at 37°C in the incubator for 3-5 min in order to allow the protease to cleave the cell surface proteins and remove the cells from the base of the flask. The cells were inspected visually by light microscopy to see if they had effectively been removed from the base of the flask and were in suspension. If not, the flask was given a gentle tap in order to aid in removal of the cells. FBS enriched media was added to the cells in order to inhibit the T/E and prevent it from further digestion of the cells.

2.2.6 Cell Counting:

Cell counting was carried out using a Nucleocounter® (Chemometec) as it allows an automated, reproducible and robust method of cell counting. To evaluate the number of viable cells present in a solution it was necessary to carry out two counts, one being the non-viable cell count which was subtracted from the second Total cell count. In order to achieve the total cell count Reagent A100 (Lysis Buffer) and Reagent B (Stabilising Buffer) were added, with the sample vortexed in between additions of buffers. These reagents diluted the cells by a factor of 3 and also lysed the cells allowing the propidium iodide present in the nucleocassette to bind the DNA of all lysed cells This count was repeated on another cell suspension without the addition of both Reagent A100 and Reagent B in order to determine the number of non-viable cells present in the solution (Figure 2.4).

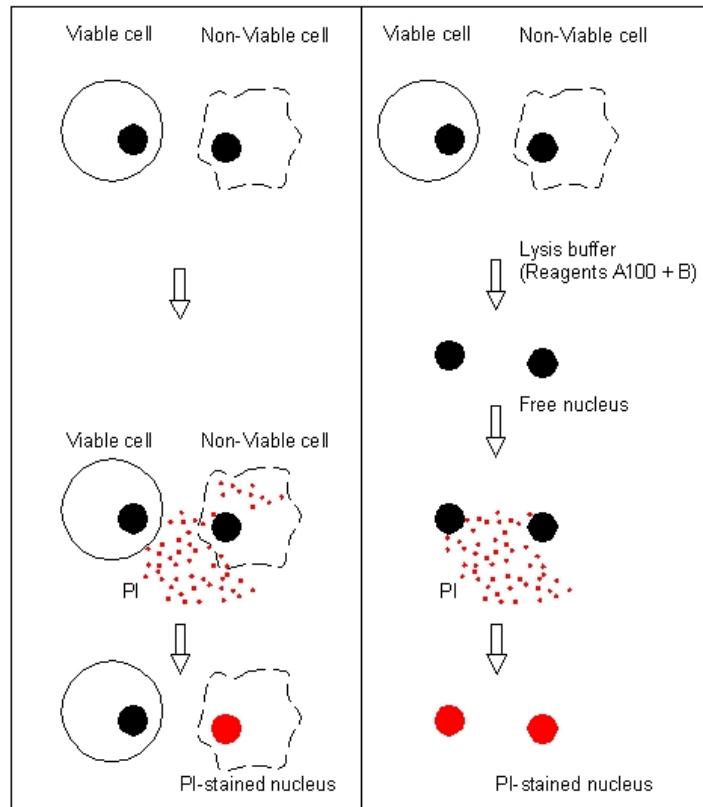


Figure 2. 4: Outline of protocol to determine the number of viable cells in a given solution [225].

The Nucleocounter[®], using a fluorescent microscope detects the number of non-viable cells present in the 2 μ l of sample present in the measurement chamber of the nucleocassette resulting in a concentration of cells/ml (Figure 2.5).

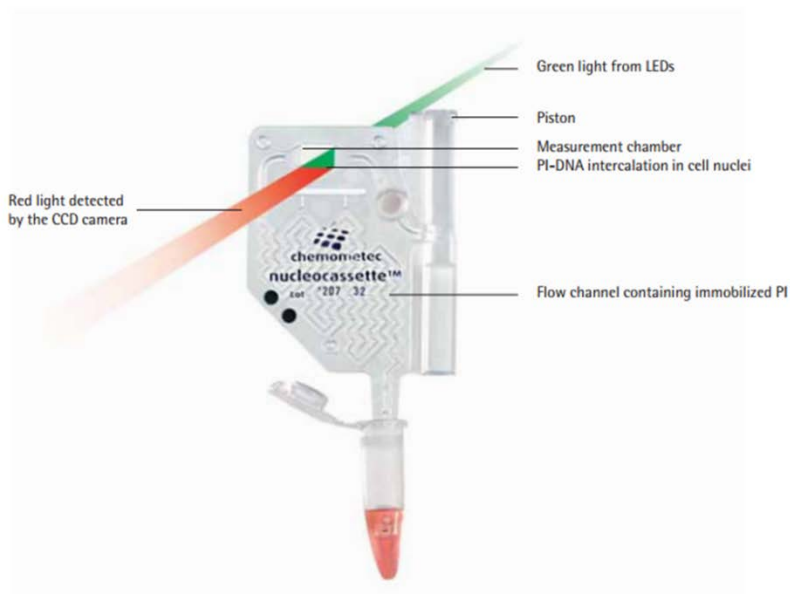


Figure 2. 5: Outline of nucleocassette (Chemometec) used for cell count [226].

In order to determine the number of viable cells the following calculation was performed:

Total no. of cells – no. of non-viable cells = no. of viable cells

2.2.7 Cryopreservation of Cells:

While growing cells, stocks were regularly made to protect against future contamination of growing cells and to prevent transformation and ageing of cells. To create stocks, cells were frozen down in complete media and 5% Dimethylated Sulphoxide (DMSO) (Sigma-Aldrich®). The DMSO prevents any crystallisation during the freezing step which could result in death of the cells. Cells were visually inspected to ensure they were viable and not contaminated. Once confirmed, cells were rinsed with PBS and Trypsinised. Cells were resuspended in complete media and centrifuged at 2,000 x g for 5 min forming a cell pellet. 2 ml Nunc Cryovials (Sarstedt) were labelled appropriately and briefly chilled on ice. Cryovials were removed from ice and 80 µl of DMSO was added to each cryovial. $1.5 - 2 \times 10^6$ cells were resuspended in 1.6 ml complete media and added to the cryovial containing DMSO which was immediately placed on ice as DMSO is toxic to cells at 37°C. The cryovials were then placed into a “Mr Frosty” (Nalgene) container. This allows for controlled freezing of cells at roughly -1°C/minute due to the presence of isopropyl alcohol. This was subsequently put into a -80°C

freezer for at least 3 hours before transportation of the frozen cells for long-term storage in liquid Nitrogen (-196°C).

2.2.8 Recovering Cells:

Frozen stocks of cells were thawed quickly to prevent any negative impact of the DMSO. For this, complete media was warmed to 37°C and the appropriate volume was added to the a T175 flask. The flask was labelled and returned to the incubator at 37°C. Cells were removed from the liquid Nitrogen and placed directly into a water bath warmed at 37°C. The cryovial was gently swirled to aid in the rapid thawing of the cells. When a small part of the cell suspension was still frozen the cryovial was sprayed with 70% IMS and placed into the LAF hood. The warmed flask was taken from the incubator and placed into the hood where the thawed cells were pipetted directly into the flask. Cells within the flask were returned to the incubator where the media was changed 24 hours later to completely remove the presence of DMSO from the cells.

2.2.9 Transduction of MSCs:

All virus-related work requires the possession of an EPA licence. To achieve stable expression of miR-379 in MSCs it was necessary to transduce the cells with a lentiviral vector from Thermo Scientific SMARTchoice shMIMIC (Figure 2.6). The lentivirus allowed for enriched expression of miR-379 or a non-targeting control (NTC), which contains a scrambled sequence that does not alter miR-379 expression. An NTC lentivirus is used as a comparison to ensure any effects witnessed on transduced cells are due to miR-379 enrichment and not as a result of the transduction with a lentivirus. This construct also contained red fluorescent protein (RFP) whose excitation/emission maxima are 553 and 574nm respectively. RFP expression made it possible to view the transduced cells by fluorescence microscopy. The vector contained 5' long terminal repeats (LTR) which allowed integration into the host genome. A Rev response element (RRE) is also present which facilitated the transfer of mRNAs from within the nucleus to the cytoplasm. The human cytomegalovirus (hCMV) promoter increased transcription of the gene while the internal ribosome entry site (IRES) allowed for the initiation of translation and for viral translation to proceed while host translation was inhibited. Importantly, the vector also contained a Puromycin resistance gene(Puro^R) which made the transduced cell resistant to the antibiotic Puromycin, allowing for subsequent positive selection of transduced cells. A woodchuck

hepatitis virus post-transcriptional regulatory element (WPRE) was also present to enhance expression in a vector, promoter and transgene independent manner. Finally, the vector contained a self-inactivating long terminal repeat (SIN LTR) as a biosafety element.



Figure 2. 6: Lentiviral construct used for transduction of cells (Adapted from the SMARTchoice shMIMIC Lentiviral miRNA Technical Manual)

To assist in lentiviral transduction Hexadimethrine Bromide (Polybrene-Sigma-Aldrich) was used which is a cationic polymer. This functions to neutralize the charge between the charged virus and Sialic acid which is present on the cell surface. For transduction, cells were trypsinised and resuspended in complete media. Cells were counted to achieve a multiplicity of infection (MOI) of 2 which is 2×10^5 cells to 4×10^5 virus particles. For Polybrene optimisation MSCs were seeded into a 96-well plate at a density of 3×10^3 cells/well. A range of concentrations of Polybrene (0, 1, 4, 8 $\mu\text{g}/\text{ml}$) were added to the cells. Following 72hrs, 20 μl MTS solution was added to each well and 3 hours later the absorbance was read @ 490 nm. Optimised Polybrene (2 $\mu\text{g}/\text{ml}$) was added to the media. The lentiviral vector was finally added to the cell suspension. Following addition of the virus the pipette tip was rinsed in bleach and all media exposed to the virus was disposed of in bleach. Pipette tips used to handle the virus, following rinsing in bleach, were placed into doubled biohazard bags and placed into an autoclave. The cell/virus suspension was centrifuged at 2,000 x g for 90 min at 37°C. Following centrifugation, the media containing the Polybrene and virus was disposed of in bleach while the cell pellet was resuspended in complete media and 2×10^5 cells were seeded into a 6-well plate. Cells were maintained in complete media for 48 hours prior to the addition of 4 $\mu\text{g}/\text{ml}$ of Puromycin for 7 days to allow for selection of transduced cells.

2.2.10 Examining Cells by Fluorescence Microscopy:

To examine any phenotypic changes undergone by the cells due to enrichment of miR-379, cells were seeded onto 4-well glass Millicell® EZ slide (Millipore) and were stained with Phalloidin (Alexafluor® 488 Invitrogen), which allowed visualisation of the actin cytoskeleton, and 4',6-diamidino-2-phenylindole (DAPI) (Sigma) in order to visualise cell nuclei. Cells were seeded at a density of 1.5×10^4 per chamber and left adhere overnight. Each chamber was washed twice with pre-warmed PBS and the chambers were subsequently removed from the slides. Cells were fixed in 3.7% Formaldehyde for 10 min at RT followed by two washes of PBS. 500 μ l of 0.1% Triton-X 100 was added to each slide for 10 min to permeabilize the cells. This was, again, followed by two rinses in PBS before the addition of 1% Bovine Serum Albumin (BSA) for 30 min which reduces background staining and binds to non-specific sites. The Phalloidin primary antibody (2 μ g/ μ l) was diluted 1:60 in 0.1% BSA solution (33 ng/ μ l) and 30 μ l was added to each slide where it was wrapped in tin foil to prevent photobleaching and let stand for 20 min at RT. Slides were protected from light for all subsequent steps. Slides underwent three rinses in PBS before the addition of DAPI at a concentration of 1 μ g/ml for 5 min. Following this, slides underwent three washes in PBS for 5 min each. Slides were dipped 40 times in each of 70%, 95% and 100% ethanol to dehydrate the cells and subsequently placed in Xylene for 3 min twice. Slides were then mounted in Dibutyl phthalate and Xylene (DPX) mounting medium and left overnight in a fume hood. Cells were visualised using the Olympus BX60 fluorescence microscope.

2.2.11 Cell Proliferation Assay:

To determine cell proliferation a 3-(4,5-dimethylthiazol-2-yl)-5-(3-carboxymethoxyphenyl)-2-(4-sulfophenyl)-2H-tetrazolium (MTS) assay (Promega) was performed. This determined cell viability based on a colorimetric assay which was founded on the reduction of the MTS tetrazolium compound by viable cells to a coloured formazan product. Cells were seeded in a 96-well plate (HCC1954/MSCs @ $1.5 \times 10^3/3 \times 10^3$ cells/well). Following growth for 24/48/72 hrs, 20 μ l of MTS solution added to each well containing cells to terminate the study. Samples were protected from light and incubated for 3 hours at 37°C. Following incubation, the absorbance in each well was read at a wavelength of 490 nm.

2.2.12 Cell Migration Assay:

Tracking of cell migration was carried out using Corning® Transwell Inserts (Sigma-Aldrich) (Figure 2.7). For the purpose of this experiment a 24 well insert with a pore size of 8 µm was implemented to allow the movement of cells through the pore in response to a chemoattractant in the well below.

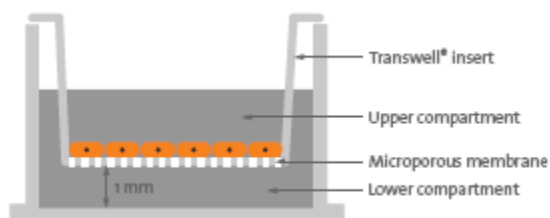


Figure 2. 7: Example of transwell insert and experimental set-up for evaluating migratory potential of cells

In the wells, there was either media supplemented with 5% FBS to serve as a positive control or basal media to serve as a negative control. Inserts were hydrated for 1 hour in basal medium prior to commencing the experiment. For this, 600 µl of basal medium was added to each well and 100 µl was added to each insert. During hydration of the inserts, MSCs were resuspended in basal media. As the inserts were lowered into the wells, MSCs ($7.5 \times 10^4/100 \mu\text{l}$) was added to each insert (Figure 2.8).

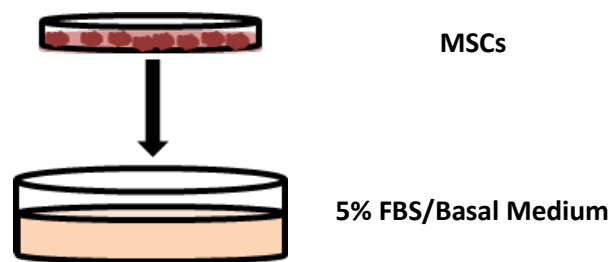


Figure 2. 8: Graphical representation of migration experiment setup

Plates with inserts added were incubated at 37°C and 5% CO₂ for 18 hrs to assess migration. Following incubation, inserts were removed using a tweezers and the inner surface was scrubbed using a cotton bud. Enough force was applied to effectively remove the cells that had not migrated, yet not so much pressure as to penetrate the membrane in the insert. The opposite end of the cotton bud was dipped into basal medium and the scrubbing was repeated to remove every cell that did not migrate. The inserts were subsequently placed into ice cold Methanol for 15 mins at room temperature (RT) which fixed the cells. Inserts were then

placed in Gill No.2 Haematoxylin (Sigma-Aldrich) to stain the cells, but for no more than 3 min to prevent staining of the pores of the insert resulting in potentially inaccurate counts. This was followed by two rinses in dH₂O to remove the Haematoxylin. Inserts were inverted on tissue and left to dry at RT. The membrane was removed with the use of a scalpel and placed onto Lenzol immersion oil (BDH) on a slide. Another drop of oil was placed on top of the membrane with a coverslip added until required for counting. For counting of the cells the membrane was viewed under a 20X magnification and counts were taken in five fields of view with the average count calculated at the end (Fig 2.9).

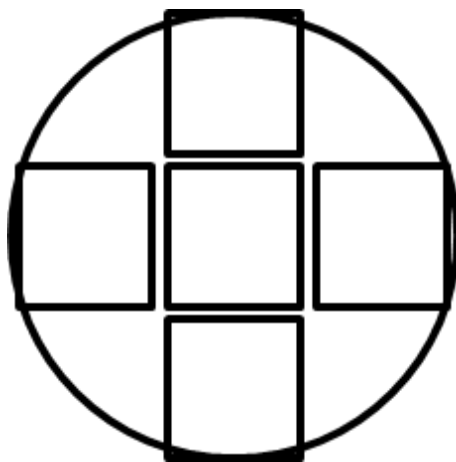


Figure 2. 9: Fields of view used to count number of migrated cells on excised insert

2.3 Exosomes

2.3.1 Exosome Isolation:

For harvesting exosomes, MSCs and breast cancer cells were grown in media containing exosome depleted fetal bovine serum (FBS). This was attained through ultracentrifugation of FBS at 100,000 x g for 16 hrs with the supernatant aliquoted and frozen at -20°C for future use. Cells grown in complete media were rinsed with PBS and trypsinised before being resuspended in exosome depleted media. Cells were seeded at 2×10^6 cells/flask and supplemented with 10 ml exosome-depleted media. The following morning, media was changed and cells were grown in 10 ml exosome depleted media for 48 hrs. The media was removed from the flasks and collected in a 50 ml Falcon tube. The tubes were centrifuged at 300 x g for 10 min, the supernatant was removed and centrifuged at 2,000 x g for 10 min (Figure 2.10). These steps removed large cellular debris contained in the media. Next the supernatant was passed through a 0.22 μ m filter to remove any particles greater than 220 nm and added to ultracentrifuge tubes (Hitachi Koki). The tubes

were balanced and placed into the ultracentrifuge (Hitachi Micro Ultracentrifuge CS150FNX) for 70 min at 100,000 x g.

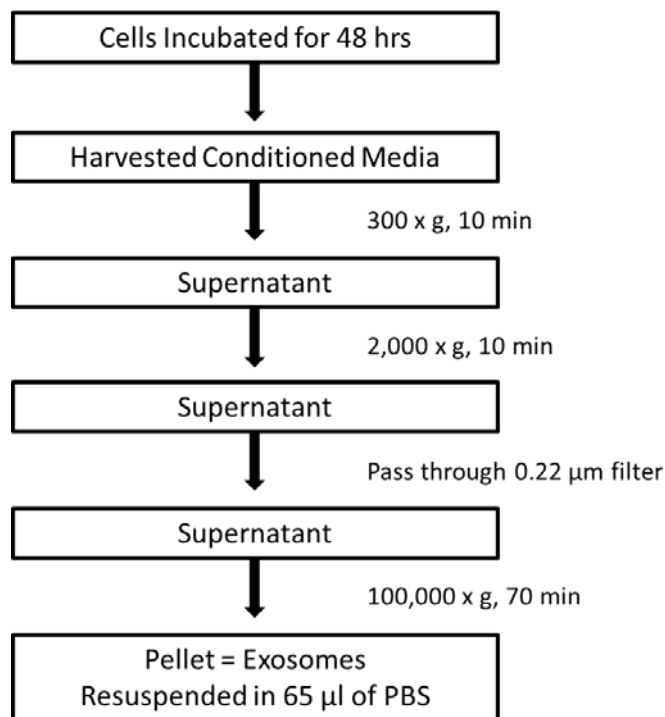


Figure 2. 10: Protocol used to isolate exosomes from cell conditioned media

After ultracentrifugation, the pellet contained exosomes and 2 ml of conditioned media was harvested in case required for future analysis and stored at -20°C. The remaining conditioned media was disposed of ensuring that each ultracentrifuge tube was devoid of any media. 65 μl of PBS was added to the first ultracentrifuge tube and scraped using a 100 μl pipette tip for 5 min focusing on the area of tube containing the pelleted exosomes. After 5 min, the same 65 μl was transferred to the second tube and this process continued for each ultracentrifuge tube containing cell medium. Upon completion, 10 μl of PBS containing exosomes was added to 40 μl of complete lysis buffer containing 1% protease inhibitor and 1% Na₃VO₄ and frozen at -20°C. 5 μl of the isolate was placed in 15 μl PBS and stored at -20 °C until required for Nanoparticle Tracking Analysis. The remaining 50 μl of PBS containing exosomes was placed in a tapered tube and frozen at -20°C until required for further use.

2.3.2 Indirect Exosome Quantification:

As a surrogate indicator of exosome content isolated, a Pierce BCA protein assay kit (ThermoFisher Scientific) was carried out on the isolated exosome samples

stored in complete lysis buffer. This quantification determines the amount of protein present in a sample. It functions on the basis of Cu^{2+} reducing to Cu^{1+} in the presence of protein while in an alkaline medium. This reduced Cu^{1+} reacts with bicinchoninic acid and results in a colour change of the media from light blue to dark purple which is read in a plate reader at 562 nm. A standard curve is formed following serial dilution of bovine serum albumin (BSA) ranging from a concentration of 2,000 $\mu\text{g}/\text{ml}$ – 0 $\mu\text{g}/\text{ml}$. 25 μl of each concentration was added to the 96-well plate in duplicate. 50 μl of isolated exosome sample was also added to two wells, 25 $\mu\text{l}/\text{well}$, to provide duplicate readings. The working reagent (WR) allowing for the colour change consisted of reagent A and B added at a ratio of 50:1. 200 μl of the WR was added last to each well in the 96-well plate. The plate was placed on a shaker for 30 sec before being incubated at 37 °C for 30 min. Absorbance in each well was read at a wavelength of 562nm.

2.3.3 Direct Exosome Quantification:

Nanoparticle Tracking Analysis (NTA) was carried out on isolated exosomes to quantify and characterise the microvesicles. This was performed on a Nanosight (NS500) by the Nanomedicine and Molecular Imaging Group based in the Institute of Molecular Medicine, Trinity College Dublin. This device was equipped with a 405 nm laser, coupled with a 430 nm long pass filter, an EMCCD camera and was thermostatically controlled. NTA allows the quantification of particles in the size range of 10nm – 2000nm, encompassing the 30 – 120nm size range of exosomes. Nano objects were characterised using the NTA software, which utilised the properties of both light scattering and Brownian motion to obtain particle size distributions. NTA functions on the basis of a laser being passed through 0.08 μl of liquid containing exosomes. The scatter of the laser from the particles is detected by a camera mounted on a microscope (Figure 2.11).

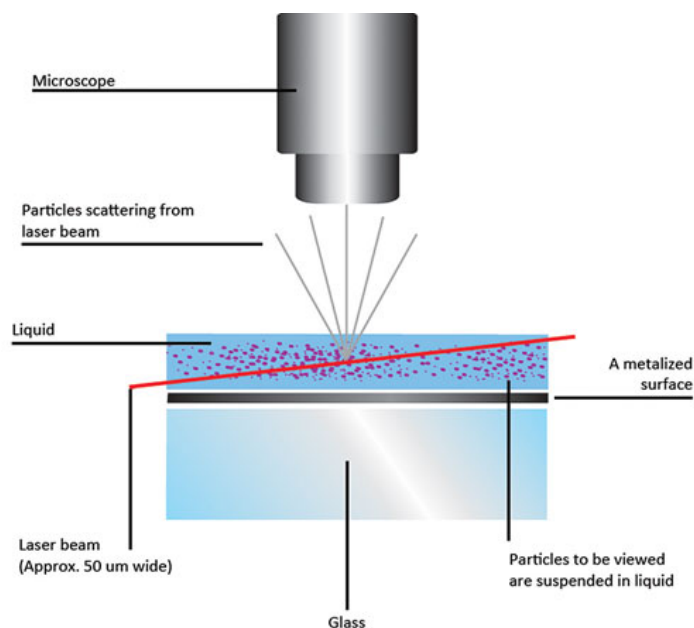


Figure 2. 11: Evaluating size and concentration of exosomes in sample by nanoparticle tracking analysis [227].

NTA provides direct quantification of exosome particles, following 5 replicate readings while also characterising the vesicles based on the size distribution.

2.3.4 Transmission Electron Microscopy:

To visualise the exosomes transmission electron microscopy (TEM) was carried out. For this the conditioned media was harvested from the cells as normal to isolate exosomes. However, when placing the samples in the ultracentrifuge they were mixed with a primary fixative. The primary fixative was made up of 4 ml 25% Gluteraldehyde, 10 ml 10% Paraformaldehyde and 25 ml 0.2M Sodium Cacodylate / HCl Buffer pH 7.2. This solution was then made up to 50 ml using dH₂O. 10 ml of primary fixative was added to 10 ml conditioned media and placed in an ultracentrifuge tube and centrifuged at 100,000 x g for 70 min. Following ultracentrifugation the conditioned media was disposed of and the exosomes were resuspended in 55 µl of PBS. The exosomes were then treated with the secondary fixative. This consisted of 2% Osmium Tetroxide and 0.2 M Sodium Cacodylate / HCl Buffer at pH 7.2 mixed together in an equal volume. 2 ml of the secondary fixative was added to 2 ml PBS and 200 µl of this solution was added to the exosomes and vortexed for 30 sec to mix the sample. Following vortexing, the samples were let stand at RT for 2 hours to allow the sample to form a density gradient resulting in a brown pellet. The secondary fixative was removed and placed into Ascorbic acid to neutralise the toxicity associated with the Osmium

solution. The pellet was then sequentially dehydrated in 30%, 50%, 70%, 90%, 95% and finally 100% Ethanol. Each step was carried out twice for 15 min each. After the final step the 100% ethanol was removed and replaced with Propylene Oxide (Sigma-Aldrich) for 20 min which allowed the sample to transition from pure ethanol to impregnation of the sample with an Epon based resin (Ladd Industries, Burlington, VT). The resin was prepared using a commercial kit and the samples were initially placed in a 50:50 mixture of resin and Propylene Oxide for 4 hours. After this, the mixture was changed to a 75:25 mixture of resin and Propylene Oxide and left on a rotator overnight. The next morning, the sample was placed in pure resin and placed on a rotator for 5-6 hours. Samples were then transferred to a 65°C oven for 48 hours to allow for polymerisation of the sample. Following polymerisation, the blocks were trimmed to a thickness of 1 µm, placed onto a glass slide and stained with 1% Toluidine Blue. These sections were then viewed by light microscopy and were referred to as 'scout sections' because they were used to deduce the tissue structure and components. Areas of interest were selected and subsequently sectioned using the ultramicrotome (Reichert-Jung Ultracut E) giving sections of a thickness 80 – 100 nm which were then placed onto copper grids. The grids were stained for 30 min in 1.5% aqueous Uranyl Acetate and 10 min Lead Citrate. Sections were dried and viewed using Hitachi H7000 Transmission Electron Microscope.

2.3.5 Confocal Microscopy of Exosome Transfer:

Exosomes were harvested as outlined previously (Section 2.3.1). Breast cancer cells were seeded onto glass coverslips (2×10^5 cells) in a 6-well plate and incubated at 37°C and 5% CO₂ overnight to ensure cells had adhered to the coverslips. Coverslips were removed using pipette tips ensuring the coverslips remained cell side up. They were transferred across to a humidification box which consisted of moist tissue with parafilm placed across it. The coverslips were placed onto the parafilm with cell side facing up. Isolated exosomes were resuspended in 20 µl of PBS for the purpose of this experiment and were added to 20 µl of exosome depleted media, thoroughly mixed and carefully added to the cells on coverslips in the humidification box. A small square of parafilm was carefully placed over the coverslips to ensure even distribution of the exosomes on the adhered cells. The humidification box was subsequently incubated at 37°C for 4 hrs. Following incubation, the coverslips were removed and rinsed in PBS

and subsequently fixed using 4% paraformaldehyde for 10 min. Once fixed, the cells were once again rinsed in PBS followed by the addition of 1 ml Triton X-100 for 10 min to permeabilise the cells. 1 ml of 1% Bovine Serum Albumin (BSA) was dissolved in 0.1% Triton X-100 and added to each coverslip for 1 hour at RT to reduce background and non-specific staining of the sample. Following this blocking step, the coverslips were washed three times in 0.1% Triton X-100. Alexafluor Phalloidin 488 was diluted 1:200 with 30 µl added to a small square of parafilm and the coverslip placed cell side down onto it ensuring the surface was flat and was evenly distributed across the coverslip. This was then incubated at 37°C for 1 hr while wrapped in tinfoil to protect the fluorescent peptide from becoming photobleached. The coverslips were then washed three times in 0.1% Triton X-100. A drop of VECTASHIELD anti-fade mounting medium with DAPI (Vector) incorporated into it was added to a slide and the cell side of the coverslips was carefully placed onto the slide. The outside of the cover slips were lined with nail varnish to prevent any leaking of the mounting medium and protected from light and allowed set overnight before imaging was carried out. Imaging was carried out on an Andor Olympus Spinning Disk Microscope (Andor, Belfast, Northern Ireland), using Andor IQ software. Images were captured as Z-Stacks once exposure time and Electron Multiplying (EM) gain were set and recorded to the channel of illumination.

2.4 Investigating the impact of miR-379 *In vivo*.

2.4.1 Ethics and Licensing:

This *In vivo* study was carried out after receiving approval from the NUI Galway Ethical Committee and after obtaining an animal licence under the Cruelty to Animals Act 1876 by the Health Products Regulatory Authority (HPRA). Basic training was provided by Laboratory Animals Science and Teaching (LAST-Ireland) where a 2 day workshop was attended and a certificate was awarded following a written exam as well as an assessment of animal handling technique (Appendix 8.2). Handling of the animals as well as procedures carried out were performed in adherence to published guidelines [228]. Refinement, Reduction and Replacement, the guiding principles introduced by Russell and Burch in 1959 were abided by throughout the duration of each *In vivo* study [229].

2.4.2 Animal Facility:

All animals were housed in the animal research facility for both *In vivo* studies. Before entering either facility, extreme care was taken to prevent the introduction of pathogens that could jeopardise the health of the immunocompromised mice. For this, the appropriate PPE was worn which consisted of shoe covers, gown, gloves, face mask and hair net which were worn throughout any work carried out within the confines of the animal research facility. Throughout the course of the study, a Named Day-to-Day Care Person was present to ensure upkeep and maintenance of animal husbandry, which included changing bedding twice a week, feeding and visual inspection of the animals. Each consumable used in the animal facility was autoclaved before use. Each cage was individually ventilated and housed 3-4 animals each. When handling the animals, all work was carried out in Class II Laminar Flow Hoods to protect the animals from any threat of infection.

2.4.3 Animal Model:

Female athymic BALB/c Nude mice (Charles River Laboratories Ltd.), aged between 6-8 weeks were the animal model used in this study. These mice lack a thymus making them immune-compromised and therefore allow the growth of human-derived tumours either subcutaneously (SC) or orthotopically. For each surgical procedure carried out Isoflurane/O₂ gas, 5% for induction and 1-2% for maintenance, was used to anaesthetise the mice prior to and for the duration of each procedure. Upon completion of the procedure, the anaesthetic was removed and mice were monitored until they could ambulate and access food and water.

2.4.3.1 Tumour Induction:

Animals were divided into groups (n=10) based on age to ensure each group had similar age distribution. To establish ER negative, HER2-amplified HCC-1954 tumours, mice received either a right flank SC injection of 4×10^6 HCC-NTC(n=10) or HCC-379 cells (n=10), or a mammary fat pad (MFP, second thoracic) (Figure 2.12) injection of 3.5×10^6 HCC-NTC(n=10) or HCC-379(n=10) cells suspended in 200 μ l RPMI medium. For tumour administration into the second thoracic MFP, the cells were directly injected into the MFP. Cell injections were performed using a 24-gauge needle and 1 ml syringe. Tumour growth was monitored, and at the appropriate time animals were sacrificed by CO₂ inhalation (week 5). Tumour

tissue was harvested, and preserved in RNAlater® or 10% Formalin until required for RNA extraction or IHC respectively.

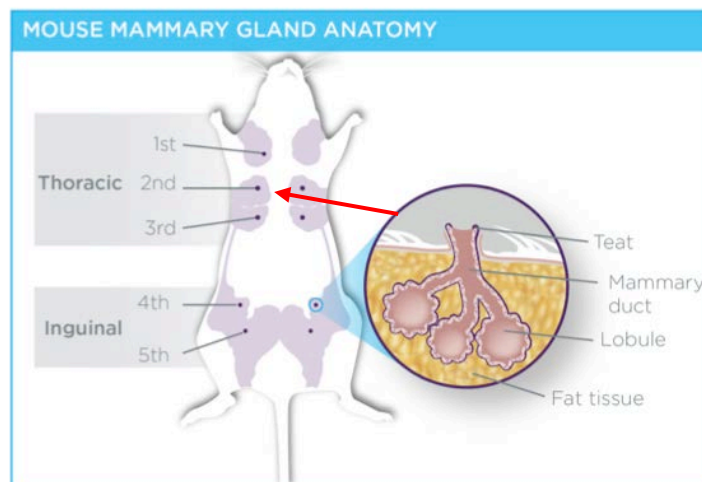


Figure 2. 12: Anatomy of mouse mammary glands exploited for tumour induction (Image adapted from aegiscreative.com)

- Group 1: (n = 10) SC, HCC-NTC
- Group 2: (n = 10) SC, HCC-379
- Group 3: (n = 10) MFP, HCC-NTC
- Group 4: (n = 10) MFP, HCC-379

2.4.3.2 Photoacoustic Imaging:

A combined photoacoustic (PA) and ultrasound (US) imaging system (VEVO LAZR VisualSonics Inc., Toronto, Canada) was operated with a 21 MHz central detection frequency linear-array transducer probe (Figure 2.13(a)). The 21 MHz probe (broadband frequency: 13-24 MHz) provides an axial resolution of 75 μm , imaging depth up to 20 mm and imaging width up to 23 mm. The mouse skin was acoustically coupled to the transducer probe head through ultrasound gel (Aquasonic® 100) for successive PA and US scans. For the oxygen saturation ($s\text{O}_2$) estimates, PA images were collected at 750- and 850-nm wavelength. A 256 element, linear array transducer, with a 21 MHz central detection frequency, was used in acquiring all images. Animals were anaesthetised as outlined previously and mounted on a platform while the imaging was carried out (Figure 2.13(b)). For imaging, contact gel was applied to both the mouse and the handheld probe. Good contact was made between the probe and area of interest on the animal.

Appropriate pressure was applied to ensure that there are no bubbles between the probe and tumour, which would distort the reading. Throughout imaging, vital signs of the animals were monitored and an anal probe monitored body temperature. Imaging of the mice yielded both a PA image as well as an US image for comparison. PAI provides information on the tumour vascularity through imaging both oxy and deoxy haemoglobin.

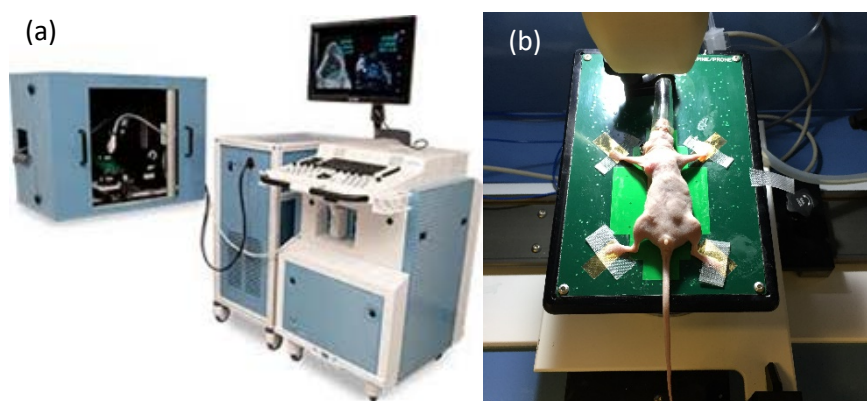


Figure 2. 13: (a) Image of Photoacoustic Imaging System (b) Picture taken of mouse prepared to undergo photoacoustic imaging

2.4.3.3 Terminal Bleed:

Mice were sacrificed 5 weeks after tumour induction. A terminal cardiac puncture was performed using a 24-gauge needle and 1 ml syringe. For this procedure, the mouse was anaesthetised and laid on their back. While approaching the base of the rib cage, the needle was held almost parallel to the position of the mouse. Upon penetration of the heart, blood having entered the syringe would pulsate at the same rhythm of the mouse heartbeat. Slowly, the plunger was withdrawn while filling with blood to a volume of roughly 1 ml. Blood samples were placed into a paediatric serum-separating tube, allowed coagulate for 30 min at RT, centrifuged at 10,000 x g for 5 min and stored at -80°C.

2.4.3.4 Animal Sacrifice and Organ Harvest:

For sacrifice, mice were placed in a CO₂ chamber which was gradually filled with CO₂ until there was an absence of respiration. Tumours were resected from the expired animal, weighed, and those large enough were cut in half and immediately placed in RNAlater® or 10% formalin for future analysis. Sentinel lymph nodes were also harvested and stored in 10% formalin for future analysis.

2.4.5 *In vivo* Investigation of therapeutic potential of miR-379:

Female BALB/c Nude mice (Charles River) were anaesthetised using Isoflurane/O₂ and maintained under anaesthetic for each procedure performed. Buprenorphine was administered to each mouse (n = 40), as an analgesic, prior to performing an incision to expose the fourth inguinal mammary gland (Figure 2.12). Mice received an injection of 1×10^7 HCC-luc cells into the fourth inguinal MFP using a 24-gauge needle and 1 ml syringe. Once palpable tumours detectable by (*In vivo* Imaging System) IVIS imaging had formed (Section 2.4.5.1), mice were divided into four groups with an equivalent size distribution of tumours in each. Mice received intravenous tail vein injections of the following: Group 1 (n=8): 1×10^6 MSC-379; Group 2 (n=8): 1×10^6 MSC-NTC; Group 3 (n=8): Four repeat doses of 2.6×10^7 exosomes derived from MSC-NTC cells, Group 4 (n=8): Four repeat doses of 2.6×10^7 exosomes derived from MSC-379 cells (Fig 2.14). Tumour growth was monitored using bioluminescent imaging (IVIS, PerkinElmer) as described in Section 2.4.5.1.

All treatments were performed through i.v. injection of the solution, using an insulin syringe, in the lateral tail vein of the mouse while the mouse was under anaesthetic as described previously (Section 2.4.3). Prior to any injection, the tip of the mouse tail was pinched to ensure the mouse was sufficiently anaesthetised.

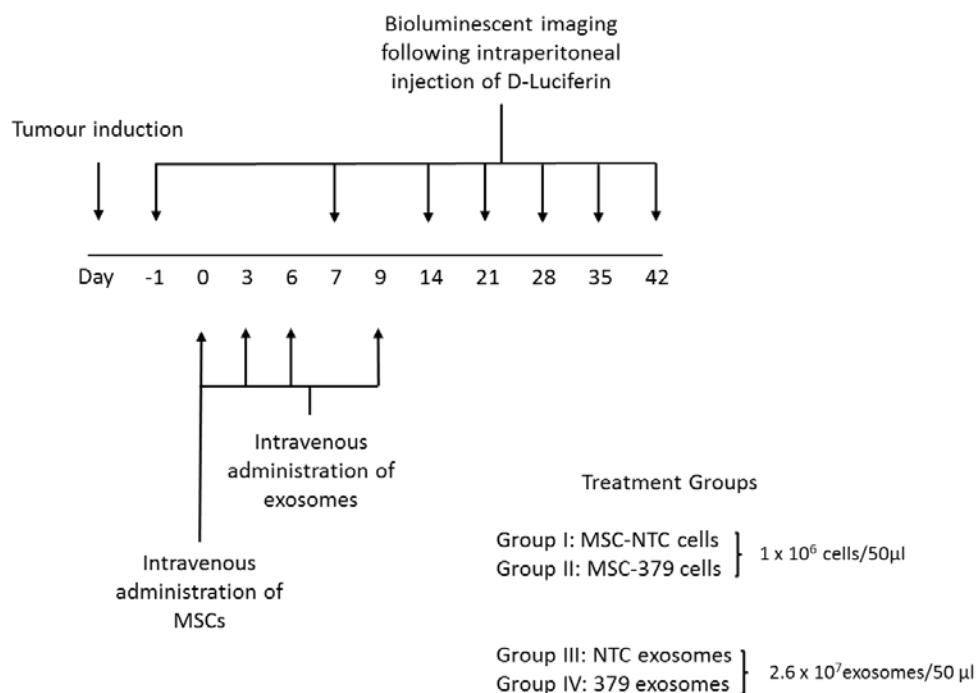


Figure 2. 14: Outline of *In vivo* study timeline

2.4.5.1 Bioluminescence Imaging:

Throughout the course of the study, mice were imaged weekly using an *In vivo* imaging system (IVIS) (PerkinElmer). Imaging was performed 12 min following intraperitoneal injection of 200 μ l D-Luciferin at a concentration of 15 mg/ml to achieve optimal activity of the reaction. This assay functions through the catalyzation of D-Luciferin by luciferase resulting in the emission of light as outlined below [230].



The mice were subsequently anaesthetised and maintained under anaesthetic throughout the course of the imaging. Images were stored and activity of the tumours calculated based on light emission. Regions of interest were automatically selected to ensure consistent selection. Measurements were recorded using Living Image Software 3.2 (IVIS Imaging Systems) (Perkin Elmer).

2.4.5.1 Study Endpoint:

Tumour growth was monitored throughout and the study was terminated 6 weeks following the first administration of a therapy. A terminal bleed was performed as outlined in Section 2.4.3.3 and animals were sacrificed through CO₂ inhalation as outlined in 2.4.3.4. Primary tumours were harvested and those large enough were divided between RNAlater[®] and 10% Formalin for subsequent analysis. Enlarged tumour draining lymph nodes were collected in 10% Formalin for future analysis.

2.5 Histological Analysis

2.5.1 Tissue processing and embedding:

Tissues were fixed in 10% Formalin for at least 72 hours at RT to ensure thorough fixation before processing. The fixed tissue samples were processed using the Leica ASP300 tissue processor. This automated process begins by dehydrating the tissue samples through immersion in 70% ethanol for 1 hour followed by a 95%/5% mixture of ethanol and methanol for a further hour. Once complete, the samples then go through four changes of 100% ethanol for 1 hour, 1 hour 30 min, 1 hour 30 min, and finally 2 hours. Following from this, the samples were cleared of ethanol by washing in Xylene in two steps that consisted of 1 hour each. This

facilitated embedding of the samples in paraffin wax twice for 1 hour each. The samples were removed from the tissue processor and immediately fixed in wax using the embedding station. Tissue samples were placed in a mould of an appropriate size. The wax was melted at 58 °C and the sample was embedded into the molten wax. After this, the cassette and mould were placed onto ice in order to solidify the wax. Once solidified, the wax moulds were removed and the embedded samples were stored in the dark at RT until required for further use.

2.5.2 Sectioning of tissue:

For analysis of embedded tissue, samples were initially sectioned using a microtome microTec cut 4055. To optimise sectioning of the samples, the wax embedded tissue was placed on ice prior to sectioning. A microtome blade MX35 35° cutting angle (Thermo Scientific Shandon) was always used throughout and replaced once the blade began to blunt. Forceps used for guiding the sectioning of the tissue were also kept on ice before use. Samples were mounted on the microtome and secured before beginning the sectioning of the tissue. It was necessary to remove the excess wax of the sample prior to sectioning. This was achieved through adjustment of the microtome to obtain sections 30 µm in thickness until full plane sections of the tissue were visible. When cutting the desired section of the tissue the microtome thickness was adjusted to 5 µm. Slices were smoothly sectioned and using a cold forceps the tissue samples were carefully placed into a 37 °C water bath. Floating samples were then placed on the Superfrost™ plus slides (Thermoscientific) where they were stored at 37 °C overnight to allow the samples to dry. Samples were removed the following day and stored in slide folders until required for further experimentation.

2.5.3 Haematoxylin and Eosin Staining:

For initial analysis of morphology of the tissue sections, Haematoxylin and Eosin (H & E) staining was performed. This causes nuclear staining through the formation of the complex hemalum which is formed by aluminium ions and oxidized haematoxylin [231]. This targets the nuclei of cells while the eosin Y counterstains eosinophilic structures. This results in a purple and pink contrasting stain that allows assessment of the morphology of the tissue.

Prior to staining of the tissue, a 1 % Eosin Y solution was made up using 10 g of Eosin Y, 200 ml dH₂O and 95% ethanol. This was thoroughly mixed and left at RT.

A working solution of 0.25% Eosin Y solution was made up using 250 ml of the 1% Eosin Y stock solution, 750ml of 80% ethanol and 5 ml of glacial acetic acid and stored at RT. Mayer's Haematoxylin (Sigma) was used for the staining of tissue samples. For staining, tissue sections were placed in a holder and were immersed in 2 changes of xylene for 10 min each to deparaffinise the samples. This was carried out within a LAF fume hood to prevent inhalation of any fumes released from the xylene. Sections were removed from the fume hood and rehydrated in 2 changes of 100% ethanol which lasted 5 min each before further changes in 95% and 70% ethanol for 2 min each. Sections were then placed into distilled water (dH₂O) before immersion in haematoxylin for 8 min. This timing is crucial as any longer will result in over staining of the tissue sections. The stained sections were placed in warm running tap water for 10 min and rinsed in dH₂O. Samples were dipped in 95% ethanol ten times prior to staining with eosin Y for 45 sec. Timing, again, is crucial to achieve optimal staining of the tissue sections. This was followed by dehydration in 95% ethanol and two changes of 100% ethanol which last 5 min each. Finally, to mount the tissue sections in DPX, the samples were immersed in two washes of xylene for 5 min each. DPX was used to mount the tissue sections to preserve the staining and mounted sections were allowed to dry at RT overnight.

2.5.4 Fluorescent staining of tissue samples:

As transduced cells used for tumour formation in groups 1-4 express red fluorescent protein (RFP) it would be possible to view infiltration of these cells into the lymph node by fluorescence microscopy. For this, 5 µm thick sections of sentinel lymph nodes harvested from the animals were stained with fluorescent nuclear dye DAPI. All the following work was carried out under protection from light where possible. For this, sectioned tissue samples were deparaffinised in xylene through two changes lasting 5 min each and subsequently rehydrated in two changes of 100% ethanol for five min each and finally 95% and 70% ethanol for 2 min each. Sections were then placed in PBS for three washes lasting five min each. Following this, sectioned tissue was immersed in a 1 µg/ml solution of DAPI for 4 min. Samples were immediately placed in another 3 rinses of PBS lasting 5 min each. Samples were dehydrated in 95% ethanol for 5 min and two washes of 100% ethanol for 5 min each before two final immersions in xylene for 5 min each. Sections were then mounted using DPX mounting medium and allowed dry

overnight under protection of light within the fume hood and stored until visualised by fluorescence microscopy using the Olympus BX60.

2.5.5 Immunohistochemistry:

Immunohistochemistry (IHC) was carried out to determine the expression of a variety of proteins of interest. All IHC experimentation was carried out using the Ventana Discovery system. This automated system ensured consistent and robust staining of the tissue. Many solutions are employed by the system to obtain optimal staining such as EZ prep solution, which is used to remove paraffin from the tissue sections. Liquid coverslip (LCS) provides a barrier between the reagents and the air which prevents evaporation of reagents and ensures a stable environment throughout the protocol. The reaction buffer provided is a Tris based buffer solution at pH 7.6 which is used to wash slides between each staining step. Furthermore, a DADMap™ kit allows detection of the antibody and consists of Copper D, DAB H₂O₂ D™, DAB D™, SA-HRP D, Blocker D™ and Inhibitor D™ all of which are stored at 4°C until required. Each section is also counterstained with haematoxylin and a bluing reagent. Two solutions were involved with pre-treatment of the tissue sections required for antigen retrieval. CC1 solution was a pH 8 pre-treatment solution while CC2 was at pH 6.

Labels were printed and placed onto each slide for a run with a maximum of 20 spaces available. For each run carried out, a positive and negative control tissue section were included (Table 2.5). The positive control tissue is derived from an organ with high expression of the target protein to ensure effective binding of the antibody. This ensures that any issues witnessed throughout the run are not related to the functionality of the antibody. A negative control section is an identical section of tissue and this does not receive any primary antibody but receives the same secondary antibody as every other section in the run. This was used as comparison for each section in the run to ensure any positive staining witnessed in the experimental samples are not artefacts of background staining of the secondary antibody. It was essential to have a positive and negative control slide for each antibody and each run carried out on a group of samples. Primary and secondary antibodies were applied manually at designated intervals with details of the antibodies used outlined in Table 2.5. Once the run was completed the slides were removed, placed in a holder, and immediately immersed into warm water containing a detergent in order to clean the slides. The sections were

Chapter 2: Materials and Methods

dipped twenty times and placed under running tap water until all detergent was removed. Samples were dipped 40 times in 70%, 95% and 100% ethanol in order to dehydrate the tissue sections. Sections were then immersed in xylene within the LAF hood twice for 3 min and subsequently mounted using DPX. Mounted sections were then left overnight within the fume hood at RT before subsequent analysis by light microscopy.

Antibody Target	Abcam Code	Dilution	Control Tissue	Pre-treatment Buffer
Cyclooxygenase-2 (COX-2)	ab52237	1/200	<i>Ex Vivo</i> Breast tumour sample	CC1
CD31	ab28364	1/50	Tonsil	CC1
Proliferating Cell Nuclear Antigen (PCNA)	ab2426	1/500	Patient breast tumour sample	CC1
Goat anti-Rabbit IgG (HRP)	ab6721	1/500	N/A	N/A

Table 2 5: Primary and Secondary antibody information Abcam: Supplier used

Chapter 3

Circulating miRNAs as Biomarkers of Breast Cancer

3.1 Introduction:

A minimally invasive method for detecting the presence of cancer would aid in reducing the health burden of the disease on a global scale [232]. Currently, there is a lack of an effective circulating biomarker of disease for patients suffering with breast cancer. miRNAs are molecules that many believe hold the key to such accurate and sensitive detection of the malignancy. These short, non-coding strands of RNA play a key role in many disease processes [233]. As a result of this, miRNAs are often dysregulated in cancer allowing these molecules to serve as ideal circulating biomarkers [234]. These molecules are believed to be tissue specific which is crucial in the detection of cancer [58]. miRNAs originating from an epithelial cancer type were shown to be stably present in the circulation of patients for the first time in 2008 [124]. In this report, patients with prostate cancer could be determined from healthy controls with significant specificity and sensitivity when analysing circulating levels of miR-144. Despite publication of this promising data almost a decade ago, miRNAs have yet to be routinely utilised in a clinical setting.

This may, in part, be due to the current lack of standardisation between different research groups. As it stands, circulating miRNAs can be analysed in either whole blood, serum or plasma. All three starting materials have been employed for analysis by many different groups (Introduction, Table 1.3). However, few have rationalised the choice of starting material used. Variances in results have been witnessed in the field which may result from different starting materials employed. For example, miR-10b was reported to be significantly elevated between breast cancer patients and controls in serum, which was not reflected in the whole blood when performed in a different study [67, 235]. Certain miRNAs, such as miR-16 and miR-451, are known to be strongly associated with cells present in the circulation, such as erythrocytes due to the miRNAs role in erythropoiesis [236, 237]. For this reason, much of the literature to date has focused on analysing the miRNA content in cell free sources, serum and plasma. When analysing cell free sources, a point worthy of consideration is haemolysis. This is the rupturing of erythrocytes which subsequently results in the release of miRNAs. Both serum and plasma samples that have suffered haemolysis prior to isolation, may be contaminated by the erythrocyte associated miRNAs [121].

Haemolysed samples can impact results seen within a study when not taken into consideration.

There are also variations evident in methods of collection, storage, extraction and normalisation of data when analysing circulating miRNAs. Collection and storage of whole blood can range from EDTA tubes to PAXgene™ tubes stored at either -80°C or 4°C [67, 73]. Extraction methods can also vary between column and chemical based methods of extraction (Table 1.4). A large array of miRNAs or other molecules have been employed for data normalisation which can have a significant impact on results (Table 1.5). Differing approaches to analysis would not be an issue if it did not result in contradictory results published in the literature. This variation in approaches to analysing circulating miRNAs is stagnating progression into the clinical setting.

Based on previous analysis of miRNAs as biomarkers carried out within this group, further studies were performed analysing miR-138, miR-504 and miR-379 in different populations of individuals to determine any potential as circulating biomarkers of breast cancer[128, 129].

3.2 Aims:

The aims of this study were:

- To determine the potential of miR-138 and miR-504 as circulating biomarkers of breast cancer in EDTA collected whole blood.
- To evaluate the impact that starting material, method of collection, storage and extraction has on the circulating miRNA profile
- To analyse the potential of miR-138, miR-504 and miR-379 as circulating biomarkers of breast cancer in PAXgene™ collected whole blood.

3.3 Materials and Methods

3.3.1 Ethical Approval:

For this study, whole blood (EDTA n=73, PAXgene™ n=94), serum (n=28) and plasma samples (n=28) were obtained from patients with breast cancer and healthy volunteers following ethical approval and informed consent.

3.3.2 Patient Clinicopathological Details:

Patient details for whole blood samples collected in EDTA tubes as shown in Table 3.1. Patient samples are representative of a population with majority of cancers of Luminal A subtype and similar numbers of and Luminal B, Basal and HER2.

	<i>Patients</i> <i>n=40</i>	<i>Controls</i> <i>n=33</i>
Median Age (Range)	57(43-86)	35(24-79)
Epithelial Subtype		
<i>Luminal A</i>	27	
<i>Luminal B</i>	4	
<i>Basal</i>	5	
<i>HER2</i>	4	
Tumour Grade		
1	3	
2	22	
3	15	
Menopausal Status		
<i>Pre</i>	6	24
<i>Peri</i>	12	2
<i>Post</i>	22	7

Table 3. 1: Patient clinicopathological details on EDTA collected whole blood

3.3.3 Sample Collection and Analysis:

Whole blood samples were either collected in EDTA tubes and subsequently stored at 4°C, or PAXgene™ tubes and subsequently stored at -80°C. Serum samples were collected in serum separating tubes while plasma samples were collected in EDTA tubes and then centrifuged and separated as described in Section 2.1.2. The RNA was extracted from PAXgene™ collected whole blood using the PreAnalytix kit while the modified TRIzol™ BD method was used for RNA extraction from EDTA collected whole blood (Section 2.1.2.2). The miRCURY™ kit was used to extract the RNA from both serum and plasma samples. All extracted RNA was quantified using the NanoDrop Spectrophotometer and samples were stored at -80°C. RQ-PCR was carried out following reverse transcription of each sample. Data was normalised to miR-16 as an endogenous control as previously reported in whole blood analysis [67]. miRNA expression was calculated using the $\Delta\Delta C_t$ method [222].

3.4 Results:

3.4.1 Analysis of Circulating miR-138 in EDTA Collected Whole Blood:

The circulating level of miR-138 was analysed in the EDTA collected whole blood of both healthy controls (n=33) and patient samples (n=40, Figure 3.1). miR-138 was detectable in every sample and was not significantly changed in the whole blood of patients with breast cancer (Mean \pm SEM, 1.36 ± 0.04 , Log_{10}RQ miR-138) when compared to healthy controls (1.48 ± 0.05 , Log_{10}RQ miR-138, 2 Sample T-test, $p = 0.06$).

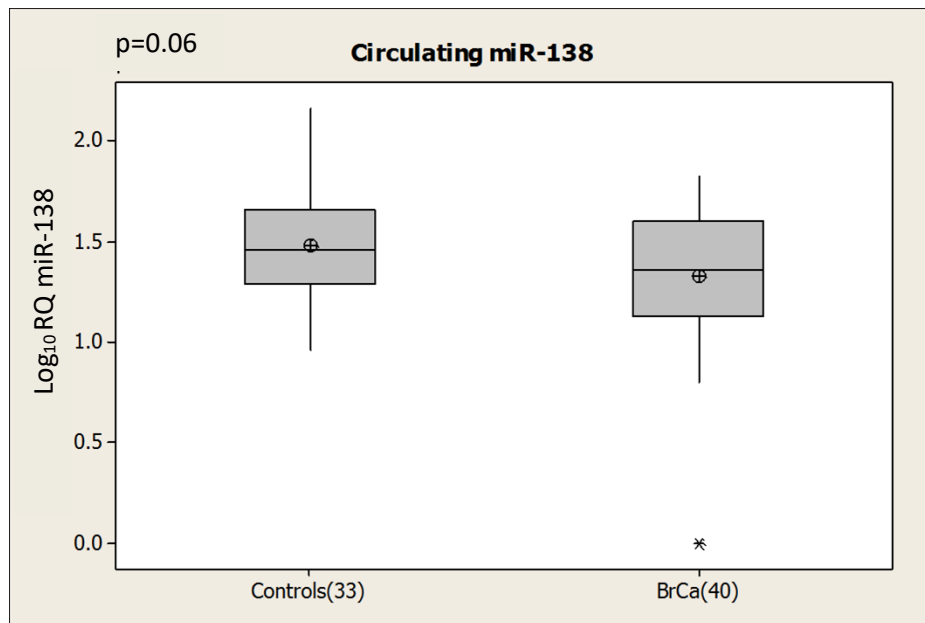


Figure 3. 1: miR-138 levels were not significantly altered in whole blood of breast cancer patients (n=40, 1.36 ± 0.04 , Log_{10}RQ miR-138) and healthy controls (n=33, 1.48 ± 0.05 , Log_{10}RQ miR-138, 2 Sample T-test, $p = 0.06$). Central horizontal line represents the median, ⊕ represents the mean and the vertical lines represent the minimum and the maximum of the data

3.4.2 Analysis of Circulating miR-504 in EDTA Collected Whole Blood:

Circulating levels of miR-504 were analysed in EDTA collected whole blood from healthy controls (n=33) and patient samples (n=40, Figure 3.2). miR-504 was detectable in all healthy control samples and 38 out of 40 (95%) patient samples. This was shown to be significantly increased in patients with breast cancer (Mean \pm SEM, 1.53 ± 0.09 Log_{10}RQ miR-504) when compared to healthy controls (0.91 ± 0.08 Log_{10}RQ miR-504, 2 Sample T-test $p=0.000$). miR-16 was used as an endogenous control and samples that expressed the miRNA within the Ct range of 14-16 were used for data normalisation.

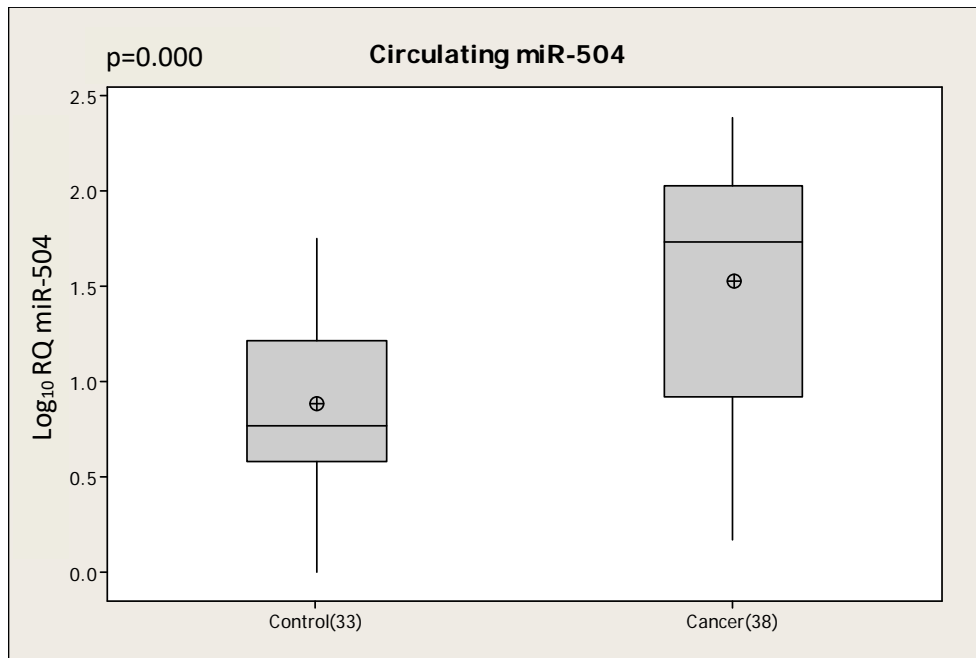


Figure 3. 2: miR-504 levels were significantly elevated in whole blood of breast cancer patients ($n=38$, 1.53 ± 0.09 Log₁₀RQ miR-504) when compared to healthy controls ($n=33$, 0.91 ± 0.08 Log₁₀RQ miR-504, 2 Sample T-test $p=0.000$). Central horizontal line represents the median, ⊕ represents the mean and the vertical lines represent the minimum and the maximum of the data

3.4.3 Impact of Collection, Storage and Extraction Method on miRNA Profile:

Due to the variability in miR-16 expression in initial analyses in EDTA collected whole blood, the miRNA was analysed in EDTA collected whole blood ($n=50$) and PAXgene™ collected samples ($n=50$) (Figure 3.3). miR-16 was analysed in a cohort of patients and healthy individuals. EDTA collected whole blood was stored at 4°C while PAXgene™ samples, once processed, were stored at -80°C. In PAXgene™ collected whole blood samples miR-16 expression ranged from 14-16 Ct, while in EDTA collected samples miR-16 expression ranged from 14-34 Ct (Figure 3.3).

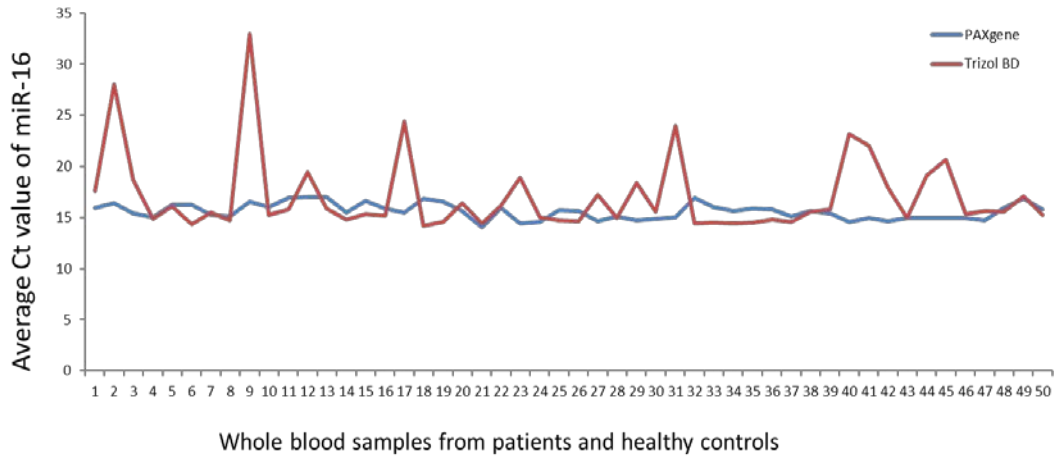


Figure 3. 3: miR-16 expression in EDTA collected whole blood and RNA extracted by modified TRIZOL™ BD method (n=50, Red line -). PAXgene™ collected whole blood and RNA extracted by PreAnalytix method (n=50, Blue line -). Whole blood from healthy individuals (samples 1-25) and patients (samples 26-50)

3.4.4 Impact of Starting Material on Endogenous Control Profile:

Due to the fluctuating levels of miR-16 expression in EDTA collected whole blood (Figure 3.3) all subsequent analysis of whole blood was carried out on PAXgene™ collected samples. The impact of starting material on the expression profile of miR-16 was analysed in matched PAXgene™ whole blood (n=28), serum (n=28) and plasma samples (n=28) (Figure 3.4). miR-16 was detectable in every sample analysed. However, miR-16 values were more variable in plasma (Ct range: 17-27) and serum (Ct range: 18-26) than in PAXgene™ stabilised blood (Ct range: 14-16) from the same individuals.

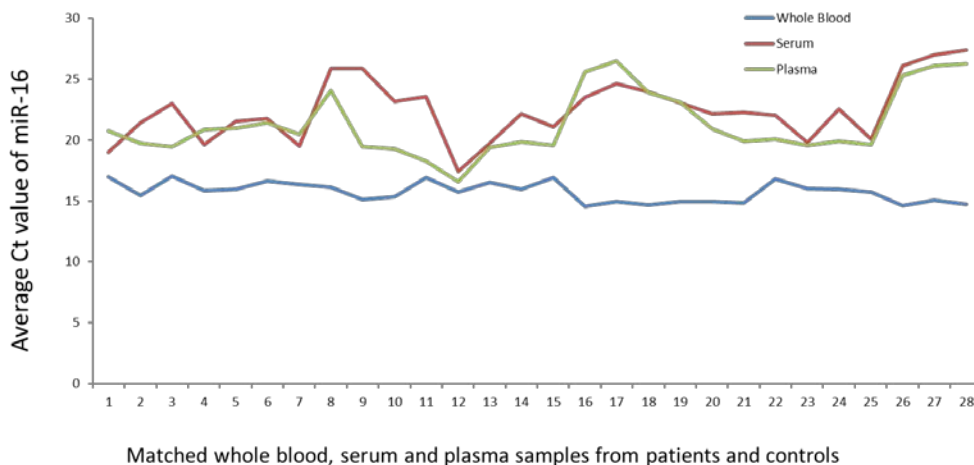


Figure 3. 4: Analysis of range of miR-16 expression in whole blood (n=28, 14-16 Ct), serum (n=28, 18-26 Ct) and plasma (n=28, 17-27 Ct) from healthy individuals (samples 1-14) and patients (samples 15-28)

3.4.5 Detecting Haemolysis in Cell-Free Sources:

As miR-16 is associated with red blood cells and PAXgene™ lyses all red blood cells, miR-16 was expressed highly in each whole blood sample. Serum and plasma samples, lacking erythrocytes, had lower (higher Ct value) expression of miR-16. However, in sample 12, miR-16 expression in serum, plasma and whole blood samples were observed to be closely associated (Figure 3.4). To determine if the samples were haemolysed, known markers of haemolysis and miRNAs associated with erythrocytes miR-144 and miR-451, were measured in these samples [121, 238] (Table 3.2). Serum and plasma that was potentially haemolysed (Sample 12) was compared to two samples of serum and plasma that did not appear to be haemolysed (Sample A, B). While miR-144 expression did not change in sample 12, miR-451 expression was slightly increased in both serum and plasma. Along with the increase in miR-16 expression observed, it would suggest that Sample 12 was haemolysed.

	miR-16 (Avg. Ct.)		miR-144(Avg. Ct.)		miR-451(Avg. Ct.)	
	Serum	Plasma	Serum	Plasma	Serum	Plasma
Sample A	22	21	32	32	24	25
Sample B	22	21	30	30	24	24
Sample 12	17	17	30	30	20	23

Table 3. 2: Measuring miR-16, miR-144 and miR-451 for presence of haemolysis in serum (n=3) and plasma (n=3) samples

3.4.6 Qualitative Analysis of the Impact of Starting Material on Circulating miRNAs:

A panel of miRNAs were then examined to assess whether all miRNAs were present in each starting material. miR-138 was examined in the same cohort of matched whole blood (n=28), serum (n=28) and plasma samples (n=28) (Figure 3.5). In this cohort, miR-138 was detectable in all whole blood samples i.e. 28 of 28 (Ct range 30 -34), while being present in 19 of 28 serum samples (Ct range 35 - 39) and 22 of 28 plasma samples (Ct range 33 - 39).

Chapter 3: Circulating miRNAs as Biomarkers of Breast Cancer

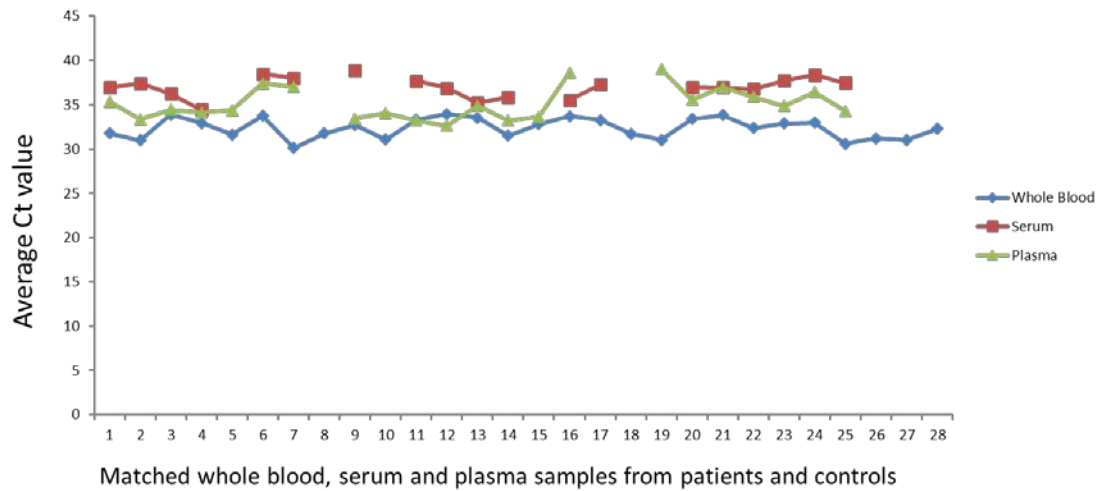


Figure 3. 5: Qualitative analysis of miR-138 in whole blood (n=28), serum (n=28) and plasma (n=28). miR-138 was detectable in every whole blood sample analysed, 19/28 serum samples and 22/28 plasma samples analysed

miR-504 was examined in the same cohort of whole blood, serum and plasma samples (total n=84, Figure 3.6). When analysing miR-504 it was detectable in all whole blood samples (Ct range 29 – 35), 13 of 28 serum samples (Ct range 36 – 39) and 21 of 28 plasma samples (Ct range 32 – 39).

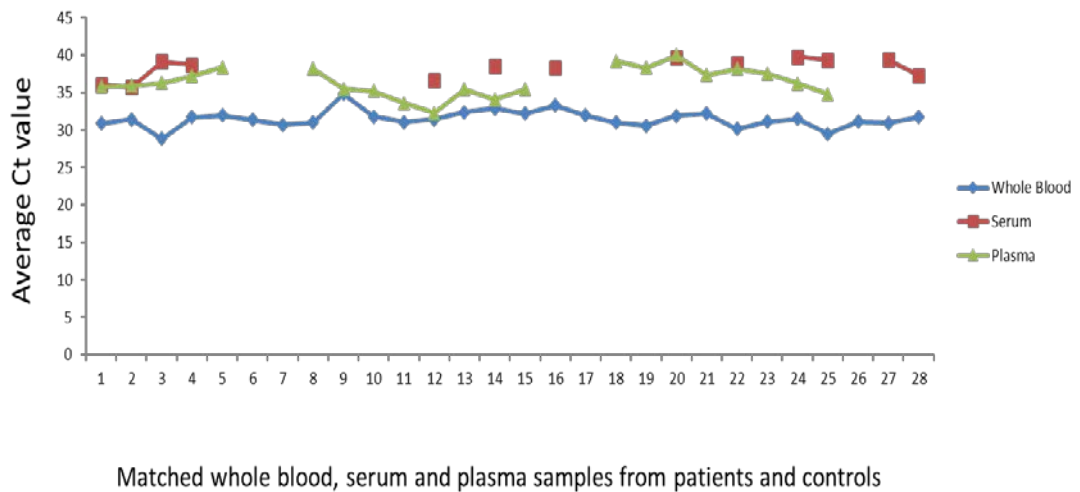


Figure 3. 6: Qualitative analysis of miR-504 in whole blood (n=28), serum (n=28) and plasma (n=28). miR-504 was detectable in all whole blood samples, 13/28 serum samples and 21/28 plasma samples

Lastly, due to exhaustion of certain samples in the cohort, miR-379 was analysed in whole blood, serum and plasma samples (total n=72, Figure 3.7). Unlike

previously analysed miR-138 and miR-504, miR-379 was detectable in all whole blood (Ct range 30 – 36), serum (Ct range 30 – 38) with the highest levels of detection in the plasma (Ct range 27 – 37).

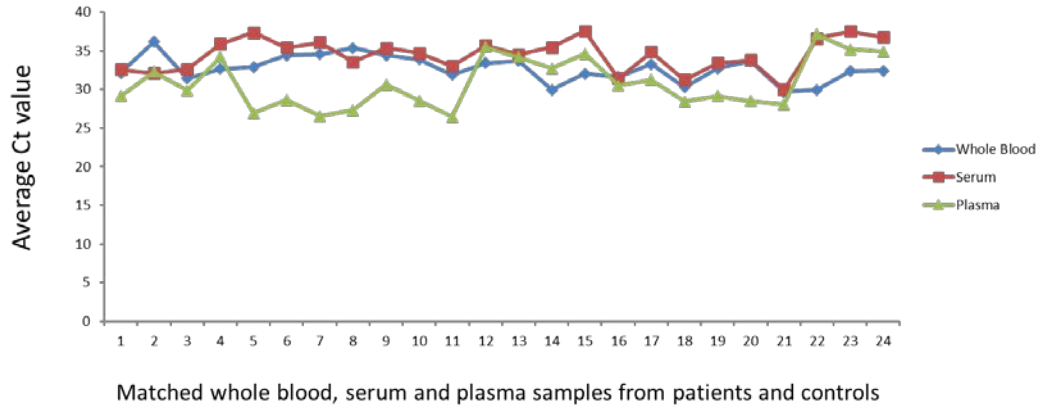


Figure 3. 7: Qualitative analysis of miR-379 in whole blood (n=24), serum (n=24) and plasma (n=24). miR-379 was detectable in every whole blood, serum and plasma sample analysed

3.4.7 miR-138 as Potential Biomarker of Breast Cancer:

Following from these analyses, PAXgene™ collected whole blood samples were used for subsequent biomarker analyses as opposed to EDTA collected whole blood samples analysed initially (Figure 3.1, 3.2). miR-138 was analysed in another cohort of healthy controls (n=44) and patients with breast cancer (n=50), clinicopathological details (Table 3.3). Patient demographics are representative of the population with a slight enrichment for the Basal subtype.

	Patients n=50	Controls n=44
Median Age (Range)	58(32-82)	29.5(20-82)
Epithelial Subtype		
Luminal A	31	
Luminal B	5	
Basal	10	
HER2	4	
Tumour Grade		
1	3	
2	28	
3	17	
N/A	2	
Menopausal Status		
Pre	13	31
Peri	7	2
Post	30	11

Table 3. 3: Patient clinicopathological details on PAXgene™ collected whole blood

Data was normalised to the endogenous control miR-16 which was stably expressed throughout the cohort (14-16 Ct). There was no significant change (2 Sample T-test, $p=0.25$) in expression of miR-138 between patient (Mean \pm SEM, 0.77 ± 0.05 Log₁₀ RQ miR-138) and control samples (0.68 ± 0.05 Log₁₀ RQ miR-138, Figure 3.8).

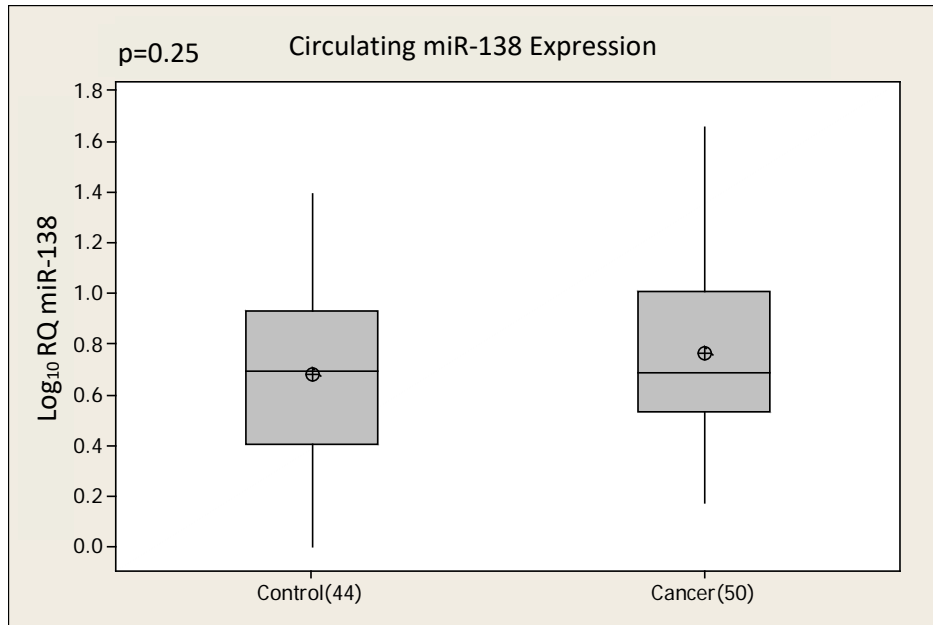


Figure 3. 8: miR-138 was not dysregulated in controls ($n=44$, 0.68 ± 0.05 Log₁₀ RQ miR-138) and patients with breast cancer ($n=50$, 0.77 ± 0.05 Log₁₀ RQ miR-138, 2 Sample T-test, $p=0.25$). Central horizontal line represents the median, \oplus represents the mean and the vertical lines represent the minimum and the maximum of the data

The cancer samples were then divided based on epithelial subtype to establish any association between miR-138 and a particular breast cancer subtype (Figure 3.9). There was not significant change in miR-138 expression witnessed across the breast cancer subtypes (ANOVA, $p=0.34$). miR-138 expression appears slightly elevated in the HER2 subtype and may be strengthened if numbers were increased. miR-138 expression was also analysed across the grades of the tumour (Grade 1-3) and no significant difference was witnessed (ANOVA, $p=0.38$, Data not shown).

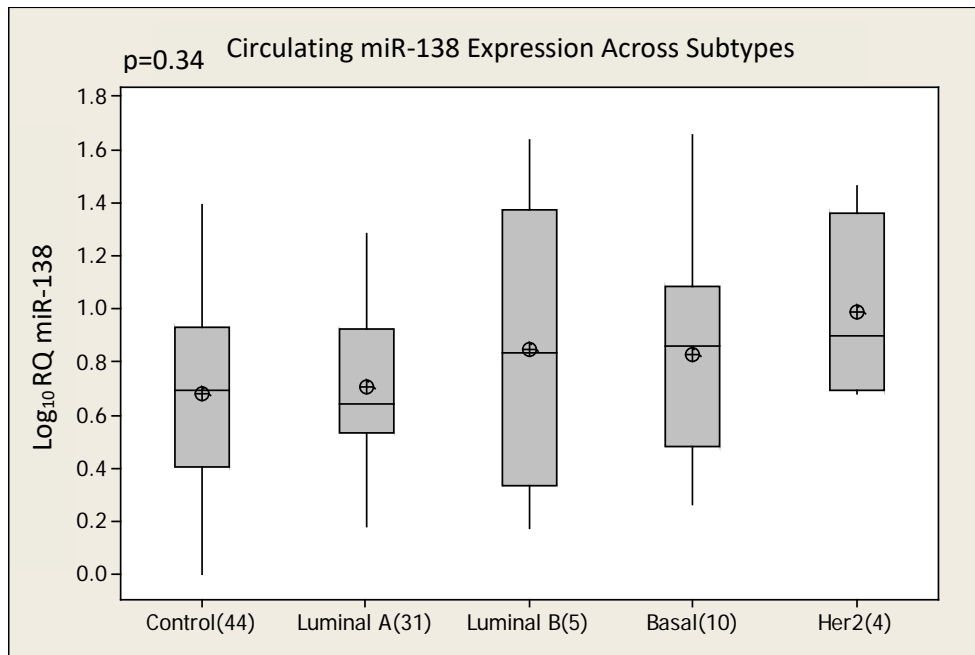


Figure 3. 9: miR-138 was not dysregulated between healthy controls and across each subtype of breast cancer (ANOVA, $p=0.34$). Central horizontal line represents the median, \oplus represents the mean and the vertical lines represent the minimum and the maximum of the data

3.4.8 miR-504 as Potential Biomarker of Breast Cancer:

miR-504 expression was analysed in a similar cohort of healthy controls ($n=44$) and breast cancer patients ($n=49$) (Figure 3.10). miR-504 was found to be significantly increased in patients (Mean \pm SEM, 1.37 ± 0.06 Log₁₀ RQ miR-504) when compared to control samples (1.18 ± 0.07 Log₁₀ RQ miR-504, 2 Sample T-test, $p=0.03$). This data was normalised to miR-16 as it was stably expressed across all samples (range 14-16 Ct).

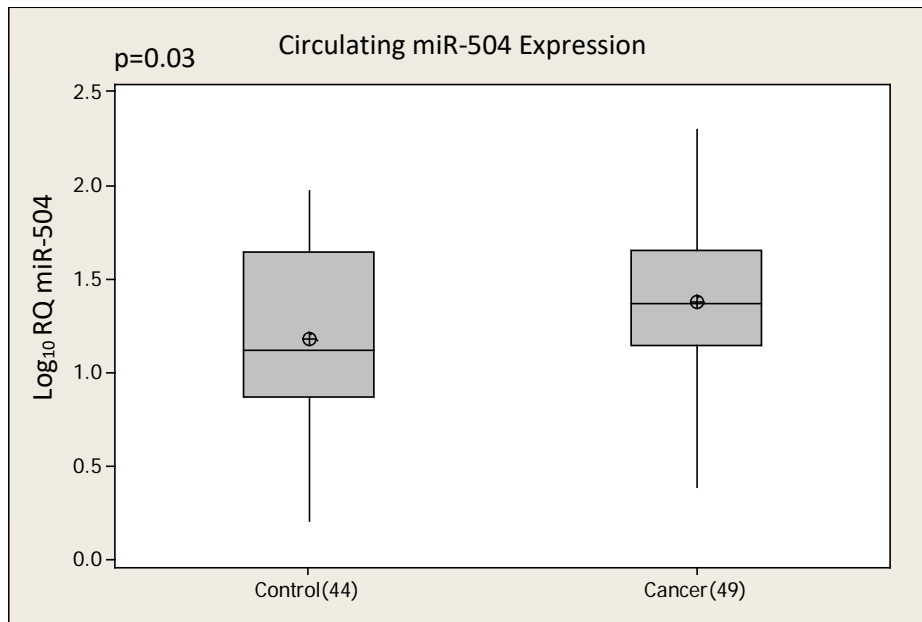


Figure 3. 10: miR-504 expression was significantly increased in patients ($n=49$, $1.37 \pm 0.06 \text{ Log}_{10} \text{ RQ miR-504}$) when compared to healthy controls ($n=44$, $1.18 \pm 0.07 \text{ Log}_{10} \text{ RQ miR-504}$, 2 Sample T-test, $p=0.03$). Analysis of miR-504 expression in healthy controls and patients with breast cancer. Central horizontal line represents the median, \oplus represents the mean and the vertical lines represent the minimum and the maximum of the data

The cancer cohort was then subdivided based on epithelial subtype and miR-504 expression was not significantly dysregulated (ANOVA, $p=0.08$, Figure 3.11). miR-504 expression was also analysed based on tumour grade (Grade 1-3) with no significant difference witnessed (ANOVA, $p=0.61$, Data not shown).

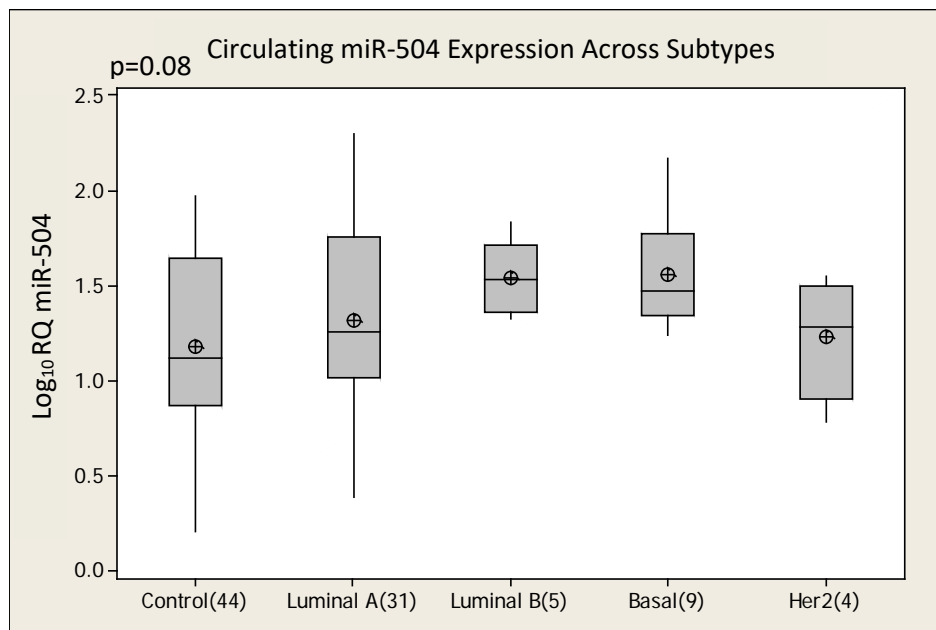


Figure 3. 11: Analysis of miR-504 between healthy controls and breast cancer subtypes revealed no dysregulated expression (ANOVA, $p=0.08$). Central horizontal line represents the median, \oplus represents the mean and the vertical lines represent the minimum and the maximum of the data

3.4.9 miR-379 as Potential Biomarker of Breast Cancer:

Finally, miR-379 was analysed in a cohort of healthy controls (n=44) and breast cancer patient samples that were not exhausted from previous analysis (n=43) (Figure 3.12). There was no significant change in miR-379 expression witnessed between patients (Mean \pm SEM, $2.01 \pm 0.09 \text{ Log}_{10} \text{ RQ miR-379}$) and controls ($1.93 \pm 0.07 \text{ Log}_{10} \text{ RQ miR-379}$, 2 Sample T-test, $p=0.47$).

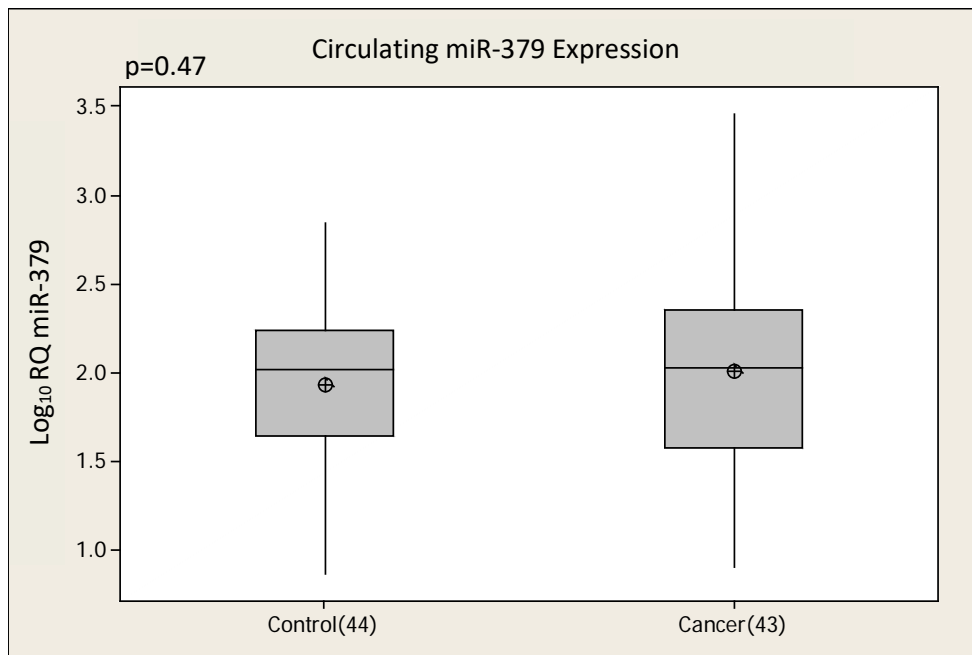


Figure 3. 12: Analysis of miR-379 in healthy controls (n=44, $1.93 \pm 0.07 \text{ Log}_{10} \text{ RQ miR-379}$) and breast cancer patient samples (n=43, $2.01 \pm 0.09 \text{ Log}_{10} \text{ RQ miR-379}$) revealed no dysregulation in expression (2 Sample T-test, $p=0.47$). Central horizontal line represents the median, \oplus represents the mean and the vertical lines represent the minimum and the maximum of the data

Samples were broken down into specific epithelial subtypes and miR-379 expression was analysed (Figure 3.13). miR-379 expression was found to remain stable across subtypes (ANOVA, $p=0.89$). miR-379 expression was also analysed across the grades of the tumour (Grade 1-3) and no significant difference was witnessed (ANOVA, $p=0.56$, Data not shown).

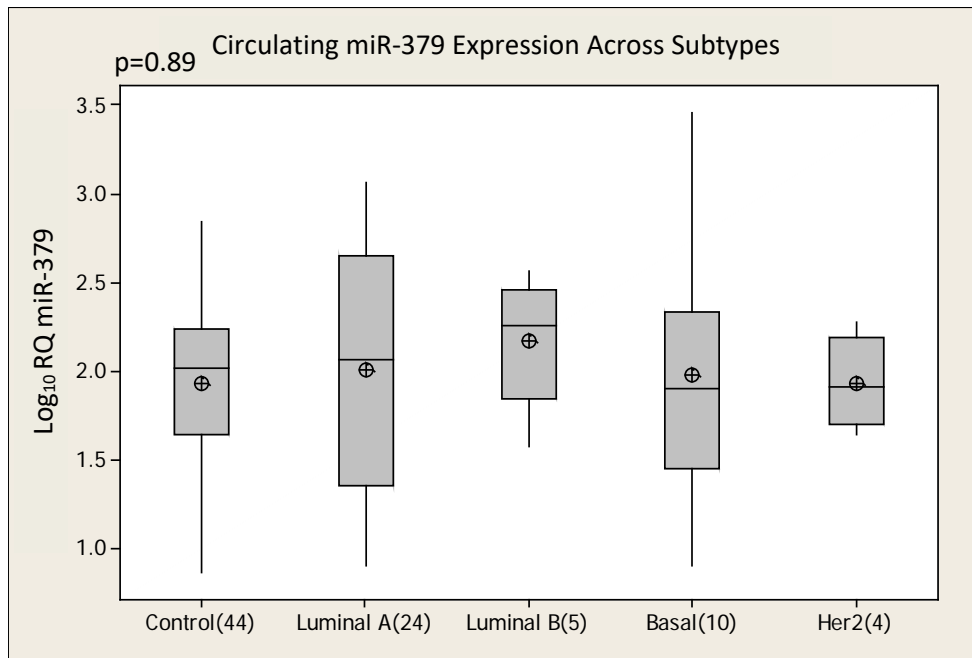


Figure 3. 13: No dysregulation of miR-379 expression in healthy controls and each subtype of breast cancer (ANOVA, $p=0.89$). Central horizontal line represents the median, \oplus represents the mean and the vertical lines represent the minimum and the maximum of the data

3.5 Discussion:

This important study highlights current issues relating to the analysis of circulating miRNAs as potential biomarkers of disease. Variations are evident in many aspects of analysis and this chapter highlights the impact that certain methodological variations have on the miRNA profile in the circulation. These variations could be misinterpreted as being related to the health status of the individual. EDTA collected whole blood stored at 4°C and extracted using the modified TRIZOL™ BD method was used for analysis of miR-138 and miR-504 as biomarkers of breast cancer, similar to previous work performed [67]. Previous reports have shown a significant elevation of miR-138 expression in the circulation of patients with breast cancer while no significant dysregulation was witnessed in this study [128]. The same method of collection and storage was used for the initial analysis in this study and the published work. Analysis of circulating levels of miR-138 in PAXgene™ collected whole blood samples found no significant change in expression of the miRNA. This contradiction between work in this study and the published report may be due to different endogenous controls used, miR-16 vs U6. This may have caused this variation in results as a Ct range of 14-16 was used for both analyses of whole blood samples performed in this study. The published report used EDTA collected whole blood and in this study both PAXgene™ and EDTA collected whole blood were used, which accounts for the difference in

collection and storage. The previously published study did not report the Ct range witnessed for U6 as an endogenous control [128]. This data should always be provided and if investigators ignore fluctuations in endogenous control expression, consistency and reproducibility of findings will remain an issue for circulating miRNAs. Different populations of individuals were also used between both studies. Individuals with different type, stage and grade of disease could account for the contradiction in results. Also, individuals in both populations may suffer from different comorbidities which may impact the pattern of expression of miR-138. Of course, a robust biomarker should maintain a strong pattern of expression despite such factors, suggesting that miR-138 is not a robust circulating biomarker of breast cancer.

Initial analyses revealed significant dysregulated expression of miR-504. Circulating levels of miR-504 have not been published previously and this initial work showing significantly elevated expression of miR-504 in patients with breast cancer highlighted a potentially promising biomarker of disease. In PAXgene™ collected whole blood there was still a significant increase ($p=0.03$) in the expression of miR-504 in patients with breast cancer but not as dramatic as previously witnessed ($p=0.000$). In each study miR-16 expression remained consistent in PAXgene™ collected whole blood and samples did not have to be excluded as a result of fluctuating levels of the miRNA. This emphasises the importance of optimising methods of analysing circulating miRNAs. This is likely to be dependent on the stability of the target miRNA and its abundance in various fractions of blood.

miR-16 has been reported as a stably expressed miRNA in the circulation of patients with breast cancer as well as healthy controls [77]. There were issues relating to miR-16 as an endogenous control as its expression fluctuated throughout the cohort of samples analysed. An endogenous control should exhibit stable expression in a large cohort of samples regardless of the presence or absence of disease. Only samples with miR-16 expression within the Ct range of 14-16 were included for analysis due to the majority of samples falling within this range of expression. The method of storage, collection and extraction of the whole blood samples was investigated as a potential cause of fluctuation witnessed in miR-16 expression in initial studies.

EDTA collected whole blood was compared to PAXgene™ collected whole blood samples, which are immediately mixed with a proprietary preservative, and can be stored at room temperature for up to three days and can be viable up to eight years when stored at -80°C [120]. PAXgene™ samples stored at -80°C and extracted using the recommended PreAnalytix kit were compared to previous methods of analysing circulating miRNAs. miR-16 is widely reported as an endogenous control in whole blood, serum and plasma samples [71, 73, 77, 83, 84, 109, 111, 112]. In the cohort of whole blood samples analysed, miR-16 expression fluctuated in the EDTA collected samples (14-34 Ct) when compared to PAXgene™ collected whole blood (14-16 Ct). Such dysregulation may be due to miRNA stability. Storage of samples at 4°C for 72 hours has been shown to impact miRNA stability [239]. In the published report, it was suggested that miR-16 may be susceptible to such degradation and the miRNA was more stable when frozen. miR-16 expression for frozen PAXgene™ whole blood samples was within a Ct range of 14-16. Such fluctuations in miR-16 expression in whole blood that was EDTA collected, stored at 4°C and extracted using TRIzol™ shows the impact that storage, collection and extraction can have on miRNA expression. Since data is expressed relative to endogenous controls, if this fluctuation were ignored, it could result in reporting a false elevation or decrease in a circulating miRNA that was not related to the patient's health status. It is essential to adhere to appropriate methods of collection and storage of clinical samples as they are such a precious resource and warrant optimal handling to fulfil the potential of each sample. For this reason, PAXgene™ collected whole blood samples were employed for all subsequent analyses in this study.

To determine the impact of starting material on miRNA expression, miR-16 was analysed in matched whole blood, serum and plasma samples. As mentioned, miR-16 has been used as an endogenous control in each starting material and was deemed an appropriate comparator for analysing the impact of different starting materials. Matched whole blood, serum and plasma samples from healthy individuals and breast cancer patients were analysed for miR-16 expression. While the expression profile of the miRNA was similar in serum and plasma samples it fluctuated to such an extent that it would not serve as an effective endogenous control within this group of samples. Such fluctuation in expression was not evident in PAXgene™ collected whole blood which had stable expression of miR-

16. In this particular cohort of serum and plasma samples, miR-16 would not effectively serve as an endogenous control. However, miR-16 expression in PAXgene™ samples would adequately function as an endogenous control. This highlights the importance of identifying an endogenous control specific to the starting material employed.

As miR-16 is associated with erythrocytes its expression can increase following rupturing of red blood cells which occurs during haemolysis [121]. miR-144 has been reported as being associated with erythrocytes and therefore it was thought that the miRNA would increase in cell free sources following haemolysis [238]. This was not evident in the samples analysed (Table 3.3). Analysis of miR-451, a miRNA associated with haemolysis, did increase in expression in one sample when compared to non-haemolysed samples [121]. However, miR-16 expression showed the greatest increase. Previously published work has shown that miR-16 is strongly affected by haemolysis [121]. This data would suggest that this sample was haemolysed. Spectrophotometry can also be performed to determine if a sample is haemolysed through measurement of the absorbance of free haemoglobin [121]. For retrospective analysis of samples with RNA already extracted, miRNAs offer promise for detecting haemolysis. However, the source of miRNAs is not possible to determine and highlights a weakness in utilizing miRNAs as a sole means of determining haemolysis. As spectrophotometry measures haemoglobin it would serve as a more accurate detector of red blood cell lysis. For the best overall results, the combination of analysis of miRNAs such as miR-16 and spectrophotometry approaches would allow for more robust detection of haemolysis.

miR-138, miR-504 and miR-379 were analysed in the same cohort of matched whole blood, serum and plasma samples. miR-138 and miR-504 revealed similar patterns of expression as both miRNAs were evident in 100% of whole blood samples while they were only present in a proportion of serum and plasma samples. However, miR-379 was detected in 100% of whole blood, serum and plasma samples. This highlights the importance of preliminary analysis for a miRNA prior to performing large studies on a particular starting material. Neither serum nor plasma would be appropriate for analysis of miR-138 or miR-504 while whole blood, serum or plasma would be appropriate for analysis of miR-379. This

type of preliminary analysis is currently lacking within the field of circulating biomarkers and consistent approaches to analysis may serve to improve progress from the laboratory into the clinical setting. Again, presence or absence of a miRNA could be incorrectly associated with disease, when it is really reflective of the choice of starting material. The presence or absence of a miRNA in a particular starting material might be as a result of how the miRNA is present in the circulation. Some miRNAs are encapsulated in vesicles such as exosomes and are present in each starting material while cell associated miRNAs would be absent from both serum and plasma [195]. As miRNAs can have short half-lives, processing time is essential and such differences between each starting material may highlight another explanation as to why certain miRNAs are absent in particular samples [122]. As serum samples were required to stand for 30 min to allow for coagulation, this may explain why this blood fraction continuously exhibited the lowest pattern of miRNA expression. While the factors impacting the presence or absence of particular miRNAs in the circulation are important, determining the optimum starting material for a miRNA of interest is essential prior to any large cohort studies are carried out.

Using PAXgene™ collected whole blood samples, an analysis was performed on miR-379 as circulating biomarkers of breast cancer. Previous reports analysed miR-379 expression in whole blood samples collected in EDTA tubes and extracted using the modified TRIzol™ BD method [129]. The published study found no significant dysregulation in the expression of circulating miR-379 which was confirmed in the data presented here (Fig 3.12). Despite different methods of analysis, overall findings in certain cases, can remain consistent.

For a miRNA to reach clinical implementation as a biomarker of breast cancer it must exhibit exceptional sensitivity and specificity in a population of patients and healthy individuals. While it is not possible to obtain a biomarker to identify every individual with cancer it is important to develop a diagnostic tool that will reduce the number of false positive and false negative diagnosis. Such a biomarker should be capable of identifying the presence of breast cancer despite previously existing comorbidities that may affect the circulating profile of miRNAs. In likelihood, one individual miRNA will not serve as a biomarker of breast cancer but rather a panel

of miRNAs, when combined may offer higher sensitivity and specificity than what is currently available.

Different approaches can reveal contrasting results and prevent optimal utilisation of important clinical samples. If using whole blood, collection in PAXgene™ tubes would be recommended where the collection and storage guidelines are strictly adhered to. For plasma and serum collection it is crucial that samples are handled extremely carefully and guidelines for temperature, time and centrifugation are followed rigidly. It is necessary to check and compensate for haemolysis in both plasma and serum samples. It is important to note that each starting material is a viable source, however, certain miRNAs, when quantified by RQ-PCR with a limit of detection of 40 cycle thresholds, are not present at sufficiently high levels to be detected in particular fractions. Therefore, it is necessary to carry out preliminary analysis prior to commencing a large study analysing a particular miRNA in the circulation.

Chapter 4

Evaluation of miR-379 as Tumour Suppressor miR *In vivo*

4.1 Introduction:

Work from this group has shown that expression of miR-379 was significantly reduced in the primary tumour tissue of patients with breast cancer when compared to healthy controls [75]. Another study analysing the miRNA in 30 osteosarcoma tissue samples also found miR-379 to have significantly reduced expression when compared to adjacent non-cancerous tissues [240]. In contrast, one study analysing miR-379 in prostate cancer cell lines showed the miRNA to have increased expression in a metastatic cancer cell line when compared to a less invasive cell population [138]. Contrastingly, this same published study found using a published dataset of clinical samples, [241], that elevated miR-379 expression correlated with patient progression-free survival.

As well as the reduction of miR-379 expression in breast tumours, our group revealed an inverse correlation between the miRNA and a key initiator of mitosis, Cyclin-B1 [129]. This same study showed that transient transfection of miR-379 in a breast cancer cell line resulted in a reduction in cell proliferation. This effect was mirrored in other studies of osteosarcoma and vascular smooth cell lines showing a reduction in proliferation and invasion when miR-379 expression was increased [75, 240, 242]. Despite a number of studies reporting a potential tumour suppressor role for miR-379, the exact mechanism of action remains unclear. To confirm tumour suppressor capacity, it is necessary to show an impact on tumour establishment and progression *In vivo*.

As discussed previously, miRNAs can have multiple gene targets and miR-379 is no exception. Multiple gene targets for the miRNA have been reported in separate disease settings. Predictive algorithms coupled with luciferase reporter assays have suggested that miR-379 targets IL-18 in mesothelioma [137], IL-11 in breast cancer cells [146], PDK1 in osteosarcoma [240] and IGF-1 in vascular smooth muscle cells [242]. miR-379 is located on chromosome region 14q32.31, a region which has been found to be down-regulated in human cancers and accounting for 12-30% of total down-regulated miRNAs [141]. In the literature to date, there is one other example of *In vivo* analysis of the miRNA in any disease setting. One group established an *In vivo* model for osteosarcoma and following injection of a miR-379 mimic directly into the tumour they showed a reduction in tumour growth, tumour weight and reduced Ki67 expression [240].

Predictive algorithms (Targetscan, PicTar, miRBase) suggested a putative binding site for miR-379 on the 3' UTR of the cyclooxygenase-2 (COX-2) mRNA [243-245]. A previous study using genome-wide gene expression analysis found downregulation of COX-2 gene expression (>1.5 fold) 24hrs after transfection of breast cancer cell line, MDA-MB-231, with a miR-379 precursor [146]. While miR-379 was shown to directly inhibit Smad-mediated transcriptional activity by luciferase assay there was no direct targeting of COX-2 shown. As high levels of COX-2 are known to be present in breast tumours the protein remains a desirable therapeutic target [246, 247]. Furthermore, COX-2 expression is also known to positively correlate with an increase in lymphangiogenesis, making it a promising therapeutic target [248, 249]. miR-146a has been shown to target COX-2 and impact both gene and protein expression of the prostaglandin in lung cancer, however miRNA regulation of COX-2 has yet to be shown in the breast cancer setting [250].

4.2 Aims:

The aims of this study were as follows:

- To determine the impact of miR-379 enrichment on breast tumour establishment and progression *In vivo*
- To establish a mechanism of action for miR-379 in an animal model of breast cancer.

4.3 Materials and Methods:

HCC1954 breast cancer cell lines had been previously transduced with a lentivirus resulting in enriched expression of miR-379 (HCC-379) or a non-targeting control sequence (HCC-NTC). The cells were transduced with a lentiviral vector (SMARTchoice shMIMIC) containing a Turbo-RFP promoter, human Cytomegalovirus (CMV) promoter and a puromycin resistance marker (Figure 2.6). Cells were transduced at a multiplicity of infection (MOI) of 2 in the presence of Polybrene (2µg/ml) for 6 hr. 48 hrs following transduction, cells were cultured in the presence of 4µg/ml puromycin for 7 days ensuring positive selection of transduced cells.

Female BALB/c Nude mice (Charles River) received either a right flank subcutaneous (S.C.) injection of 4×10^6 HCC-NTC (n=10) or HCC-379 (n=10) cells. Other mice received a second thoracic mammary fat pad (M.F.P.) injection of 3.5×10^6 HCC-NTC (n=10) or HCC-379 cells (n=10). Mice and tumour growth were monitored over the course of 5 weeks and the mice were sacrificed by CO₂ inhalation. The tumour tissue was harvested immediately into either RNAlater® or 10% Formalin until further required. All animal experiments were licensed by the HPRA, and carried out according to the guidelines of the Institutional Animal Ethics Committee.

Upon resection of the tumour, the tissue was placed directly into 10% formalin. Fixed samples were processed in a Leica ASP300 tissue processor followed by paraffin embedding. Tissue samples were cut to a thickness of 5 µm and subsequently stained with Haematoxylin and Eosin (H & E) or prepared for immunohistochemistry. Immunohistochemistry was performed using the Ventana Discovery system targeting COX-2, CD31 and proliferating cell nuclear antigen (PCNA). Full details are provided in Section 2.5.5.

4.4 Results

4.4.1 Confirmation of HCC1954 Transduction:

Successful transduction of HCC-NTC/379 cells was confirmed by fluorescence microscopy and RQ-PCR (Figure 4.1). An increase in miR-379 expression (376-fold) was confirmed in triplicates of the HCC-379 (Mean \pm SEM, $3.54 \pm 0.16 \text{ Log}_{10}$ Relative Quantity(RQ) miR-379) cell line when compared to the control population HCC-NTC ($1.08 \pm 0.134 \text{ Log}_{10}$ RQ miR-379, Figure 4.1 (a)). Following growth in puromycin for 7 days, red fluorescence was visualised in 100% of both HCC-NTC and HCC-379 cell populations, confirming successful transduction (Figure 4.1 (b)).

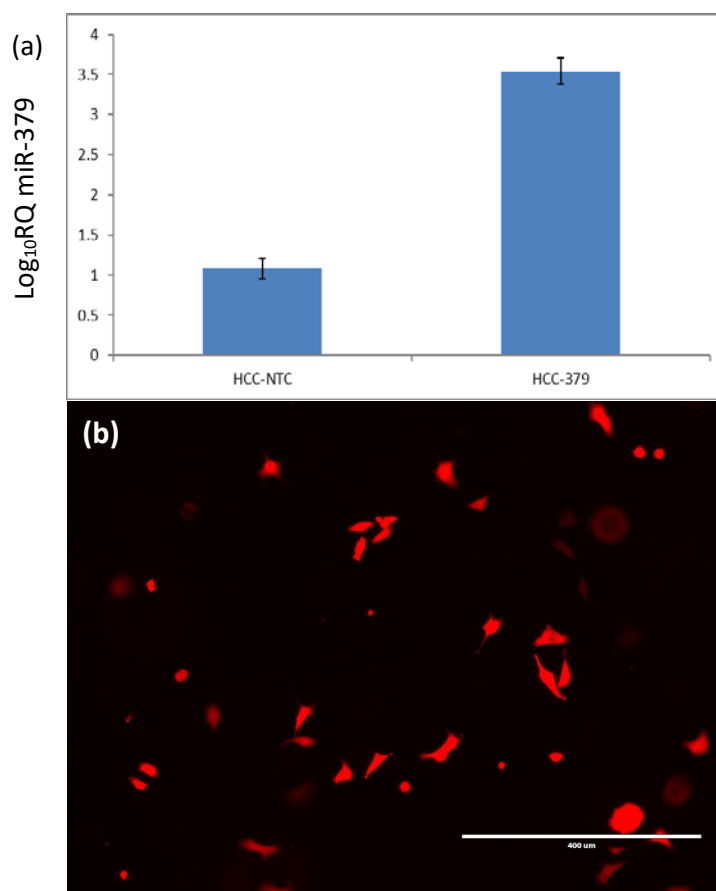


Figure 4. 1: Confirmation of transduction of breast cancer cell line HCC1954 with lentivirus by (a)RQ-PCR analysis of miR-379 expression in HCC-NTC ($n=3$, $1.08 \pm 0.134 \text{ Log}_{10}$ RQ miR-379) compared to HCC-379 cells ($n=3$, $3.54 \pm 0.16 \text{ Log}_{10}$ RQ miR-379) and (b)Visualisation of Red Fluorescing Protein (RFP) in HCC-NTC cells following lentiviral transduction (10X, scale bar 400 μm).

4.4.2 Impact of Transduction on HCC1954 Cell Viability:

Once transduced, an MTS assay was carried out in triplicate to establish any effect that miR-379 enrichment might have on cell viability (Figure 4.2). For analysis, each cell line was normalised to absorbance at 24 hrs as 100% and marked as a percentage change for subsequent 48hr, [HCC-NTC (Mean \pm SEM, $12 \pm 7.65 \%$

increase in cell growth), HCC-379 (46 ± 7.59 % increase in cell growth)] and 72hr timepoints, [HCC-NTC (29 ± 9.71 % increase in cell growth), HCC-379 (67 ± 12.16 % increase in cell growth)]. There was a significant increase in cell proliferation in the HCC-379 cell population when compared to HCC-NTC cells (ANOVA, $p=0.01$) (Figure 4.2).

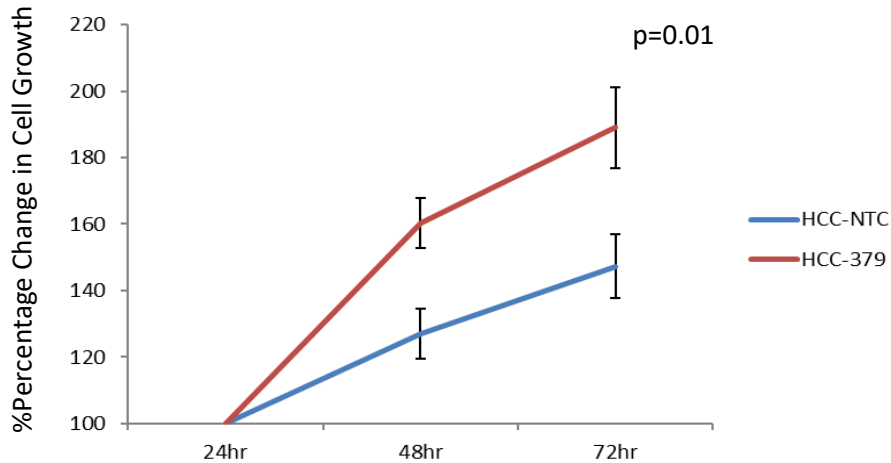


Figure 4. 2: MTS assay showing an increase in cell viability in HCC-379 cells ($n=3$) compared to HCC-NTC cell lines ($n=3$, ANOVA, $p=0.01$) over a 72hr period

4.4.3 Subcutaneous vs Mammary Fat Pad Tumour Administration:

This *In vivo* study administered tumours either subcutaneously (SC) in the right flank of the animal and orthotopically in the second thoracic mammary fat pad (MFP) of the mice. H & E staining of sectioned tumours revealed clear morphological differences between both subsets (Figure 4.3). An apparent increase in the amount stromal like cells within the tumours grown in the MFP environment (Figure 4.3 i-ii) was evident when compared to SC grown tumours (Figure 4.3 iii-iv).

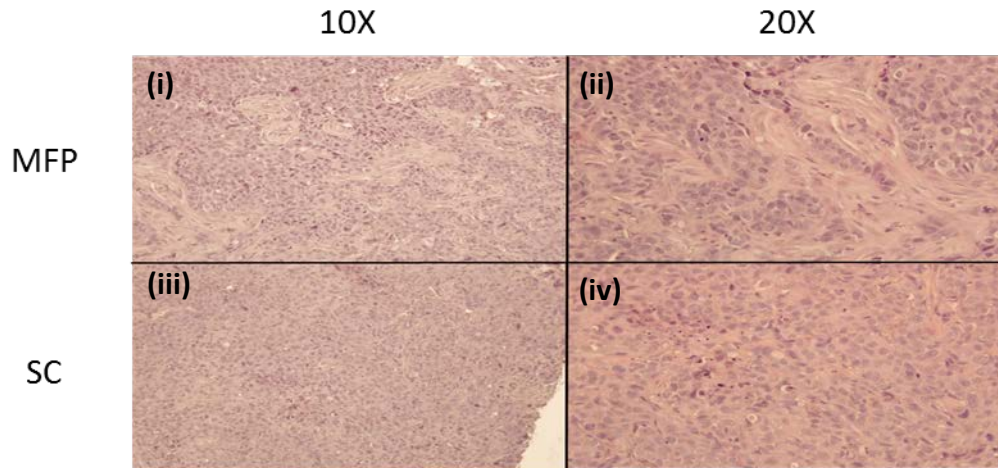


Figure 4. 3: H & E staining of both MFP and SC tumours imaged at 10X and 20X

4.4.4 *In vivo* Imaging of Tumour Vascularity:

Photoacoustic imaging (PAI) was carried out on mice with MFP tumours during the study to analyse the vascularity of the tumour *in situ* (Figure 4.4). This system measured the concentration of oxy (red) and deoxy (blue)-haemoglobin within the tumour. An area devoid of vascularity can be seen in the centre of the HCC-379 tumour (Figure 4.4, B (ii)). Upon resection of tumours, these tumours were found to be fluid filled and an increase in weight was observed in the HCC-379 (Mean \pm SEM, 386.47 \pm 57.38 mg) tumours when compared to the HCC-NTC (89.51 \pm 16.24 mg) tumours ($p=0.000$). The greater weight of the HCC-379 tumours was due to the presence of fluid within the tumours.

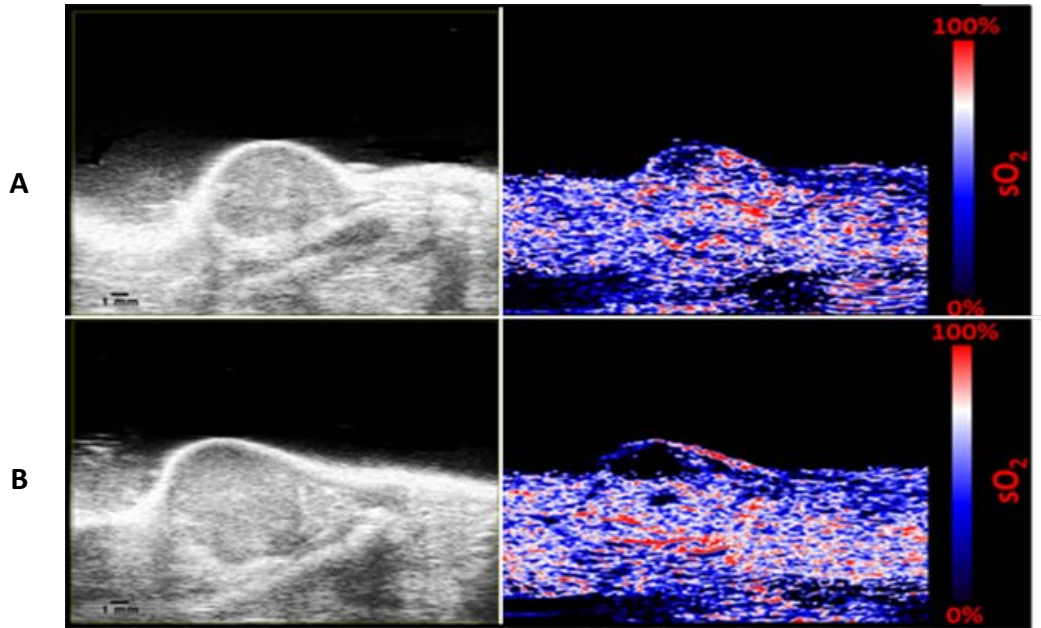


Figure 4. 4: Ultrasound and Photoacoustic images from a HCC-NTC tumour, A (i,ii) and compared to a HCC-379 tumour, B (i,ii). Images taken in the range of 680 – 970 nm allowing for detection of oxy and deoxyhaemoglobin

4.4.5 Histological Analysis of Tumours:

Following tumour resection, samples were H & E stained (Figure 4.5). HCC-379 tumours lacked tissue within the centre of the tumour. Samples were sent to a pathologist to determine any morphological differences between the HCC-NTC and HCC-379 cohorts. Following blinded analysis by collaborating pathologist, Dr. Helen Ingoldsby, a difference in the degree of necrosis was witnessed between both cohorts. There was an increase in the degree of necrosis in the HCC-379 tumours (n=11, $\leq 5-50$, Figure 4.5 (C)) when compared to tumours established from HCC-NTC cells (n=9, %necrosis $\leq 5-20$).

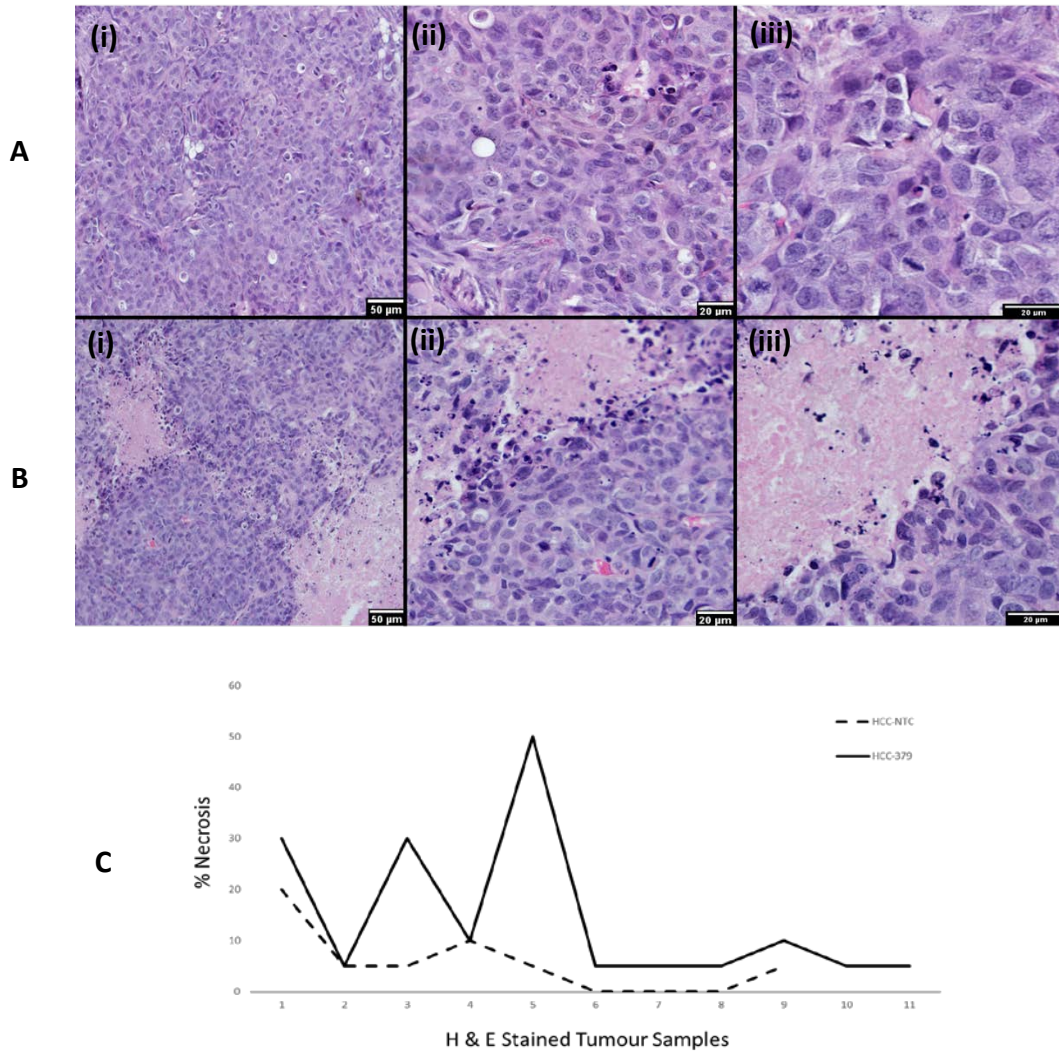


Figure 4. 5: Images from sectioned MFP tumours derived from HCC-NTC, (A) and HCC-379, (B) cells stained for H & E and imaged at 10X (i), 20X (ii) and 40X (iii). (C) Graph of H & E stained tumours scored for necrosis by a pathologist showing an increase in necrosis in HCC-379 tumours (n=11, \leq 5-50% necrosis) when compared to HCC-NTC tumours (n=9, \leq 5-20% necrosis)

4.4.6 Evaluation of Lymph Node Infiltration:

Enlarged sentinel lymph node samples harvested from the animals were also sectioned, DAPI stained and imaged by fluorescence microscopy (Figure 4.6). As both sets of HCC-NTC and HCC-379 tumours were transduced with a lentivirus to ensure expression of RFP, infiltrating tumour cells would be visualised using fluorescence microscopy. An increase in the number of tumour derived RFP-expressing cells was witnessed in the HCC-NTC associated lymph nodes (Figure 4.6(i-iv)) when compared to that of an animal bearing HCC-379 tumours (Figure 4.6 (v-viii)).

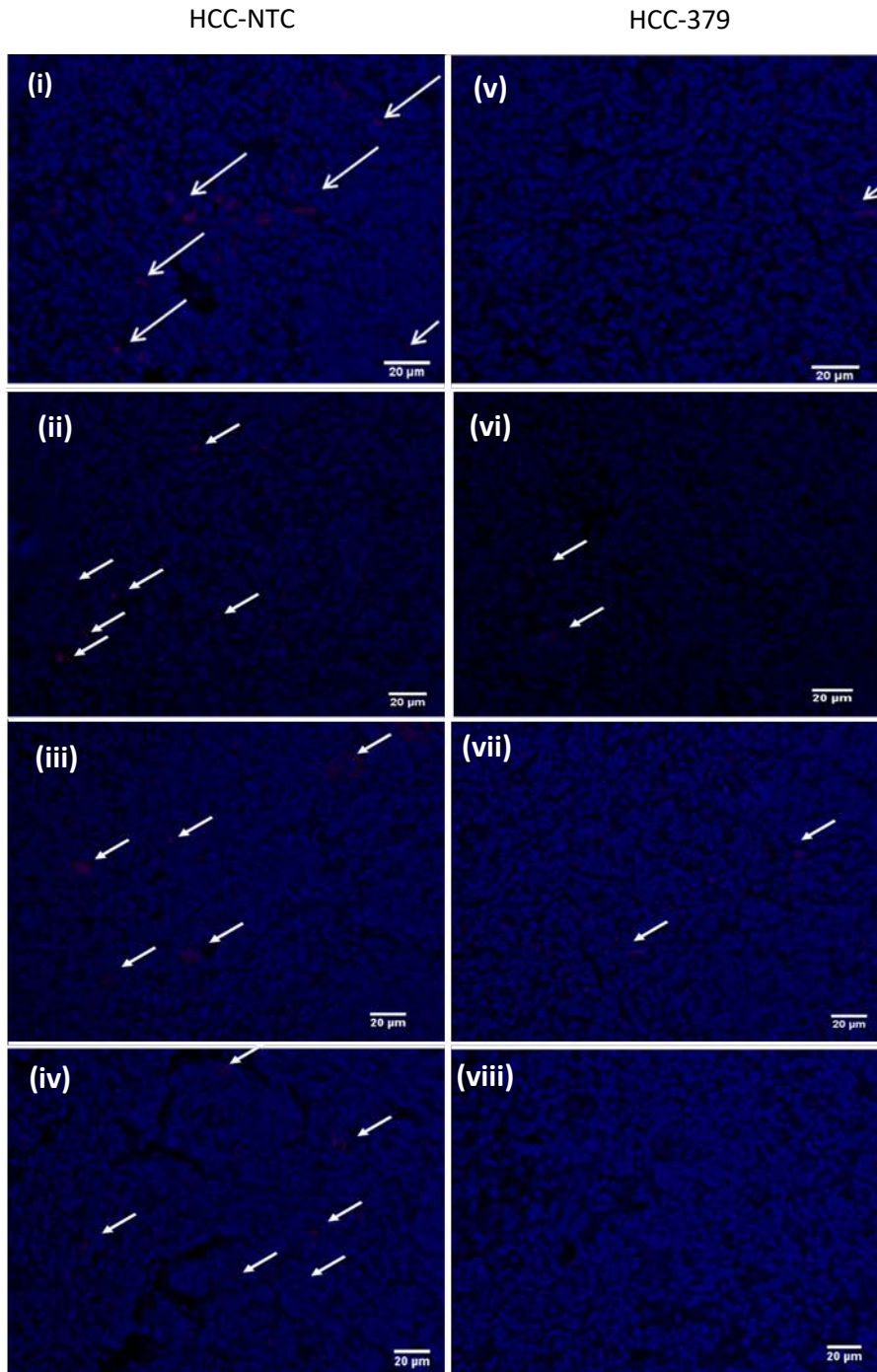


Figure 4. 6: Fluorescence microscopy imaging of DAPI stained (i-iv) HCC-NTC (n=4) and (v-viii) HCC-379 (n=4) sentinel lymph nodes showing an increase in red fluorescing tumour cell infiltration

4.4.7 Confirmation of miR-379 Enrichment *In vivo*:

RNAlater® preserved tumour samples were analysed by RQ-PCR. Firstly, enrichment of miR-379 was confirmed in each tumour group with a 112.5-fold increase in HCC-379 SC tumours (Mean \pm SEM, 479 ± 149 RQ) when compared to HCC-NTC samples (4 ± 2 RQ). There was an 81-fold increase in HCC-379 MFP

tumours (532 ± 97 RQ) when compared to HCC-NTC tumours (7 ± 2 RQ) (Figure 4.7). Expression was normalised relative to miR-16 expression.

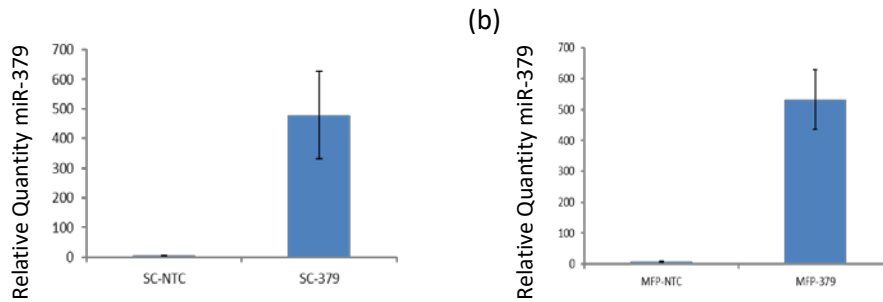


Figure 4. 7: RQ-PCR confirmation of enriched expression of miR-379 in (a) subcutaneous HCC-379 ($n=9$, 479 ± 149 RQ) compared to HCC-NTC tumours ($n=5$, 4 ± 2 RQ) tumours and (b) mammary fat pad HCC-379 tumours ($n=9$, 532 ± 97 RQ) compared to HCC-NTC tumours ($n=3$, 7 ± 2 RQ)

4.4.8 Impact of Elevated miR-379 Expression on COX-2 Expression:

Predictive algorithms suggested a binding site for miR-379 on the 3'UTR of COX-2 [243-245]. Another study also found COX-2 mRNA to have reduced expression following transfection of a breast cancer cell line with miR-379 (>1.5-fold) [146].

Gene expression analysis was performed on *In vivo* tumour samples ($n=23$). A potential correlation between miR-379 expression and COX-2 gene expression was determined by the Pearson correlation coefficient and a moderate, yet significant inverse correlation was observed ($r=-0.48$, $p=0.02$ Figure 4.8).

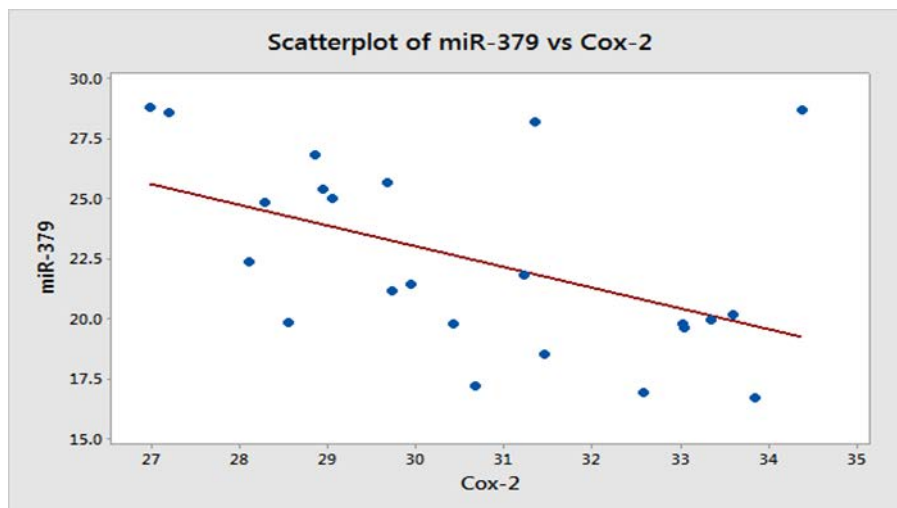


Figure 4. 8: RQ-PCR data showing an inverse correlation between miR-379 expression plotted against COX-2 gene expression in the same Ex-Vivo tumour samples ($n=23$, $r=-0.48$, $p=0.02$)

COX-2 protein analysis was carried out on tissue sections by immunohistochemistry. For all antibodies analysed, a positive and negative control were included to ensure effective, accurate staining of the target protein.

Breast tumour samples with high COX-2 expression served as control tissue and underwent all the same steps, however, the negative control was not incubated with the primary antibody (Figure 4.9). The lack of staining evident on this *In vivo* tumour sample served as reference for any positive staining observed.

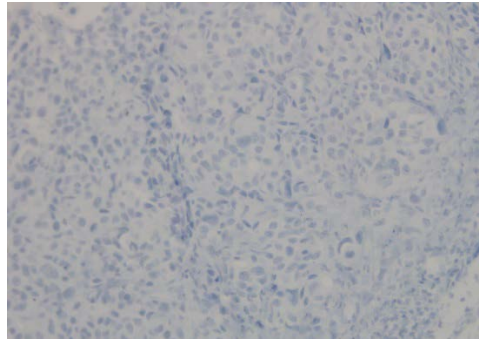


Figure 4. 9: Image of COX-2 primary antibody free negative control of *In vivo* tumour sample, with Haematoxylin stained nuclei (blue) (magnification 20X)

COX-2 was detectable in all HCC-NTC (n=14) and HCC-379 (n=17) tumour samples. Positive staining for the protein is evident in the cell cytoplasm on the membrane of the microsome and endoplasmic reticulum. Analysis of stained tissue sections showed a reduction in expression of the COX-2 protein in the HCC-379 (A i-iii) tumours when compared to the HCC-NTC sections (B i-iii, Figure 4.10).

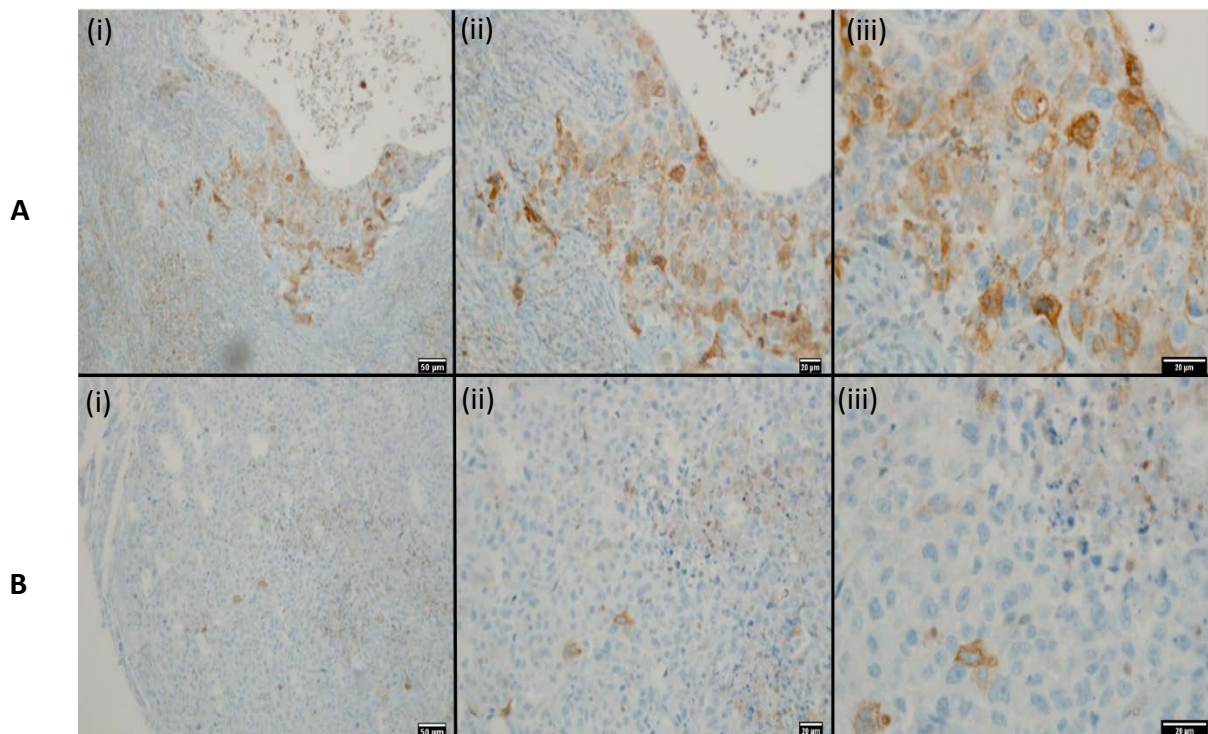


Figure 4. 10: Images from sectioned MFP tumours derived from (A) HCC-NTC, and (B) HCC-379, cells stained for the COX-2 protein and imaged at 10X (i), 20X (ii) and 40X (iii)

4.4.9 Analysis of Tumour Vascularity:

Further staining was carried out targeting CD31, an endothelial cell marker, to establish any impact that miR-379 expression may have on tumour angiogenesis. Staining was also performed on tonsil tissue which served as a positive control for the antibody with a primary antibody free section as a negative control (Figure 4.11). Effective staining for CD31 was confirmed in the positive control section on the membrane of endothelial cells lining the blood vessel. The absence of staining was evident in the negative control section of tonsil tissue.

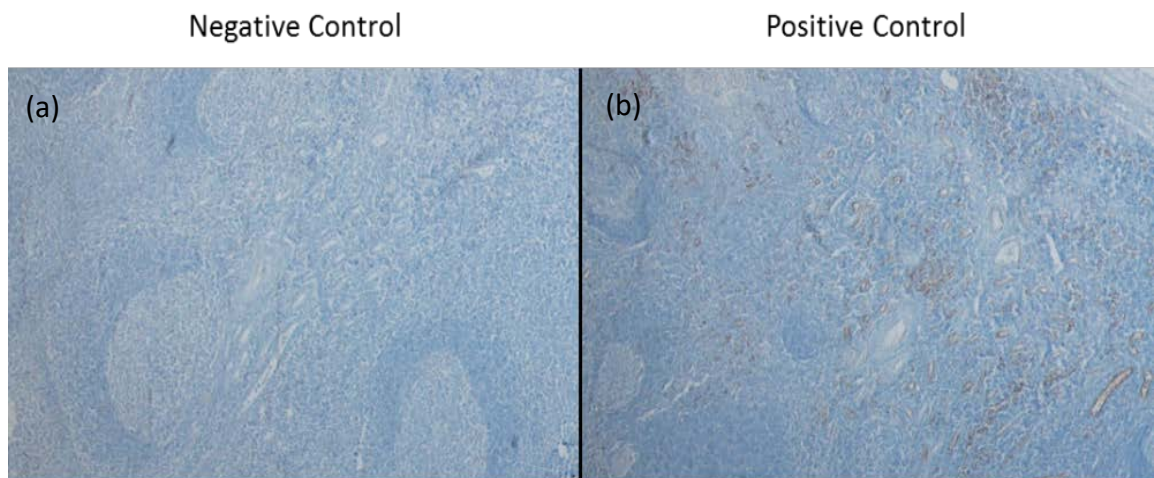


Figure 4. 11: (a) Image of tonsil tissue which served as a primary antibody free negative control and a (b) positive control, both images at 4X magnification

Once effective staining of CD31 was confirmed, analysis of tumour sections revealed no appreciable difference in expression of CD31 between HCC-NTC and HCC-379 tumours (Figure 4.12).

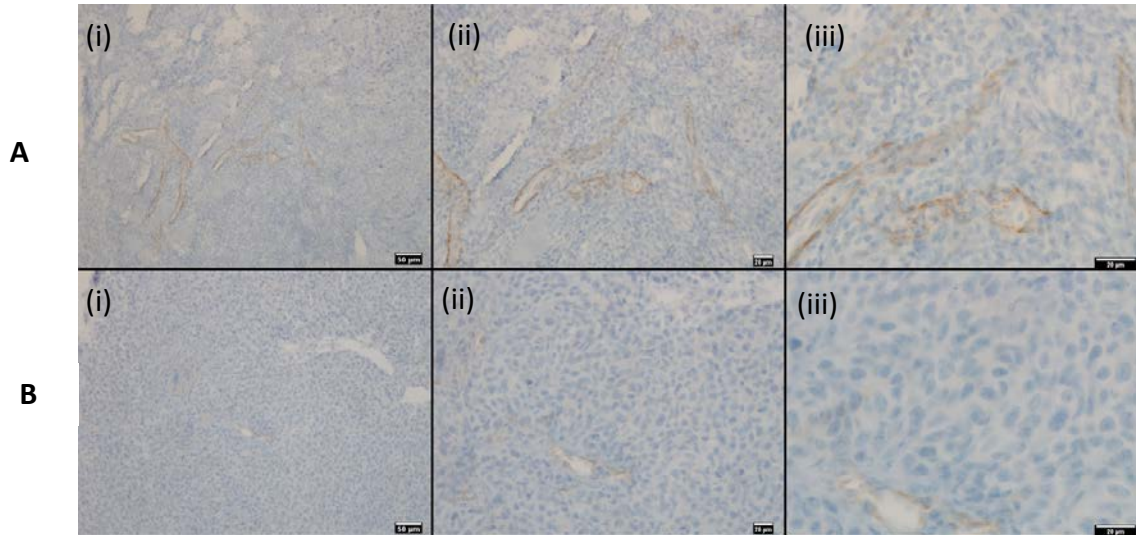


Figure 4. 12: Images from sectioned MFP tumours derived from (A) HCC-NTC, and (B) HCC-379, cells stained for the CD31 protein and imaged at 10X (i), 20X (ii) and 40X (iii)

4.4.10 Impact of Elevated miR-379 Expression on Tumour Cell Proliferation:

The tumour tissue was also stained for proliferating cell nuclear antigen (PCNA). PCNA staining is localised to the nucleus of cells while they are undergoing DNA replication. No significant difference was discovered between HCC-NTC and HCC-379 tumour tissues, with diffuse positive staining for the protein observed in all sections analysed (Figure 4.13).

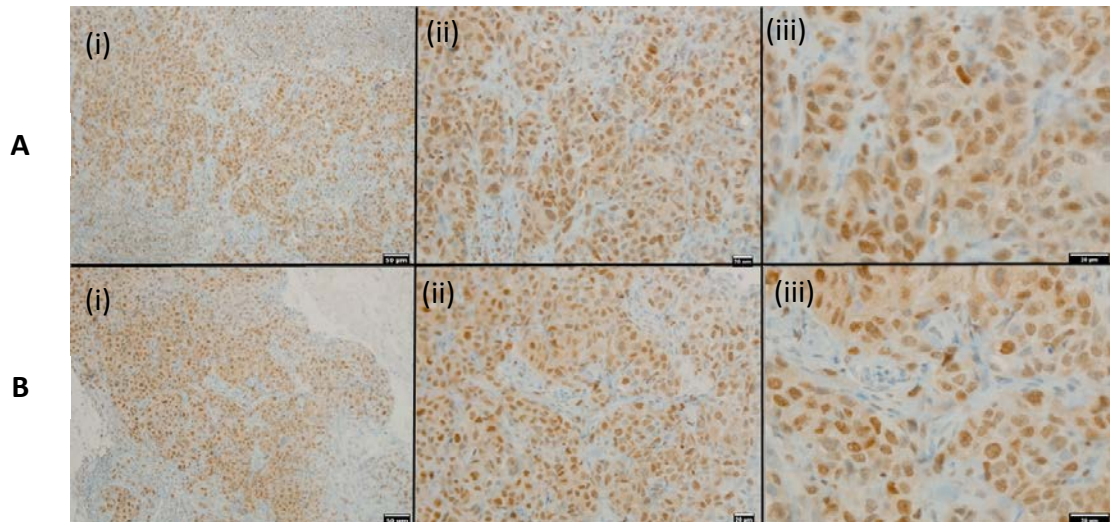


Figure 4. 13: Images from sectioned MFP tumours derived from (A) HCC-NTC, and (B) HCC-379, cells stained for the PCNA protein and imaged at 10X (i), 20X (ii) and 40X (iii)

4.5 Discussion:

This exciting data further supports a tumour **modulatory** role for miR-379 and highlights one potential mechanism of action for the miRNA. This has never been evaluated in an *In vivo* model of breast cancer despite previous work evaluating the miRNA as a potential tumour suppressor miR in a variety of diseases, including breast cancer [137, 146, 240].

In this study, cells were transduced with a lentiviral vector which ensured stable long term expression of the miRNA. This contrasted with other reports utilising transient expression of the miRNA in transfected cells [137, 146, 240]. Initially, transduction was confirmed in the HCC-NTC/379 cells through RQ-PCR analysis and fluorescence microscopy. RQ-PCR analysis confirmed enrichment of miR-379 in the HCC-379 cell line while fluorescence microscopy confirmed expression of RFP in both HCC-NTC and HCC-379 populations following selection with puromycin for 7 days.

An MTS assay (Promega) revealed a significant increase in proliferation in HCC-379 cells when compared to HCC-NTC cells. This contradicted previous findings showing reduced proliferation of cancer cells following enrichment of miR-379 [75, 240, 242]. It must be noted that the MTS assay is not a true measurement of cell proliferation as much as it is an assay to determine cell viability, and has come into question as it has been stated to be dependent on the efficiency of metabolic enzymes [251]. For a true evaluation of cell proliferation, DNA binding cyanine dyes such as PicoGreen and CyQuant are recommended. For this study the MTS assay was deemed appropriate as it can determine the impact of miR-379 enrichment on cell viability overall and could be directly compared to the impact the miRNA was seen to have had on T47D cells in the previous study [129]. This difference could be as a result of different cell lines used.

As the aim of this study was to determine the impact of miR-379 on tumour establishment and progression *In vivo*, an animal model was established to examine the tumour suppressive potential of the miRNA. Balb/c nude mice were the animal model used for this experiment as they were immunocompromised allowing for the growth of human breast cancer cells. There were two arms to the *In vivo* study examining the impact of miR-379 on transduced HCC1954 cells. Tumours were administered both subcutaneously and orthotopically into the

second thoracic mammary fat pad. Much published work on mouse models of breast cancer administer tumours subcutaneously. Subcutaneous administration is often chosen because it is easier to both administer the cells and to track tumour growth by Vernier calliper measurement. Ectopic tumours do not reflect the environment associated with breast tumours while orthotopic models of disease can result in an increased likelihood of developing a model of metastatic disease [252]. In this study, there was a greater degree of stromal cell infiltration within orthotopic tumours when compared to those grown subcutaneously. This heterogeneity reflects tumours which are known to contain stromal cells that can encourage progression [253]. MFP tumours with this mix of cells mimics what is seen in clinical tumour samples to a greater extent than what is evident in tumours developed subcutaneously [252]. This may be further highlighted as lymph node infiltration was witnessed in the MFP cohort and not in the SC group. This reflects findings in the literature showing orthotopic models of breast cancer to be more invasive when compared to ectopic models [252].

During the course of tumour growth *In vivo*, animals were imaged using the novel photoacoustic imaging (PAI) system. This system functions on the basis of the photoacoustic effect which is something that was witnessed by Alexander Graham Bell in 1880. Simply, it refers to the generation of acoustic waves following absorption of optical energy. This is an imaging modality that has offered promise in the field of breast cancer screening [254]. For the purpose of this study the system was employed to analyse vascularity of the tumours during growth. Tumours were imaged in the range 680 – 970 nm. Deoxygenated haemoglobin has stronger optical absorption in the range of 650- 780 nm while oxygenated haemoglobin has stronger absorption in the range of 950 – 1065 nm [255]. Therefore, the chosen optical window can distinguish between oxy and deoxyhaemoglobin. Furthermore, water has a peak absorption coefficient at around 975nm which falls outside the window used [256]. There was no impact on tumour volume evident in the tumours with HCC-379 cells. However, when imaged with the PAI system there was a central area devoid of vascularity in the HCC-379 tumours. As water is outside the optical window used, this area lacking any absorption within the borders of the tumour was thought to be fluid. At the time of resection, it was confirmed that many of these tumours contained large volumes of fluid. Another study utilised PAI to measure the oxygen saturation in

mouse tumours where they could differentiate between normal/hyperplasia and invasive disease [257]. Similarly this report measured oxy and deoxy-haemoglobin within the tumours. PAI has also been performed on patients with breast cancer previously and images were shown to correlate with vascularity patterns witnessed by CD31 staining [258]. For work in this thesis, the PAI system allowed evaluation of tumours grown subcutaneously and in the mammary fat pad of mice. It also provided information on the vascularity and, in this case, allowed identification of fluid filled centres prior to study completion. PAI also provided information on tumour biology in real time *In vivo*.

Following H & E staining of sectioned tumour samples, a pathologist carried out a blinded analysis. It was reported that HCC-379 tumours exhibited a greater degree of necrosis. This suggests that despite the larger size of the tumours, they may be lacking functional centres. However, one group has published a study stating that tumours exhibiting necrosis may elicit a more aggressive phenotype and the tumours outgrow the vascular supply, resulting in central areas of necrosis [259]. In order to assess if these tumours were more aggressive the invasive potential was analysed using the sentinel lymph nodes.

Lymph node samples were DAPI stained and imaged by fluorescence microscopy. As both HCC-NTC and HCC-379 populations of tumour cells express RFP, cells that originated from the tumour and successfully infiltrated into the lymph node could be detected by fluorescence microscopy. Imaging showed a greater number of infiltrating tumour cells in the HCC-NTC associated lymph nodes when compared to HCC-379 lymph nodes. This suggests that HCC-379 tumours were less invasive than the HCC-NTC cohort. In this circumstance, this study suggests that the greater degree of necrosis witnessed in the HCC-379 primary tumour is reflective of less invasive tumours with necrotic centres. Unfortunately the fluorescence was not quantified in this study but such quantification could aid in scoring the degree of tumour cell infiltration.

Following confirmation of miR-379 enrichment, gene expression of COX-2 was analysed. A significant inverse correlation was witnessed between miR-379 and COX-2 gene expression across all samples suggesting a potential role for this miRNA in the regulation of COX-2 expression.

As reduced gene expression does not always correlate to reduced protein expression and miRNAs ultimately elicit an impact in preventing translation to protein, immunohistochemistry was performed on all tumour samples [260]. Positive targeting of COX-2 staining of the microsome and endoplasmic reticulum membranes in the cell cytoplasm, was seen in all sectioned tumour samples. There was a clear reduction in the expression of the COX-2 protein in HCC-379 tumours when compared to HCC-NTC tumours. Combined with gene expression data, this confirms reduced COX-2 expression in the presence of elevated miR-379. As increased COX-2 expression is associated with an increase in lymphangiogenesis, miR-379 regulation of COX-2 may explain the reduced number of tumour infiltrating cells in sentinel lymph nodes in this study [248, 249]. As COX-2 can promote angiogenesis, miR-379 suppression of the enzyme may have reduced blood vessel infiltration of the tumours resulting in large fluid filled centres and the increase in areas of necrosis witnessed [261].

While this study shows that COX-2 protein expression is reduced in the presence of elevated miR-379, it has not confirmed any direct interaction between the miRNA and mRNA. Further studies would be required to confirm that miR-379 directly inhibits COX-2 gene expression. A luciferase assay could be performed to show direct binding of the miRNA to the 3' UTR of COX-2. Another *in vitro* study could introduce a mutation into the binding site on the 3' UTR of the COX-2 mRNA and this could also confirm direct binding of miR-379. This type of experiment could also be used to confirm that miR-379 functionally suppresses COX-2. Such studies would be required to determine if miR-379 directly inhibits COX-2.

However, when analysing CD31 expression there was no significant difference witnessed between staining of the endothelial cells in the HCC-379 and HCC-NTC cohorts. As CD31 does not detect newly formed blood vessels, nestin has been suggested by one group as a novel method of evaluating angiogenesis in tumour tissue samples [262]. An alternative approach could use nestin which detects newly formed vessels it would be more appropriate in evaluating a response to treatment. As CD31 identifies formed blood vessels within the tumour it was a preferred method of analysing tumour vasculature for this study.

Detection of PCNA was used to determine any impact of miR-379 enrichment on tumour cell proliferation. There was no significant difference evident between the

staining intensity of PCNA between all HCC-NTC and HCC-379 tumour sections. In order to obtain a more accurate evaluation of tumour cell proliferation, the addition of Ki-67 could be worthwhile. Ki-67 is present at late G1, S, G2 and M phases of the cell cycle while PCNA is expressed during the G1/S phase of the cell cycle [263]. While both markers are widely used for measuring cell proliferation in the literature, Ki-67 is used routinely by Pathologists in the clinical setting as it has been shown to be more sensitive and specific than PCNA [263].

The data presented strongly supports miR-379 as a tumour modulator in the breast cancer setting with potential as a tumour suppressor. To confirm miR-379 as a tumour suppressor further experiments would be required. Migration assays could evaluate the impact of miR-379 on tumour cell motility. Angiogenesis assays could determine any impact of miR-379 on the ability of the cells to form neovasculature. Enrichment of miR-379 did not impact tumour formation in transduced HCC1954 cells. However, this has been performed within our group previously on a less invasive cell line, T47D (unpublished). This study, while using small numbers found a reduction in tumour formation in animals with enriched miR-379 expression (n=2/5) compared to each control animal forming tumours (n=5/5). This trend was not reflected in the more aggressive HCC1954 cells used in this study. The primary HCC-NTC and HCC-379 tumours used in this chapter grew at such a rate that animals were sacrificed within five weeks of induction. If a lower number of cells were administered at tumour induction the length of the study could have been increased and it would be easier to assess any impact of miR-379 enrichment on tumour progression. Such an assessment *in vivo* would further highlight the potential of miR-379 to function as a tumour suppressor. Also, primary tumours could be resected which could allow for recurrence to be analysed and also serve to determine if animals with original tumours enriched with miR-379 would have an increase in survival. Such studies were beyond the scope of this thesis but should be performed prior to branding miR-379 as a tumour suppressor.

miR-379 enrichment resulted in increased tumour necrosis and reduced invasiveness *In vivo*, something which has never been reported previously in the literature. This study further elucidated COX-2 as a potential target of the miRNA and confirmed an inverse correlation between the miRNA and protein. Targeting

Chapter 4: Evaluation of miR-379 as Tumour Suppressor miR *In vivo*

and functional repression of the COX-2 protein has therapeutic relevance and exciting potential in the breast cancer setting.

Chapter 5

Evaluating Therapeutic Impact of Systemic Delivery of miR-379

5.1 Introduction:

Mesenchymal Stem Cells (MSCs) hold great promise for tissue regeneration due to their capacity to differentiate into osteoblasts, chondrocytes and adipocytes [264]. Another important feature is the ability of the cells to migrate and engraft into primary tumours and sites of metastases [150]. Therefore, MSCs can potentially facilitate the delivery of a therapy directly to tumour cells [265].

Despite the therapeutic promise miRNAs hold, application has been suspended due to the difficulties associated with tumour targeted delivery of the miRNAs as well as poor uptake into tumour cells [266]. While MSCs may overcome issues relating to targeted delivery, exosomes may aid in uptake of the miRNA into tumour cells. MSCs are known to secrete an abundance of exosomes which can transfer genetic material in a juxtacrine, paracrine or endocrine manner [218]. Exosomes are also known to reflect the characteristics of the parent cell and as MSCs can migrate and engraft into tumours, it may be possible for MSC secreted exosomes to also migrate to the site of the tumour [215]. It is known that exosomes have the capacity to migrate to specific regions and exert an impact on cells in a manner that reflects the cell of origin [201]. This would suggest that exosomes derived from a cell with a therapeutic capacity, may exert a therapeutic impact when systemically administered alone which has been proven [217]. One study has proven systemic administration of MSC-derived exosomes elicited a cardioprotective effect in a mouse model [217]. Another study analysed the biodistribution of systemically administered exosomes and microvesicles derived from human embryonic kidney cells in subcutaneous glioma tumour bearing mice [267]. Tracking of the vesicles 60 min following administration, revealed accumulation of the vesicles at the site of the tumour. This study confirmed that vesicle encapsulated RNA impacted the NF κ B pathway. However, this study did also confirm uptake of the vesicles in kidneys, liver, lung, heart, brain and muscle. This highlights the potential of exosomes alone as a systemic therapy and also underlines the necessity to increase our overall understanding of exosome biology and factors impacting migratory itinerary.

MSC exosomal content has been engineered for enriched expression of miRNAs. This was utilised for the treatment of glioma in an animal model [213]. This finding involved one direct administration of 50 μ g of exosomes derived from

MSCs with enriched expression of miR-146b into the tumour. Animals were sacrificed 5 days after treatment and it resulted in a significant reduction in tumour growth. Systemic administration of exosomes offers potential and research has been performed on exosomes derived from different cell lines. Another study systemically administered exosomes derived from human embryonic kidney cells following engineering of the surface expression [205]. Expressing the GE11 peptide on the surface of exosomes allowed targeted delivery of the therapeutic miRNA let-7a to EGFR positive tumour cells. This targeted delivery significantly suppressed tumour growth in the mammary fat pad of immunocompromised mice. These studies highlight the potential of exosomes enriched with tumour suppressive miRNAs.

While the work presented in this thesis thus far has highlighted the tumour suppressive capability of miR-379, targeted delivery of the miRNA *In vivo* remains a challenge. Systemic administration of MSCs engineered for enriched expression of miR-379 may serve as a therapy *In vivo*. Also, cell free exosome mediated delivery of miR-379 may serve as a therapeutic option *In vivo*. There has been no published work to date analysing the impact that elevated expression of miR-379 may have on MSCs and what therapeutic effect these engineered cells or secreted exosomes may elicit.

5.2 Aim:

The aims of this study were as follows:

- To investigate the potential to engineer MSC derived exosomes with enriched expression of miR-379
- To evaluate the therapeutic impact of miR-379 enriched MSCs or derivative exosomes on tumour progression *In vivo*.

5.3 Materials and Methods:

MSCs were obtained from the Regenerative Medicine Institute at NUI Galway. After ethical approval and informed consent, bone marrow was aspirated from the iliac crest of healthy volunteers in accordance with a defined clinical protocol [268, 269]. MSCs were transduced with a lentivirus as previously described (Section 2.2.9), to generate MSC-379 or MSC-NTC cells.

For exosome isolation, MSCs were incubated in exosome depleted media for 48 hours, prior to differential centrifugation, micro-filtration and ultra-centrifugation. Exosomes were resuspended in PBS and stored at -80 °C until further required for RQ-PCR, nanoparticle tracking analysis (NTA), transmission electron microscopy (TEM), confocal microscopy or further experimentation.

HCC1954 cells expressing luciferase (HCC-luc) were employed for tumour establishment. Female BALB/c Nude mice (n=32, Charles River) received an injection of 1×10^7 HCC-luc cells into the fourth inguinal mammary fat pad (MFP). Tumours and animals were monitored weekly and upon formation of palpable tumours that were detectable by IVIS, treatments were administered. Animal groupings were formed based on an even distribution of tumour sizes in each group. Mice received 4 repeat intravenous tail vein injections of 2.6×10^7 exosomes derived from either MSC-NTC (n=8) or MSC-379 cells (n=8) resuspended in PBS, or one injection of 1×10^6 MSC-NTC (n=8)/ or MSC-379 cells (n=8) resuspended in 50µl of serum free media (Figure 2.14). Tumour growth was monitored weekly by *In vivo* Imaging System (IVIS, PerkinElmer) following intraperitoneal injection of luciferin at (150mg/kg).

5.4 Results:

5.4.1 Optimisation of MSC Transduction:

To optimise MSC transduction with a lentivirus it was necessary to establish the optimal concentration of Polybrene. In a 96-well plate format, MSCs were incubated with a range of concentrations of Polybrene (0-8 $\mu\text{g}/\text{ml}$) and the impact on cell viability was determined. Experiments were performed in triplicate and there was no inhibition of MSC growth resulting from any concentration of Polybrene (Figure 5.1). Initial transduction experiments were thus performed at a concentration of 8 $\mu\text{g}/\text{ml}$ of Polybrene in line with previously published work [270].

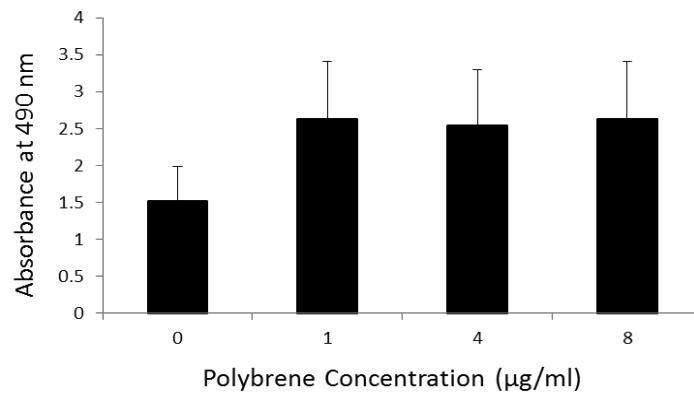


Figure 5. 1: MTS assay analysing impact of varying concentrations of Polybrene on MSC viability following 72hrs performed in triplicate

As the lentivirus contained a Puromycin resistance gene, transduced cells could be positively selected following exposure to the antibiotic Puromycin. The optimum puromycin concentration ie. lowest concentration necessary to induce death of non-transduced cell was determined. Cells were incubated with a range of puromycin concentrations (0-8 μg) in a 96-well plate format and assay was performed in triplicate. Puromycin at 4 $\mu\text{g}/\text{ml}$, was deemed the optimal concentration for inhibiting MSC growth (Figure 5.2).

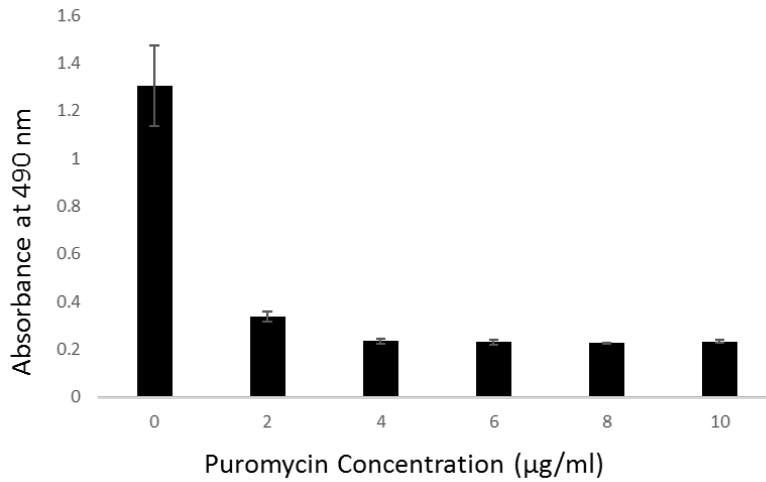


Figure 5. 2: MTS assay analysing impact of Puromycin concentrations on MSC viability over the course of 7 days performed in triplicate

5.4.2 Transduction of MSCs:

Fluorescence imaging was carried out on MSCs 48 hrs after transduction (Figure 5.3 (iii)) and following puromycin selection (Figure 5.3 (iv)). While at the earlier timepoint only a subpopulation of MSCs were RFP positive, following selection, it was confirmed that all RFP negative cells had been depleted (Figure 5.3 (ii), (iv)). MSCs were fixed onto slides and stained with DAPI and Phalloidin for subsequent fluorescence imaging (Figure 5.3 (v)). Expression of the red fluorescent protein (RFP) was confirmed in both MSC-NTC and MSC-379 cell populations (Figure 5.3 (vi)).

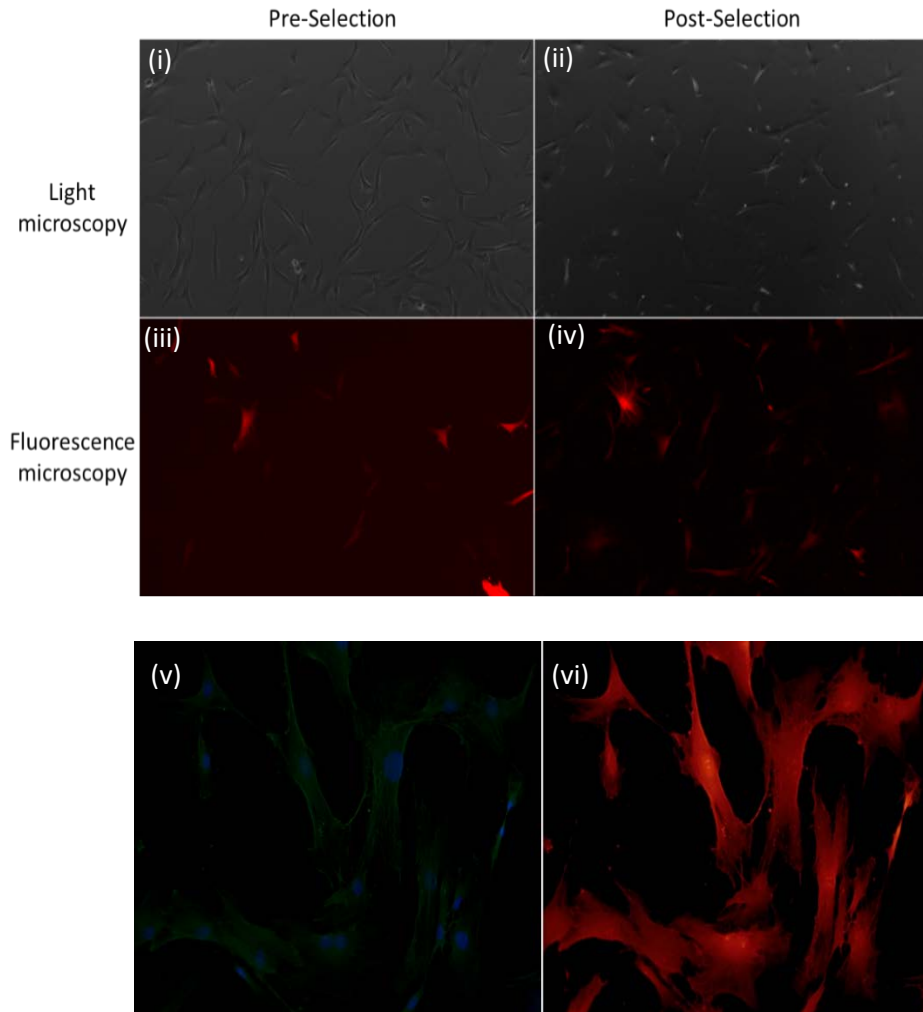


Figure 5. 3: Light (i,ii) and fluorescent (iii,iv) images taken at 10X of MSCs showing successful selection using 4 μ g/ml puromycin. Fluorescent images of (v) DAPI and Phalloidin (vi) MSCs readily expressing RFP following transduction, imaged at a magnification of 40X

Transduction of MSCs was also confirmed by RQ-PCR where a 476-fold increase in expression of miR-379 was evident in MSC-379 cells (Mean \pm SEM, 2.71 ± 0.29 , Log_{10} RQ miR-379) when compared to MSC-NTC cells (0.151 ± 0.08 Log_{10} RQ miR-379) performed in triplicate (Figure 5.4 (a)).

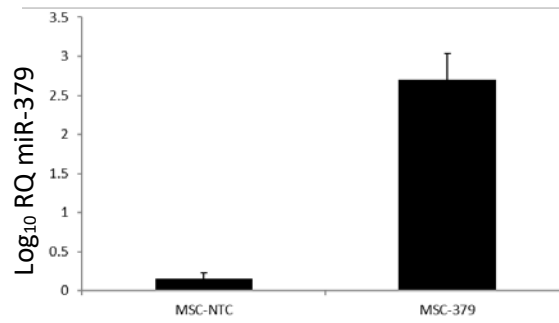


Figure 5. 4: RQ-PCR confirmation of a 476-fold increase in miR-379 expression in MSC-379 cells (2.71 ± 0.29 , Log_{10} RQ miR-379) compared to MSC-NTC cells (0.151 ± 0.08 Log_{10} RQ miR-379) following transduction performed in triplicate

5.4.3 Impact of miR-379 Enrichment on MSCs:

Following transduction of both MSC-NTC and MSC-379 cell populations an MTS assay was carried out in triplicate over the course of 72 hours on both cell populations to determine any impact of miR-379 enrichment on MSC viability (Figure 5.5). There was no significant impact on cell growth witnessed between MSC-379 cells (Mean \pm SEM, 6.67 ± 10.68 % increase in cell growth, ANOVA $p=0.89$) and MSC-NTC cells (9 ± 8.88 % increase in cell growth) after 72hrs.

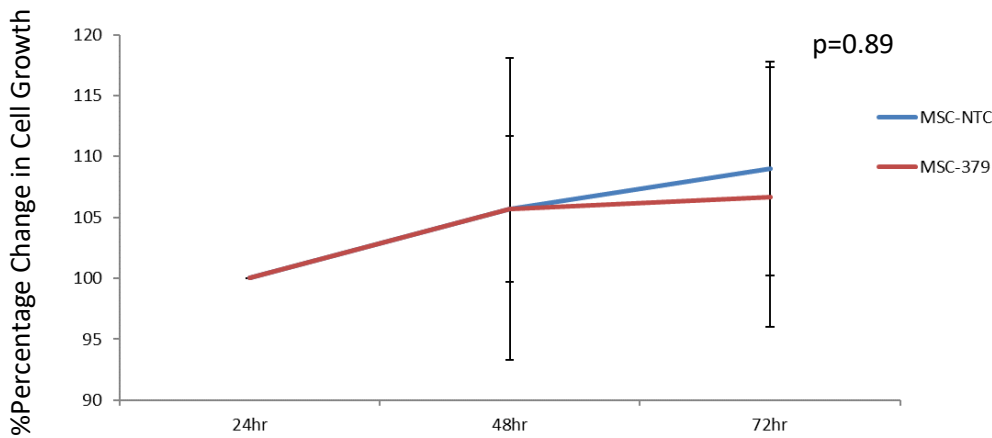


Figure 5. 5: MTS assay showing no significant impact of miR-379 enrichment on cell viability in MSC-NTC and MSC-379 cell lines performed in triplicate (ANOVA $p=0.89$)

As transduced MSCs are required to migrate to sites of the tumour *In vivo*, a transwell migration assay was performed in triplicate to ensure there was no negative impact of miR-379 enrichment on MSC migration (Figure 5.6). Migration towards 5% FBS media was used as a positive control and serum free media served as a negative control. There was no significant impact witnessed on migration between of MSC-NTC and MSC-379 cell lines (2 Sample T-test, $p=0.261$).

There was a significant difference between the negative and positive controls (2 Sample T-test, $p=0.02$).

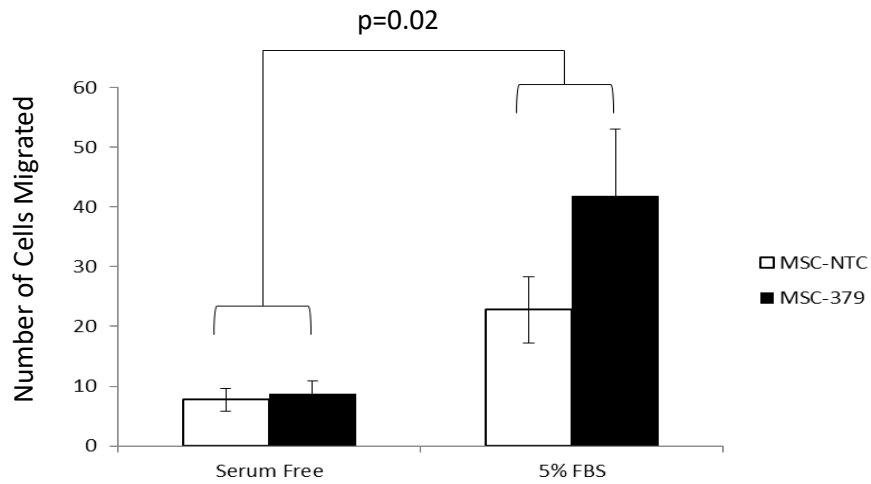


Figure 5. 6: Migration assay quantifying the number of migrated cells at a magnification of 20X. A significant increase in migration was evident between positive and negative controls (2 Sample T-test, $p=0.02$) with no significant difference evident between MSC-NTC and MSC-379 cells (2 Sample T-test $p=0.261$) performed in triplicate

5.4.4 Characterisation and Quantification of Exosomes:

Exosomes were isolated from both cell lines as described previously. To ensure that the isolates were in fact exosomes, TEM was carried out to evaluate whether the vesicles were of the appropriate size range and morphology (Figure 5.7).

Although there were some larger vesicles present, the vast majority were roughly 30-120 nm in diameter and of the appropriate morphology.

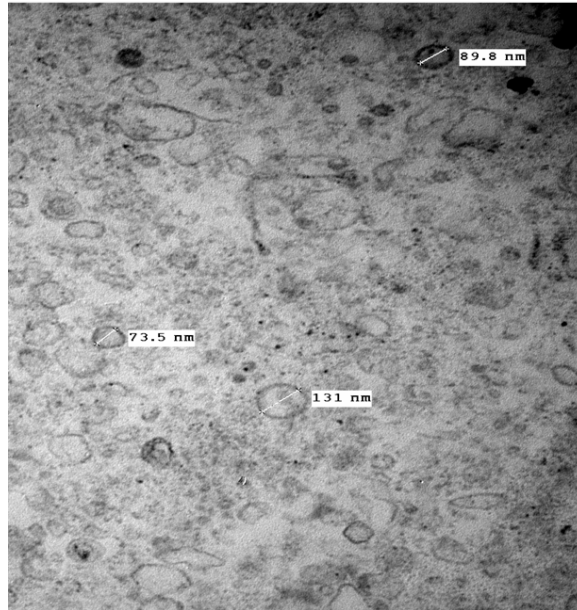


Figure 5. 7: TEM image at 40,000X of isolated exosomes

Further characterisation and quantification was carried out by NTA. This allows characterisation of exosomes based on the size of the particles and also allows for quantification of exosomes. It is necessary for the exosomes to be evenly dispersed to attain an accurate measurement of the samples (Figure 5.8 (a, b)). This is an example of a sample which does not contain aggregates of exosomes and allows for accurate quantification of the isolates. Figure 5.8 (a) shows five separate readings taken of the sample. Figure 5.8 (b) is a snapshot of a recording which shows clear dispersal of exosomes in solution. Figure 5.8 (c, d) are from a sample that contained aggregation of exosomes. In Figure 5.8 (c) the average of five readings \pm SEM (red) are shown. The size distribution within this sample was not representative of a population of exosomes. The snapshot (Figure 5.8 (d)) shows aggregation of the exosomes and light scattering as a result. This yields an inaccurate quantification of exosomes and would need to be excluded from further analysis.

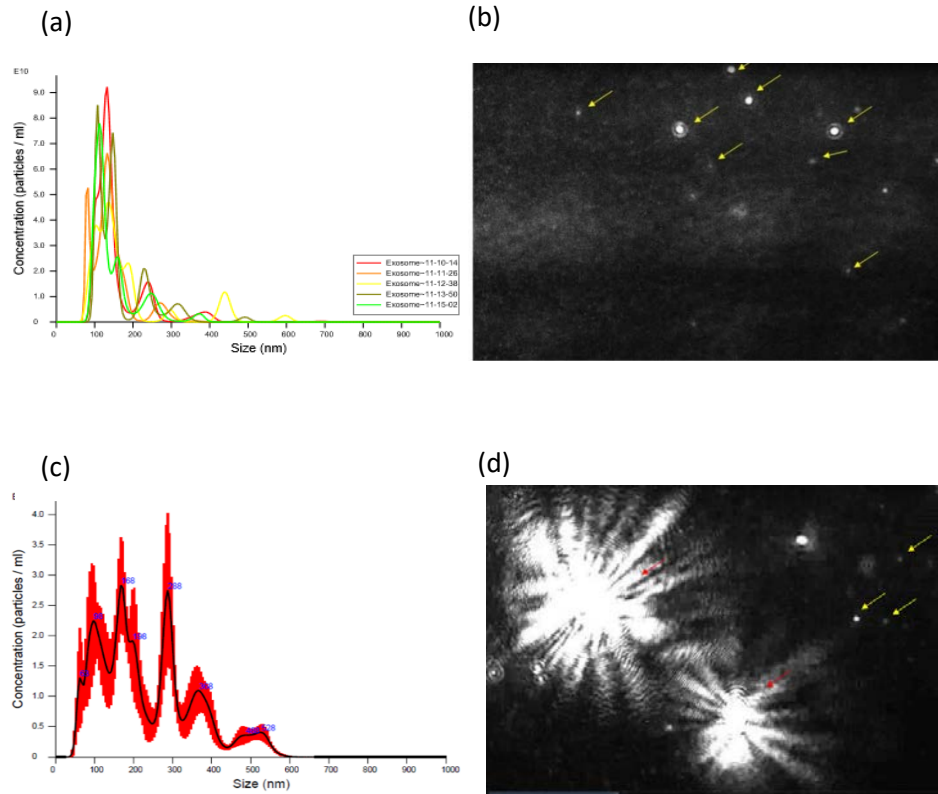


Figure 5. 8: Images from NTA of isolated exosomes. (a,c) Graph showing size distribution of and average of 5 analyses of isolates showing SEM in red. (b,d) Snapshot from video analysis showing individual exosomes or aggregates

Indirect quantification of exosomes was also performed by bicinchoninic acid (BCA) assay for each sample isolated. For each assay a standard curve was obtained based on serial dilutions of bovine serum albumin (BSA) standards. Using 4 samples, protein estimation and NTA were compared to determine if any correlation existed between both methods of quantifying exosomes (Table 5.1). There was no relationship between both methods of quantifying exosomes in this small cohort of samples. As a result of this, NTA was utilised for accurate quantification of exosomes for the remainder of this study.

Cell Source of Exosomes	Particles/ μ l	Protein Estimation (ng/ μ l)
MSC-NTC	5.42E+05	423.2
MSC-379	2.40E+05	601.8
HCC-NTC	2.58E+07	320
HCC-379	1.35E+05	781.172

Table 5. 1: Lack of a correlation between quantification of exosomes by protein estimation and NTA

5.4.5 Quantification of Exosome-Encapsulated miR-379:

Exosomes isolated from MSC-NTC and MSC-379 cell lines were analysed in triplicate by RQ-PCR to determine if it was possible to enrich miR-379 in MSC-379 secreted exosomes. Analysis was normalised based on exosome sample loading and was expressed relative to miR-16. There was a 2.5-fold increase in expression of miR-379 in the MSC-379 associated conditioned media (Mean \pm SEM, 15 ± 1 , RQ miR-379) when compared to MSC-NTC conditioned media (6 ± 3 RQ miR-379, 2 Sample T-test, $p=0.09$) (Figure 5.9). Analysis of the exosomal content revealed a significant (2 Sample T-test, $p=0.02$), 5-fold increase in expression of miR-379 in MSC-379 secreted exosomes (25 ± 3 RQ miR-379) compared to MSC-NTC derived exosomes (5 ± 3 RQ miR-379).

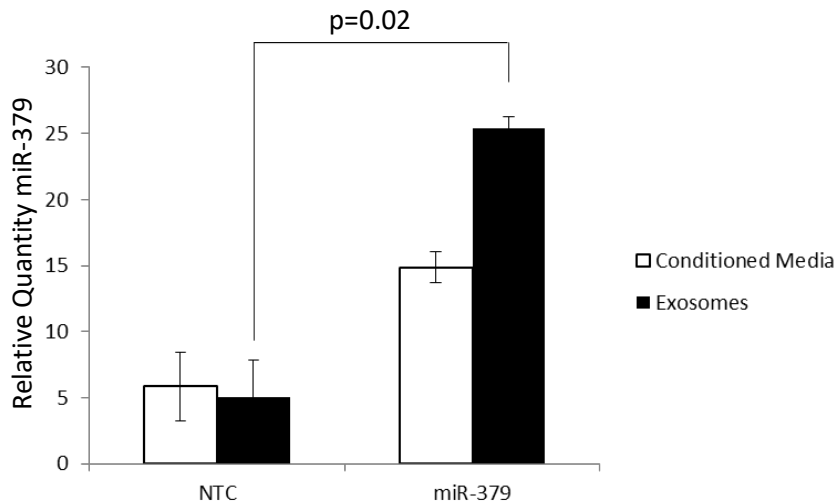


Figure 5. 9: RQ-PCR analysis of significant elevation of miR-379 expression in exosomes isolated from MSC-NTC (5 ± 3 RQ miR-379) and MSC-379 cell lines (25 ± 3 RQ miR-379, 2 Sample T-test $p=0.02$) performed in triplicate

5.4.6 Confocal Microscopy of Exosomal Co-Localisation:

Confocal microscopy was carried out to visualise transfer of RFP expressing exosomes onto recipient, non-RFP cell populations. HCC1954 cells were fixed and imaged following incubation with engineered RFP exosomes derived from MSC-379 cells (Figure 5.10). Areas of red fluorescence were detected over the HCC1954 cells that were incubated with exosomes (Figure 5.10 (c,d)). To confirm that this was not background or auto-fluorescence a control slide with no exosomes was analysed (Figure 5.10 (a,b)).

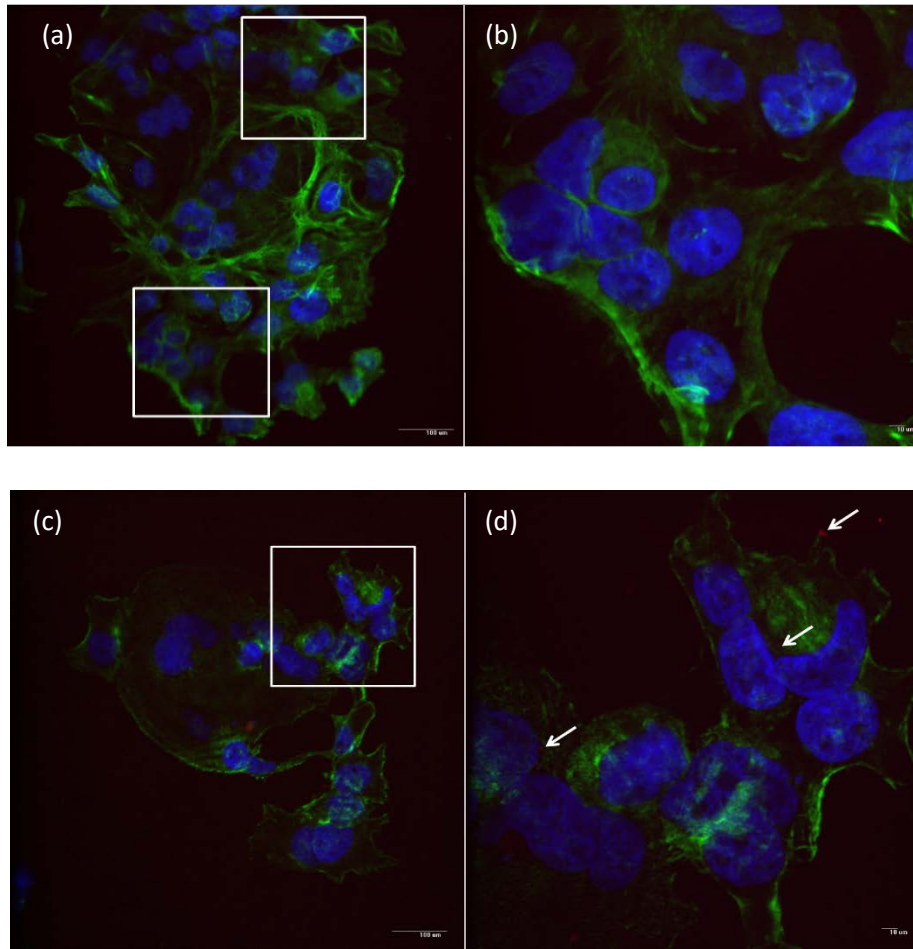


Figure 5. 10: (a) 20X, (b) 60X image of HCC1954 cells incubated with PBS. (c) 20X, (d) 60X image of HCC1954 cells incubated with engineered exosomes derived from MSCs

5.4.7 Impact of Exosomal Transfer on Breast Cancer Cell Proliferation:

An MTS assay was performed in triplicate on HCC1954 cells to determine any impact on cell viability following transfer of exosomes from both MSC-NTC and MSC-379 cell lines (Figure 5.11). There was no significant impact on cell viability following a single administration of exosomes from either MSC-NTC or MSC-379 cells (ANOVA, $p=0.59$).

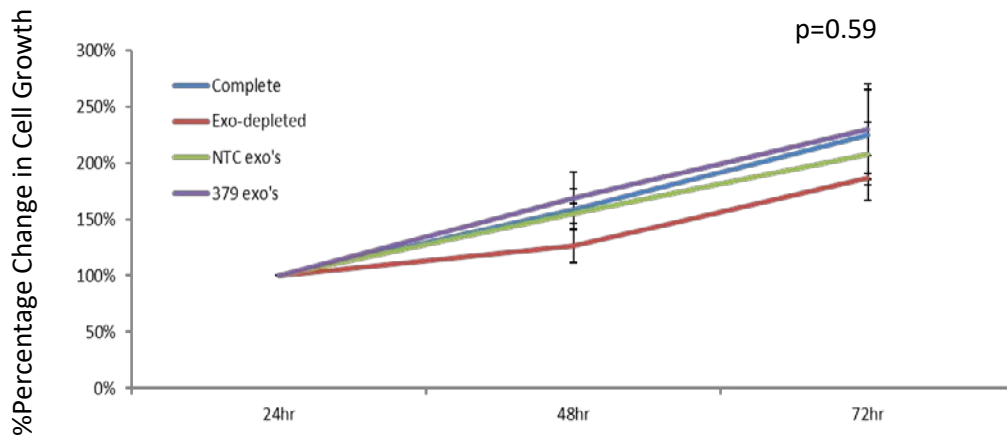
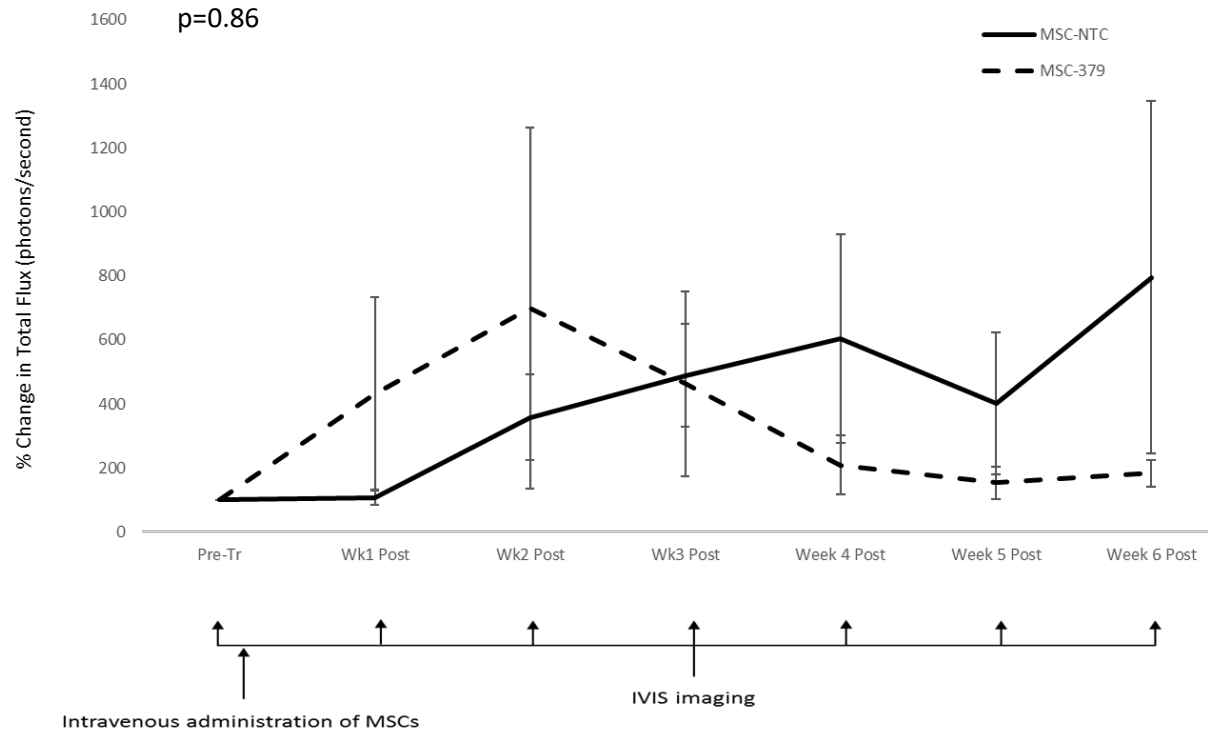


Figure 5. 11: MTS assay showing no significant impact of MSC derived exosomes on cell viability over 72 hours performed in triplicate

5.4.8 Evaluating Therapeutic Efficacy of Systemically Administered Engineered MSCs:

A pilot *In vivo* study was carried out using HCC1954-luc cells to determine the impact of systemically administered MSC-379 cells on tumour progression. Upon tumour formation, MSC-NTC or MSC-379 cells (1×10^6 /cells) were intravenously injected into the tail vein of the mice. Animals were imaged weekly for 6 weeks to determine any impact on tumour progression (Figure 5.12). Based on bioluminescence, tumour activity and progression was quantified over the 6 weeks following therapeutic administration. Data was normalised to pre-treatment readings and given a baseline of 100%. Over the duration of the study there was no significant change in activity (ANOVA, $p=0.86$, Figure 5.12 (a)) between animals that received MSC-NTC cells ($n=8$) and MSC-379 cells ($n=8$). Sample images in Figure 5.12 (b) show sample IVIS images throughout course of the study with similar rates of tumour progression in both treatment groups.

(a)



(b)

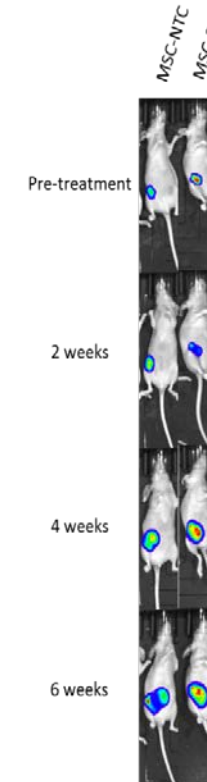


Figure 5. 12: (a) IVIS imaging and quantification of bioluminescence of tumours over 6 weeks showing no significant change in tumour activity (ANOVA $p=0.86$) in animals that received MSC-NTC cells ($n=8$) and MSC-379 cells ($n=8$). (b) Sample images of mice before and following administration of MSC-NTC and MSC-379 cells showing similar rates of tumour progression

5.4.9 Therapeutic Impact of Systemic Administration of Cell-Free Engineered Exosomes:

Prior to injection, exosomes derived from MSC-NTC and MSC-379 cells were characterised and quantified by NTA. Upon tumour formation, four repeat injections of NTC and miR-379 enriched exosomes (2.6×10^7 exosomes in 50ul PBS) were performed and subsequent IVIS imaging was carried out for 6 weeks following the first injection (Figure 5.13). Data was normalised to pre-treatment readings assigned a baseline of 100%. Exosome injections were well tolerated with no adverse effects observed. Over the course of the study there was a significant reduction in tumour activity observed in animals that received exosomes enriched with miR-379 (n=8) when compared to animals that received NTC exosomes (n=8, ANOVA p=0.000, Figure 5.13 (a)). Sample IVIS images show a reduction in tumour size in an animal that received miR-379 exosomes compared to NTC treatment (Figure 5.13 (b)).

Chapter 5: Evaluating Therapeutic Impact of Systemic Delivery of miR-379

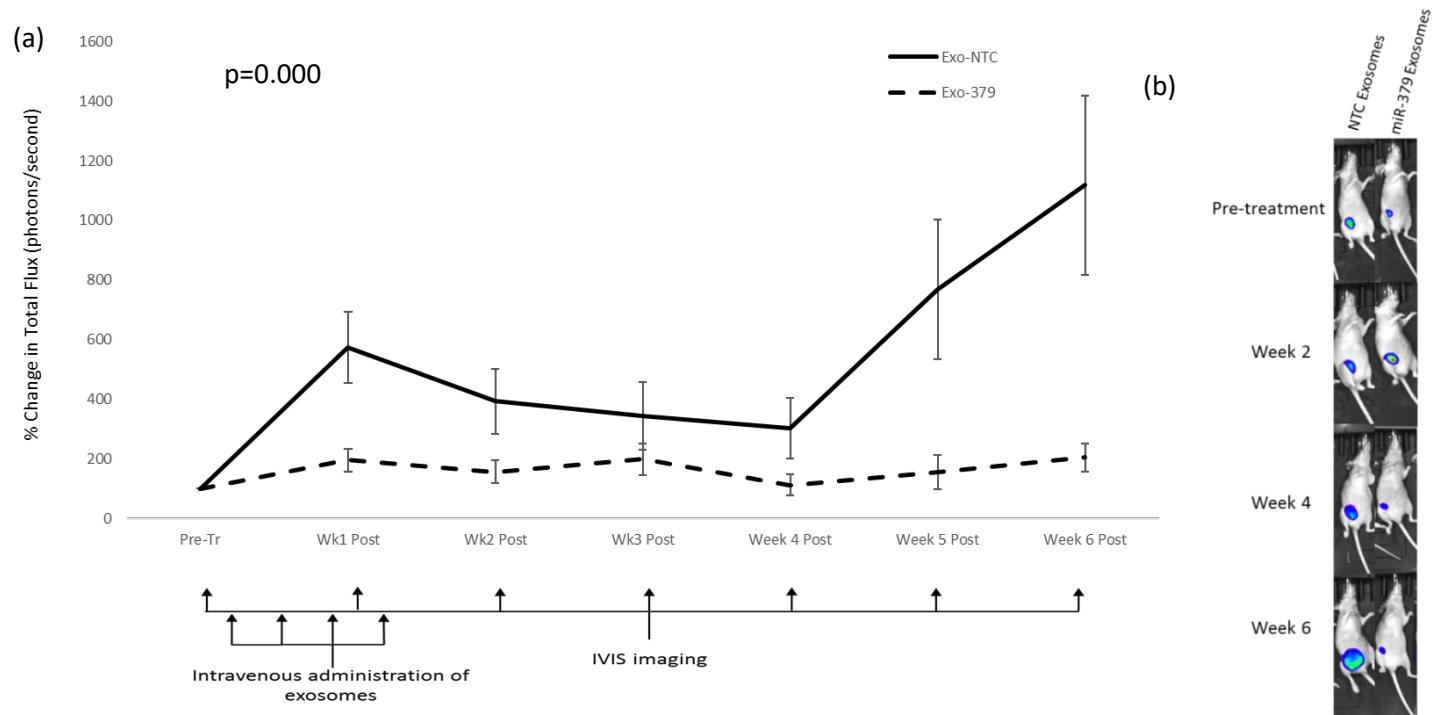


Figure 5. 13: (a) IVIS imaging and quantification of bioluminescence of tumours over 6 weeks showing a significant reduction in tumour activity (ANOVA, $p=0.000$) of animals that received Exo-379 ($n=8$) compared to those in receipt of Exo-NTC ($n=8$) (b) Sample images of mice before and following repeat doses of miR-379 enriched exosomes and NTC exosomes

5.5 Discussion:

This study investigated the therapeutic potential for engineered MSCs and secreted exosomes in an animal model of breast cancer. As MSCs hold such promise as tumour targeted delivery vehicles of a therapy, this study looked to engineer the stromal cells for enriched expression of the tumour suppressive miRNA, miR-379. In order to attain long term expression of the miRNA in the MSCs, a lentivirus was chosen as it permanently integrates into the host genome. Although use of lentivirus raises safety concerns in the patient context, this study design involves the lentivirus at the *In vitro* stage. Furthermore, concerns associated with direct viral administration are averted as the virus would not directly be administered into patients. Incubation of MSCs with a lentivirus alone results in low transduction efficiencies, so it is necessary to add a compound such as polybrene [270]. Prior to transduction, the optimal concentration of polybrene was first evaluated and there was no negative impact on cell viability witnessed from Polybrene over 72 hours. 8 µg/ml has commonly been used on cells in the literature and for preliminary attempts at transducing MSCs in this group, 8 µg/ml was chosen [270]. However, it was found that polybrene inhibits MSC growth 3 weeks after transduction [270]. Our MTS assay analysed the impact on the cells over 72 hrs which was not sufficient time to witness the effect of Polybrene on MSC proliferation and as a result no impact on cell proliferation was observed. Reducing the concentration and exposure time of MSCs to Polybrene was suggested as a method of avoiding the negative effect on cell growth [270]. Based on this another method of transducing the cells was opted for. Previously published work has centrifuged cells in the presence of an adenovirus to obtain efficient transfection of MSCs [167]. In order to expose the MSCs to polybrene for as short a time as possible, lentiviral transduction of the MSCs was performed through centrifugation of the cells with a low concentration of polybrene (2 µg/ml) for 90 min. MSCs were also transduced in the presence of FGF-2 which aids in lentiviral transduction as a lentivirus more easily transduces rapidly dividing cells [271]. This resulted in effective lentiviral transduction and following selection in optimised puromycin at 4 µg/ml, there was a homogenous population of transduced MSCs.

To ensure MSCs were effectively transduced, RQ-PCR confirmed a 476-fold increase in the expression of miR-379 in the MSC-379 cohort. As this only

confirmed effective transduction in MSC-379 cells, fluorescence microscopy confirmed expression of the red fluorescent protein in both MSC-NTC and MSC-379 cell populations. While other studies have measured transduction efficiency by flow cytometry [271], this was not performed in this study as the number of MSCs transduced was very low 4×10^5 . It was essential to culture these cells for optimal exosome isolation which requires roughly 3×10^7 cells at as low a passage number as possible. As the transduced MSCs underwent selection in puromycin media, it ensured 100% expression of the lentiviral vector in the resulting culture.

Upon confirmation of lentiviral transduction, experiments were performed to determine the impact of miR-379 enrichment on native MSC characteristics. It was essential to culture a high number of MSCs in as short a time as possible for isolation of exosomes. This was done to prevent any negative impacts of *In vitro* culturing on MSCs, such as a reduction in population doublings associated with ageing [272]. There was no significant impact on cell growth witnessed between MSC-NTC and MSC-379 cells.

As the aim of this study was to systemically administer MSC-379 cells *In vivo*, a migration assay was performed to confirm that MSC-379 cells maintained their migratory ability. In this study, a migration assay using inserts (8 μm) was utilised instead of a wound healing assay as, *In vivo*, the MSCs will migrate towards a stimulus provided by the tumour. Previous reports have shown consistency in the migration of MSCs *In vitro* with *In vivo* studies [154]. Despite elevated miR-379 expression, MSC-379 cells maintained a migratory capacity following enrichment of miR-379.

Isolation of exosomes yields heterogenous populations of vesicles and as result, extensive characterisation is required. Recently, an initiative known as EV-TRACK has been established to standardise methods of isolating and characterising vesicles [187]. This report states that in 1,742 experiments recorded on the system there were 190 unique isolation methods and 1,038 unique protocols implemented when isolating extracellular vesicles. 17% of registered studies did not provide any characterisation of the vesicles. EV-METRIC consists of nine experimental parameters to abide by for reporting on exosomal research which will improve consistency of reporting. EV-TRACK will hopefully increase transparency of reporting and ultimately allow for reproducibility of findings. As it

stands, there are challenges associated with interpretation of existing data due to a lack of standardisation.

Exosomes were isolated from both MSC-NTC and MSC-379 populations.

Transmission Electron Microscopy (TEM) confirmed vesicles in the appropriate size range (30 - 120nm) and morphology distinctive of exosomes. Part of the definition of exosomes is based upon the size (30 – 120 nm) of the vesicles, when visualised by TEM, however, other microvesicles are also present within this size range [170]. However, other microvesicles within the size range would be present. The exosomes should have a 'cup-shape' morphology which was only evident through high powered microscopy such as TEM [215].

Quantification of exosomes remains a contentious issue within the field. Initially, studies indirectly quantified exosomes based on the total mass of protein present in a solution, such as the BCA method [273]. However, other soluble proteins may be present in a solution and it is known that exosomes may have differences in protein content which could skew results. Initial work relating to exosomes within our group quantified isolates using a BCA assay. However, Nanoparticle Tracking Analysis (NTA) was more recently performed which provides quantification based on particles of a designated size [273]. This is now a preferred method for quantifying exosomes as it provides real time data and accurate measurements of exosomes within a sample. Importantly, it is essential for isolates to be evenly dispersed in order to yield an accurate count. Aggregation of particles results in light scatter and inaccurate readings. In this small sample size of four isolates there was no correlation evident between isolates quantified by protein estimation and NTA. The aim of this study was to ultimately compare exosomes derived from different cell populations (MSC-NTC/379) in an *In vivo* model. For this reason, an accurate method of exosome quantification was required and NTA was deemed more reliable than protein estimation. This ensured that equal amounts of therapeutic and control exosomes were administered to tumour bearing animals.

Isolated exosomes and conditioned media from MSC-NTC and MSC-379 cells were analysed by RQ-PCR to determine if there was an increase in secretion of miR-379. There was a 2.5-fold increase in the expression of miR-379 in the non-exosomal conditioned media derived from the MSC-379 cells when compared to the MSC-

NTC cells. There was a 5-fold increase in the expression of miR-379 in the exosomes derived from the MSC-379 cells when compared to MSC-NTC exosomes, demonstrating that miR-379 was enriched within exosomes specifically. Despite studies saying that the majority of miRNAs are exosome/microvesicle free in culture media, this data showed that miR-379 was enriched within the exosome fraction [274].

In an attempt to visualise exosomal transfer, confocal microscopy was performed to visualise the co-localisation of engineered exosomes onto recipient breast cancer cells. When cells incubated with exosomes were analysed there are clear areas of red fluorescence. At 60X magnification each pixel shows a size of roughly 260 nm so it is not possible that each pixel of red fluorescence is an individual exosome. However, it is possible that they represent areas of aggregated or conjoined exosomes. Other studies have shown uptake of exosomes by means of confocal microscopy [275]. While in this study this is not confirmation of exosomal uptake, it strongly suggests transfer of exosomes onto recipient cell populations.

There was no impact on breast cancer cell viability witnessed in cells that received exosomes enriched with miR-379 when compared to cells receiving NTC exosomes. Another group have carried out similar methodologies for analysing the effect of exosomal transfer on cell proliferation [276]. This study added exosomes at 24, 48 and 72 hr timepoints and found an increase in recipient cell proliferation. Repeat dosing of engineered MSC exosomes, as demonstrated in the published study, may result in a significant alteration in cell proliferation. Similar to the data presented, another study transferred 2 µg of engineered exosomes from Hs578Ts(i)₈ cells onto recipient Hs578Ts(i)₈ cells and analysed cell growth using an acid phosphatase assay [191]. Transfer of exosomes significantly impacted migration and invasion of recipient cells. However, that study did not find any significant impact on cell proliferation, similar to work presented in this chapter.

A pilot *In vivo* study was established to determine the impact of systemically administered MSC-379 cells on tumour progression. Once tumour formation was evident, IVIS imaging was carried out following intraperitoneal administration of luciferin. 1 x 10⁶ of MSC-NTC and MSC-379 cells, based on previous studies, were injected into the tail vein of the mice [167]. Importantly no adverse reaction was

evident in any animal that received engineered MSCs over the duration of the study. Mice were imaged over the course of 6 weeks and bioluminescence of luciferase was quantified. This has been shown to be an accurate method of measuring tumours *In vivo* [277]. There was no significant impact on tumour activity witnessed between animals that received systemic MSC-379 and MSC-NTC cells. Tumour activity is the measurement of the signal intensity resulting from uptake of the D-Luciferin into tumour cells actively expressing luciferase resulting in subsequent bioluminescence [230]. Over the course of the study, animals with excessively large tumours were sacrificed. By week 6 treatment groups consisted of MSC-NTC (n=5) and MSC-379 (n=3). This explains the narrow range of bioluminescence evident in the MSC-379 group compared to the broader range in the MSC-NTC grouping. The sacrifice of animals with large tumours introduces a selection bias that is unavoidable within this study. Furthermore, there is a lack of a consistent reference throughout the study. Introduction of a phantom that expresses a consistent bioluminescent signal would allow for any fluctuations in weekly imaging to be accounted for. For this study, timing between injection of luciferin and imaging was standardised throughout to account for such fluctuations.

Cell-free exosomes alone, derived from both MSC-NTC and MSC-379 cell lines were administered to tumour bearing mice. Previous work injecting exosomes has quantified the content administered based on protein [201, 205, 206, 213]. Data from this lab has shown that there is not any correlation between protein quantification and the number of exosomes. As a result there is no pre-existing data to identify the optimal dose of exosomes. This is an area that will require significant investigation going forward to determine the optimal dose of administration *In vivo* that can be safely extrapolated to patients. In this study, exosomes were quantified based on NTA yields. 2.6×10^7 exosomes were administered at four evenly spaced time points. Every animal tolerated the repeat doses of exosomes and there was no negative impact witnessed from the therapeutic intervention over the course of the study. Following 6 weeks of IVIS imaging there was a significant reduction in tumour activity in the cohort of animals that received exosomes enriched for miR-379 when compared to animals in receipt of NTC exosomes. Animals were sacrificed in the group that received exo-379 resulting in (n=5) from week 4 of analysis. This selection bias removed

animals with excessively large tumours and impacted subsequent bioluminescent imaging. To avoid this type of impact a survival study of mice could be performed which would monitor mice over a significantly longer time than 6 weeks post treatment. The sample of IVIS images show an animal that over the course of 6 weeks had a response to exosomes enriched with miR-379. While this data is preliminary, more work is required to establish if the effects are miR-379 mediated. This positive trend suggests a possible therapeutic application for exosome encapsulated miR-379. Another study by Katakowski et al engineered the miRNA content of MSC-derived exosomes and showed therapeutic efficacy *In vivo* [213]. In contrast, that study directly administered the exosomes into the tumour and also quantified the vesicles based on protein content. For treatment of advanced breast cancer, direct administration is not possible so a study delivering the vesicles systemically offers more promise. Another study engineered the surface of exosomes derived from human embryonic kidney cells to systemically deliver let-7a [205]. This strategy was therapeutically efficacious when the vesicles were systemically administered. In this report, the exosomes were also administered at four times over four weeks. However, the vesicles were quantified based on protein estimation. If MSC derived exosomes maintain the tumour-homing capacity of the parent cell, as suggested in this study, then it would be a preferred approach of miRNA delivery as engineering of surface expression would not be required.

IVIS imaging would allow for the tracking of metastasis *in vivo*, but this was not utilised in this study. Measures were taken to block the signal released from the primary tumour in order to detect any signal from distant organs within the animal but no bioluminescent was visualised. This study was carried out over a relatively short time frame and extending the duration of the study may allow for evaluation of metastasis. Resection of the primary tumour may also aid in detection of recurrence of the tumour and study the impact that our treatment strategy would have on its prevalence. While this preliminary study suggests a therapeutic impact for exosome encapsulated miR-379, further experiments would be required to evaluate its true efficacy.

Overall, this promising data has evaluated a novel mechanism of tumour targeted delivery of a therapy in the breast cancer setting. It is possible to enrich the

expression of MSC secreted exosomes with miR-379 following lentiviral transduction of the parent cell. Systemic administration of exosomes enriched with miR-379 alone reduced tumour activity in animals bearing orthotopic tumours of breast cancer. While further work is required to evaluate the mechanism of action of this exosome mediated tumour suppression, the results offer promise for a novel systemic method of treating breast cancer.

Chapter 6

Discussion

6.1 Discussion:

There is an abundance of evidence available in the literature that highlights the potential of miRNAs as biomarkers of breast cancer. Detecting breast cancer at an early stage may be the most effective method of improving patient survival [2]. Therefore, molecules such as miRNAs offer immense potential for the detection of cancer in a non-invasive, sensitive and specific manner. Despite the large degree of research invested into circulating miRNAs, currently there are only two clinical trials (NCT01957332, NCT01722851) analysing circulating miRNAs as biomarkers of breast cancer. NCT01957332 is attempting to correlate circulating miRNA expression in venous blood to receptor status, imaging & clinical follow-up data and is expected to complete in 2018. NCT01722851 is an Irish run trial attempting to correlate miRNA expression in whole blood with patient response to both neoadjuvant and adjuvant chemotherapy. Estimated primary completion date for this trial is 2017. While circulating miRNAs were discovered in the circulation almost ten years ago, clinical implementation still evades the non-coding molecules [124]. The variations in approaches to analysing circulating miRNAs is a large contributing factor to the stagnated progression of the molecules. Other studies, similar to those described Chapter 3, have analysed the pre-analytic variables associated with circulating miRNAs [127, 239, 278]. McDonald et al, [239] found that miRNAs were more abundant in the plasma when compared to serum. This was performed on matched samples from a small number of healthy volunteers (n=10). The impact on miRNA expression resulting from different centrifugation protocols was also analysed and that was the first paper to analyse the impact of preanalytic variations on miRNA expression. Even further variations might be expected in patients with co-morbidities present. Similarly, the impact of differing centrifugation protocols was also described by Duttagupta et al [278]. Pritchard et al, [279] highlighted many issues relating to data analysis and interpretation, sample type and extraction methods in a review which recognised the issue of varying approaches. However, there has not been as robust an analysis of matched whole blood, serum and plasma samples performed to date. Work presented in this thesis clearly shows the impact that collection, storage and extraction method can have on an endogenous control, miR-16. The choice of starting material, whole blood, serum or plasma impacted expression of the same endogenous control. This has not been addressed to this extent in research articles relating to circulating miRNAs and can significantly impact the profile of

expression reported. Haemolysis clearly impacted miRNA expression in the group of samples analysed in this thesis. This is an issue worthy of caution for researchers utilizing cell free starting materials and something that has been addressed in certain studies [121, 127, 280]. Kirschener et al, [121] confirmed that miR-16 and miR-451 were both proportional to the degree of haemolysis in plasma samples. This finding was mirrored in another analysis performed by Pritchard et al, [127] where both miR-16 and miR-451 were significantly increased in haemolysed plasma samples. Fortunato et al, [280] have established an absorbance ratio (414/375 nm) and a miRNA signature which allows for detection of haemolysis in plasma samples. Similar caution to each pre-analytical variable such as starting material, collection, storage, extraction and endogenous controls used should allow for miRNAs to fulfil the potential promised. Qualitative analysis of miR-138, miR-504 and miR-379 in all 3 starting materials revealed differing patterns of detection. Interestingly, miR-379 was the only miRNA that was present in all samples analysed. This shows the importance of preliminary investigation prior to analysing a miRNA in a large number of samples. As highlighted through the analysis of circulating levels of miR-138 in EDTA and PAXgene™ collected whole blood within this study and other work previously published from this same group, contradictions can exist when different methods of analyses are employed [128]. Such contradictions can be harmful to the progression of such promising biomarkers. However, when care and attention is paid to variables such as endogenous control expression, then reproducible results can be attained. This was shown in both analyses finding a significant increase in circulating miR-504 expression in patients with breast cancer even with different methods of collection, storage and extraction were utilised. It is crucial that miRNA expression reflects disease status rather than different methodological approaches employed. Overall, a consistent and thoughtful approach to the analysis of circulating miRNAs, similar to work performed in this study, should allow for miRNAs to achieve the clinical potential that is currently promised. These variations impact reporting of findings showing a significant change in a miRNA that is not related to the disease but rather due to the methodological approach employed. This is evident in contrasting reports of miR-10b elevated in serum while not changed in whole blood of breast cancer patients compared to controls

[66, 67]. This lack of reproducibility is as a result of different approaches to analysing circulating miRNAs and is an issue that requires attention.

While miRNAs have been heralded as potential biomarkers of breast cancer there is also a significant volume of work highlighting the therapeutic potential of the molecules. Based on previous data showing reduced miR-379 expression in breast cancer, [129] miR-379 was assessed as a potential tumour suppressor miR. Data is present in the literature that highlights the tumour suppressive potential of miR-379 [129, 134, 137, 138, 141, 146, 240, 242]. However, to determine if a miRNA is a tumour suppressor an *In vivo* study analysing the impact of the miR-379 on tumour formation and progression is required. To date, such a study has not been performed. Research performed in Chapter 4 analysed impact of miR-379 expression in HER2 amplified breast cancer cells and no significant difference on tumour volume was evident over the course of the study. Photoacoustic imaging in real time showed a difference between tumour groups. This highlights the benefit of this imaging method as it gave the first indication that the characteristics of miR-379 enriched tumours may be different. Tissue analysis revealed an increase in necrosis in HCC-379 tumours, highlighting the importance of *Ex-Vivo* histological analysis. Predictive algorithms suggested that miR-379 had a putative binding site on the 3' UTR of COX-2 mRNA. A previously published report found down regulation of COX-2 gene expression (>1.5-fold) in a cell line in the presence of elevated miR-379 *In vitro* without showing any impact on protein expression [146]. This study analysed the relationship between miR-379 and COX-2 expression in *Ex-Vivo* samples. Gene expression analysis showed that miR-379 inversely correlated with COX-2. Further investigation of protein expression revealed miR-379 mediated inhibition of COX-2. Such a miRNA mediated downregulation of COX-2 has never been shown in a breast cancer model of disease. COX-2 is associated with increased lymph node infiltration [143] and staining of *Ex-Vivo* tumour draining lymph nodes revealed an apparent reduction in RFP tumour cell infiltration in animals with HCC-379 tumours. This data suggests that miR-379 reduces COX-2 expression while resulting in a reduction in lymph node infiltration and therefore invasive potential of the tumour. As COX-2 is associated with the promotion of angiogenesis, this inhibition mediated through miR-379 may serve as an explanation to the large areas of necrosis and fluid filled centres that were evident in HCC-379 tumours [143]. miRNA mediated regulation

of COX-2 could serve as a potent therapy in the breast cancer setting. This study demonstrated miR-379 as a potential tumour suppressor miR. A mechanism of action for miR-379 was also elucidated and confirmed in animal tissue samples. Overall, this was the most thorough evaluation of the tumour modulatory capabilities of miR-379 to date.

Demonstration of such a miRNA with therapeutic potential raises interest in the possibility of therapeutic application. However, there are limitations with targeted delivery of tumour suppressive miRNAs, such as miR-379. Tissue specific delivery of miRNAs in a means that will allow for efficient uptake into the recipient cells remains elusive. The potential of such therapeutic miRNAs is limited because they lack translational strategies of delivery.

This study attempted to utilise the tumour targeting capacity of Mesenchymal Stem Cells (MSCs) as vehicles for delivery of a therapy, as has been previously performed by this group [167]. Like all cell types, MSCs secrete an abundance of exosomes and published reports have presented a rationale for the enrichment of a miRNA in the parent MSC for subsequent encapsulation into secreted exosomes [213]. For the study presented in this thesis, miR-379 was utilised as the systemically administered therapy. MSCs enriched with miR-379 were employed as tumour targeted delivery vehicles. Another study implemented MSC mediated delivery of an exosome encapsulated miRNA to a tumour *In vivo* [281]. That report administered MSCs into an orthotopic model of glioma in the ipsilateral hemisphere. This delivery method was more direct than the systemic administration, which is more relevant to advanced breast cancer, utilised in this thesis. That report confirmed transfer of the miRNA via exosomes in a contact dependent manner once the cells had engrafted into the site of the tumour. In this study, MSC-379 cells did not significantly reduce tumour activity when measured by luciferase activity.

Exosomes enriched for miR-379 were systemically administered at four equal time points to mimic the consistent secretion of exosomes in the MSC-379 study. There was a significant reduction in tumour activity in the group of animals that received exosomes enriched for miR-379 when compared to animals that received NTC exosomes. Exosome encapsulated miRNA treatment of breast cancer has been achieved *In vivo* previously [205]. In that paper, surface expression of the

exosomes derived from HEK293 cell was engineered to contain the GE11 peptide to achieve targeted delivery to EGFR expressing cells. Similar to the approach taken in this study, the exosomes were also administered at four time points, however they were spaced by a week instead of 3 days and tumour growth was also quantified by IVIS imaging. Contrastingly, the vesicles were quantified based on protein estimation compared to the NTA quantification in this thesis. Protein estimation and NTA do not correlate and as a result treatment doses cannot be compared between this study and the reported finding. Initiatives such as EV-TRACK will aim to alleviate, or account for such variations in methodologies taken in exosome analysis [187]. EV-METRIC consists of nine experimental parameters which include isolation methods, protein characterisation and electron microscopy of the vesicles. This initiative is representative of the careful consideration that was required ten years ago in the analysis of circulating miRNAs. The current landscape of circulating miRNAs outlined in Chapter 3 is an example of what exosomal researchers are working to avoid. Due to the promise that exosomes hold as both diagnostics and therapeutics, many researchers are beginning to invest efforts into utilising the vesicles. This has resulted in a rapidly developing field of research. Only a few years ago, the commonly accepted method of quantifying exosomes was based on protein estimation but more recently NTA has been utilised to quantify the vesicles. EV-TRACK will focus efforts and avoid the range of variations that can be seen within circulating miRNA research.

MSC secreted exosomes used in this study may exhibit the same tumour targeted capacity of the parent cells. While possible to engineer the surface expression of exosomes to achieve targeted miRNA delivery, reducing the degree of manipulation for administered exosomes is beneficial. This is the first study to show miRNA therapy mediated through systemic administration of MSC derived exosomes *In vivo*. Importantly, there was no adverse reaction in any animal that received repeat administration of exosomes. Having shown that miR-379 is a potent tumour suppressor miR, this initial study has now developed a method of systemically delivering the miRNA.

6.2 Future Work:

Further *in vitro* studies should be performed to determine if miR-379 directly regulates COX-2. If direct regulation is present subsequent studies should confirm that miR-379 functionally suppresses COX-2. Such analysis would be required prior to confirmation of miR-379 as a regulator of COX-2. Similarly, *in vivo*, impact of miR-379 on different invasive breast cancer cell lines should be investigated. Also any impact of miR-379 enrichment on breast cancer metastasis could be analysed in a longer running study which could also determine the impact of elevated miR-379 expression on animal overall survival.

Further analysis will determine if the therapeutic effect witnessed was in fact miR-379 mediated. Samples will have to be analysed for targets of miR-379, including COX-2. Dosing of exosomes was quantified based on Nanoparticle Tracking Analysis (NTA) and yields may not reflect a clinically relevant dose as there is no previous literature in which to refer. Dose escalation studies will be essential in determining an effective and clinically relevant dose of exosomes. Consistent repeated treatment of mice with exosomes may serve to further improve the therapeutic response witnessed. This study had a follow-up of 6 weeks which is longer than has been reported. This would need to be extended further to detect any potential resurgence of the disease. A longer follow-up would also allow for the identification of circulating biomarkers that may indicate when further doses are required.

An analysis utilising an immune competent animal will allow any immune related effects of allogenic exosomes to be studied. Certain exosomes are known to express the MHC Class I molecule and studies performed in immunodeficient mice may be preventing full realisation of allogenic exosome administration [282]. A published report suggests that exosomes may be cleared by macrophages when systemically administered, highlighting the role of the immune response [283]. This could potentially impact therapeutic effects that have been seen to date in immunocompromised mouse models. One study implemented systemic delivery of xenogenic adipose MSC-derived exosomes into a rat model [284]. This study stated that no immune reaction was evident in the brain, heart, lung, liver and kidney of the animals. This would suggest that exosomes derived from immune privileged MSCs may reflect that capacity. This important finding further strengthens the rationale for using MSC derived exosomes as a therapeutic

delivery vehicle. While promising, this would have to be confirmed in an immune competent model of breast cancer.

Tracking of systemically administered exosomes would allow for biodistribution of the vesicles to be determined and improve understanding of any off-target effects. This has been achieved previously in exosomes with the surface expression engineered for GE11 [205]. Exosomes, following incubation with lipophilic near-infrared dye XenoLight DiR, were imaged and tracked to the site of the tumour *In vivo* by IVIS. To determine off target effects on non-targeted organs, samples were harvested 24 hrs following injection and imaged *Ex Vivo*. Similar work has been performed for extracellular vesicles (40-1000 nm) [267] Using exosome-mimetic vesicles, imaging was performed through incubation of macrophage-derived exosome-mimetic vesicles with ^{99m}Tc-hexamethylpropyleneamineoxime (HMPAO) [285]. This facilitated SPECT/CT imaging of the vesicles *In Vivo*. Approaches such as these are required to fully understand the mechanism of action of exosomes in the circulation but the sensitivity required to image vesicles on a nano scale is difficult to achieve. If optimised, similar imaging techniques could improve the understanding of the tumour-homing potential of MSC derived exosomes.

While miR-379 alone has shown potent therapeutic effects, it may be more efficacious in combination with other therapeutic miRNAs. Enriching the expression of a panel of tumour suppressive miRNAs into secreted exosomes could increase the potency of the therapy. Such a study has not been performed but may be necessary as one miRNA is unlikely to cure breast cancer.

Exosomes enriched with miR-379 may also offer systemic benefits. Exosomes have been proven to aid in the establishment of a pre-metastatic niche [201]. Exosomes with a therapeutic capacity may inhibit this process, thus reducing potential for metastasis.

6.3 Conclusion:

In conclusion, this study firstly demonstrated the impact that different methods of analysis have on circulating miRNAs. There is a need for standardisation in approaches taken to analyse circulating miRNAs. Researchers need to be transparent in reporting of findings to allow for comparison of results and improved reproducibility. miR-379 has potential as a tumour suppressor whose

impact is in part mediated through a reduction in the expression of pro-tumourigenic COX-2 protein. Systemic administration of MSC-secreted exosomes enriched for miR-379 significantly reduced tumour activity. Overall, this study evaluated a therapeutic miRNA in breast cancer and established a novel method for systemic delivery.

Chapter 7

References

Chapter 7: References

Chapter 7: References

1. World Health Organization, W., *Global Health Estimates*. <http://www.who.int/cancer/detection/breastcancer/en/index1.html>, 2013.
2. NCRI, *Cancer in Ireland 1994-2011: Annual Report*, in <http://www.ncri.ie/sites/ncri/files/pubs/annual%20report%202014.pdf>. 2014.
3. Society, I.C. <https://www.cancer.ie/cancer-information/breast-cancer/male-breast-cancer#sthash.GZTrEvG4.dpbs>. 2015.
4. Singletary, S.E. and J.L. Connolly, *Breast cancer staging: working with the sixth edition of the AJCC Cancer Staging Manual*. CA Cancer J Clin, 2006. **56**(1): p. 37-47; quiz 50-1.
5. Slamon, D.J., et al., *Use of chemotherapy plus a monoclonal antibody against HER2 for metastatic breast cancer that overexpresses HER2*. N Engl J Med, 2001. **344**(11): p. 783-92.
6. Hopkins, J. <http://pathology.jhu.edu/breast/grade.php>. 2015.
7. Bloom, H.J. and W.W. Richardson, *Histological grading and prognosis in breast cancer; a study of 1409 cases of which 359 have been followed for 15 years*. Br J Cancer, 1957. **11**(3): p. 359-77.
8. Perou, C.M., et al., *Molecular portraits of human breast tumours*. Nature, 2000. **406**(6797): p. 747-52.
9. Sorlie, T., et al., *Gene expression patterns of breast carcinomas distinguish tumor subclasses with clinical implications*. Proc Natl Acad Sci U S A, 2001. **98**(19): p. 10869-74.
10. Rouzier, R., et al., *Breast cancer molecular subtypes respond differently to preoperative chemotherapy*. Clin Cancer Res, 2005. **11**(16): p. 5678-85.
11. Spears, M. and J. Bartlett, *The potential role of estrogen receptors and the SRC family as targets for the treatment of breast cancer*. Expert Opin Ther Targets, 2009. **13**(6): p. 665-74.
12. Early Breast Cancer Trialists' Collaborative, G., et al., *Relevance of breast cancer hormone receptors and other factors to the efficacy of adjuvant tamoxifen: patient-level meta-analysis of randomised trials*. Lancet, 2011. **378**(9793): p. 771-84.
13. Ellis, M.J., et al., *Whole-genome analysis informs breast cancer response to aromatase inhibition*. Nature, 2012. **486**(7403): p. 353-60.
14. Hudis, C.A., *Trastuzumab--mechanism of action and use in clinical practice*. N Engl J Med, 2007. **357**(1): p. 39-51.
15. Kaufman, B., et al., *Trastuzumab plus anastrozole versus anastrozole alone for the treatment of postmenopausal women with human epidermal growth factor receptor 2-positive, hormone receptor-positive metastatic breast cancer: results from the randomized phase III TAnDEM study*. J Clin Oncol, 2009. **27**(33): p. 5529-37.
16. Badve, S., et al., *Basal-like and triple-negative breast cancers: a critical review with an emphasis on the implications for pathologists and oncologists*. Mod Pathol, 2011. **24**(2): p. 157-67.
17. Livasy, C.A., et al., *Phenotypic evaluation of the basal-like subtype of invasive breast carcinoma*. Mod Pathol, 2006. **19**(2): p. 264-71.
18. Saslow, D., et al., *American Cancer Society guidelines for breast screening with MRI as an adjunct to mammography*. CA Cancer J Clin, 2007. **57**(2): p. 75-89.
19. Bassett, L.W., *Mammographic analysis of calcifications*. Radiol Clin North Am, 1992. **30**(1): p. 93-105.

Chapter 7: References

20. Heywang-Kobrunner, S.H., A. Hacker, and S. Sedlacek, *Advantages and Disadvantages of Mammography Screening*. Breast Care (Basel), 2011. **6**(3): p. 199-207.
21. Baines, C.J., *Are There Downsides to Mammography Screening?* The Breast Journal, 2005. **11**(s1): p. S7-S10.
22. Breastcancer.org.
<http://www.breastcancer.org/symptoms/testing/types/mri/screening>. 2016.
23. Feldman, E.D., B.A. Oppong, and S.C. Willey, *Breast cancer screening: clinical, radiologic, and biochemical*. Clin Obstet Gynecol, 2012. **55**(3): p. 662-70.
24. Halsted, W.S., I. *The Results of Radical Operations for the Cure of Carcinoma of the Breast*. Ann Surg, 1907. **46**(1): p. 1-19.
25. Yu, K.D., S. Li, and Z.M. Shao, *Different annual recurrence pattern between lumpectomy and mastectomy: implication for breast cancer surveillance after breast-conserving surgery*. Oncologist, 2011. **16**(8): p. 1101-10.
26. Albertini, J.J., et al., *Lymphatic mapping and sentinel node biopsy in the patient with breast cancer*. JAMA, 1996. **276**(22): p. 1818-22.
27. Robson, D. and S. Verma, *Anthracyclines in early-stage breast cancer: is it the end of an era?* Oncologist, 2009. **14**(10): p. 950-8.
28. Silver, D.P., et al., *Efficacy of neoadjuvant Cisplatin in triple-negative breast cancer*. J Clin Oncol, 2010. **28**(7): p. 1145-53.
29. Early Breast Cancer Trialists' Collaborative, G., *Effects of chemotherapy and hormonal therapy for early breast cancer on recurrence and 15-year survival: an overview of the randomised trials*. Lancet, 2005. **365**(9472): p. 1687-717.
30. Kirova, Y.M., *Recent advances in breast cancer radiotherapy: Evolution or revolution, or how to decrease cardiac toxicity?* World J Radiol, 2010. **2**(3): p. 103-8.
31. Delaney, G., M. Barton, and S. Jacob, *Estimation of an optimal radiotherapy utilization rate for breast carcinoma: a review of the evidence*. Cancer, 2003. **98**(9): p. 1977-86.
32. John W. Park, D.T., Michael J. Campbell and Laura J. Esserman, *Biological Therapy of Breast Cancer*. BioDrugs, 2000. **14**(4): p. 221-246.
33. Baum, M., *Current status of aromatase inhibitors in the management of breast cancer and critique of the NCIC MA-17 trial*. Cancer Control, 2004. **11**(4): p. 217-21.
34. Osborne, C.K., *Tamoxifen in the treatment of breast cancer*. N Engl J Med, 1998. **339**(22): p. 1609-18.
35. Junttila, M.R. and F.J. de Sauvage, *Influence of tumour micro-environment heterogeneity on therapeutic response*. Nature, 2013. **501**(7467): p. 346-54.
36. Chen, K., Y.H. Huang, and J.L. Chen, *Understanding and targeting cancer stem cells: therapeutic implications and challenges*. Acta Pharmacol Sin, 2013. **34**(6): p. 732-40.
37. Shering, S.G., et al., *Preoperative CA 15-3 concentrations predict outcome of patients with breast carcinoma*. Cancer, 1998. **83**(12): p. 2521-7.
38. Kokko, R., K. Holli, and M. Hakama, *Ca 15-3 in the follow-up of localised breast cancer: a prospective study*. Eur J Cancer, 2002. **38**(9): p. 1189-93.
39. Wang, J., et al., *Tumor-associated circulating microRNAs as biomarkers of cancer*. Molecules, 2014. **19**(2): p. 1912-38.

Chapter 7: References

40. Lee, R.C., R.L. Feinbaum, and V. Ambros, *The C. elegans heterochronic gene lin-4 encodes small RNAs with antisense complementarity to lin-14*. Cell, 1993. **75**(5): p. 843-54.
41. Huntzinger, E. and E. Izaurralde, *Gene silencing by microRNAs: contributions of translational repression and mRNA decay*. Nat Rev Genet, 2011. **12**(2): p. 99-110.
42. Rajewsky, N., *microRNA target predictions in animals*. Nat Genet, 2006. **38** **Suppl**: p. S8-13.
43. Krek, A., et al., *Combinatorial microRNA target predictions*. Nat Genet, 2005. **37**(5): p. 495-500.
44. Kozomara, A. and S. Griffiths-Jones, *miRBase: integrating microRNA annotation and deep-sequencing data*. Nucleic Acids Res, 2011. **39**(Database issue): p. D152-7.
45. Rodriguez, A., et al., *Identification of mammalian microRNA host genes and transcription units*. Genome Res, 2004. **14**(10A): p. 1902-10.
46. Murchison, E.P. and G.J. Hannon, *miRNAs on the move: miRNA biogenesis and the RNAi machinery*. Curr Opin Cell Biol, 2004. **16**(3): p. 223-9.
47. Heneghan, H.M., N. Miller, and M.J. Kerin, *MiRNAs as biomarkers and therapeutic targets in cancer*. Curr Opin Pharmacol, 2010. **10**(5): p. 543-50.
48. Asgari, S., *Role of MicroRNAs in Insect Host-Microorganism Interactions*. Front Physiol, 2011. **2**: p. 48.
49. McDermott, A.M., et al., *The therapeutic potential of microRNAs: disease modulators and drug targets*. Pharm Res, 2011. **28**(12): p. 3016-29.
50. Jackson, R.J. and N. Standart, *How do microRNAs regulate gene expression?* Sci STKE, 2007. **2007**(367): p. re1.
51. Hussain M., F.F.D., Moreira L. A., O'Neill S. L., Asgari S. , *Wolbachia utilizes host microRNAs to manipulate host gene expression and facilitate colonization of the dengue vector Aedes aegypti*. PNAS, 2011. **108**.
52. Ma, F., et al., *MicroRNA-466l upregulates IL-10 expression in TLR-triggered macrophages by antagonizing RNA-binding protein tristetraprolin-mediated IL-10 mRNA degradation*. J Immunol, 2010. **184**(11): p. 6053-9.
53. Henke, J.I., et al., *microRNA-122 stimulates translation of hepatitis C virus RNA*. EMBO J, 2008. **27**(24): p. 3300-10.
54. Chang, T.C. and J.T. Mendell, *microRNAs in vertebrate physiology and human disease*. Annu Rev Genomics Hum Genet, 2007. **8**: p. 215-39.
55. Avril-Sassen, S., et al., *Characterisation of microRNA expression in post-natal mouse mammary gland development*. BMC Genomics, 2009. **10**: p. 548.
56. Calin, G.A., et al., *Frequent deletions and down-regulation of micro- RNA genes miR15 and miR16 at 13q14 in chronic lymphocytic leukemia*. Proc Natl Acad Sci U S A, 2002. **99**(24): p. 15524-9.
57. Gurtner, A., et al., *Dysregulation of microRNA biogenesis in cancer: the impact of mutant p53 on Drosha complex activity*. J Exp Clin Cancer Res, 2016. **35**: p. 45.
58. Lu, J., et al., *MicroRNA expression profiles classify human cancers*. Nature, 2005. **435**(7043): p. 834-8.
59. Shi, M., et al., *Metastasis-related miRNAs, active players in breast cancer invasion, and metastasis*. Cancer Metastasis Rev, 2010. **29**(4): p. 785-99.

Chapter 7: References

60. Lowery, A.J., et al., *MicroRNA signatures predict oestrogen receptor, progesterone receptor and HER2/neu receptor status in breast cancer*. *Breast Cancer Res*, 2009. **11**(3): p. R27.
61. Riaz, M., et al., *miRNA expression profiling of 51 human breast cancer cell lines reveals subtype and driver mutation-specific miRNAs*. *Breast Cancer Res*, 2013. **15**(2): p. R33.
62. Iorio, M.V., et al., *MicroRNA gene expression deregulation in human breast cancer*. *Cancer Res*, 2005. **65**(16): p. 7065-70.
63. Calin, G.A., et al., *A MicroRNA signature associated with prognosis and progression in chronic lymphocytic leukemia*. *N Engl J Med*, 2005. **353**(17): p. 1793-801.
64. Chen, X., et al., *Secreted microRNAs: a new form of intercellular communication*. *Trends Cell Biol*, 2012. **22**(3): p. 125-32.
65. Bertoli, G., C. Cava, and I. Castiglioni, *MicroRNAs: New Biomarkers for Diagnosis, Prognosis, Therapy Prediction and Therapeutic Tools for Breast Cancer*. *Theranostics*, 2015. **5**(10): p. 1122-43.
66. Mar-Aguilar, F., et al., *Serum circulating microRNA profiling for identification of potential breast cancer biomarkers*. *Disease Markers*, 2013. **34**(3): p. 163-169.
67. Heneghan, H.M., et al., *Systemic miRNA-195 differentiates breast cancer from other malignancies and is a potential biomarker for detecting noninvasive and early stage disease*. *Oncologist*, 2010. **15**(7): p. 673-82.
68. Wang, F., et al., *Correlation and quantitation of microRNA aberrant expression in tissues and sera from patients with breast tumor*. *Gynecol Oncol*, 2010. **119**(3): p. 586-93.
69. Cookson, V.J., et al., *Circulating microRNA profiles reflect the presence of breast tumours but not the profiles of microRNAs within the tumours*. *Cell Oncol (Dordr)*, 2012. **35**(4): p. 301-8.
70. Ng, E.K.O., et al., *Circulating microRNAs as Specific Biomarkers for Breast Cancer Detection*. *PLoS One*, 2013. **8**(1).
71. Wu, X.W., et al., *De novo sequencing of circulating miRNAs identifies novel markers predicting clinical outcome of locally advanced breast cancer*. *J Transl Med*, 2012. **10**.
72. Schwarzenbach, H., et al., *Diagnostic potential of PTEN-targeting miR-214 in the blood of breast cancer patients*. *Breast Cancer Research and Treatment*, 2012. **134**(3): p. 933-941.
73. Schrauder, M.G., et al., *Circulating micro-RNAs as potential blood-based markers for early stage breast cancer detection*. *PLoS One*, 2012. **7**(1): p. e29770.
74. Sieuwerts, A.M., et al., *mRNA and microRNA expression profiles in circulating tumor cells and primary tumors of metastatic breast cancer patients*. *Clin Cancer Res*, 2011. **17**(11): p. 3600-18.
75. Khan, S., et al., *miR-379 Regulates Cyclin B1 Expression and Is Decreased in Breast Cancer*. *PLoS One*, 2013. **8**(7).
76. Heneghan, H.M., et al., *Circulating microRNAs as Novel Minimally Invasive Biomarkers for Breast Cancer*. *Annals of Surgery*, 2010. **251**(3): p. 499-505.
77. McDermott, A.M., M.J. Kerin, and N. Miller, *Identification and validation of miRNAs as endogenous controls for RQ-PCR in blood specimens for breast cancer studies*. *PLoS One*, 2013. **8**(12): p. e83718.
78. Waters, P.S., et al., *Impact of Tumour Epithelial Subtype on Circulating microRNAs in Breast Cancer Patients*. *PLoS One*, 2014. **9**(3).

Chapter 7: References

79. Waters, P.S., et al., *Relationship between Circulating and Tissue microRNAs in a Murine Model of Breast Cancer*. PLoS One, 2012. **7**(11).
80. Wang, P.Y., et al., *Higher expression of circulating miR-182 as a novel biomarker for breast cancer*. Oncology Letters, 2013. **6**(6): p. 1681-1686.
81. Eichelser, C., et al., *Deregulated Serum Concentrations of Circulating Cell-Free MicroRNAs miR-17, miR-34a, miR-155, and miR-373 in Human Breast Cancer Development and Progression*. Clinical Chemistry, 2013. **59**(10): p. 1489-1496.
82. Sun, Y., et al., *Serum MicroRNA-155 as a Potential Biomarker to Track Disease in Breast Cancer*. PLoS One, 2012. **7**(10).
83. Si, H.Y., et al., *Circulating microRNA-92a and microRNA-21 as novel minimally invasive biomarkers for primary breast cancer*. Journal of Cancer Research and Clinical Oncology, 2013. **139**(2): p. 223-229.
84. Wang, H.J., et al., *Circulating MiR-125b as a Marker Predicting Chemoresistance in Breast Cancer*. PLoS One, 2012. **7**(4).
85. van Schooneveld, E., et al., *Expression profiling of cancerous and normal breast tissues identifies microRNAs that are differentially expressed in serum from patients with (metastatic) breast cancer and healthy volunteers*. Breast Cancer Research, 2012. **14**(1).
86. Asaga, S., et al., *Direct Serum Assay for MicroRNA-21 Concentrations in Early and Advanced Breast Cancer*. Clinical Chemistry, 2011. **57**(1): p. 84-91.
87. Zhu, W., et al., *Circulating microRNAs in breast cancer and healthy subjects*. BMC Res Notes, 2009. **2**: p. 89.
88. Li, J., et al., *Genetic heterogeneity of breast cancer metastasis may be related to miR-21 regulation of TIMP-3 in translation*. Int J Surg Oncol, 2013. **2013**: p. 875078.
89. Godfrey, A.C., et al., *Serum microRNA expression as an early marker for breast cancer risk in prospectively collected samples from the Sister Study cohort*. Breast Cancer Res, 2013. **15**(3): p. R42.
90. Tang, D., et al., *The expression and clinical significance of microRNA-1258 and heparanase in human breast cancer*. Clin Biochem, 2013. **46**(10-11): p. 926-32.
91. Zhao, F.L., et al., *Serum overexpression of microRNA-10b in patients with bone metastatic primary breast cancer*. J Int Med Res, 2012. **40**(3): p. 859-66.
92. Guo, L.J. and Q.Y. Zhang, *Decreased serum miR-181a is a potential new tool for breast cancer screening*. Int J Mol Med, 2012. **30**(3): p. 680-6.
93. Wang, X., et al., *[Serum miR-103 as a potential diagnostic biomarker for breast cancer]*. Nan Fang Yi Ke Da Xue Xue Bao, 2012. **32**(5): p. 631-4.
94. Wu, Q., et al., *Analysis of serum genome-wide microRNAs for breast cancer detection*. Clin Chim Acta, 2012. **413**(13-14): p. 1058-65.
95. Hu, Z., et al., *Serum microRNA profiling and breast cancer risk: the use of miR-484/191 as endogenous controls*. Carcinogenesis, 2012. **33**(4): p. 828-34.
96. Appaiah, H.N., et al., *Persistent upregulation of U6:SNORD44 small RNA ratio in the serum of breast cancer patients*. Breast Cancer Res, 2011. **13**(5): p. R86.
97. Wu, Q., et al., *Next-generation sequencing of microRNAs for breast cancer detection*. J Biomed Biotechnol, 2011. **2011**: p. 597145.

Chapter 7: References

98. Gotte, M., *MicroRNAs in breast cancer pathogenesis*. *Minerva Ginecol*, 2010. **62**(6): p. 559-71.
99. Roth, C., et al., *Circulating microRNAs as blood-based markers for patients with primary and metastatic breast cancer*. *Breast Cancer Res*, 2010. **12**(6): p. R90.
100. Anfossi, S., et al., *High Serum miR-19a Levels Are Associated with Inflammatory Breast Cancer and Are Predictive of Favorable Clinical Outcome in Patients with Metastatic HER2(+) Inflammatory Breast Cancer*. *PLoS One*, 2014. **9**(1): p. e83113.
101. Guo, L., et al., *Genome-wide screen for aberrantly expressed miRNAs reveals miRNA profile signature in breast cancer*. *Mol Biol Rep*, 2013. **40**(3): p. 2175-86.
102. Lyng, M.B., et al., *Prospective validation of a blood-based 9-miRNA profile for early detection of breast cancer in a cohort of women examined by clinical mammography*. *Mol Oncol*, 2016. **10**(10): p. 1621-1626.
103. Hamam, R., et al., *microRNA expression profiling on individual breast cancer patients identifies novel panel of circulating microRNA for early detection*. *Sci Rep*, 2016. **6**: p. 25997.
104. Motawi, T.M., et al., *Study of microRNAs-21/221 as potential breast cancer biomarkers in Egyptian women*. *Gene*, 2016. **590**(2): p. 210-9.
105. Zhang, L., et al., *A circulating miRNA signature as a diagnostic biomarker for non-invasive early detection of breast cancer*. *Breast Cancer Res Treat*, 2015. **154**(2): p. 423-34.
106. Jung, E.J., et al., *Plasma microRNA 210 levels correlate with sensitivity to trastuzumab and tumor presence in breast cancer patients*. *Cancer*, 2012. **118**(10): p. 2603-14.
107. Cuk, K., et al., *Plasma microRNA panel for minimally invasive detection of breast cancer*. *PLoS One*, 2013. **8**(10): p. e76729.
108. Leidner, R.S., L. Li, and C.L. Thompson, *Dampening Enthusiasm for Circulating MicroRNA in Breast Cancer*. *PLoS One*, 2013. **8**(3).
109. Zeng, R.C., et al., *Down-regulation of miRNA-30a in human plasma is a novel marker for breast cancer*. *Medical Oncology*, 2013. **30**(1).
110. Liu, J.J., et al., *Analysis of miR-205 and miR-155 expression in the blood of breast cancer patients*. *Chinese Journal of Cancer Research*, 2013. **25**(1): p. 46-54.
111. Chen, W., et al., *The level of circulating miRNA-10b and miRNA-373 in detecting lymph node metastasis of breast cancer: potential biomarkers*. *Tumour Biol*, 2013. **34**(1): p. 455-62.
112. Kumar, S., et al., *Overexpression of circulating miRNA-21 and miRNA-146a in plasma samples of breast cancer patients*. *Indian J Biochem Biophys*, 2013. **50**(3): p. 210-4.
113. Madhavan, D., et al., *Circulating miRNAs as Surrogate Markers for Circulating Tumor Cells and Prognostic Markers in Metastatic Breast Cancer*. *Clinical Cancer Research*, 2012. **18**(21): p. 5972-5982.
114. Zhao, R.H., et al., *Plasma miR-221 as a Predictive Biomarker for Chemoresistance in Breast Cancer Patients who Previously Received Neoadjuvant Chemotherapy*. *Onkologie*, 2011. **34**(12): p. 675-680.
115. Zhao, H., et al., *A Pilot Study of Circulating miRNAs as Potential Biomarkers of Early Stage Breast Cancer*. *PLoS One*, 2010. **5**(10).
116. Tjensvoll, K., et al., *miRNA expression profiling for identification of potential breast cancer biomarkers*. *Biomarkers*, 2012. **17**(5): p. 463-70.

117. Zhao, Q., et al., *A direct quantification method for measuring plasma MicroRNAs identified potential biomarkers for detecting metastatic breast cancer*. *Oncotarget*, 2016. **7**(16): p. 21865-74.
118. Madhavan, D., et al., *Circulating miRNAs with prognostic value in metastatic breast cancer and for early detection of metastasis*. *Carcinogenesis*, 2016. **37**(5): p. 461-70.
119. Freres, P., et al., *Circulating microRNA-based screening tool for breast cancer*. *Oncotarget*, 2016. **7**(5): p. 5416-28.
120. Shaffer, J., *miRNA profiling from blood — challenges and recommendations*. Qiagen, 2012.
121. Kirschner, M.B., et al., *Haemolysis during sample preparation alters microRNA content of plasma*. *PLoS One*, 2011. **6**(9): p. e24145.
122. Sethi, P. and W.J. Lukiw, *Micro-RNA abundance and stability in human brain: specific alterations in Alzheimer's disease temporal lobe neocortex*. *Neurosci Lett*, 2009. **459**(2): p. 100-4.
123. Kroh, E.M., et al., *Analysis of circulating microRNA biomarkers in plasma and serum using quantitative reverse transcription-PCR (qRT-PCR)*. *Methods*, 2010. **50**(4): p. 298-301.
124. Mitchell, P.S., et al., *Circulating microRNAs as stable blood-based markers for cancer detection*. *Proc Natl Acad Sci U S A*, 2008. **105**(30): p. 10513-8.
125. McDonald, J.S., et al., *Analysis of circulating microRNA: preanalytical and analytical challenges*. *Clinical Chemistry*, 2011. **57**(6): p. 833-40.
126. McDermott, A.M., M.J. Kerin, and N. Miller, *Identification and Validation of miRNAs as Endogenous Controls for RQ-PCR in Blood Specimens for Breast Cancer Studies*. *PLoS One*, 2013. **8**(12).
127. Pritchard, C.C., et al., *Blood cell origin of circulating microRNAs: a cautionary note for cancer biomarker studies*. *Cancer Prev Res (Phila)*, 2012. **5**(3): p. 492-7.
128. Waters, P.S., et al., *Impact of tumour epithelial subtype on circulating microRNAs in breast cancer patients*. *PLoS One*, 2014. **9**(3): p. e90605.
129. Khan, S., et al., *miR-379 regulates cyclin B1 expression and is decreased in breast cancer*. *PLoS One*, 2013. **8**(7): p. e68753.
130. Esau, C.C. and B.P. Monia, *Therapeutic potential for microRNAs*. *Adv Drug Deliv Rev*, 2007. **59**(2-3): p. 101-14.
131. Krutzfeldt, J., et al., *Silencing of microRNAs in vivo with 'antagomirs'*. *Nature*, 2005. **438**(7068): p. 685-9.
132. Kota, J., et al., *Therapeutic microRNA delivery suppresses tumorigenesis in a murine liver cancer model*. *Cell*, 2009. **137**(6): p. 1005-17.
133. Mingozzi, F. and K.A. High, *Immune responses to AAV vectors: overcoming barriers to successful gene therapy*. *Blood*, 2013. **122**(1): p. 23-36.
134. Chen, J.S., et al., *MicroRNA-379-5p inhibits tumor invasion and metastasis by targeting FAK/AKT signaling in hepatocellular carcinoma*. *Cancer Lett*, 2016. **375**(1): p. 73-83.
135. Clancy, C., et al., *Screening of exosomal microRNAs from colorectal cancer cells*. *Cancer Biomark*, 2016.
136. Chen, J.S., et al., *[Effects of microRNA-379-5p on proliferation, migration and invasion of hepatocellular carcinoma cell line]*. *Zhonghua Yi Xue Za Zhi*, 2016. **96**(18): p. 1450-3.
137. Yamamoto, K., et al., *MiR-379/411 cluster regulates IL-18 and contributes to drug resistance in malignant pleural mesothelioma*. *Oncol Rep*, 2014. **32**(6): p. 2365-72.

138. Gururajan, M., et al., *miR-154* and miR-379 in the DLK1-DIO3 microRNA mega-cluster regulate epithelial to mesenchymal transition and bone metastasis of prostate cancer*. Clin Cancer Res, 2014. **20**(24): p. 6559-69.
139. Dai, R., R. Lu, and S.A. Ahmed, *The Upregulation of Genomic Imprinted DLK1-Dio3 miRNAs in Murine Lupus Is Associated with Global DNA Hypomethylation*. PLoS One, 2016. **11**(4): p. e0153509.
140. Nadal, E., et al., *A MicroRNA cluster at 14q32 drives aggressive lung adenocarcinoma*. Clin Cancer Res, 2014. **20**(12): p. 3107-17.
141. Laddha, S.V., et al., *Genome-wide analysis reveals downregulation of miR-379/miR-656 cluster in human cancers*. Biol Direct, 2013. **8**: p. 10.
142. Singh-Ranger, G. and K. Mokbel, *The role of cyclooxygenase-2 (COX-2) in breast cancer, and implications of COX-2 inhibition*. Eur J Surg Oncol, 2002. **28**(7): p. 729-37.
143. Costa, C., et al., *Cyclo-oxygenase 2 expression is associated with angiogenesis and lymph node metastasis in human breast cancer*. J Clin Pathol, 2002. **55**(6): p. 429-34.
144. Ristimaki, A., et al., *Prognostic significance of elevated cyclooxygenase-2 expression in breast cancer*. Cancer Research, 2002. **62**(3): p. 632-635.
145. Holmes, M.D., et al., *COX-2 expression predicts worse breast cancer prognosis and does not modify the association with aspirin*. Breast Cancer Research and Treatment, 2011. **130**(2): p. 657-662.
146. Pollari, S., et al., *Identification of microRNAs inhibiting TGF-beta-induced IL-11 production in bone metastatic breast cancer cells*. PLoS One, 2012. **7**(5): p. e37361.
147. Pittenger, M.F., et al., *Multilineage potential of adult human mesenchymal stem cells*. Science, 1999. **284**(5411): p. 143-7.
148. Dominici, M., et al., *Minimal criteria for defining multipotent mesenchymal stromal cells. The International Society for Cellular Therapy position statement*. Cytotherapy, 2006. **8**(4): p. 315-7.
149. Uccelli, A., L. Moretta, and V. Pistoia, *Mesenchymal stem cells in health and disease*. Nat Rev Immunol, 2008. **8**(9): p. 726-36.
150. Kidd, S., et al., *The (in) auspicious role of mesenchymal stromal cells in cancer: be it friend or foe*. Cytotherapy, 2008. **10**(7): p. 657-67.
151. Dvorak, H.F., *Tumors: wounds that do not heal. Similarities between tumor stroma generation and wound healing*. N Engl J Med, 1986. **315**(26): p. 1650-9.
152. Spaeth, E., et al., *Inflammation and tumor microenvironments: defining the migratory itinerary of mesenchymal stem cells*. Gene Ther, 2008. **15**(10): p. 730-8.
153. De Becker, A. and I.V. Riet, *Homing and migration of mesenchymal stromal cells: How to improve the efficacy of cell therapy?* World J Stem Cells, 2016. **8**(3): p. 73-87.
154. Dwyer, R.M., et al., *Monocyte chemotactic protein-1 secreted by primary breast tumors stimulates migration of mesenchymal stem cells*. Clin Cancer Res, 2007. **13**(17): p. 5020-7.
155. Maestroni, G.J., E. Hertens, and P. Galli, *Factor(s) from nonmacrophage bone marrow stromal cells inhibit Lewis lung carcinoma and B16 melanoma growth in mice*. Cell Mol Life Sci, 1999. **55**(4): p. 663-7.
156. Spaeth, E.L., et al., *Mesenchymal stem cell transition to tumor-associated fibroblasts contributes to fibrovascular network expansion and tumor progression*. PLoS One, 2009. **4**(4): p. e4992.

Chapter 7: References

157. Karnoub, A.E., et al., *Mesenchymal stem cells within tumour stroma promote breast cancer metastasis*. Nature, 2007. **449**(7162): p. 557-63.
158. Zhu, W., et al., *Mesenchymal stem cells derived from bone marrow favor tumor cell growth in vivo*. Exp Mol Pathol, 2006. **80**(3): p. 267-74.
159. Muehlberg, F.L., et al., *Tissue-resident stem cells promote breast cancer growth and metastasis*. Carcinogenesis, 2009. **30**(4): p. 589-97.
160. Nakamura, K., et al., *Antitumor effect of genetically engineered mesenchymal stem cells in a rat glioma model*. Gene Ther, 2004. **11**(14): p. 1155-64.
161. Stoff-Khalili, M.A., et al., *Mesenchymal stem cells as a vehicle for targeted delivery of CRAbs to lung metastases of breast carcinoma*. Breast Cancer Res Treat, 2007. **105**(2): p. 157-67.
162. Kim, S.M., et al., *Gene therapy using TRAIL-secreting human umbilical cord blood-derived mesenchymal stem cells against intracranial glioma*. Cancer Res, 2008. **68**(23): p. 9614-23.
163. Mishra, P.J., et al., *Carcinoma-associated fibroblast-like differentiation of human mesenchymal stem cells*. Cancer Res, 2008. **68**(11): p. 4331-9.
164. Dembinski, J.L., et al., *Reduction of nontarget infection and systemic toxicity by targeted delivery of conditionally replicating viruses transported in mesenchymal stem cells*. Cancer Gene Ther, 2010. **17**(4): p. 289-97.
165. Gao, Y., et al., *Human mesenchymal stem cells overexpressing pigment epithelium-derived factor inhibit hepatocellular carcinoma in nude mice*. Oncogene, 2010. **29**(19): p. 2784-94.
166. Sasportas, L.S., et al., *Assessment of therapeutic efficacy and fate of engineered human mesenchymal stem cells for cancer therapy*. Proc Natl Acad Sci U S A, 2009. **106**(12): p. 4822-7.
167. Dwyer, R.M., et al., *Mesenchymal Stem Cell-mediated delivery of the sodium iodide symporter supports radionuclide imaging and treatment of breast cancer*. Stem Cells, 2011. **29**(7): p. 1149-57.
168. Marote, A., et al., *MSCs-Derived Exosomes: Cell-Secreted Nanovesicles with Regenerative Potential*. Front Pharmacol, 2016. **7**: p. 231.
169. Trams, E.G., et al., *Exfoliation of membrane ecto-enzymes in the form of micro-vesicles*. Biochim Biophys Acta, 1981. **645**(1): p. 63-70.
170. Braicu, C., et al., *Exosomes as divine messengers: are they the Hermes of modern molecular oncology?* Cell Death Differ, 2015. **22**(1): p. 34-45.
171. Vlassov, A.V., et al., *Exosomes: current knowledge of their composition, biological functions, and diagnostic and therapeutic potentials*. Biochim Biophys Acta, 2012. **1820**(7): p. 940-8.
172. Schageman, J., et al., *The complete exosome workflow solution: from isolation to characterization of RNA cargo*. Biomed Res Int, 2013. **2013**: p. 253957.
173. Kourembanas, S., *Exosomes: vehicles of intercellular signaling, biomarkers, and vectors of cell therapy*. Annu Rev Physiol, 2015. **77**: p. 13-27.
174. Azmi, A.S., B. Bao, and F.H. Sarkar, *Exosomes in cancer development, metastasis, and drug resistance: a comprehensive review*. Cancer Metastasis Rev, 2013. **32**(3-4): p. 623-42.
175. Gruenberg, J., G. Griffiths, and K.E. Howell, *Characterization of the early endosome and putative endocytic carrier vesicles in vivo and with an assay of vesicle fusion in vitro*. J Cell Biol, 1989. **108**(4): p. 1301-16.

Chapter 7: References

176. Pant, S., H. Hilton, and M.E. Burczynski, *The multifaceted exosome: biogenesis, role in normal and aberrant cellular function, and frontiers for pharmacological and biomarker opportunities*. *Biochem Pharmacol*, 2012. **83**(11): p. 1484-94.
177. Conde-Vancells, J., et al., *Characterization and comprehensive proteome profiling of exosomes secreted by hepatocytes*. *J Proteome Res*, 2008. **7**(12): p. 5157-66.
178. Raposo, G., et al., *B lymphocytes secrete antigen-presenting vesicles*. *J Exp Med*, 1996. **183**(3): p. 1161-72.
179. Ji, H., et al., *Difference gel electrophoresis analysis of Ras-transformed fibroblast cell-derived exosomes*. *Electrophoresis*, 2008. **29**(12): p. 2660-71.
180. Thery, C., et al., *Proteomic analysis of dendritic cell-derived exosomes: a secreted subcellular compartment distinct from apoptotic vesicles*. *J Immunol*, 2001. **166**(12): p. 7309-18.
181. Clayton, A., et al., *Analysis of antigen presenting cell derived exosomes, based on immuno-magnetic isolation and flow cytometry*. *J Immunol Methods*, 2001. **247**(1-2): p. 163-74.
182. Petersen, K.E., et al., *A review of exosome separation techniques and characterization of B16-F10 mouse melanoma exosomes with AF4-UV-MALS-DLS-TEM*. *Anal Bioanal Chem*, 2014. **406**(30): p. 7855-66.
183. Hiemstra, T.F., et al., *Human urinary exosomes as innate immune effectors*. *J Am Soc Nephrol*, 2014. **25**(9): p. 2017-27.
184. Liga, A., et al., *Exosome isolation: a microfluidic road-map*. *Lab Chip*, 2015. **15**(11): p. 2388-94.
185. Van Deun, J., et al., *The impact of disparate isolation methods for extracellular vesicles on downstream RNA profiling*. *J Extracell Vesicles*, 2014. **3**.
186. Soo, C.Y., et al., *Nanoparticle tracking analysis monitors microvesicle and exosome secretion from immune cells*. *Immunology*, 2012. **136**(2): p. 192-7.
187. Consortium, E.-T., et al., *EV-TRACK: transparent reporting and centralizing knowledge in extracellular vesicle research*. *Nat Methods*, 2017. **14**(3): p. 228-232.
188. Valadi, H., et al., *Exosome-mediated transfer of mRNAs and microRNAs is a novel mechanism of genetic exchange between cells*. *Nat Cell Biol*, 2007. **9**(6): p. 654-9.
189. Thery, C., *Exosomes: secreted vesicles and intercellular communications*. *F1000 Biol Rep*, 2011. **3**: p. 15.
190. Henderson, M.C. and D.O. Azorsa, *The genomic and proteomic content of cancer cell-derived exosomes*. *Front Oncol*, 2012. **2**: p. 38.
191. O'Brien, K., et al., *miR-134 in extracellular vesicles reduces triple-negative breast cancer aggression and increases drug sensitivity*. *Oncotarget*, 2015. **6**(32): p. 32774-89.
192. Skog, J., et al., *Glioblastoma microvesicles transport RNA and proteins that promote tumour growth and provide diagnostic biomarkers*. *Nat Cell Biol*, 2008. **10**(12): p. 1470-6.
193. Matsuo, H., et al., *Role of LBPA and Alix in multivesicular liposome formation and endosome organization*. *Science*, 2004. **303**(5657): p. 531-4.

Chapter 7: References

194. Keerthikumar, S., et al., *ExoCarta: A Web-Based Compendium of Exosomal Cargo*. J Mol Biol, 2016. **428**(4): p. 688-92.
195. Lin, J., et al., *Exosomes: novel biomarkers for clinical diagnosis*. ScientificWorldJournal, 2015. **2015**: p. 657086.
196. Rabinowits, G., et al., *Exosomal microRNA: a diagnostic marker for lung cancer*. Clin Lung Cancer, 2009. **10**(1): p. 42-6.
197. Lau, C., et al., *Role of pancreatic cancer-derived exosomes in salivary biomarker development*. J Biol Chem, 2013. **288**(37): p. 26888-97.
198. Feng, D., et al., *Cellular internalization of exosomes occurs through phagocytosis*. Traffic, 2010. **11**(5): p. 675-87.
199. Morelli, A.E., et al., *Endocytosis, intracellular sorting, and processing of exosomes by dendritic cells*. Blood, 2004. **104**(10): p. 3257-66.
200. Thery, C., et al., *Molecular characterization of dendritic cell-derived exosomes. Selective accumulation of the heat shock protein hsc73*. J Cell Biol, 1999. **147**(3): p. 599-610.
201. Costa-Silva, B., et al., *Pancreatic cancer exosomes initiate pre-metastatic niche formation in the liver*. Nat Cell Biol, 2015. **17**(6): p. 816-26.
202. Eldh, M., et al., *Exosomes communicate protective messages during oxidative stress; possible role of exosomal shuttle RNA*. PLoS One, 2010. **5**(12): p. e15353.
203. Ibrahim, A.G., K. Cheng, and E. Marban, *Exosomes as critical agents of cardiac regeneration triggered by cell therapy*. Stem Cell Reports, 2014. **2**(5): p. 606-19.
204. Alvarez-Erviti, L., et al., *Delivery of siRNA to the mouse brain by systemic injection of targeted exosomes*. Nat Biotechnol, 2011. **29**(4): p. 341-5.
205. Ohno, S., et al., *Systemically injected exosomes targeted to EGFR deliver antitumor microRNA to breast cancer cells*. Mol Ther, 2013. **21**(1): p. 185-91.
206. Tian, Y., et al., *A doxorubicin delivery platform using engineered natural membrane vesicle exosomes for targeted tumor therapy*. Biomaterials, 2014. **35**(7): p. 2383-90.
207. Yang, T., et al., *Exosome delivered anticancer drugs across the blood-brain barrier for brain cancer therapy in Danio rerio*. Pharm Res, 2015. **32**(6): p. 2003-14.
208. Shtam, T.A., et al., *Exosomes are natural carriers of exogenous siRNA to human cells in vitro*. Cell Commun Signal, 2013. **11**: p. 88.
209. Bryniarski, K., et al., *Antigen-specific, antibody-coated, exosome-like nanovesicles deliver suppressor T-cell microRNA-150 to effector T cells to inhibit contact sensitivity*. J Allergy Clin Immunol, 2013. **132**(1): p. 170-81.
210. Zeelenberg, I.S., et al., *Targeting tumor antigens to secreted membrane vesicles in vivo induces efficient antitumor immune responses*. Cancer Res, 2008. **68**(4): p. 1228-35.
211. Mizrak, A., et al., *Genetically engineered microvesicles carrying suicide mRNA/protein inhibit schwannoma tumor growth*. Mol Ther, 2013. **21**(1): p. 101-8.
212. Munoz, J.L., et al., *Delivery of Functional Anti-miR-9 by Mesenchymal Stem Cell-derived Exosomes to Glioblastoma Multiforme Cells Conferred Chemosensitivity*. Mol Ther Nucleic Acids, 2013. **2**: p. e126.
213. Katakowski, M., et al., *Exosomes from marrow stromal cells expressing miR-146b inhibit glioma growth*. Cancer Lett, 2013. **335**(1): p. 201-4.

Chapter 7: References

214. Bellavia, D., et al., *Interleukin 3- receptor targeted exosomes inhibit in vitro and in vivo Chronic Myelogenous Leukemia cell growth*. *Theranostics*, 2017. **7**(5): p. 1333-1345.
215. Fevrier, B. and G. Raposo, *Exosomes: endosomal-derived vesicles shipping extracellular messages*. *Curr Opin Cell Biol*, 2004. **16**(4): p. 415-21.
216. Timmers, L., et al., *Reduction of myocardial infarct size by human mesenchymal stem cell conditioned medium*. *Stem Cell Res*, 2007. **1**(2): p. 129-37.
217. Lai, R.C., et al., *Exosome secreted by MSC reduces myocardial ischemia/reperfusion injury*. *Stem Cell Res*, 2010. **4**(3): p. 214-22.
218. Yeo, R.W., et al., *Mesenchymal stem cell: an efficient mass producer of exosomes for drug delivery*. *Adv Drug Deliv Rev*, 2013. **65**(3): p. 336-41.
219. Ohno, S.I., et al., *Systemically Injected Exosomes Targeted to EGFR Deliver Antitumor MicroRNA to Breast Cancer Cells*. *Mol Ther*, 2013. **21**(1): p. 185-191.
220. Roche. https://roche-biochem.jp/catalog/category_33552.
221. Ayakannu, T., et al., *Validation of endogenous control reference genes for normalizing gene expression studies in endometrial carcinoma*. *Mol Hum Reprod*, 2015. **21**(9): p. 723-35.
222. Livak, K.J. and T.D. Schmittgen, *Analysis of relative gene expression data using real-time quantitative PCR and the 2(-Delta Delta C(T)) Method*. *Methods*, 2001. **25**(4): p. 402-8.
223. Ryan, C.M., et al., *ROCK activity and the Gbetagamma complex mediate chemotactic migration of mouse bone marrow-derived stromal cells*. *Stem Cell Res Ther*, 2015. **6**: p. 136.
224. Choi, S.C., et al., *Fibroblast growth factor-2 and -4 promote the proliferation of bone marrow mesenchymal stem cells by the activation of the PI3K-Akt and ERK1/2 signaling pathways*. *Stem Cells Dev*, 2008. **17**(4): p. 725-36.
225. <https://chemometec.com/cell-counters/cell-counter-nc-100-nucleocounter/>.
226. <http://www.kubus-sa.com/en/product/nucleocounter-cassettes-1x100/>.
227. <http://www.genengnews.com/gen-articles/exosome-and-microvesicle-characterization/4056>.
228. Wolfensohn S., L.M., *Handbook of laboratory animal management and welfare*. Wiley-Blackwell, 2013. **4th ed**.
229. Balls, M. and D.W. Straughan, *The three Rs of Russell & Burch and the testing of biological products*. *Dev Biol Stand*, 1996. **86**: p. 11-8.
230. Bronstein, I., et al., *Chemiluminescent and Bioluminescent Reporter Gene Assays*. *Analytical Biochemistry*, 1994. **219**(2): p. 169-181.
231. Cooksey, C., *Hematoxylin and related compounds--an annotated bibliography concerning their origin, properties, chemistry, and certain applications*. *Biotech Histochem*, 2010. **85**(1): p. 65-82.
232. Etzioni, R., et al., *The case for early detection*. *Nat Rev Cancer*, 2003. **3**(4): p. 243-52.
233. Esquela-Kerscher, A. and F.J. Slack, *Oncomirs - microRNAs with a role in cancer*. *Nat Rev Cancer*, 2006. **6**(4): p. 259-69.
234. Calin, G.A. and C.M. Croce, *MicroRNA signatures in human cancers*. *Nat Rev Cancer*, 2006. **6**(11): p. 857-66.

Chapter 7: References

235. Mar-Aguilar, F., et al., *Serum circulating microRNA profiling for identification of potential breast cancer biomarkers*. *Dis Markers*, 2013. **34**(3): p. 163-9.
236. Vasilatou, D., et al., *The role of microRNAs in normal and malignant hematopoiesis*. *Eur J Haematol*, 2010. **84**(1): p. 1-16.
237. Bruchova, H., et al., *Regulated expression of microRNAs in normal and polycythemia vera erythropoiesis*. *Exp Hematol*, 2007. **35**(11): p. 1657-67.
238. Rasmussen, K.D., et al., *The miR-144/451 locus is required for erythroid homeostasis*. *J Exp Med*, 2010. **207**(7): p. 1351-8.
239. McDonald, J.S., et al., *Analysis of circulating microRNA: preanalytical and analytical challenges*. *Clin Chem*, 2011. **57**(6): p. 833-40.
240. Li, Z., et al., *MicroRNA-379 suppresses osteosarcoma progression by targeting PDK1*. *J Cell Mol Med*, 2017. **21**(2): p. 315-323.
241. Taylor, B.S., et al., *Integrative genomic profiling of human prostate cancer*. *Cancer Cell*, 2010. **18**(1): p. 11-22.
242. Li, K., et al., *miR-379 Inhibits Cell Proliferation, Invasion, and Migration of Vascular Smooth Muscle Cells by Targeting Insulin-Like Factor-1*. *Yonsei Med J*, 2017. **58**(1): p. 234-240.
243. TargetScanHuman. http://www.targetscan.org/vert_71/. 2016.
244. PicTar, <http://pictar.mdc-berlin.de/>. 2007.
245. miRBase, <http://www.mirbase.org/>. 2014.
246. Soslow, R.A., et al., *COX-2 is expressed in human pulmonary, colonic, and mammary tumors*. *Cancer*, 2000. **89**(12): p. 2637-2645.
247. Parrett, M.L., et al., *Cyclooxygenase-2 gene expression in human breast cancer*. *International Journal of Oncology*, 1997. **10**(3): p. 503-507.
248. Zhang, X.H., et al., *Coexpression of VEGF-C and COX-2 and its association with lymphangiogenesis in human breast cancer*. *Bmc Cancer*, 2008. **8**.
249. Timoshenko, A.V., et al., *COX-2-mediated stimulation of the lymphangiogenic factor VEGF-C in human breast cancer*. *Br J Cancer*, 2006. **94**(8): p. 1154-1163.
250. Cornett, A.L. and C.S. Lutz, *Regulation of COX-2 expression by miR-146a in lung cancer cells*. *RNA*, 2014. **20**(9): p. 1419-30.
251. Quent, V.M., et al., *Discrepancies between metabolic activity and DNA content as tool to assess cell proliferation in cancer research*. *J Cell Mol Med*, 2010. **14**(4): p. 1003-13.
252. Khanna, C. and K. Hunter, *Modeling metastasis in vivo*. *Carcinogenesis*, 2005. **26**(3): p. 513-23.
253. Shekhar, M.P., et al., *Breast stroma plays a dominant regulatory role in breast epithelial growth and differentiation: implications for tumor development and progression*. *Cancer Res*, 2001. **61**(4): p. 1320-6.
254. Wang, M.X.a.L.V., *Photoacoustic Imaging in Biomedicine*. Review of Scientific Instruments, 2006.
255. Roggan, A., et al., *Optical Properties of Circulating Human Blood in the Wavelength Range 400-2500 nm*. *J Biomed Opt*, 1999. **4**(1): p. 36-46.
256. Xu, Z., C. Li, and L.V. Wang, *Photoacoustic tomography of water in phantoms and tissue*. *J Biomed Opt*, 2010. **15**(3): p. 036019.
257. Wilson, K.E., et al., *Multiparametric spectroscopic photoacoustic imaging of breast cancer development in a transgenic mouse model*. *Theranostics*, 2014. **4**(11): p. 1062-71.

Chapter 7: References

258. Heijblom, M., et al., *Photoacoustic image patterns of breast carcinoma and comparisons with Magnetic Resonance Imaging and vascular stained histopathology*. *Sci Rep*, 2015. **5**: p. 11778.
259. Leek, R.D., et al., *Necrosis correlates with high vascular density and focal macrophage infiltration in invasive carcinoma of the breast*. *Br J Cancer*, 1999. **79**(5-6): p. 991-5.
260. Greenbaum, D., et al., *Comparing protein abundance and mRNA expression levels on a genomic scale*. *Genome Biol*, 2003. **4**(9): p. 117.
261. Gately, S. and W.W. Li, *Multiple roles of COX-2 in tumor angiogenesis: a target for antiangiogenic therapy*. *Semin Oncol*, 2004. **31**(2 Suppl 7): p. 2-11.
262. Matsuda, Y., M. Hagi, and T. Ishiwata, *Nestin: a novel angiogenesis marker and possible target for tumor angiogenesis*. *World J Gastroenterol*, 2013. **19**(1): p. 42-8.
263. Bologna-Molina, R., et al., *Comparison of the value of PCNA and Ki-67 as markers of cell proliferation in ameloblastic tumors*. *Med Oral Patol Oral Cir Bucal*, 2013. **18**(2): p. e174-9.
264. Mackay, A.M., et al., *Chondrogenic differentiation of cultured human mesenchymal stem cells from marrow*. *Tissue Eng*, 1998. **4**(4): p. 415-28.
265. Shah, K., *Mesenchymal stem cells engineered for cancer therapy*. *Adv Drug Deliv Rev*, 2012. **64**(8): p. 739-48.
266. Chen, Y., D.Y. Gao, and L. Huang, *In vivo delivery of miRNAs for cancer therapy: challenges and strategies*. *Adv Drug Deliv Rev*, 2015. **81**: p. 128-41.
267. Lai, C.P., et al., *Dynamic biodistribution of extracellular vesicles in vivo using a multimodal imaging reporter*. *ACS Nano*, 2014. **8**(1): p. 483-94.
268. Barry, F. and J. Murphy, *Mesenchymal stem cells: clinical applications and biological characterization*. *Int J Biochem Cell Biol*, 2004. **36**(4): p. 568-84.
269. Martin, F.T., et al., *Potential role of mesenchymal stem cells (MSCs) in the breast tumour microenvironment: stimulation of epithelial to mesenchymal transition (EMT)*. *Breast Cancer Res Treat*, 2010. **124**(2): p. 317-26.
270. Lin, P., et al., *Polybrene inhibits human mesenchymal stem cell proliferation during lentiviral transduction*. *PLoS One*, 2011. **6**(8): p. e23891.
271. Lin, P., et al., *Efficient lentiviral transduction of human mesenchymal stem cells that preserves proliferation and differentiation capabilities*. *Stem Cells Transl Med*, 2012. **1**(12): p. 886-97.
272. Bonab, M.M., et al., *Aging of mesenchymal stem cell in vitro*. *BMC Cell Biol*, 2006. **7**: p. 14.
273. Boon Siew Chia, Y.P.L., Qing Wang, Pin Li, Zhiqiang Gao, *Advances in exosome quantification techniques*. *TrAC Trends in Analytical Chemistry*, 2017. **86**: p. 93-106.
274. Turchinovich, A., et al., *Characterization of extracellular circulating microRNA*. *Nucleic Acids Res*, 2011. **39**(16): p. 7223-33.
275. Parolini, I., et al., *Microenvironmental pH is a key factor for exosome traffic in tumor cells*. *J Biol Chem*, 2009. **284**(49): p. 34211-22.
276. Qu, J.L., et al., *Gastric cancer exosomes promote tumour cell proliferation through PI3K/Akt and MAPK/ERK activation*. *Dig Liver Dis*, 2009. **41**(12): p. 875-80.

Chapter 7: References

277. Jenkins, D.E., et al., *Bioluminescent imaging (BLI) to improve and refine traditional murine models of tumor growth and metastasis*. Clin Exp Metastasis, 2003. **20**(8): p. 733-44.
278. Duttagupta, R., et al., *Impact of cellular miRNAs on circulating miRNA biomarker signatures*. PLoS One, 2011. **6**(6): p. e20769.
279. Pritchard, C.C., H.H. Cheng, and M. Tewari, *MicroRNA profiling: approaches and considerations*. Nat Rev Genet, 2012. **13**(5): p. 358-69.
280. Fortunato, O., et al., *Assessment of circulating microRNAs in plasma of lung cancer patients*. Molecules, 2014. **19**(3): p. 3038-54.
281. Lee, H.K., et al., *Mesenchymal stem cells deliver synthetic microRNA mimics to glioma cells and glioma stem cells and inhibit their cell migration and self-renewal*. Oncotarget, 2013. **4**(2): p. 346-61.
282. Lynch, S., et al., *Novel MHC class I structures on exosomes*. J Immunol, 2009. **183**(3): p. 1884-91.
283. Imai, T., et al., *Macrophage-dependent clearance of systemically administered B16BL6-derived exosomes from the blood circulation in mice*. J Extracell Vesicles, 2015. **4**: p. 26238.
284. Chen, K.H., et al., *Intravenous administration of xenogenic adipose-derived mesenchymal stem cells (ADMSC) and ADMSC-derived exosomes markedly reduced brain infarct volume and preserved neurological function in rat after acute ischemic stroke*. Oncotarget, 2016. **7**(46): p. 74537-74556.
285. Hwang, D.W., et al., *Noninvasive imaging of radiolabeled exosome-mimetic nanovesicle using (99m)Tc-HMPAO*. Sci Rep, 2015. **5**: p. 15636.

Chapter 7: References

Chapter 8

Appendices

Circulating MicroRNAs in Cancer

Killian P. O'Brien, Eimear Ramphul, Linda Howard, William M. Gallagher, Carmel Malone, Michael J. Kerin, and Róisín M. Dwyer

Abstract

It is believed that microRNAs have potential as circulating biomarkers of disease; however, successful clinical implementation remains a challenge. This chapter highlights broad variations in approaches to microRNA analysis where whole blood, serum and plasma have each been employed as viable sources. Further discrepancies in approaches are seen in endogenous controls and extraction methods utilized. This has resulted in contradictory publications, even when the same microRNA is targeted in the same disease setting.

Analysis of blood samples highlighted the impact of both collection method and storage, on the microRNA profile. Analysis of a panel of microRNAs across whole blood, serum, and plasma originating from the same individual emphasized the impact of starting material on microRNA profile. This is a highly topical field of research with immense potential for translation into the clinical setting. Standardization of sample harvesting, processing and analysis will be key to this translation. Methods of sample harvesting, preservation, and analysis are outlined, with important mitigating factors highlighted.

Key words Circulating microRNAs, Breast Cancer, Whole blood, Serum, Plasma

1 Introduction

1.1 MicroRNAs Once microRNAs were shown to be detectable in the circulation of patients with cancer, a surge of interest regarding these molecules implementation as biomarkers for the disease quickly ensued. Further research discovered that microRNAs could be protein bound or encapsulated in vesicles in the circulation [1].

In the breast cancer field alone, this breakthrough has resulted in the emergence of a significant number of studies analyzing breast cancer patient blood samples for the possibility of identifying clinically relevant microRNAs. Despite tremendous potential, microRNAs have not yet been implemented in the clinical setting as a biomarker of disease. There is not a standardized approach to investigating these molecules, resulting in many different methods being employed. All three starting materials (whole blood, plasma, or serum) have been analyzed following differing methods of

extraction (TRIzol or column-based) with data generated being normalized to a large variety of endogenous controls. This variance in approaches to circulating microRNAs has resulted in opposing published results. Contradictory results can be seen in this field even when the same target microRNA is being investigated. For example, in one study circulating levels of miR-10b were found at significantly higher levels in the serum of breast cancer patients when compared to healthy controls, while another study reported no significant difference in the whole blood of patients versus healthy individuals [2 , 3]. This pattern was mirrored in other studies where miR-106a and miR-155 were found to be elevated in the serum of patients with breast cancer when compared to healthy individuals [4 , 5]. However, when these microRNAs were analyzed in plasma samples by other research groups, no significant change was observed in breast cancer patients compared to healthy controls [4 , 5]. miR-145 was also analyzed in the plasma and serum of breast cancer patients and compared to healthy controls by two separate groups [2 , 6]. Analyzing miR-145 in the serum suggested a significant increase in the patient cohort, while it was found to be decreased in the plasma of patients when compared to healthy controls [2 , 6].

However, separate studies using different source materials can achieve similar results. For example, two separate groups carried out analysis of miR-21 in serum and plasma respectively, and both concluded that it was up-regulated in patients when compared to healthy controls [4 , 6].

Variation is not limited to starting material, but is also witnessed in methods of extracting microRNA with some implementing TRIzol based methods, while others opt for column-based approaches on the same source material [7 , 8]. Storage and handling of samples vary across the studies also, with some utilizing storage of whole blood at -80°C in PAXgene™ tubes while others report storage in EDTA tubes at 4°C [3 , 9]. These contrasting approaches to analysis could impact results seen, thus inhibiting publication of consistent findings and preventing the progression of the field into the clinical setting.

1.2 Sample Source Circulating microRNAs have been analyzed in serum , plasma and whole blood of breast cancer patients and healthy controls. MicroRNAs are found to be relatively stable in these starting materials as well as other fluids such as saliva and urine. This is due to being either protein bound or encapsulated in exosomes; this makes each source material a viable option for analysis [1]. It is imperative for these samples to be stored appropriately. Whichever starting material is routinely collected in the host lab is likely to be the greatest influencing factor for researchers when choosing a starting material. A review of the literature revealed publications using each of these sources, with serum employed in the majority of studies (Table 1).

Table 1**Overview of starting material used in studies analyzing circulating microRNAs in breast cancer**

Source of extracted microRNAs	Studies Published to Date	References
Whole Blood	8	[3 , 9 , 17 , 20 , 26 – 29]
Serum	26	[2 , 4 , 7 , 8 , 18 , 21 , 22 , 30 – 48]
Plasma	13	[5 , 6 , 15 , 19 , 23 , 24 , 49 – 55]

1.3 Whole Blood

results analyzing circulating microRNAs in the whole blood of patients with breast cancer. This would be an ideal source of identifying and analyzing circulating microRNAs as it could be tested after taking a simple pinprick sample from an individual. While some studies reported use of whole blood collected in standard EDTA tubes, more recently, PAXgene™ tubes have been employed for analysis of whole blood. PAXgene™ tubes contain a blend of proprietary reagents that lyse all cells, allowing immediate stabilization of RNA. This stability is maintained for 3 days when stored at room temperature, and up to 8 years when stored at -80°C [10]. RNA extracted from whole blood will result in greater amounts of RNA available for downstream analysis when compared to the lower, but adequate, quantity of RNA extracted from serum and plasma.

However, whole blood contains many cellular constituents, which may impact upon levels of microRNAs being detected. The presence of red blood cells can impact particular microRNAs. For example, miR-16 and miR-451 have been found to be at much higher levels on erythrocytes [11]. As a result of the many cellular elements existing in whole blood, a published study took white cell counts, hemoglobin and hematocrit levels into account in order to reduce the likelihood of sample-to-sample variability [3].

An issue when using whole blood as a source of microRNAs is storage of the sample. Samples can be collected in EDTA and PAXgene™ tubes and can then be frozen for long term storage at -80°C . However, some studies also reported the long term storage of whole blood in EDTA tubes at 4°C [3]. Stabilizing the RNA in the collected sample is crucial, as it is now understood that certain microRNAs have very short half-lives, some as short as an hour [12]. This highlights the necessity to standardize methods of collecting samples in order to reduce potential variability associated with particular microRNA instability.

1.4 Plasma

Eight papers have published

As whole blood contains many factors such as erythrocytes that are capable of effecting levels of particular microRNAs, cell-free sources

have been
employed to

analyze circulating microRNAs. There have been 13 published papers that analyzed this source in

the breast cancer setting. As with the two other sources of circulating microRNAs, many publications did not provide a rationale as to why plasma was chosen. Plasma is obtained through a centrifugation process and contains certain clotting factors such as fibrinogen, requiring the addition of anticoagulants such as heparin. This addition has been shown to inhibit the downstream process of PCR analysis while citrate and EDTA have been deemed acceptable [13]. Plasma is advantageous when used for retrospective studies as it is routinely stored at -80°C where it has been reported to remain stable and suitable for subsequent analysis. One study has shown that freeze thawing of plasma samples stored at -80°C does not affect microRNAs present at high levels [14]. There is a risk of contaminating plasma samples with cells when aspirating the sample as this can subsequently result in detection of cellular based microRNAs as well as increasing levels of certain circulating microRNAs in the extracted RNA [13].

There are certain preanalytic variabilities associated with plasma. The time between sample collection and processing can significantly impact sample quality so it is important to standardize this time for each sample [13]. Differences can also be seen in how samples are centrifuged. Some studies report that samples were spun at $1300 \times g$ for 20 min at 10°C , and others at $600 \times g$ for 15 min at room temperature [6 , 15].

1.5 Serum The most studied source of circulating microRNAs is serum and this is represented by 26 published studies in breast cancer alone. Serum is also a cell-free source, but unlike plasma, the sample must first undergo the coagulation process prior to centrifugation [13]. Similar to plasma, serum can be stored at -80°C for long periods of time. A study was carried out where plasma and serum samples from the same group of individuals were compared for certain microRNAs [16]. This study found miR-15b, -16, and -24 to be detected at higher levels in plasma when compared to serum of matched individuals. This study stated that results from serum and plasma samples are not interchangeable when looking at microRNA levels. It states the need for a rigorous protocol for centrifugation to be set in place in order to standardize this method. It was also discovered that hemolysis can lead to the detection of artificially high levels of miR-15b and miR-16 [16].

2 Materials

1. EDTA tubes, serum-separating tubes and PAXgene™ tubes.
2. TRIzol, bromoanisole (BAN), isopropanol, and 75 % ethanol, store at room temperature (RT).
3. PreAnalytix kit (Qiagen/BD).
 - (a) RNase-free water
 - (b) Buffer BM1
 - (c) Buffer BM2
 - (d) Buffer BM3 (add 100 % ethanol as indicated)
 - (e) Buffer BM4 (add 100 % ethanol as indicated)
 - (f) BR5
 - (g) Proteinase K
 - (h) DNase 1 stock solution (dissolve in RNase-free water) store at 4 °C
 - (i) Buffer RDD
 - (j) PAXgene™ shredder spin column
 - (k) PAXgene™ RNA spin column
4. miRCURY™ kit (Exiqon):
 - (a) Collection tubes
 - (b) microRNA mini spin column BF
 - (c) Lysis solution BF
 - (d) Protein precipitation solution BF
 - (e) Wash solution 1 BF
 - (f) Wash solution 2 BF (add 100 % as outlined)
 - (g) RNase-free water
5. Nuclease-free water, store at 4 °C.
6. Isopropanol.
7. NanoDrop-1000 (ND-1000) Spectrophotometer.
8. Deoxynucleotide mix, 10× RT Buffer (100 mM), RNase Inhibitor (20 U/μL), Multiscribe (50 U/μL), Stem loop primer and a Probe (Applied Biosystems), store at -20 °C.
9. GeneAmp PCR system 9700 (Applied Biosystems).
10. TaqMan Fast mix (Applied Biosystems) store at 4 °C.
11. MicroAmp® Fast Optical 96-well Reaction Plate with Barcode (0.1 mL) and a MicroAmp optical adhesive film (Applied Biosystems).
12. 7900HT Fast Real Time PCR system (Life Technologies).

3 Methods

3.1

Serum and Plasma Separation

13. Shaker-Incubator PHMT (Grant-Bio).
14. 75 % Ethanol: 125 mL dH₂O and 375 mL 100 % Ethanol (make up to 500 mL and store at RT).
15. 100 % Ethanol.

3.2.2 From PAXgene™

Collected Whole Blood

1. Serum: collect whole blood in serum separating tubes and let stand at RT for 30 min for sample to coagulate prior to centrifugation at $3000 \times g$ for 5 min, remove supernatant and subsequently store at -80°C .
2. Plasma : collect whole blood directly into EDTA tubes in order to prevent coagulation of the sample. Samples are then centrifuged at $3000 \times g$ for 5 min, remove supernatant and store at -80°C .

3.2 E

xtraction of RNA

3.2.1 From EDTA Collected Whole Blood Using TRIzol BD [17] Method

1. Collect whole blood directly into an EDTA tube to prevent any coagulation of the sample and store sample at 4°C as quickly as possible until extraction.
2. Add 3 mL of TRIzol to a 5 mL tube.
3. Add 200 μL of BAN to the TRIzol and the sample is mixed.
4. Add 1 mL of whole blood to the mixture and sample is thoroughly mixed until entire sample is homogenous.
5. Stand samples at RT for 5 min prior to centrifugation at $18,000 \times g$ for 15 min at 4°C where samples will undergo phase separation leaving a clear aqueous upper phase which contains the required RNA.
6. Remove 1 mL of the aqueous phase without interfering with the middle interphase layer. Discard remaining sample.
7. Add 1 mL of isopropanol to the aqueous phase and stand at RT for 5 min.
8. Spin sample at $18,000 \times g$ for 5 min at 18°C .
9. Remove supernatant completely from the pellet.
10. Add 1 mL of 75 % ethanol to pellet and mix by vortex.
11. Centrifuge sample at $18,000 \times g$ for 5 min at 18°C .
12. Remove ethanol without disturbing the pellet and repeat addition of 75 % ethanol and centrifugation step.
13. After removing 75 % ethanol for a second time allow pellet to air-dry at RT for up to 5 min, or until the pellet has dried sufficiently.
14. Add 30 μL of NFW and vortex the sample before leaving it stand at RT for 5 min.

1. Collect whole blood directly into PAXgene™ tube and store at RT for 2 h prior to long term storage at -80°C (*see* **Note 1**).
2. Thaw sample at RT for at least 1 h prior to extraction.
3. Centrifuge sample at $4500 \times g$ for 10 min.
4. Remove and discard supernatant from pellet.
5. Add 4 mL RNase-free water, seal tube using a new Hemogard closure and vortex sample to suspend pellet.
6. Centrifuge at $4500 \times g$ for 10 min.
7. Remove and discard supernatant; add 350 μL of buffer BM1 and vortex until pellet is dissolved.
8. Transfer sample into 1.5 mL microcentrifuge tube.
9. Add 300 μL buffer BM2 to sample and then 40 μL proteinase K and vortex for 5 s.
10. Incubate sample for 10 min at 55°C and 900 RPM on shaker-incubator.
11. Pipet sample into PAXgene™ Shredder spin column and centrifuge at $20,000 \times g$ for 3 min.
12. Transfer supernatant to fresh microcentrifuge tube without disrupting pellet.
13. Add 700 μL of isopropanol to supernatant and vortex sample to mix.
14. Pipet 700 μL of sample into PAXgene™ RNA spin column and centrifuge at $20,000 \times g$ for 1 min.
15. Discard flow-through and repeat **Step 14** until entire sample has passed through PAXgene™ RNA spin column.
16. Add 350 μL of buffer BM3 and centrifuge sample at $20,000 \times g$ for 15 s.
17. Add 10 μL DNase 1 stock solution to 70 μL buffer RDD in a separate microcentrifuge tube.
18. Add 80 μL of mixture directly onto PAXgene™ RNA spin column membrane and incubate at RT for 15 min.
19. Add 350 μL of buffer BM3 to column and centrifuge at $20,000 \times g$ for 15 s.
20. Discard flow-through, add 500 μL of buffer BM4 to column and centrifuge at $20,000 \times g$ for 2 min.
21. Repeat **Step 20** .

22. Discard flow-through and centrifuge column at $20,000 \times g$ for 1 min.
23. Place column into fresh collection tube and pipet 40 μL of buffer BR5 directly onto column membrane and centrifuge at $20,000 \times g$ for 1 min.
24. Pipet another 40 μL of buffer BR5 onto column membrane and centrifuge at $20,000 \times g$ for 1 min.
25. Incubate eluate at 65°C for 5 min in shaker-incubator.
26. Following incubation place sample directly on ice or store at -80°C for future use.

3.2.3 From Serum and Plasma

3.3 Determining RNA Quality and Quantity

3.4 *c* DNA Synthesis of MicroRNA

1. Allow samples to thaw on ice.
2. Once thawed, centrifuge samples at $3000 \times g$ for 5 min.
3. Transfer 200 μL of sample to microcentrifuge tube and add 60 μL of Lysis solution BF.
4. Vortex for 5 s and incubate for 5 min at RT.
5. Add 20 μL of protein precipitation solution BF and vortex for 5 s.
6. Incubate at RT for 1 min and then centrifuge at $11,000 \times g$ for 3 min.
7. Transfer supernatant to fresh tube without disturbing pellet.
8. Add 270 μL isopropanol to sample and vortex for 5 s.
9. Put microRNA Mini Spin Column BF into a collection tube and add sample to column.
10. Incubate at RT for 2 min and then centrifuge at $11,000 \times g$ for 30 s.
11. Discard flow-through and repeat **Steps 9** and **10** if there is sample remaining.
12. Add 100 μL wash solution 1 BF to column and centrifuge at $11,000 \times g$ for 30 s.
13. Discard flow-through, add 700 μL wash solution 2 BF to column and centrifuge at $11,000 \times g$ for 30 s.
14. Discard flow-through, add 250 μL wash solution 2 BF to column and centrifuge at $11,000 \times g$ for 2 min.

15. Place column in fresh collection tube and add 50 μL RNase-free water directly onto the column membrane.
16. Incubate for 1 min at RT and centrifuge at $11,000 \times g$ for 1 min.
17. Store samples at -80°C for future use.

1. Place 1.1 μL of NFW on pedestal of ND-1000 spectrophotometer to act as a blank (see **Note 2**).

2. Adjust wavelength to 260 nm for analysis of RNA. Add 1.1 μL of sample onto pedestal and acquire reading to determine quantity and quality of RNA extracted.

1. Appropriate amount of RNA required for cDNA synthesis (25–100 ng) is calculated based on yield following analysis on ND-1000 spectrophotometer.

2. NFW is added to RNA to achieve a final volume of 5 μL .

3. A premix of 10 μL is made up for each sample of extracted RNA and each microRNA being reverse transcribed as follows (Table 2):

3.5 R Q-PCR Analysis of MicroRNA

3.6 Comparing microRNA Profile in Whole Blood, Serum, and Plasma from Same Individual Table 2

Components of cDNA synthesis premix

Component	Volume (μL)
dNTP mix (100 mM)	0.17
10 \times RT Buffer	1.65
NFW	4.57
RNase Inhibitor (20 U/ μL)	0.21
Multiscribe (50 U/ μL)	1.1
Stem Loop Primer	3.1

4. Add components of the premix as outlined in (Table 2).

5. Add 10 μL of premix to 5 μL of RNA. Samples are thoroughly mixed and centrifuged in a microcentrifuge for < 1 min.

6. Place samples into a GeneAmp PCR system 9700 and are set to one cycle of 30 min at 16°C , 30 min at 42°C , and 5 min at 4°C . Samples are then maintained at 4°C until required.

7. Store samples at -20°C until further use.

1. Make premix up to 9.3 μL for each sample and target microRNA being analyzed, consisting of 5 μL Fast Mastermix, 3.8 μL of NFW and 0.5 μL of microRNA Probe.
2. Add 0.7 μL of cDNA to each well of the 96-well plate.
3. Add the corresponding 9.3 μL of premix to the appropriate cDNA sample where every sample is run in triplicate (*see Note 3*).
4. After all samples and premix are added seal the plate with MicroAmp optical adhesive film and centrifuged at $1000 \times g$ for 1 min.
5. Plates are then run on a Thermocycler where cycles of 20 s at 95 $^{\circ}\text{C}$, 1 s at 95 $^{\circ}\text{C}$, and 20 s at 60 $^{\circ}\text{C}$ are repeated.
6. Data is collected and analyzed.

Whole blood, plasma, and serum samples, originating from the same patient were collected and subsequently had the microRNA profile analyzed (Fig. 1). Whole blood was collected and stored in PAXgene™ tubes, while plasma samples were collected in EDTA tubes and serum samples were collected in serum separating tubes. Plasma and serum samples were centrifuged at $3000 \times g$ for 5 min. miR-16 was used for this comparison due to its frequent use as an endogenous control.

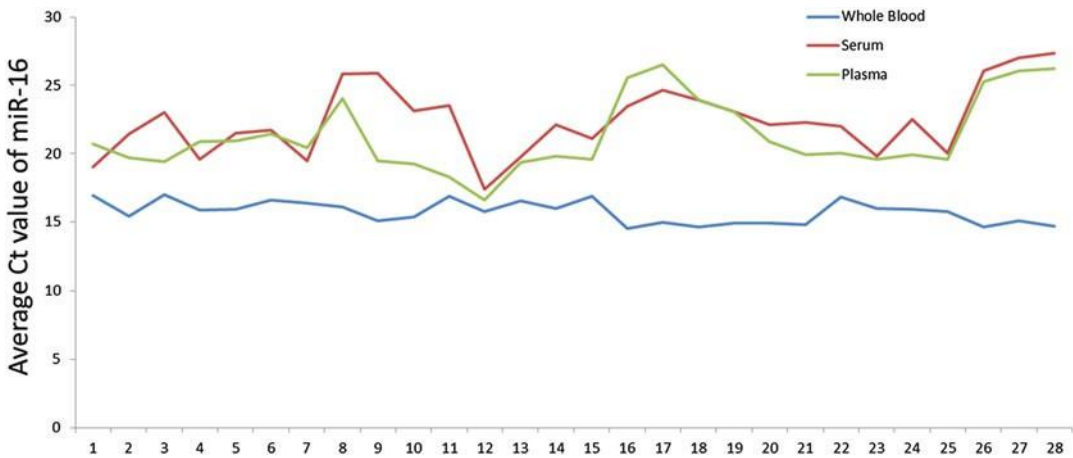


Fig. 1 Comparing levels of miR-16 across whole blood, plasma, and serum from the same individuals

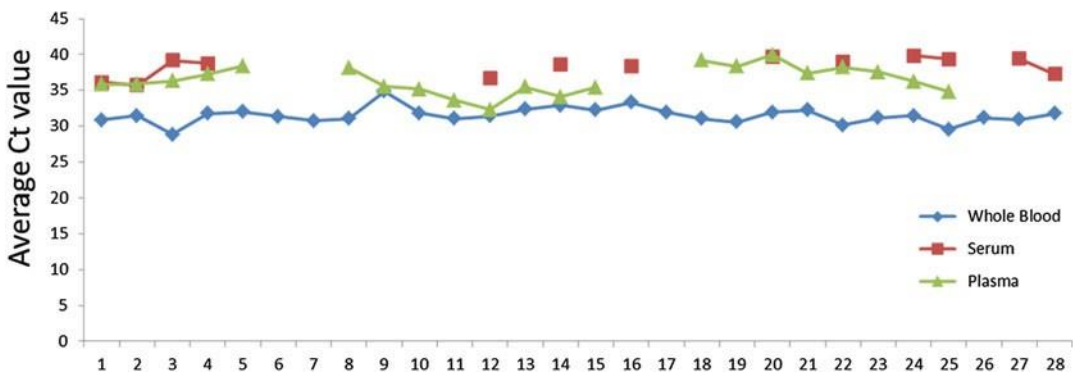


Fig. 2 Comparing levels of miR-504 across whole blood, plasma, and serum from the same individuals

miR-16 was detectable in all samples analyzed (Fig. 1). Different trends in miR-16 levels can be seen across the three sources with similar patterns noticed between certain individuals when analyzing plasma and serum. However, the miR-16 values were clearly more variable in plasma (Ct range: 17–27) and serum (Ct range: 18–26) than in PAXgene™ stabilized blood (Ct range: 14–16) from the same individuals.

Two more microRNAs were also analyzed across these same matching samples, miR-138 and miR-504. Firstly, miR-504 was detected in all whole blood samples. In contrast, it was detected in 46 % of serum samples and 75 % of plasma samples (Fig. 2). This suggests that when analyzing particular microRNAs, source material may be crucial for accurate analysis.

Analysis of miR-138 in the same cohort of samples yielded similar results with the microRNA detectable in every whole blood sample analyzed, while it was detected in only 68 % of serum samples and 79 % of plasma samples (data not shown).

3.7 Impact A very important issue to consider when using serum and plasma **of Hemolysis** as a source for microRNA analysis is hemolysis. Hemolysis is the rupturing of erythrocytes and can be measured by quantifying levels of free hemoglobin in the sample (see Note 4). This is achieved using a spectrophotometer to analyze levels of oxy-hemoglobin, which is detected when peaks at wavelength $\lambda = 414$ are observed indicating that a sample is hemolyzed [11]. Another method of detecting hemolysis is to analyze particular microRNAs that are known to be enriched in erythrocytes, such as miR-451 and miR-144 [11]. These steps are necessary when determining the quality of the source material as hemolysis does have an effect on the portrait of microRNAs seen in these samples.

Hemolysis is an issue that was ignored at first but as the field developed it became far too great a problem not to be addressed. It has been shown to effect levels of certain microRNAs, such as miR-16, miR-15b, and miR-24 [11]. As miR-16 has been employed as endogenous control for studies looking at circulating microRNAs in both serum and plasma, it makes the issue of hemolysis a major factor in data analysis and something that cannot be overlooked [18, 19].

3.8 Impact There is a large variation in extraction methods when looking **of Variations** across all publications regarding circulating microRNAs in breast **in Extraction Methods** cancer, with nine different methods employed, eight of which are column-based (Table 3).

As part of the current study, analysis of particular microRNAs in whole blood was carried out on samples stored in EDTA tubes followed by TRIzol BD extraction, as well as microRNAs analyzed

Table 3

Different extraction methods used in analysis of circulating microRNAs in breast cancer. (X indicating at least 1 published use of technique)

Method	Whole Blood	Serum	Plasma
mirVana miRNA isolation kit		X	X
mirVana PARIS kit		X	
miRNeasy mini kit	X	X	X
TRIzol LS method		X	X
TRIzol BD method	X	X	X
BioChain miRNA isolation kit		X	
MagMax viral RNA isolation kit		X	
Norgens RNA purification kit		X	X
Allprep DNA/RNA micro kit	X		

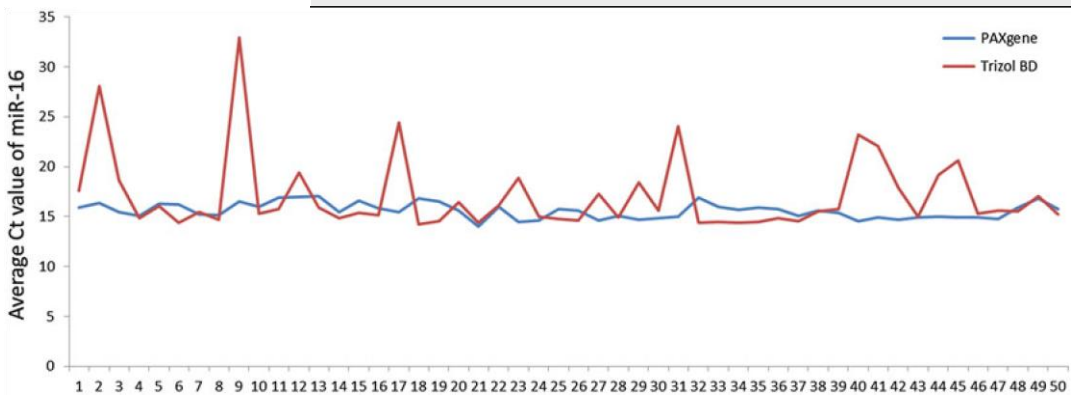


Fig. 3 Comparison of miR-16 levels in whole blood harvested into PAXgene™ tubes followed by PreAnalytix extraction, or EDTA tubes followed by TRIzol BD method respectively

in whole blood samples collected in PAXgene™ tubes followed by extraction using the PreAnalytix kit (Qiagen). Levels of miR-16 were analyzed and detected using RQ-PCR analysis (Fig. 3).

miR-16 was detected at high levels (low Ct value) as it is robustly present in whole blood. Expression was found to be more stable in the PAXgene™ processed samples, with miR-16 ranging from 14 to 16 Ct. In contrast, whole blood collected in EDTA tubes with subsequent TRIzol extraction was found to be much less stable, with miR-16 ranging from 14 to 34 Ct. In samples collected, stored and extracted in

this manner, miR-16 would not be deemed a suitable endogenous control.

3.9 Impact Following a similar pattern, there is also inconsistency in relation **of Endogenous** to which endogenous controls are employed for the analysis of

Controls circulating microRNAs in breast cancer, with 12 different endogenous controls used for analysis of serum microRNAs alone (Table 4). An endogenous control would ideally be stably expressed across all samples used for analysis so that sample-to-sample variability can be accounted for, as well as variations in template loading and varying efficiencies of reaction.

These endogenous controls range from microRNAs to ribosomal RNAs, to spiked in controls. Entire studies are carried out to establish appropriate endogenous controls for analysis of blood [20]. Many published studies determine suitability of endogenous control across a range of samples to ensure that it is stably expressed prior to employment [21].

miR-16 is seen as an appropriate endogenous control for each source material and one that has featured in several publications [7, 9, 18 – 20, 22 – 24]. There has also been work stating that miR-16 along with other microRNAs are impacted by blood cells and hemolysis [25]. As shown in Fig. 3, miR-16 can fluctuate depending on storage and extraction method. In our hands it was found to be robust and stable in PAXgene™ collected whole blood.

Table 4
Variation in endogenous controls used in literature of circulating microRNAs in breast cancer

Endogenous Control	Whole Blood	Serum	Plasma
5 s rRNA		X	
18S rRNA		X	
cel-miR-3 9		X	X
miR-16	X	X	X
GAPDH		X	
miR-1825		X	
U6 s nRNA		X	
RNU6B		X	X
miR-191		X	

miR-484	X
SNORD44	X
miR- 192	X
U6	X
miR- 92	X

One study chose to normalize the data to the mean and median of all microRNAs measured in a sample [26]. As endogenous controls heavily influence data analysis it is crucial that there is not a large degree of variability seen in this sector of the field. Standardization of starting material, methods of harvesting, storage and extraction will impact endogenous controls.

3.10 Conclusion This chapter highlights a number of issues that have a significant impact on the outcome of circulating microRNA studies. This in turn is preventing the realization of the full potential of microRNAs as biomarkers of disease. Standardization of approaches to analyzing microRNAs in the circulation could help establishment of these molecules as clinically relevant biomarkers.

Whole blood, plasma, and serum have all been shown to be appropriate for analyzing circulating microRNAs, and each with varying methods of sample collection and storage. This shows that there are many ways of analyzing microRNAs and that overall, no one method is necessarily superior to another. The issue is reproducibility, and that the different starting materials are not suitable for comparison. Consistency is required to support reliable comparison of data generated by different groups. Until the factors influencing microRNA presence, stability and detection in the circulation are clearly defined it is imperative that there is an attempt at standardization.

Understanding and addressing the mitigating factors that can negatively impact upon a study, such as hemolysis, is critical in achieving standardization across this field and resulting in more consistent and reproducible findings. If achieved, this may allow microRNAs to fulfill their potential as circulating biomarkers of many diseases.

3.11 Outcome If using whole blood, authors recommend collection in PAXgene™ tubes where the collection and storage guidelines are strictly adhered to. For plasma and serum collection it is crucial that samples are handled carefully and guidelines for temperature, time and centrifugation are followed rigidly. It is necessary to check and compensate for hemolysis in both plasma and serum samples. It is important to note that each starting material is a viable source; however, certain

microRNAs are not present at sufficiently high levels to be detected in particular fractions. Therefore, it is necessary to carry out preliminary analysis prior to commencing a large study analyzing a particular microRNA in the circulation.

4 Notes

1. When collecting whole blood into PAXgene™ tubes it is important for samples to be incubated for 2 h at RT in order to allow the reagents in the tube to lyse the whole blood sample.
2. When analyzing samples on the ND-1000 it is important to pay particular attention to both the 260/230 nm and 260/280 nm ratios. If ratios are not in the required range of 1.8–2.1 for samples analyzed, it could impact subsequent RQ-PCR analysis.
3. For RQ-PCR analysis keep mixtures containing the probe in opaque tubes in order to prevent any photo-bleaching of the fluorophore which may impact analysis.
4. When harvesting serum and plasma, care in handling is critical in order to prevent hemolysis of the sample. When carrying out analysis on a patient cohort it is important to take hemolysis into consideration. As hemolysis is not always readily detectable through visual analysis, it is important to analyze samples by means mentioned previously in this chapter.

Acknowledgements

This material is based upon works supported by the Irish Cancer Society collaborative cancer research centre BREAST-PREDICT Grant CCRC13GAL and funding agency “Breast Cancer Research”.

References

1. Chen X, Liang H, Zhang J et al (2012) Secreted microRNAs: a new form of intercellular communication. *Trends Cell Biol* 22(3):125–132. doi: [10.1016/j.tcb.2011.12.001](https://doi.org/10.1016/j.tcb.2011.12.001), doi:S0962-8924(11)00238-8 [pii]
2. Mar-Aguilar F, Mendoza-Ramirez JA, Malagon-Santiago I et al (2013) Serum circulating microRNA profiling for identification of potential breast cancer biomarkers. *Dis Markers* 34(3):163–169. doi: [10.3233/Dma-120957](https://doi.org/10.3233/Dma-120957)
3. Heneghan HM, Miller N, Kelly R et al (2010) Systemic miRNA-195 differentiates breast cancer from other malignancies and is a potential biomarker for detecting noninvasive and early stage disease. *Oncologist* 15(7):673–682. doi: [10.1634/theoncologist.2010-0103](https://doi.org/10.1634/theoncologist.2010-0103), doi:theoncologist.2010-0103 [pii]
4. Wang F, Zheng Z, Guo J et al (2010) Correlation and quantitation of microRNA aberrant expression in tissues and sera from patients with breast tumor. *Gynecol Oncol* 119(3):586–593. doi: [10.1016/j.ygyno.2010.07.021](https://doi.org/10.1016/j.ygyno.2010.07.021), S0090-8258(10)00550-0 [pii]
5. Cookson VJ, Bentley MA, Hogan BV et al (2012) Circulating microRNA profiles reflect the presence of breast tumours but not the profiles of microRNAs within the tumours. *Cell Oncol (Dordr)* 35(4):301–308. doi: [10.1007/s13402-012-0089-1](https://doi.org/10.1007/s13402-012-0089-1)
6. Ng EKO, Li RFN, Shin VY et al (2013) Circulating microRNAs as specific biomarkers for breast cancer detection. *PLoS One* 8(1), e53141, doi:ARTN e53141. DOI 10.1371/journal.pone.0053141
7. Wu XW, Somlo G, Yu Y et al (2012) De novo sequencing of circulating miRNAs identifies novel markers predicting clinical outcome of locally

- advanced breast cancer. *J Transl Med* 10:42. doi: [10.1186/1479-5876-10-42](https://doi.org/10.1186/1479-5876-10-42)
8. Schwarzenbach H, Milde-Langosch K, Steinbach B et al (2012) Diagnostic potential of PTEN-targeting miR-214 in the blood of breast cancer patients. *Breast Cancer Res Treat* 134(3):933–941. doi: [10.1007/s10549-012-1988-6](https://doi.org/10.1007/s10549-012-1988-6)
 9. Schrauder MG, Strick R, Schulz-Wendtland R et al (2012) Circulating micro-RNAs as potential blood-based markers for early stage breast cancer detection. *PLoS One* 7(1), e29770. doi: [10.1371/journal.pone.0029770](https://doi.org/10.1371/journal.pone.0029770) , PONE-D-11-17907 [pii]
 10. S haffer J (2012) miRNA profi ling from blood — challenges and recommendations. Qiagen
 11. Kirschner MB, Kao SC, Edelman JJ et al (2011) Haemolysis during sample preparation alters microRNA content of plasma. *PLoS One* 6(9), e24145. doi: [10.1371/journal.pone.0024145](https://doi.org/10.1371/journal.pone.0024145)
 12. Sethi P, Lukiw WJ (2009) Micro-RNA abundance and stability in human brain: specifi c alterations in Alzheimer's disease temporal lobe neocortex. *Neurosci Lett* 459(2):100–104. doi: [10.1016/j.neulet.2009.04.052](https://doi.org/10.1016/j.neulet.2009.04.052)
 13. Kroh EM, Parkin RK, Mitchell PS et al (2010) Analysis of circulating microRNA biomarkers in plasma and serum using quantitative reverse transcription-PCR (qRT-PCR). *Methods* 50(4):298–301. doi: [10.1016/j.ymeth.2010.01.032](https://doi.org/10.1016/j.ymeth.2010.01.032)
 14. Mitchell PS, Parkin RK, Kroh EM et al (2008) Circulating microRNAs as stable blood-based markers for cancer detection. *Proc Natl Acad Sci U S A* 105(30):10513–10518. doi: [10.1073/pnas.0804549105](https://doi.org/10.1073/pnas.0804549105), 0804549105 [pii]
 15. Leidner RS, Li L, Thompson CL (2013) Dampening enthusiasm for circulating MicroRNA in breast cancer. *PLoS One* 8(3), e57841. doi: [10.1371/journal.pone.0057841](https://doi.org/10.1371/journal.pone.0057841)
 16. McDonald JS, Milosevic D, Reddi HV et al (2011) Analysis of circulating microRNA: preanalytical and analytical challenges. *Clin Chem* 57(6):833–840. doi: [10.1373/clinchem.2010.157198](https://doi.org/10.1373/clinchem.2010.157198)
 17. Heneghan HM, Miller N, Lowery AJ et al (2010) Circulating microRNAs as novel minimally invasive biomarkers for breast cancer. *Ann Surg* 251(3):499–505. doi: [10.1097/Sla.0b013e3181cc939f](https://doi.org/10.1097/Sla.0b013e3181cc939f)
 18. Si HY, Sun XM, Chen YJ et al (2013) Circulating microRNA-92a and microRNA-21 as novel minimally invasive biomarkers for primary breast cancer. *J Cancer Res Clin* 139(2):223–229. doi: [10.1007/s00432-012-1315-y](https://doi.org/10.1007/s00432-012-1315-y)
 19. Zeng RC, Zhang W, Yan XQ et al (2013) Downregulation of miRNA-30a in human plasma is a novel marker for breast cancer. *Med Oncol* 30(1):477. doi: [10.1007/S12032-013-0477-Z](https://doi.org/10.1007/S12032-013-0477-Z)
 20. McDermott AM, Kerin MJ, Miller N (2013) Identifi cation and validation of miRNAs as endogenous controls for RQ-PCR in blood specimens for breast cancer studies. *PLoS One* 8(12), e83718. doi: [10.1371/journal.pone.0083718](https://doi.org/10.1371/journal.pone.0083718)
 21. Anfossi S, Giordano A, Gao H et al (2014) High serum miR-19a levels Are associated with infl ammatory breast cancer and Are predictive of favorable clinical outcome in patients with metastatic HER2(+) infl ammatory breast cancer. *PLoS One* 9(1), e83113. doi: [10.1371/journal.pone.0083113](https://doi.org/10.1371/journal.pone.0083113)
 22. Wang HJ, Tan G, Dong L et al (2012) Circulating MiR-125b as a marker predicting chemoresistance in breast cancer. *PLoS One* 7(4), e34210. doi: [10.1371/journal.pone.0034210](https://doi.org/10.1371/journal.pone.0034210)
 23. Chen W, Cai F, Zhang B et al (2013) The level of circulating miRNA-10b and miRNA-373 in detecting lymph node metastasis of breast cancer: potential biomarkers. *Tumour Biol* 34(1):455–462. doi: [10.1007/s13277-012-0570-5](https://doi.org/10.1007/s13277-012-0570-5)
 24. Kumar S, Keerthana R, Pazhanimuthu A et al (2013) Overexpression of circulating miRNA 21 and miRNA-146a in plasma samples of breast cancer patients. *Indian J Biochem Biophys* 50(3):210–214
 25. Pritchard CC, Kroh E, Wood B et al (2012) Blood cell origin of circulating microRNAs: a cautionary note for cancer biomarker studies. *Cancer Prev Res (Phila)* 5(3):492–497. doi: [10.1158/1940-6207.CAPR-11-0370](https://doi.org/10.1158/1940-6207.CAPR-11-0370)
 26. Sieuwerets AM, Mostert B, Bolt-de Vries J et al (2011) mRNA and microRNA expression profiles in circulating tumor cells and primary tumors of metastatic breast cancer patients. *Clin Cancer Res* 17(11):3600–3618. doi: [10.1158/1078-0432.CCR-11-0255](https://doi.org/10.1158/1078-0432.CCR-11-0255)
 27. Khan S, Brougham CL, Ryan J et al (2013) miR-379 regulates cyclin B1 expression and is decreased in breast cancer. *PLoS One* 8(7):e68753. doi: [10.1371/journal.pone.0068753](https://doi.org/10.1371/journal.pone.0068753)
 28. Waters PS, Dwyer RM, Brougham C et al (2014) Impact of tumour epithelial subtype on circulating microRNAs in breast cancer patients. *PLoS One* 9(3), e90605. doi: [10.1371/journal.pone.0090605](https://doi.org/10.1371/journal.pone.0090605)

29. Waters PS, McDermott AM, Wall D et al (2012) Relationship between circulating and tissue microRNAs in a murine model of breast cancer. *PLoS One* 7(11), e50459. doi: [10.1371/journal.pone.0050459](https://doi.org/10.1371/journal.pone.0050459)
30. Wang PY, Gong HT, Li BF et al (2013) Higher expression of circulating miR-182 as a novel biomarker for breast cancer. *Oncol Lett* 6(6):1681–1686. doi: [10.3892/OL.2013.1593](https://doi.org/10.3892/OL.2013.1593)
31. Eichelsler C, Flesch-Janys D, Chang-Claude J et al (2013) Deregulated serum concentrations of circulating cell-free MicroRNAs miR-17, miR-34a, miR-155, and miR-373 in human breast cancer development and progression. *Clin Chem* 59(10):1489–1496. doi: [10.1373/clinchem.2013.205161](https://doi.org/10.1373/clinchem.2013.205161)
32. Sun Y, Wang MJ, Lin GG et al (2012) Serum MicroRNA-155 as a potential biomarker to track disease in breast cancer. *PLoS One* 7(10), e47003. doi: [10.1371/journal.pone.0047003](https://doi.org/10.1371/journal.pone.0047003)
33. van Schooneveld E, Wouters MCA, Van der Auwera I et al (2012) Expression profiling of cancerous and normal breast tissues identifies microRNAs that are differentially expressed in serum from patients with (metastatic) breast cancer and healthy volunteers. *Breast Cancer Res* 14(1):R34. doi: [10.1186/Bcr3127](https://doi.org/10.1186/Bcr3127)
34. Asaga S, Kuo C, Nguyen T et al (2011) Direct serum assay for MicroRNA-21 concentrations in early and advanced breast cancer. *Clin Chem* 57(1):84–91. doi: [10.1373/clinchem.2010.151845](https://doi.org/10.1373/clinchem.2010.151845)
35. Zhu W, Qin W, Atasoy U et al (2009) Circulating microRNAs in breast cancer and healthy subjects. *BMC Res Notes* 2:89. doi: [10.1186/1756-0500-2-89](https://doi.org/10.1186/1756-0500-2-89)
36. Li J, Zhang Y, Zhang W et al (2013) Genetic heterogeneity of breast cancer metastasis may be related to miR-21 regulation of TIMP-3 in translation. *Int J Surg Oncol* 2013:875078. doi: [10.1155/2013/875078](https://doi.org/10.1155/2013/875078)
37. Godfrey AC, Xu Z, Weinberg CR et al (2013) Serum microRNA expression as an early marker for breast cancer risk in prospectively collected samples from the Sister Study cohort. *Breast Cancer Res* 15(3):R42. doi: [10.1186/bcr3428](https://doi.org/10.1186/bcr3428)
38. Tang D, Zhang Q, Zhao S et al (2013) The expression and clinical significance of microRNA-1258 and heparanase in human breast cancer. *Clin Biochem* 46(10-11):926–932. doi: [10.1016/j.clinbiochem.2013.01.027](https://doi.org/10.1016/j.clinbiochem.2013.01.027)
39. Zhao FL, Hu GD, Wang XF et al (2012) Serum overexpression of microRNA-10b in patients with bone metastatic primary breast cancer. *J Int Med Res* 40(3):859–866
40. Guo LJ, Zhang QY (2012) Decreased serum miR-181a is a potential new tool for breast cancer screening. *Int J Mol Med* 30(3):680–686. doi: [10.3892/ijmm.2012.1021](https://doi.org/10.3892/ijmm.2012.1021)
41. Wang X, Wu X, Yan L et al (2012) Serum miR-103 as a potential diagnostic biomarker for breast cancer. *Nan Fang Yi Ke Da Xue Xue Bao* 32(5):631–634
42. Wu Q, Wang C, Lu Z et al (2012) Analysis of serum genome-wide microRNAs for breast cancer detection. *Clin Chim Acta* 413(13-14):1058–1065. doi: [10.1016/j.cca.2012.02.016](https://doi.org/10.1016/j.cca.2012.02.016)
43. Hu Z, Dong J, Wang LE et al (2012) Serum microRNA profiling and breast cancer risk: the use of miR-484/191 as endogenous controls. *Carcinogenesis* 33(4):828–834. doi: [10.1093/carcin/bgs030](https://doi.org/10.1093/carcin/bgs030), doi:bgs030 [pii]
44. Appaiah HN, Goswami CP, Mina LA et al (2011) Persistent upregulation of U6:SNORD44 small RNA ratio in the serum of breast cancer patients. *Breast Cancer Res* 13(5):R86. doi: [10.1186/bcr2943](https://doi.org/10.1186/bcr2943)
45. Wu Q, Lu Z, Li H et al (2011) Next-generation sequencing of microRNAs for breast cancer detection. *J Biomed Biotechnol* 2011:597145. doi: [10.1155/2011/597145](https://doi.org/10.1155/2011/597145)
46. Gotte M (2010) MicroRNAs in breast cancer pathogenesis. *Minerva Ginecol* 62(6):559–571
47. Roth C, Rack B, Muller V et al (2010) Circulating microRNAs as blood-based markers for patients with primary and metastatic breast cancer. *Breast Cancer Res* 12(6):R90. doi: [10.1186/bcr2766](https://doi.org/10.1186/bcr2766), doi:bcr2766 [pii]
48. Guo L, Zhao Y, Yang S et al (2013) Genome-wide screen for aberrantly expressed miRNAs reveals miRNA profile signature in breast cancer. *Mol Biol Rep* 40(3):2175–2186. doi: [10.1007/s11033-012-2277-5](https://doi.org/10.1007/s11033-012-2277-5)
49. Jung EJ, Santarpia L, Kim J et al (2012) Plasma microRNA 210 levels correlate with sensitivity to trastuzumab and tumor presence in breast cancer patients. *Cancer* 118(10):2603–2614. doi: [10.1002/cncr.26565](https://doi.org/10.1002/cncr.26565)
50. Cuk K, Zucknick M, Madhavan D et al (2013) Plasma microRNA panel for minimally invasive detection of breast cancer. *PLoS One* 8(10), e76729. doi: [10.1371/journal.pone.0076729](https://doi.org/10.1371/journal.pone.0076729)
51. Liu JJ, Mao QX, Liu Y et al (2013) Analysis of miR-205 and miR-155 expression in the blood of breast cancer patients. *Chin J Cancer Res* 25(1):46–54. doi: [10.3978/j.issn.1000-9604.2012.11.04](https://doi.org/10.3978/j.issn.1000-9604.2012.11.04)
52. Madhavan D, Zucknick M, Wallwiener M et al (2012) Circulating miRNAs as Surrogate

- Markers for Circulating Tumor Cells and Prognostic Markers in Metastatic Breast Cancer. *Clin Cancer Res* 18(21):5972–5982. doi: [10.1158/1078-0432.Ccr-12-1407](https://doi.org/10.1158/1078-0432.Ccr-12-1407)
53. Zhao RH, Wu JN, Jia WJ et al (2011) Plasma miR-221 as a Predictive Biomarker for Chemoresistance in Breast Cancer Patients who Previously Received Neoadjuvant Chemotherapy. *Onkologie* 34(12):675–680. doi: [10.1159/000334552](https://doi.org/10.1159/000334552)
54. Zhao H, Shen J, Medico L et al (2010) A Pilot Study of Circulating miRNAs as Potential Biomarkers of Early Stage Breast Cancer. *PLoS One* 5(10), e13735. doi: [10.1371/journal.pone.0013735](https://doi.org/10.1371/journal.pone.0013735)
55. Tjensvoll K, Svendsen KN, Reuben JM et al (2012) miRNA expression profiling for identification of potential breast cancer biomarkers. *Biomarkers* 17(5):463–470. doi: [10.3109/1354750X.2012.686061](https://doi.org/10.3109/1354750X.2012.686061)



LAST – Ireland

17th & 18th June 2014

Category; A,B,C,D Species : Rat & Mouse

This is to certify that

Killian O'Brien

*Attended a course and passed an assessment of the course, based on the **EU EWG guidelines contained in the framework document, which fulfill the requirements under article 23 and 24 of directive 2010/63 EU for the Categories of persons stated below.*
A skills attainment record should be presented with this certificate.*

Module	Title of Core Module
1	National Legislation (Irish SI 543/12)
2	Ethics, Animal welfare and the 3 Rs (level 1)
3.1	Basic and Appropriate Biology (species noted on certificate)
4	Animal care, health and management (species noted on certificate)
5	Recognition of pain, suffering and distress (species noted on certificate)
6.1	Humane methods of euthanasia (theory)
7	Minimally invasive procedures without anaesthesia.
9	Ethics, Animal welfare and the 3 Rs (level 2)
10	Design of procedures and projects (level 1)
11	Design of procedures and projects (level 2)
	Title of Practical Module
3.2	Basic and appropriate biology (species noted on certificate)
8	Minimally invasive procedures without anaesthesia
6.2	Humane methods of euthanasia
	Title of Additional Module
20	Anaesthesia for minor procedures
22	Principles of surgery
30	Introduction to local environment

**** extract from** National Competent Authorities for the implementation of Directive 2010/63/EU on the protection of animals used for scientific purposes A working document on the development of a common education and training framework to fulfill the requirements under Articles 23 and 24 - Replacing consensus document 1 of 22-23 March 2012 – 18/19 Sept 2013

Signed

Peter F. Nowlan (Course organiser)

Contact information:

PO Box 12172 Glenageary Co. Dublin

E-Mail: sec@last-ireland.ie ; www.last-ireland.ie

Peter
Nowlan

Digitally signed by Peter Nowlan
DN: cn=Peter Nowlan,
o=LAST Ireland, ou,
email=certs@last-ireland.org,
c=IE
Location: TCD
Date: 2014.08.04 12:55:52
+01'00'

*Category A: Persons carrying out procedures on animals, Category B; Persons designing procedures and projects
Category C; Persons taking care of animals, Category D; persons performing euthanasia

IRISH MEDICINES BOARD ACTS 1995 AND 2006
Authorisation of Individual pursuant to Part 8 of the European Union
(Protection of Animals Used for Scientific Purposes) Regulations 2012
(S.I. No. 543 of 2012)

Authorisation Number: AE19125/I074
Case no: 7018616

The Health Products Regulatory Authority, in exercise of the powers conferred on it under the European Union (Protection of Animals Used for Scientific Purposes) Regulations 2012 (S.I. No. 543 of 2012) and Directive 2010/63/EU of the European Parliament and of the Council of 22 September 2010 on the protection of animals used for scientific purposes, hereby grants authorisation pursuant to Part 8 of the European Union (Protection of Animals Used for Scientific Purposes) Regulations 2012 (S.I. No. 543 of 2012) to

Mr. Killian O'Brien

subject to the provisions of the European Union (Protection of Animals used for Scientific Purposes) Regulations 2012 (S. I. No. 543 of 2012) and the terms and conditions set out in this authorisation

The authorisation, unless varied, suspended or revoked, shall continue in force from 22 August 2014 until 21 August 2019.

Signed on behalf of the Health Products Regulatory Authority on 22 August 2014



A person authorised in that behalf by the Health Products Regulatory Authority

(NOTE: This authorisation replaces any previous authorisation in respect of this individual at this particular establishment.)

TERMS OF THE AUTHORISATION

- 1 INDIVIDUAL AUTHORISATION NUMBER**
AE19125/1074
- 2 PURPOSE FOR WHICH THE INDIVIDUAL IS AUTHORISED PURSUANT TO PART 8 OF S.I. NO. 543 OF 2012**
Carrying out procedures
- 3 ESTABLISHMENT(S) AT WHICH THE INDIVIDUAL IS AUTHORISED FOR THE PURPOSE SPECIFIED ABOVE PURSUANT TO S.I. NO. 543 OF 2012**
National University of Ireland, Galway
- 4 SPECIES / CATEGORY OF ANIMALS WITH RESPECT TO WHICH THE INDIVIDUAL IS AUTHORISED FOR THE PURPOSE SPECIFIED ABOVE PURSUANT TO S.I. NO. 543 OF 2012**
Rodents
- 5 CATEGORY OF PROCEDURE / METHOD OF EUTHANASIA (I.E. ACTIVITIES) WHICH THE INDIVIDUAL IS AUTHORISED FOR THE PURPOSE SPECIFIED ABOVE PURSUANT TO S.I. NO. 543 OF 2012**
Surgical procedures involving general anaesthesia and analgesia
Non-recovery procedures (including surgical procedures) conducted under terminal general anaesthesia
Minor/minimally invasive procedures involving sedation, analgesia or general anaesthesia
Minor/minimally invasive procedures not requiring sedation, analgesia or general anaesthesia

Appendix 3

GENERAL CONDITIONS

- 1 The holder of the authorisation shall ensure that he/she carries out only the activities listed in the Terms of the authorisation and that the said activities are conducted in the establishment(s) listed in the Terms of the authorisation with respect to the species of animals listed in the Terms of the authorisation.
- 2 Where the authorisation is for the purpose of carrying out the role of project manager (designated pursuant to Regulation 47 of S.I. No. 543 of 2012), the holder of the authorisation shall, in particular –
 - a) ensure that he/she fulfils the requirements of Regulations 47 and 49 of S.I. No. 543 of 2012,
 - b) cooperate with the management of the establishment(s) in relation to the formation, maintenance and provision of records and information, including statistical information, required under Part 10 of S.I. No. 543 of 2012.
- 3 Where the authorisation is for the purpose of carrying out procedures pursuant to the requirements of S.I. No. 543 of 2012, the holder of the authorisation shall, in particular –
 - a) ensure that at all times animals are treated as sentient creatures and with sensitivity and respect. The holder of the authorisation shall ensure that surgical procedures she/he carries out on animals at the establishment(s) are appropriately conducted,
 - b) ensure that he/she complies with Part 4 of S.I. No. 543 of 2012,
 - c) cooperate with the management of the establishment in relation to the formation, maintenance and provision of records and information, including statistical information, required under Part 10 of S.I. No. 543 of 2012,
 - d) inform the staff responsible for the care and welfare of the animals of any issue arising from the conduct of any procedure that is relevant to the recovery or amelioration of pain, suffering or distress of the animal from a procedure,
 - e) inform the establishment's animal welfare body (set up under Regulation 50 of S.I. No. 543 of 2012) and designated veterinarian or expert (designated pursuant to Regulation 48 of S.I. No. 543 of 2012) of any deviation in relation to:
 - f) the conduct of a procedure that negatively impacts upon animal welfare, or
 - g) the conditions of a project authorisation which results in any unexpected adverse impact to animal welfare, or an increase in the level of severity or adverse effects seen in the animal subjects,
 - h) ensure that where the severity classification of procedures authorised under a project authorisation granted by the HPRA are exceeded, the fact is brought to the attention of the establishment's animal welfare body (set up under Regulation 50 of S.I. No. 543 of 2012) and designated veterinarian or expert (designated pursuant to Regulation 48 of S.I. No. 543 of 2012) and the HPRA.
- 4 Where the individual authorisation is for the purpose of euthanising animals pursuant to the requirements of S.I. No. 543 of 2012, the holder of the authorisation shall, in particular –
 - a) ensure that animals are handled in a humane and respectful manner,

Appendix 3

- b) ensure that animals are euthanised out of sight of other animals and in accordance with Regulation 8 of S.I. No. 543 of 2012,
- c) cooperate with the management of the establishment in relation to the formation, maintenance and provision of records and information, including statistical information, required under Part 10 of S.I. No. 543 of 2012,
- d) cooperate with the management of the establishment in relation to the disposal of dead animals in an environmentally safe manner.

5 The holder of the authorisation shall –

- a) apply to the HPRA to amend the authorisation in respect of one or more of the following circumstances:
 - (i) Addition of or change to a category of procedure(s)/method of euthanasia which the individual is authorised to perform.
 - (ii) Addition of or change to a new species / category of animal for the purpose(s) specified in the authorisation.
 - (iii) Addition of or change to a new purpose(s) to the authorisation.
- b) ensure that he/she is aware of and, where appropriate, complies with guidelines issued by the HPRA pursuant to Regulation 5(4) of S.I. No. 543 of 2012.

6 The authorisation is subject to all requirements specified in S.I. No. 543 of 2012.

SPECIFIC CONDITIONS

None

Appendix 4 Ethical Approval



Feidhmeannacht na Seirbhíse Sláinte
Health Service Executive



Ospidéal Réigiúin Pháirc na Muirlinne
Merlin Park Regional Hospital,
Galway, Ireland.

Tel: (091) 757 631

Research Ethics Committee
Unit 4
Merlin Park Hospital
Galway.

27th January, 2006.

Professor Michael Kerin
Department of Surgery
Clinical Science
University College Hospital
Galway.

*Ref: 45/05 - The Provision of a Breast Cancer BioBank research resource for use in
Molecular and Cellular Studies and Clinical Trials*

Dear Michael,

The informed consent form for participation in the BioBank was approved by the CREC subject to a single amendment. It was felt that a stronger statement should be included to ensure that participants were aware their histological details would be linked to their clinical data and to their overall health outcome.

Yours sincerely,

Dr. S. T O'Keeffe
Chairman Research Ethics Committee.



GALWAY UNIVERSITY HOSPITALS - BIOBANK INFORMED CONSENT Patient Information

Introduction

We would like to invite you to participate in a clinical research initiative at Galway University Hospitals to establish a BioBank. The purpose of the BioBank is to set up a resource that can support a diverse range of research programmes intended to improve the prevention, diagnosis and treatment of cancer. You are under no obligation to take part and if, having read the information below, you would prefer not to participate, we will accept your decision without question.

Although major advances have been made in the management of cancer, many aspects of the disease are not fully understood. It is hoped that our understanding of the disease will be improved through research. Galway University Hospitals are actively involved in research that aims to identify markers that will predict how a cancer develops, progresses and responds to a variety of treatments. This type of work requires the use of tissue and blood samples. It is hoped that it will eventually lead to improvements in the diagnosis, treatment and outcome for those who have cancer. Although this study may have no direct benefit to you, it is hoped that the results may benefit patients like you in the future.

Your Involvement

If you volunteer to participate in our BioBank, there will be no additional risks to you outside those of your standard investigation and treatment. Your identity will remain confidential. Your name will not be published or disclosed to anyone outside the study group. All research is covered by standard institutional indemnity insurance and is approved by a Research Ethics Committee that ensures the ethical nature of the research. Nothing in this document restricts or curtails your rights. You may withdraw your consent at any time. If you decide not to participate, or if you withdraw your consent, your standard of treatment will not be affected in any way.

Procedure

We invite all patients who are undergoing treatment and/or investigation to participate. All samples for research will be taken at the time you are attending the hospital for routine diagnostic tests. **You may also be asked to complete a short questionnaire at your clinic visit and annually thereafter. This questionnaire will ask about your use of medicines, lifestyle, and health status, for example.**

(i) Tissue Samples

By participating, you give us consent to retain small pieces of your tissue obtained at the time of surgery. These samples will be stored and used in the future for research. They may be analysed in the surgical laboratory at GUH, or may be transferred to another laboratory for additional analysis using specialised equipment which is not yet available in Ireland. This will not affect your diagnosis in any way.

(ii) Blood Samples

By participating, you give us consent to take an extra blood sample (equivalent of 4 teaspoonfuls) at the same time that your blood is being taken for routine tests. These samples will be stored and used in the future for research. They may be analysed in the surgical laboratory at GUH, or may be transferred to another laboratory for additional analysis using specialised equipment which is not yet available in Ireland.

(iii) Clinical & Questionnaire Information

By participating, you give us consent to collect and store information relating to your diagnosis and treatment, and questionnaire responses on a database.

Information from this database will be anonymised and coded with a unique study number before being made available to researchers not directly involved in research within the Surgical Research Unit.

(iv) Relating to those with a Diagnosis of Cancer: Health Information

By participating, you give us consent to access information about your cancer held by the National Cancer Registry. The National Cancer Registry is funded by the Department of Health and has permission under the law to collect information on every cancer diagnosed in the Republic of Ireland since 1994. The Registry has information on how your cancer was diagnosed, treatments you received, and medicines prescribed for you by your doctors. You can read more about the Registry on their website: www.ncri.ie.

Further Information

If you would like further information about our BioBank, your participation and your rights, please contact the Surgical Research Unit (Tel: 091 524390).

If you would like further information about research projects that may be conducted, please contact your Consultant.

Thank you in anticipation of your assistance. Please read and sign the Consent section.

I have read the attached information sheet on the above project, dated _____

Please Initial Box

GALWAY UNIVERSITY HOSPITALS - BIOBANK INFORMED CONSENT

PARTICIPANT DECLARATION

I have read, or had read to me, this consent form. I have had the opportunity to ask questions and all my questions have been answered to my satisfaction. I freely and voluntarily agree to be part of this research study, though without prejudice to my legal and ethical rights. I have received a copy of this agreement and I understand that, if there is a sponsoring company, a signed copy will be sent to that sponsor. I understand that I may withdraw from the study at any time.

(Name of sponsor):

PARTICIPANT'S NAME:

CONTACT DETAILS:

PARTICIPANT'S SIGNATURE:

DATE:

Where the participant is incapable of comprehending the nature, significance and scope of the consent required, the form must be signed by a person competent to give consent to his or her participation in the research study (other than a person who applied to undertake or conduct the study). If the participant is a minor (under 18 years old) the signature of parent or guardian must be obtained:

NAME OF CONSENTER, PARENT, OR

GUARDIAN:

SIGNATURE:

RELATION TO PARTICIPANT:

DECLARATION OF INVESTIGATOR'S RESPONSIBILITY

I have explained the nature and purpose of this research study, the procedures to be undertaken and any risks that may be involved. I have offered to answer any questions and fully answered such questions. I believe that the participant understands my explanation and has freely given informed consent.

NAME OF RESEARCH NURSE OR

INVESTIGATOR:

SIGNATURE:

DATE:

CONSULTANT:

Keep the original of this form in the investigators file, give one copy to the participant, and send one copy to the sponsor (if there is a sponsor).